UNIVERSITY OF LONDON THESIS

Degree PhD   Year 2005   Name of Author IRVINE, I.P

COPYRIGHT
This is a thesis accepted for a Higher Degree of the University of London. It is an unpublished typescript and the copyright is held by the author. All persons consulting the thesis must read and abide by the Copyright Declaration below.

COPYRIGHT DECLARATION
I recognise that the copyright of the above-described thesis rests with the author and that no quotation from it or information derived from it may be published without the prior written consent of the author.

LOAN
Theses may not be lent to individuals, but the University Library may lend a copy to approved libraries within the United Kingdom, for consultation solely on the premises of those libraries. Application should be made to: The Theses Section, University of London Library, Senate House, Malet Street, London WC1E 7HU.

REPRODUCTION
University of London theses may not be reproduced without explicit written permission from the University of London Library. Enquiries should be addressed to the Theses Section of the Library. Regulations concerning reproduction vary according to the date of acceptance of the thesis and are listed below as guidelines.

A.   Before 1962. Permission granted only upon the prior written consent of the author. (The University Library will provide addresses where possible).

B.   1962 - 1974. In many cases the author has agreed to permit copying upon completion of a Copyright Declaration.

C.   1975 - 1988. Most theses may be copied upon completion of a Copyright Declaration.

D.   1989 onwards. Most theses may be copied.

This thesis comes within category D.
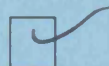
☑ This copy has been deposited in the Library of UCL

☐ This copy has been deposited in the University of London Library, Senate House, Malet Street, London WC1E 7HU.

A METABOLIC ENGINEERING APPROACH TO STUDY OVERFLOW METABOLISM IN *E. COLI*

A Thesis Submitted to the University of London for the Degree of
DOCTOR OF PHILOSOPHY

2004

Helen Patricia Irvine

THE ADVANCED CENTRE FOR BIOCHEMICAL ENGINEERING

UNIVERSITY COLLEGE LONDON

UMI Number: U592060

UMI

Dissertation Publishing

ProQuest

ABSTRACT

Aerobic fermentations of *Escherichia coli* grown with glucose accumulate organic acids in the culture medium. These by-products of glucose metabolism are synthesised and excreted when the glucose uptake rate is greater than its conversion to biomass and carbon dioxide. Acetate is the most abundant overflow metabolite produced in aerobic cultures of *E. coli*. Its production is strain and media specific, being greatest in dense nutrient-rich cultures. In industrial fermentations, *E. coli* is widely employed for production of recombinant proteins. However, acetate excretion reduces process efficiency by lowering cell growth rate, and decreasing the amount of substrate carbon converted to recombinant protein product.

This thesis describes the construction of three plasmid vectors designed to express antisense RNA targeted against phosphotransacetylase and acetate kinase, which convert acetyl CoA to acetate. Antisense RNA was used as a metabolic engineering tool in this study, to enable examination of the central carbon flux distribution before, during and after enzyme downregulation. The aim was to decrease expression of these enzymes in *E. coli*, and thus decrease acetate production. *E. coli* MG1655 was transformed with a) a plasmid construct encoding an antisense RNA fragment, b) two compatible plasmids encoding different antisense RNA fragments. The resulting strains were cultivated in a 2L bioreactor, and the effect of antisense RNA expression evaluated. Assays to monitor the enzyme activities of phosphotransacetylase and acetate kinase were conducted, along with metabolite analysis to determine organic acid excretion profiles. Flux balance analysis, which is a method of modelling metabolism, was applied to the central carbon pathways in *E. coli* to provide insight into the partitioning of internal carbon fluxes. Information about the mechanisms used by *E. coli* to cope with partial shutdown of the acetate synthesis pathway was gained by comparing the flux distribution of a control strain with an antisense RNA-expressing strain.

TABLE OF CONTENTS

2. MATERIALS AND METHODS — 46

LIST OF FIGURES

CHAPTER 7

LIST OF TABLES

14

ACKNOWLEDGEMENTS

CHAPTER 1

INTRODUCTION

Escherichia coli is one of the most widely used hosts for recombinant protein production (Demain, 2000; Lee, 1996). It is particularly suitable for this role due to its ability to grow rapidly to high cell densities using inexpensive substrates. Furthermore, *E. coli* genetics and physiology are well characterised and there are an increasingly large number of mutant *E. coli* strains and cloning vectors available (Baneyx, 1999). However, under the commonly used fermentation conditions of aerobic growth in excess glucose, *E. coli* produces the toxic by-product acetate, which accumulates in the culture medium and reduces cell growth and recombinant protein production (Jensen and Carlsen, 1990; Luli and Strohl, 1990). In an attempt to overcome this problem, a great deal of research has focused on understanding why acetate is produced by *E. coli* and on developing strains with reduced acetate production.

Strain optimisation has traditionally been accomplished by using chemical mutagens and ionising radiation, combined with screening and selection techniques to identify superior strains. There are many examples of success with this approach in the areas of amino acid, antibiotic, solvent and vitamin production, however mutagenesis is essentially a random process (Stephanopoulos *et al.*, 1998). In contrast, *Metabolic Engineering* is a rational, directed approach to strain optimisation that combines molecular biology techniques for DNA recombination with advanced tools for metabolic pathway analysis (Koffas et al., 1999; Nielsen, 2001).

Metabolic engineering is usually an iterative process that involves several stages. For example, the process may begin with design and construction of a recombinant strain, followed by analysis of the resulting strain compared with the original strain background and then identification of the next target for genetic engineering. Alternatively, detailed analysis of the metabolic network may be required in order to identify the targets for genetic engineering before proceeding to the construction stage and subsequent analysis of the recombinant strain. Consequently, metabolic engineering entails continuous improvement of cellular properties. The main areas of research where metabolic engineering has been applied are: heterologous protein production; extension of substrate range; pathways leading to new products; pathways for degradation of xenobiotics; engineering of cellular physiology for process improvement; elimination or reduction of by-product formation and improvement of yield or productivity (Nielsen, 2001).

This research aimed to reduce acetate production by *E. coli,* using a metabolic engineering approach. To this end, recombinant *E. coli* strains were developed to express antisense RNA targeted against the enzymes of the primary acetate production pathway. Antisense RNA-expressing cultures were analysed using experimental and mathematical tools, and compared with the original strain background. The challenge is to determine the effectiveness of antisense RNA in suppressing expression of the target enzymes and redirecting the central carbon metabolism of *E. coli.*

1.1 AEROBIC ACETATE PRODUCTION BY *E. COLI*

In *E. coli* the uptake rate of some carbon sources such as glycerol, is tightly regulated to permit the precise balance of carbon flux to biosynthesis and energy production. These carbon sources are converted to new biomass and carbon dioxide with no by-product formation, however the control imposed on carbon uptake limits the cellular growth rate. For other carbon sources such as glucose, the uptake rate is not as rigorously controlled and carbon flux through the central metabolic pathways exceeds the demands for biosynthesis and energy production (Holms, 1986). In particular, carbon flux through glycolysis is thought to exceed the capacity of the TCA cycle and result in acetate production (El-Mansi and Holms, 1989; Han et al., 1992; Majewski and Domach, 1989). This outlet for excess carbon allows *E. coli* to maintain a rapid growth rate and in addition, the acetate production pathway (*ackA-pta* pathway) generates ATP, unlike the lactate or ethanol by-product pathways. It is commonly observed that 10-30% of glucose is excreted as acetate even in a fully aerated culture, depending on the particular strain type.

1.1.1 ACETATE PRODUCTION AND CONSUMPTION PATHWAYS

There are two known pathways for production of acetate in *E. coli,* which are illustrated in Figure 1.1. Acetate can be produced directly from pyruvate by the enzyme pyruvate oxidase (*poxB*). However, the main acetate production pathway is the *ackA-pta* pathway, which involves a two-step conversion of acetyl CoA to acetate. In the first step acetyl CoA is converted to acetyl phosphate by phosphotransacetylase (Pta), and in the second step acetate kinase (Ack) converts acetyl phosphate to acetate with concomitant production of ATP (Brown *et al.,* 1977). The *ackA-pta* pathway is reversible, although acetate kinase has a low affinity for acetate. Consequently, the pathway is only thought to function in the reverse mode when acetate is present in high concentrations in the media (e.g. when it is utilised as the main carbon source). In summary, the *ackA-pta*

pathway functions primarily in a catabolic role, excreting acetate and generating ATP during growth on excess glucose (Brown *et al.*, 1977).

The *ackA-pta* pathway intermediate acetyl phosphate is a high-energy phosphate compound that has been implicated in a range of important cellular functions. These include the glucose phosphotransferase system, flagellar expression and expression of porin proteins that control the permeability of the *E. coli* outer membrane (Fox et al., 1986b; Heyde et al., 2000; PruB, 1998; PruB and Wolfe, 1994; Shin and Park, 1995). In addition, acetyl phosphate is thought to function as a phosphate donor for many signal transduction response regulators including CheY, PhoB, NR1, and OmpR (McCleary and Stock, 1994). Perturbations in the production of acetyl phosphate have been shown to affect expression of the phosphate regulon (Pho) (Wanner and Wilmes-Riesenberg, 1992), the nitrogen regulon (Ntr) (Feng *et al.*, 1992), and the glucose starvation stimulon (Nystrom, 1994). Intracellular levels of acetyl phosphate vary widely with carbon source (McCleary and Stock, 1994), cell growth phase and temperature (PruB and Wolfe, 1994). In summary, perturbations in acetyl phosphate production are likely to have far-reaching affects on *E. coli* cellular activities.

There are two pathways for acetate consumption in *E. coli*, which are illustrated in Figure 1.1. As mentioned above, the reversible *ackA-pta* pathway is thought to consume acetate when it is present in relatively high concentrations in the media, and activate it to acetyl CoA. The second route for acetate uptake comprises a two-step pathway catalysed by the enzyme acetyl CoA synthetase (Acs). This enzyme is thought to function as a scavenger when acetate is present at a low concentration in the culture (Kumari et al., 1995). In the first step of this pathway, acetate is converted to the intermediary compound acetyl-AMP by acetyl CoA synthetase and in the second step acetyl-AMP is converted to acetyl CoA by acetyl CoA synthetase. As the first reaction is irreversible, the pathway can only consume acetate. Once acetate has been activated to acetyl CoA, it can be further metabolised through the TCA cycle and the glyoxylate bypass. Incidentally, acetyl CoA synthetase is cotranscribed with the acetate membrane-carrier protein, acetate permease (*actP*; formerly designated *yjcG*) (Gimenez *et al.*, 2003). An additional gene, *yjcH*, is cotranscribed with *acs* and *actP*. The *yjcH* gene codes for a putative membrane protein of 104 amino acids and is highly conserved in many bacterial species but still has no defined function (Gimenez *et al.*, 2003).
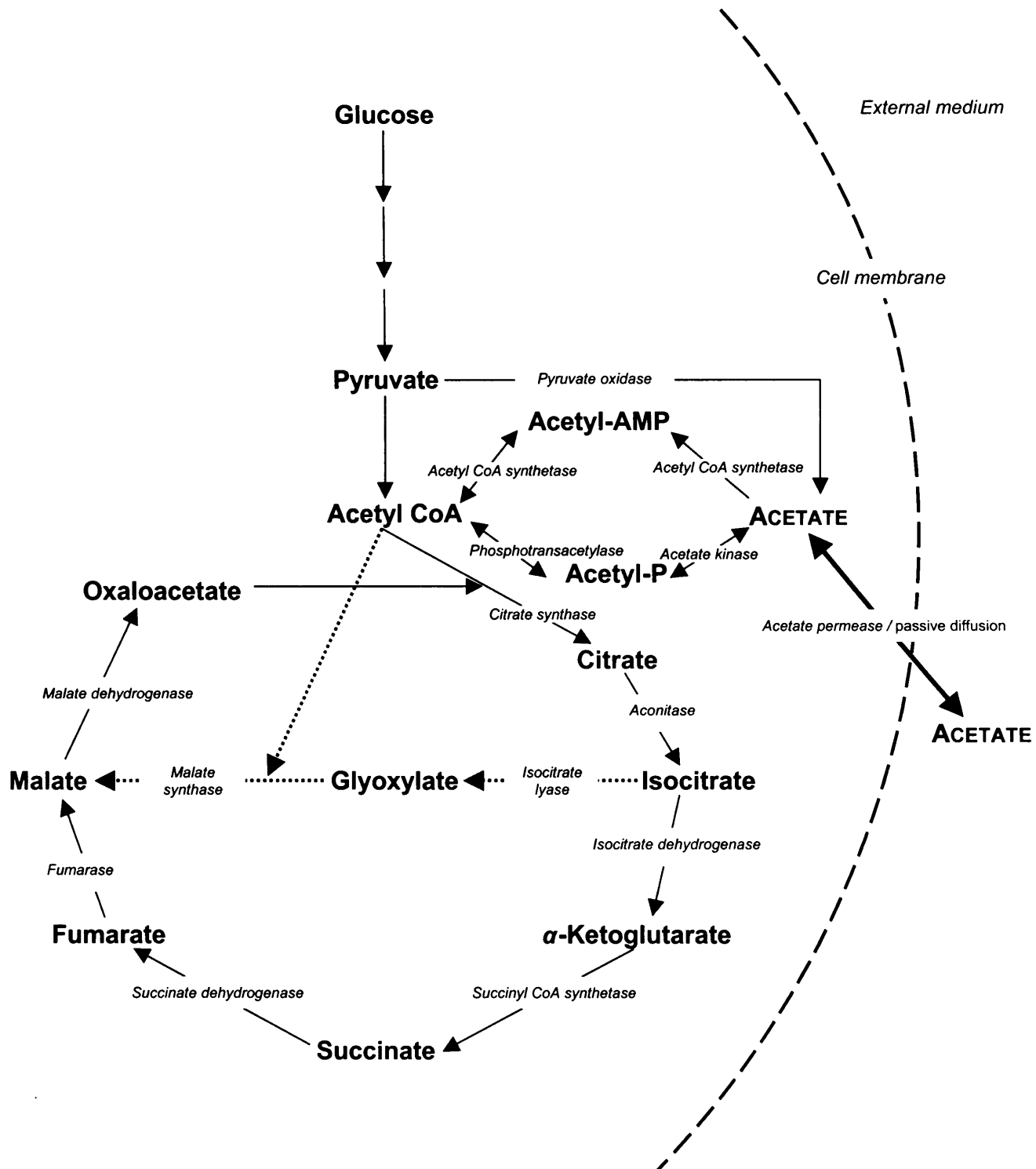
Figure 1.1 Acetate production and consumption pathways in *E. coli*.

1.1.2   STRAIN SPECIFIC DIFFERENCES IN ACETATE PRODUCTION BY *E. COLI*

Acetate production in *E. coli* is strain-specific. For example, *E. coli* B derivatives, such as BL21, are low acetate producers, whereas *E. coli* K derivatives, such as JM109, are high acetate producers. The difference is thought to be due to different expression levels of the enzymes responsible for acetate production and consumption in *E. coli* (van de Walle and Shiloach, 1998). A recent study has confirmed that the glyoxylate shunt and acetyl CoA synthetase are constitutively expressed in the low-acetate producing *E. coli* BL21, while the same enzymes are repressed in *E. coli* JM109, which produces high levels of acetate (Phue and Shiloach, 2004). This trend was consistently observed in both low and high glucose growth. It is possible that expression of the glyoxylate shunt pathway is correlated with expression of acetyl CoA synthetase, because the glyoxylate shunt requires additional acetyl CoA that is supplied through acetate uptake by acetyl CoA synthetase. The findings suggest that the ability of *E. coli* B to grow on glucose without producing high levels of acetate is a result of its capability to operate the TCA cycle and the glyoxylate pathway simultaneously. No clear difference was observed in expression levels of the *ackA-pta* pathway between the two strains, however higher transcription levels of pyruvate oxidase were found in the high-acetate producing *E. coli* JM109 (Phue and Shiloach, 2004).

In addition to the inherent strain-specific differences in acetate production, growth phase-related changes in the operation of acetate production and consumption pathways in *E. coli* have been observed. Some *E. coli* cultures undergo a metabolic switch from glucose to acetate utilisation, as the cells enter stationary phase (Kleman and Strohl, 1994). It has been proposed that as the cells divide exponentially, they excrete acetate via the *ackA-pta* pathway. Then when they begin the transition to stationary phase, they resorb acetate, even in the presence of remaining glucose, using acetyl CoA synthetase, and utilise it to generate energy and biosynthetic components via the TCA cycle and the glyoxylate shunt respectively (Kumari et al., 2000).

1.1.3   EFFECT OF ACETATE ON *E. COLI* PHYSIOLOGY

Acetate is a weak acid and a well-known growth inhibitor. The undissociated form produced intracellularly freely permeates the cell membrane and accumulates in the culture medium. Subsequently, undissociated extracellular acetate re-enters the cell where it dissociates due to the higher intracellular pH. Consequently, acetate dissipates the pH component of the proton motive force and lowers the cytoplasmic pH, causing growth stasis due to irreversible denaturation of DNA and protein (Stephanopoulos *et al.*,

1998). In addition, acetate reduces the cellular efficiency for recombinant protein production. Acetate levels of 40 mM have been shown to reduce recombinant protein production by 35% without significantly effecting biomass yield (Jensen and Carlsen, 1990).

Global analysis of the effect of acetate accumulation (100 mM) on *E. coli* gene expression revealed a complex cellular response, involving significant change in the expression level of 86 genes (Arnold *et al.*, 2001). The expression of 60 genes was reduced by at least two-fold, including 48 genes that encode components of the transcription-translation machinery. Expression of 26 genes was increased two-fold or more, and of these, six encoded products are known to be important for survival at low pH. In addition, proteomic studies using 2D-gel electrophoresis have led to the identification of 37 proteins whose expression is increased and 17 proteins whose expression is decreased, by acetate accumulation (50 mM) in the culture media (Kirkpatrick *et al.*, 2001).

It is well established that acetate has a detrimental effect on *E. coli* that is brought about by reducing the intracellular pH, however a recent study has shown that acetate-treated cells accumulate the toxic intermediate homocysteine (Roe *et al.*, 2002). Therefore, it has been proposed that acetate may inhibit the activity of an enzyme in the lower part of the methionine biosynthetic pathway, leading to accumulation of toxic homocysteine. This theory agrees with a previous observation that the growth inhibition of *E. coli* caused by acetate can be alleviated by supplementing the culture with methionine (Han et al., 1993). Growth inhibition caused by acetate can therefore be partly attributed to a partial auxotrophy for methionine combined with accumulation of an inhibitory pathway intermediate (Roe *et al.*, 2002).

1.2 METABOLIC ENGINEERING

1.2.1 BACKGROUND

Metabolic engineering was defined in 1991 as the 'improvement of cellular activities by manipulation of enzymatic, transport and regulatory functions of the cell with the use of recombinant DNA technology' (Bailey, 1991). At that time, metabolic engineering consisted of little more than a collection of examples and most of the research involved changes in a single gene, operon or gene cluster. However many potential applications for metabolic engineering were identified and grouped into the following two categories: (1) recruiting heterologous activities for strain improvement, and (2) redirecting metabolite flow.

Early research that used enzyme amplification to enhance production of a specific metabolite had limited success, which highlighted the complexities of metabolic regulation. Consequently, the term metabolic network rigidity was coined to describe the inherent resistance of metabolism to alterations in flux. In addition, a methodology to define the flexibility of metabolic nodes was proposed (Stephanopoulos and Vallino, 1991). According to the system, nodes can be described as flexible, weakly rigid or rigid, depending on how readily flux partitioning into each branch changes to meet metabolic demands. A 'principle node' is defined as a branch point in which the partitioning of flux into each branch affects the rate of formation of a specific product. Application of these concepts can improve the identification of targets for metabolic engineering.

In recent years, advances in genomics and analytical tools have facilitated the rapid expansion of the field of metabolic engineering. Whole genome sequencing and new and improved techniques for gene cloning have increased the repertoire of heterologous genes that can be recruited from many different organisms and expressed in novel hosts. Also, additional tools for expression of heterologous genes have been generated, such as segregationally stable plasmids present in low copy numbers (Jones and Keasling, 1998) and RNA secondary structures that reduce mRNA degradation (Carrier and Keasling, 1997). In addition, powerful experimental techniques have been developed for analysis of gene expression and protein levels, including microarrays, RT-PCR and 2-dimensional gel electrophoresis (Lee and Lee, 2003).

1.2.2   EXPERIMENTAL AND MATHEMATICAL METHODS FOR ANALYSING COMPLEX METABOLIC NETWORKS

An integral part of metabolic engineering is *Metabolic Pathway Analysis,* which is the study of complex metabolic networks. There are three distinct areas, described as 1) identification of metabolic network structure, 2) quantification of flux through pathways of the metabolic network, and 3) identification of control structures within the metabolic network (Nielsen, 2001). Incidentally, *metabolic flux* is defined as 'the rate at which material is processed through a metabolic pathway' (Stephanopoulos, 1999).

1.2.2.1   IDENTIFICATION OF METABOLIC NETWORK STRUCTURE

A powerful experimental method that can be used to determine the structure of a metabolic network or specific metabolic flux distribution, involves isotopic tracer experiments' with ^{13}C-labelled substrate (Kelleher, 2001). The labelling pattern of ^{13}C in intracellular metabolites is analysed using nuclear magnetic resonance (NMR) or gas chromatography and mass spectrometry (GC-MS). The ^{13}C NMR technique has the disadvantage of relatively low sensitivity and therefore requires a large amount of sample. By contrast, GC-MS is highly sensitive and cheaper than NMR, which makes it more suitable for metabolic pathway analysis (Zhao and Shimizu, 2003).

Mathematical approaches can also be employed to examine the structure of complex metabolic networks. Two closely related methods that were developed for this purpose are elementary flux mode analysis and extreme pathway analysis. Elementary flux modes (EFM) are defined as the complete set of routes that convert a given substrate to a specific product. Elementary flux mode analysis aims to identify the number of alternative routes for a certain task, the 'optimal' routes, and the sensitivity of these pathways towards disturbances such as mutations. Extreme pathways (EP) are a subset of elementary modes, which are intended to represent a minimal set of pathways capable of describing all steady-state flux distributions (Klamt and Stelling, 2003). Due to the tight constraints, there is a danger that extreme pathways may exclude physiologically important pathways, and therefore elementary flux mode analysis is generally viewed as the most suitable method of the two for analysing metabolic pathways.

1.2.2.2   QUANTIFICATION OF FLUX THROUGH PATHWAYS OF THE METABOLIC NETWORK

The study and quantification of metabolic fluxes through the branches of a metabolic network can be achieved by *Metabolic Flux Analysis* (Edwards et al., 1999; Holms, 1999). This is a mathematical method, which is used to calculate a specific set of intracellular fluxes by formulating a stoichiometric model of the metabolic reaction network and applying mass balances around the intracellular metabolites. Measured extracellular fluxes, such as the substrate uptake and product secretion rates, are used as inputs for the calculation. The outcome is a flux map, which shows the reaction pathways included in the model, along with an estimated steady-state rate (flux) for each reaction. Individual metabolic flux maps contain information about the relative contributions of various pathways to the overall processes of substrate utilisation and product formation. However, the real value of these maps lies in the differences that are observed when flux maps that are obtained from different strains or under different conditions are compared (Stephanopoulos *et al.*, 1998). Through these comparisons, the impact of genetic or environmental perturbations can be evaluated and the importance of specific pathways identified. Although metabolic flux analysis has been widely used, it has several important limitations. Information regarding gene expression levels and enzyme regulation is not incorporated, therefore the results should be carefully analysed in the light of current biochemical knowledge about the pathways involved. This may be possible for small reaction networks, but is a more daunting task for large, complex networks. Metabolic flux analysis is described in more detail in chapter 8.

1.2.2.3   IDENTIFICATION OF CONTROL STRUCTURES WITHIN THE METABOLIC NETWORK

An important goal of metabolic engineering is to understand the control of metabolic flux in order to approach the rational modification of metabolic pathways. *Metabolic Control Analysis* (MCA) is a mathematical method which was developed in the 1960's and 70's to quantify flux control (Heinrich and Rapoport, 1974; Higgins, 1963; Kacser and Burns, 1973). In this system the degree of flux control exercised by specific enzymes in a pathway is expressed in terms of a flux control coefficient (Fell, 1998). According to the theory, over-expressing an enzyme with a high flux control coefficient is likely to increase overall flux through the pathway. However, metabolic control analysis is essentially a 'linear perturbation theory' of the inherently non-linear problem of enzyme kinetics of metabolic networks, therefore predictions and subsequent extrapolations made using this method should be regarded as tentative (Stephanopoulos et al., 1998).

1.2.3   USE OF CONTINUOUS CULTURE METHODS FOR ANALYSING METABOLISM AT STEADY STATE

Cultivation of cells can be carried out in batch, fed-batch or continuous culture. In batch culture, the cells environment constantly changes due to substrate depletion, product formation and biomass accumulation. This is reflected in the different growth phases that are commonly observed in batch culture i.e. lag phase, exponential growth phase and stationary phase. In fed-batch culture, nutrients are added in a stepwise fashion throughout the course of fermentation, which allows some degree of control over the cells environment. This method is commonly used for achieving high cell densities. In continuous culture, an equilibrium concentration of the growth-controlling substrate is established, independently of culture density and time, which allows the culture to grow at the set dilution rate by maintaining stable environmental growth conditions and hence the same physiological state (Kovarova-Kovar and Egli, 1998).

For metabolic engineering purposes, it is desirable to study metabolism under steady state conditions. Therefore, continuous culture methods for cell cultivation are particularly well suited. Several types of continuous culture have been developed, including chemostat, where the dilution rate is kept constant, and turbidostat, where the biomass concentration is kept constant. However, these methods are time consuming to implement and use large volumes of medium. Typically, 4-5 cultures volumes are required to obtain the steady state. In recent years, modified continuous culture methods have been developed, such as the A-stat technique where the rate of change of the dilution rate is kept constant (Paalme et al., 1995). This system is thought to mimic the gradually changing growth conditions that are found in nature and many industrial processes, and may therefore be even more informative for practical purposes (Kasemets et al., 2003).

Several metabolic engineering studies have employed continuous culture methods for cell cultivation under steady state conditions. These include: use of an oxygen-limited chemostat culture to analyse carbon flow through the central metabolic pathways of *Candida tropicalis* grown on xylose (Granstrom et al., 2002); use of a phosphate-limited chemostat culture to study carbon flow and antibiotic production in *Streptomyces lividans* (Avignone Rossa et al., 2002); and use of a carbon-limited chemostat culture to analyse the effect of increasing NADH availability on the carbon flow through *Escherichia coli* central metabolism (Berrios-Rivera et al., 2002). In this study, batch fermentation was used in order to mimic the fermentation conditions that are most commonly employed in the Biotechnology industry.

1.2.4   EXAMPLES OF METABOLIC ENGINEERING APPROACHES TO REDUCE ACETATE PRODUCTION BY *E. COLI*

Many operational strategies have been proposed and tested to reduce acetate production and accumulation in *E. coli* culture (Yang et al., 1998). The approaches include: increasing the agitation speed or enriching the culture with pure oxygen to avoid dissolved oxygen limitation; controlled feeding to restricting the glucose uptake rate by *E. coli;* and removal of acetate from spent medium using devices such as a perfusion system (Akesson et al., 2001; Curless et al., 1991; Konstantinov et al., 1990). Although these methods can lead to improved process performance, they are often difficult to scale up and costly to implement. An alternative approach is to develop *E. coli* strains that inherently produce less acetate under optimal fermentation conditions. Metabolic engineering has been employed for this purpose and several examples are described below.

1.2.4.1   RESTRICTING THE RATE OF GLUCOSE UPTAKE BY *E. COLI*

It is well established that glucose uptake by *E. coli* is loosely regulated. When glucose is present in the culture medium in excess amounts, glucose uptake normally exceeds the cellular requirements for biosynthesis and energy production, resulting in acetate excretion. However, when glucose is the sole carbon source in minimal media it is used by *E. coli* to generate energy and for macromolecule synthesis, therefore its uptake rate plays a critical role in dictating cellular activities. Under these conditions, reducing the glucose uptake rate often results in a reduced specific growth rate. By contrast, *E. coli* grown in a complex medium derives most building blocks as already synthesised compounds from media components such as yeast extract and casamino acids, and uses glucose primarily as an energy supply. Therefore, decreasing the glucose uptake rate has less of an impact on cellular growth rate (Neidhardt et al., 1987).

The glucose uptake rate by *E. coli* can be reduced by supplementing the culture with methyl *a*-glucoside, which is a glucose analogue that is non-toxic and metabolically inert (Chou et al., 1994a). It acts as a competitive inhibitor to enzyme II of the glucose phosphotransferase system, thereby reducing the rate of glucose uptake into the cell. This strategy of partial disruption to the glucose phosphotransferase system has also been achieved by inactivating the *ptsG* gene, which encodes enzyme II in the glucose phosphotransferase system (Chou et al., 1994b). In batch cultures, the growth rate of the *ptsG* mutant strain was reduced by 20% in glucose minimal media, but was not affected in complex media. Furthermore, in complex media the *ptsG* mutant strain exhibited

significantly reduced levels of acetate production and enhanced recombinant protein production. These results indicate that modulation of the glucose uptake rate is an effective approach to minimise the inhibitory effects of acetate accumulation by *E. coli*, grown under aerobic conditions in complex media.

1.2.4.2 ENGINEERING *E. COLI* TO PRODUCE A USEFUL OR LESS TOXIC END-PRODUCT AT THE EXPENSE OF ACETATE PRODUCTION

Advances in molecular biology tools allow metabolic engineers to clone and express heterologous genes in *E. coli* in order to generate novel pathways and produce new compounds of interest. However, as metabolism is inherently resistant to change it can be difficult to anticipate whether a heterologous enzyme will be able to compete successfully with native enzymes for a substrate in central metabolism. It is more straightforward if a heterologous enzyme is simply extending an existing linear pathway and does not have to compete with other enzymes for its substrate.

Flux partitioning at the pyruvate node in *E. coli* central metabolism can be altered by expressing the *Bacillus subtilis* acetolactate synthase (ALS) gene, which catalyses the conversion of pyruvate to acetoin, via the intermediary compound *a*-acetolactate (Figure 1.2). This approach has been used with the aim of redirecting carbon flux away from acetate production and towards formation of acetoin, which is less toxic than acetate (Aristidou *et al.*, 1994). Fermentation results from batch cultures revealed that recombinant *E. coli* grown under aerobic conditions, and expressing the active acetolactate synthase enzyme reached double the final cell density of the parent strain with a six-fold reduction in total acetate accumulated in the culture medium. In addition, the ALS strain was shown to be capable of enhancing the production of a recombinant CadA/beta-galactosidase fusion protein in *E. coli* by about 60% (Aristidou *et al.*, 1995). These results indicate that expression of a heterologous enzyme can redirect carbon flux and reduce acetate production by *E. coli*, grown under aerobic conditions.

Under anaerobic conditions, *E. coli* excrete large quantities of the partially oxidised byproducts acetate, formate and ethanol (Figure 1.2). Metabolic flux analysis has been used to study the effects of *Bacillus subtilis* acetolactate synthase expression on the metabolic flux distribution in anaerobic *E. coli* (Aristidou *et al.*, 1999). Batch fermentation results showed that anaerobic *E. coli* expressing *Bacillus subtilis* acetolactate synthase (ALS) produced three-fold less acetate and about 30% less formate compared to the parent strain. Ethanol production was not significantly affected. Metabolic flux analysis calculated that ALS expression resulted in a reduced flux from pyruvate to acetyl CoA,

although flux to ethanol was unaffected at the expense of acetate production. The undisturbed flux to ethanol may be due to the crucial role of the ethanol production pathway in NADH regeneration in anaerobic E. coli, indicating that partitioning of flux at the acetyl CoA node into ethanol or acetate is determined by the redox state of the cell. As a result, the acetyl CoA branch point was classified as a 'weakly rigid node', characterised by a dominant branch (ethanol) and a subordinate branch (acetate). In addition, metabolic flux analysis showed that the ALS strain has the ability to channel excess pyruvate to acetoin. This study demonstrates that even under anaerobic conditions, expression of Bacillus subtilis acetolactate synthase has the ability to redirect central carbon flux and reduce acetate production by E. coli.

Glucose

Succinate

$NAD^+ + ATP$

$NADH + ADP$

Fumarate

$NAD^+ + Aspartate$

$NADH + NH_4^-$

Phosphoenolpyruvate $\longrightarrow$ Oxaloacetate

CO_2

ADP

ATP

CO_2

a-Acetolactate $\longleftarrow$ Pyruvate $\longrightarrow$ Lactate

NADH NAD^+

CO_2

Acetoin

CoA

Formate

CO_2

H_2

Acetyl CoA $\longrightarrow$ Acetyl-P

2 NADH

NAD^+

ADP

ATP

Ethanol   Acetate
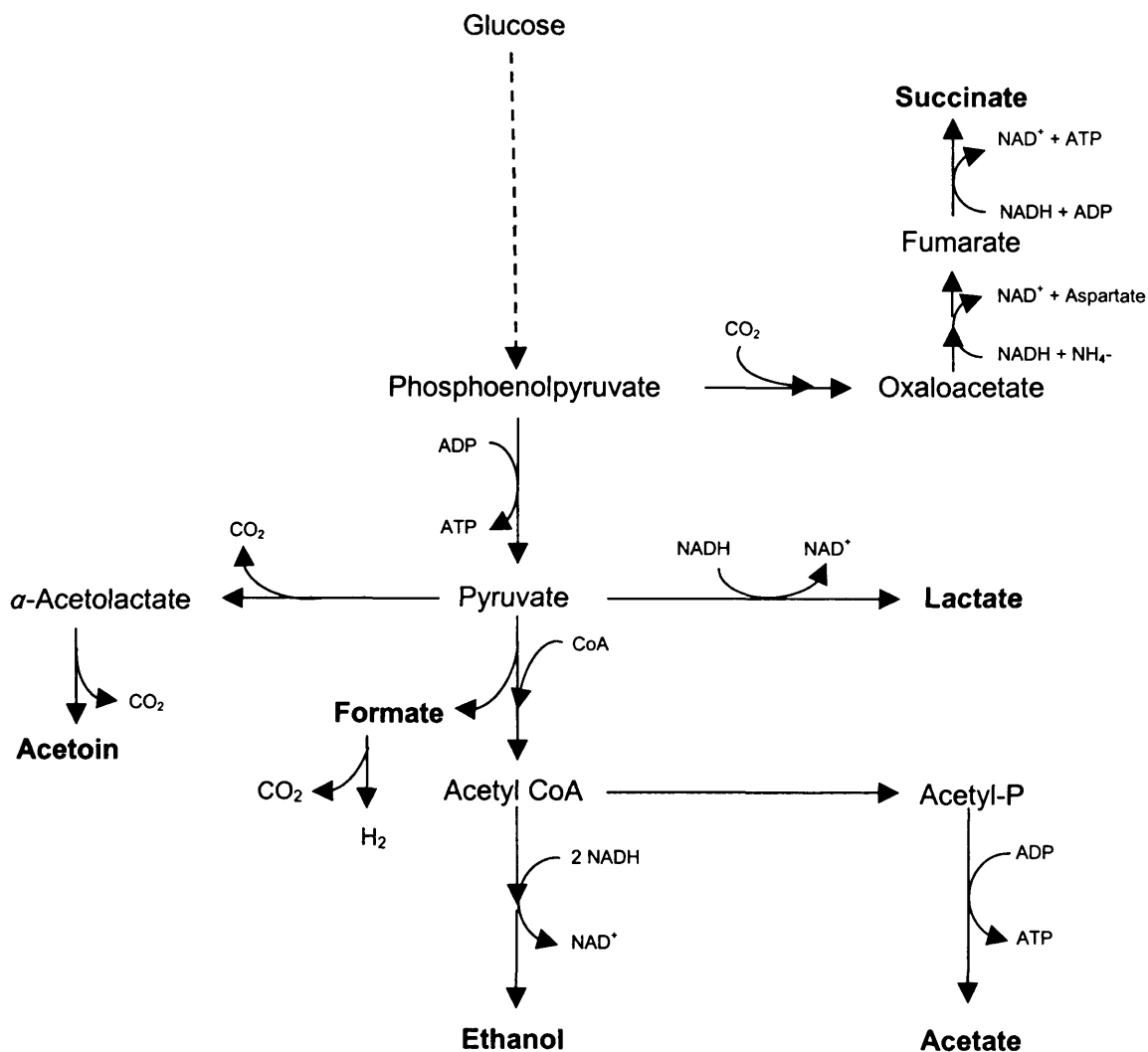
Figure 1.2 Central metabolic pathways of anaerobically grown E. coli and the additional heterologous pathway for acetoin production (adapted from Aristidou et al., 1999). The principle fermentation products are represented in boldface.

1.2.4.3   INACTIVATING PHOSPHOTRANSACETYLASE AND ACETATE KINASE TO REDUCE ACETATE PRODUCTION

The major acetate production pathway in *E. coli* (*ackA-pta* pathway) consists of the enzymes phosphotransacetylase and acetate kinase, which convert acetyl CoA to acetate via the intermediate acetyl phosphate. The effect of deleting the *ackA-pta* pathway on the flux distribution in central carbon metabolism was studied in anaerobic *E. coli* using metabolic flux analysis (Yang *et al.*, 1999a). Batch fermentation results showed that the *ackA⁻ pta⁻* mutant strain exhibited an increased lactate production rate with a concomitant decrease in formate, ethanol, and acetate production. Excretion of pyruvate was also detected. Lactate dehydrogenase (LDH), which catalyses the conversion of pyruvate to lactate, is typically induced under anaerobic conditions at low pH and is allosterically activated by pyruvate (Ruijun *et al.*, 2001). Therefore, it was suggested that deleting the *ackA-pta* pathway resulted in an elevated intercellular pyruvate pool, inducing allosteric activation of lactate dehydrogenase and subsequent lactate production. Alternatively, it has been suggested that acetyl phosphate, which is the *ackA-pta* pathway intermediate, may be involved in suppressing expression of lactate dehydrogenase (Bunch *et al.*, 1997). If this were the case, abolishing acetyl phosphate production would deregulate lactate dehydrogenase and result in lactate production.

Expression of *Bacillus subtilis* acetolactate synthase (ALS), which converts pyruvate to acetoin, in the *ackA⁻ pta⁻* mutant resulted in a further reduction in acetate excretion by anaerobic *Escherichia* and more importantly, the fluxes to lactate, formate and ethanol were restored to similar levels as the parent strain. This suggests that expression of ALS alleviates a probable elevated intracellular pyruvate pool in *ackA⁻ pta⁻* mutants (Yang *et al.*, 1999a). To investigate the flux distribution around the pyruvate node further, an *E. coli* strain bearing mutations in *ackA, pta* and *ldhA* was studied under anaerobic conditions (Yang *et al.*, 1999b). These combined mutations were found to be detrimental to cell growth.

Following the observation that *ackA⁻ pta⁻* mutant strains excrete increased lactate, an *E. coli* strain over-expressing lactate dehydrogenase (*ldhA*) was constructed and studied to determine whether over-expressing this enzyme in the parent strain could effectively divert carbon flux from central metabolism towards lactate production and thereby reduce acetate production (Yang *et al.*, 1999b). However, batch fermentation results revealed that even a 10-fold increase in lactate dehydrogenase activity was unable to divert a significant fraction of the central carbon flux to lactate. Metabolic flux analysis revealed that carbon flux through pyruvate and to all products increased at the expense of flux to

30

biomass. Measurement of intracellular pyruvate levels showed that over-expression of LDH in anaerobic *E. coli* depletes the intracellular pyruvate pool. Similarly, it has been reported that over-expression of LDH in aerobic *E. coli* inhibits growth in minimal media, presumably due to depletion of the intracellular pyruvate pool (Bunch *et al.*, 1997).

1.2.4.4 UP-REGULATION OF ANAPLEUROTIC REACTIONS TO UTILISE EXCESS CARBON IN CENTRAL METABOLISM

Aerobic acetate production by *E. coli* is generally believed to arise from an imbalance between glucose uptake and cellular demands for biosynthesis and energy production, but the cause of this imbalance is largely unknown. Farmer and Liao (1997) hypothesised that increasing the flux through anapleurotic reactions in *E. coli* central metabolism would utilise the excess carbon and reduce acetate production. Anapleurotic pathways replenish the supply of important intermediate metabolites, such as oxaloacetate, which is crucial for the functioning of the TCA cycle. It is produced from phosphoenolpyruvate by PEP-carboxylase. Another example of an anapleurotic reaction is the glyoxylate bypass, which converts isocitrate to malate via glyoxylate. The enzymes of the glyoxylate bypass, isocitrate lyase and malate synthase, are active during growth of *E. coli* on acetate, but usually repressed in the presence of glucose or under anaerobic conditions.

Metabolic flux analysis indicated that increasing the expression of PEP-carboxylase and deregulating the glyoxylate bypass would reduce acetate production in glucose minimal media (Farmer and Liao, 1997). A recombinant *E. coli* strain was developed to test this theory. Batch fermentation results showed that under aerobic conditions in glucose minimal media the mutant strain exhibited a four-fold decrease in acetate accumulation compared to the parent strain, with no substantial decrease in growth rate. There was no evidence for simultaneous production and utilisation of acetate by the culture, suggesting that deregulation of the glyoxylate bypass reduces acetate production by promoting better utilisation of acetyl CoA. This study suggests that *E. coli* is not optimised for growth on glucose. The reason for this remains unclear, but it has been argued that during the course of *E. coli* evolution, glucose was not the major carbon source available (Holms, 1986). Fructose and glycerol, which do not result in acetate production, may have predominated, however *E. coli* grows relatively slowly on these substrates, making them an unpopular choice for industrial fermentation.

Recent research has revealed that the glyoxylate bypass is constitutively expressed in the low acetate-producing strain *E. coli* BL21 (Phue and Shiloach, 2004; van de Walle and Shiloach, 1998). In contrast, in the high acetate-producing strain *E. coli* JM109 there

is no apparent transcription of the enzymes of the glyoxylate bypass under the same conditions. These observations confirm that increasing flux through the anapleurotic pathways is a logical approach to reducing acetate production by *E. coli*.

1.3   ANTISENSE RNA

For a long time, RNA molecules were thought to function either as messengers (mRNA) or as part of the translational machinery (tRNA, rRNA). However, since the discovery of ribozymes, which have catalytic activity (Puerta-Fernandez et al., 2003), and antisense RNA and RNA interference, which are posttranscriptional regulators of gene expression (Brantl, 2002; Cottrell and Doering, 2003), it has become widely recognised that RNA has a diverse range of cellular functions. The following sections focus on antisense RNA, and highlight its use as an experimental tool to downregulate the expression of target genes in metabolic engineering research.

1.3.1   ANTISENSE RNA REGULATED SYSTEMS IN PROKARYOTES

Antisense RNA occurs naturally in all three kingdoms of life, although most antisense RNA-regulated systems have been identified in prokaryotes and only a few examples are known from eukaryotes and one from archaea (Stolt and Zillig, 1993). By contrast, RNA interference (gene silencing triggered by double stranded RNA), only occurs in eukaryotes. RNA interference does not occur in prokaryotic cells due to the presence of RNase III, which is a fast and efficient enzyme that specifically degrades double-stranded RNA molecules as short as 12 bp. This enzyme prevents the short interfering RNAs (siRNA), which are the effectors of RNA interference, from stably existing long enough to bind to the target mRNA and induce cleavage and subsequent degradation (Brantl, 2002).

Antisense RNAs are small, highly structured RNA molecules that bind via sequence complementarity to their target mRNAs. They are usually between 35 and 150 nucleotides long and contain multiple stem-loop structures that are important for metabolic stability and target recognition. Antisense RNAs function as posttranscriptional regulators of target gene expression by either activating or repressing translation of their target mRNAs or destabilising the message. The majority of antisense RNAs repress translation by binding to the 5' untranslated region of target mRNA, around the Shine-Dalgarno sequence, and physically blocking ribosome binding and subsequent translation of the mRNA into protein (Brantl, 2002).

1.3.1.1   PLASMID-ENCODED ANTISENSE RNA SYSTEMS

Many antisense RNA-regulated systems have been identified in plasmids, transposons and bacteriophages. In most cases, the antisense RNA is transcribed from a promoter located on the opposite strand of the same DNA molecule and is therefore fully complementary to the target mRNA. However, some antisense RNAs are encoded in a different location from the target mRNA (i.e. *trans*-encoded). *Trans*-encoded antisense RNAs have only partial complementarity to their targets and often have multiple mRNA targets. Antisense RNAs are involved in control of plasmid replication, conjugation and maintenance (Wagner and Simons, 1994). Several of the most well characterised examples are described below.

1.3.1.1.1   REPLICATION CONTROL OF PLASMID COLE1: ANTISENSE RNA REGULATES PRIMER RNA CONFORMATION

ColE1 is a small multicopy plasmid whose replication is initiated by transcription of the primer RNA II. RNA I is a 108 nucleotide antisense RNA which is expressed from the same region and is complementary to the 5' end of RNA II. Binding of RNA I to RNA II triggers a conformational change in RNA II that prevents it binding to the ColE1 plasmid and initiating plasmid replication. A plasmid-encoded protein, Rom, binds to and stabilizes the RNA I-RNA II complex, enhancing antisense RNA control (Tomizawa, 1984; Tomizawa, 1986; Tomizawa et al., 1981). The antisense RNA, RNA I, is rapidly synthesised and extremely unstable, therefore its concentration is proportional to the plasmid copy number. Consequently, if ColE1 copy number decreases the concentration of RNA I is reduced and plasmid replication proceeds. By contrast, if ColE1 copy number increases the concentration of RNA I also increased and plasmid replication ceases. Therefore, antisense RNA control of replication determines plasmid copy number (Tomizawa and Itoh, 1981). Antisense RNA control of plasmid replication also determines plasmid compatibility properties. Two distinguishable ColE1-type plasmids that have identical replication control will not stably co-exist in the same cell. This is because the control system cannot differentiate between the plasmid types, and since replication and segregation are random, the ratio of plasmid types will vary between cells and eventually result in the loss of one of the plasmid types (Wagner and Simons, 1994).

1.3.1.1.2   REPLICATION CONTROL OF PLASMID R1: ANTISENSE RNA INHIBITS TRANSLATION OF AN INITIATOR PROTEIN

Plasmid R1 is a low copy number self-transmissible plasmid, whose replication is dependent on the initiator protein RepA. Expression of the *repA* gene is subject to

posttranscriptional control by a 90 nucleotide antisense RNA called *copA*, which basepairs with the 5' region of *repA* mRNA and indirectly inhibits its translation into protein (Riise et al., 1982; Stougaard et al., 1981). The region on *repA* mRNA to which *copA* binds is known as CopT (for cop target). Immediately downstream of the CopT site there is a short open reading frame that encodes a translational activator polypeptide (*tap*) for RepA, and its translation is inhibited by *copA*-CopT binding. Translation of *tap* is coupled to translation of *repA,* and therefore in the presence of *copA* antisense RNA RepA translation is suppressed. As with ColE1 type plasmids, the antisense RNA regulator is rapidly synthesised and extremely unstable therefore it efficiently regulates plasmid copy number and determines plasmid compatibility properties.

1.3.1.1.3   MAINTENANCE OF PLASMID R1: ANTISENSE RNA INHIBITS EXPRESSION OF A HOST-KILLER GENE

Many bacterial plasmids employ host-killing systems to ensure that if plasmid-free cells arise they do not persist within a population (Summers, 1996). The *hok/sok* system of plasmid R1 is an example. Three genes are involved, namely *hok* (host killing), *mok* (modulator of killer) and *sok* (suppressor of killer). The 'host-killing' protein encoded by *hok* is a 50 amino acid membrane-associated polypeptide. Expression of this protein leads to loss of cell membrane potential, arrest of respiration, changes in cell morphology and ultimately cell death. Sok encodes a relatively unstable, *trans*-acting 67 nucleotide antisense RNA which protects plasmid-harbouring cells by indirectly blocking translation of *hok* mRNA. Translation of *mok* mRNA is required for *hok* mRNA translation. The system functions by *sok* antisense RNA basepairing with the ribosome-binding region of *mok* mRNA, which inhibits translation of *mok* and therefore indirectly blocks translation of *hok*. Hok mRNA is unusually stable, therefore if a plasmid-free cell arises the unstable *sok* antisense RNA degrades and allows the stable *hok* mRNA to be translated into a host killing protein which results in death of the plasmid-free cell (Gerdes et al., 1986b; Gerdes et al., 1986a).

1.3.1.2   CHROMOSOMALLY-ENCODED ANTISENSE RNA SYSTEMS IN *E. COLI*

Only a small number of antisense RNAs have been identified in bacterial chromosomes and in contrast to most plasmid-encoded antisense RNAs, the majority of chromosomal antisense RNAs are *trans*-encoded i.e. at genetic loci other than their target genes. Generally, *trans*-encoded antisense RNAs have only partial complementarity to their target mRNA, and they often have multiple targets (Altuvia and Wagner, 2000; Brantl, 2002). In *E. coli*, over 50 genes have been identified that encode small untranslated RNAs (sRNA), however most of these are uncharacterised and therefore their cellular roles are unknown (Hershberg et al., 2003). The number is set to increase further as

many of the genes that have been predicted by computational methods to encode sRNAs are waiting for experimental testing. Many of these newly identified sRNAs could potentially function as antisense RNAs.

At present there are five identified sRNAs (*micF, oxyS, dsrA, spf and ryhB*) that are known to act as antisense regulators in *E. coli* (Altuvia et al., 1997; Lease et al., 1998; Masse and Gottesman, 2002; Mizuno et al., 1983; Moller et al., 2002b). They function by basepairing with their target mRNAs to activate or repress translation, or to destabilise the message. Many of the chromosomally encoded antisense RNAs are expressed in response to stress conditions in *E. coli*. They function by activating or repressing the translation of a global response regulator, which in turn controls the expression of a multitude of specific genes to protect the cell from stress, such as increased or reduced temperature, oxidative stress or exposure to toxic agents (Brescia et al., 2004). Several examples of the antisense RNA systems encoded by the *E. coli* genome are described below.

1.3.1.2.1 REGULATION OF OUTER MEMBRANE PORIN EXPRESSION BY *micF* ANTISENSE RNA

The first chromosomally-encoded antisense RNA to be identified in *E. coli* was the 93 nucleotide *micF* antisense RNA (Mizuno et al., 1983; Mizuno et al., 1984). It regulates the expression of outer membrane protein F (OmpF) in response to stress conditions such as elevated temperature, high osmolarity and redox stress by basepairing with the *ompF* mRNA, inhibiting translational of the OmpF protein and inducing degradation of the message. Regulation of *ompF* gene expression is important for *E. coli* because the ability to control permeability of molecules through the outer membrane is a major factor in survival of the cell under conditions of environmental stress (Delihas and Forst, 2001). The *micF* gene is also present in *Salmonella typhimurium, Klebsiella pneumonia* and *Pseudomonas aeruginosa,* which are Gram-negative bacteria that are related to *E. coli* (Esterling and Delihas, 1994).

1.3.1.2.2 REGULATION OF THE TRANSCRIPTIONAL ACTIVATOR FHLA AND THE STATIONARY PHASE SIGMA FACTOR σ^s BY *oxyS* ANTISENSE RNA

The 109 nucleotide *oxyS* antisense RNA is induced in response to oxidative stress in *E. coli* and functions to protect the cell against DNA damage (Altuvia et al., 1997). It regulates expression of the *fhlA* gene, which encodes a transcriptional activator, by basepairing with *fhlA* mRNA and repressing translation (Altuvia et al., 1998; Argaman and Altuvia, 2000) . In addition, *oxyS* suppresses expression of the stationary phase sigma factor σ^s encoded by *rpoS*, by basepairing with *rpoS* mRNA and inhibiting

translation (Zhang et al., 1998).

1.3.1.2.3 Regulation of the Stationary Phase Sigma Factor σ^s by DSRA Antisense RNA

In contrast to oxyS, basepairing of the 85 nucleotide dsrA antisense RNA with rpoS mRNA, leads to increased translation of the stationary phase sigma factor σ^s (Lease et al., 1998; Majdalani et al., 1998). dsrA antisense RNA promotes translation by binding to the 5' end of rpoS mRNA and preventing the formation of an inhibitory secondary structure with normally blocks the ribosome binding site. dsrA antisense RNA also regulates expression of the hns gene, which encodes a nucleoid-associated protein that mediates transcriptional silencing of multiple genes in E. coli. Consequently, dsrA indirectly regulates the transcription of many genes by overcoming H-NS-mediated transcriptional silencing. Hence, dsrA antisense RNA is a riboregulator that can either activate or repress translation.

1.3.1.2.4 Regulation of the Galactose Operon by SPF Antisense RNA

The spf gene encodes a 109 nucleotide antisense RNA, which acts to differentially regulate expression from the E. coli galactose operon (Moller et al., 2002b). It specifically binds to the galK mRNA in the region of the ribosome binding site and blocks translation of the message. The physiological significance of differential expression of the gal operon genes is unclear. However, the GalE, T and K enzymes form part of a pathway that produces substrates for biosynthesis of lipopolysaccharides. When E. coli derives its energy from galactose all three of the enzymes are required, but when the cell derives its energy from other carbon sources, a relatively high level of GalE is required to produce UDP-galactose for biosynthetic glycosylations. Therefore, spf antisense RNA may be important for optimal utilisation of carbon sources in E. coli (Moller et al., 2002b).

1.3.1.2.5 Accessory Proteins Involved in E. COLI Antisense RNA-Regulated Systems

Basepairing between the antisense RNA and target mRNA is known to occur at recognition sites in stem-loop RNA structures. Additional accessory proteins are involved in many cases and function to modulate the stability of RNA-RNA duplexes. The protein Hfq is required in the majority of chromosomally-encoded antisense RNA systems in E. coli that have been characterised so far (Brescia et al., 2003; Moller et al., 2002a; Sledjeski et al., 2001; Storz et al., 2004; Zhang et al., 2002). Exactly how the Hfq protein functions is not well understood, but it has been suggested that it may act as a RNA chaperone to increase RNA unfolding and therefore ensure that the antisense RNA and/or target mRNA are in the correct conformation for binding. Alternatively it may bring

together the antisense RNA and target mRNA by binding simultaneously to both molecules (Storz et al., 2004). A common feature of chromosomally-encoded antisense RNAs in *E. coli* is their susceptibility to digestion by RNase E (Schmidt and Delihas, 1995). However, Hfq binding sites and sites of RNase E cleavage share sequence similarity. therefore it is thought that Hfq protects antisense RNA from digestion by RNase E by blocking the cleavage site (Zhang et al., 2003). Furthermore it has been suggested that when Hfq-dependent antisense RNAs binds to their target mRNA, the Hfq protein is displaced, allowing access by RNase E and subsequent degradation of the RNA-RNA duplex (Masse et al., 2003). In addition, the DNA binding protein H-NS is thought to bind to and alter the stability of some antisense RNA-mRNA duplexes. Recent research has shown that it specifically binds to the antisense RNA *dsrA* and its target *rpoS* mRNA, and appears to enhance their degradation (Brescia et al., 2004).

1.3.2   USE OF ARTIFICIALLY-DESIGNED ANTISENSE RNA AS A RESEARCH TOOL TO DOWN-REGULATE THE EXPRESSION OF TARGET GENES

In recent years, functional synthetic RNA molecules have been used as experimental tools for proteomic and genomic research. The range of RNA tools includes small interfering RNAs (siRNAs); aptamers (protein-binding RNA motifs); ribozymes, maxizymes and aptazymes (catalytic RNAs); and antisense RNA (Famulok and Verma, 2002). These molecules allow modulation of gene function at the mRNA or protein level and are effective and highly specific tools for elucidating the biological function of individual genes, and identifying essential genes for the growth of an organism (De Backer et al., 2001; van den Berg et al., 1991). In addition to applications in functional genomics and proteomics, genetic knockdown technologies such as RNA interference (RNAi) and antisense RNA have been used in medical research to identify drug targets and to develop therapeutics (Shuey et al., 2002; Thompson, 2002).

Artificially designed antisense RNAs can be used as specific inhibitors of gene expression, without directly manipulating the gene of interest. One of the first studies to employ artificial antisense RNA for gene-specific silencing was published in 1984 (Coleman *et al.*, 1984). Having studied the naturally-occurring *micF* antisense RNA, a 174 nucleotide untranslated RNA that inhibits expression of the OmpF protein in *E. coli* (Mizuno et al., 1983; Mizuno et al., 1984), this group decided to develop an artificial 'mic' (mRNA-interfering complementary RNA) system. A plasmid was constructed to express antisense RNA targeted against the *lpp* gene in *E. coli*, which encodes the major outer membrane lipoprotein. Results showed that induction of the *lpp* antisense RNA significantly reduced the amount of *lpp* mRNA and efficiently blocked lipoprotein

production.

1.3.2.1   DESIGN OF ANTISENSE RNA OLIGONUCLEOTIDES

Antisense RNA oligonucleotides are usually designed to bind to the 5' region of the target mRNA, encompassing the ribosome-binding site and the translation initiation site. This strategy mirrors many naturally occurring antisense RNAs and aims to suppress translation of the target mRNA (Mirochnitchenko and Inouye, 2000). Several studies have confirmed that basepairing of the antisense RNA and target mRNA at the ribosome binding site is essential/optimal for effectiveness of antisense RNA-mediated gene silencing (Coleman et al., 1984; Stefan et al., 2003). There are two main mechanisms for artificial antisense RNA production. The first is to chemically synthesise the oligonucleotides *in vitro* and then introduce them into the cell. The second is to construct an expression system to produce antisense RNA *in vivo*, which can be achieved by cloning a fragment of the target gene into a plasmid vector in an antisense orientation, under the control of a promoter. Use of an inducible promoter allows conditional expression of antisense RNA during fermentation.

Although antisense RNA technology appears straightforward, its success is rather unpredictable and can vary widely depending on both the sense and antisense sequences involved. To address this problem several studies have aimed to develop methods for the rational design of antisense RNA oligonucleotides (Nellen and Sczakiel, 1996). The accessibility of an RNA strand, which is determined by its structure, and the extent of intramolecular interactions are likely to be important for efficient base pairing with a complimentary RNA strand, therefore attempts have been made to correlate these parameters with antisense RNA effectiveness. One study conducted in *Clostridium acetobutylicum* found that antisense RNA effectiveness increased as the extent of intramolecular binding increased, and concluded that this is likely to be due to greater metabolic stability and less RNase degradation (Tummala et al., 2003). Another study found that introducing a stem-loop stability element, at the 5' end of an antisense RNA resulted in greater suppression of target gene expression (Engdahl et al., 2001). Therefore, it seems likely that stability of the antisense RNA oligonucleotide is a key factor in determining its effectiveness in suppressing target gene expression.

1.3.2.2   USE OF ANTISENSE RNA FOR METABOLIC ENGINEERING RESEARCH

Antisense RNA has a number of potential advantages over gene inactivation for metabolic engineering purposes. It is relatively quick to implement compared to the time

taken for gene knockouts and antisense RNA can avoid the pitfalls of lethal mutations, as complete gene silencing is not likely. Furthermore, by using an inducible promoter for conditional expression *in vivo,* antisense RNA can be used to study metabolism before and after gene downregulation. In addition, antisense RNA may be used to downregulate the products of multiple genes by expressing multiple antisense RNAs from a single plasmid, or from multiple compatible plasmids. Examples of using antisense RNA to suppress the expression of target genes and alter metabolism in *E. coli and Clostridium acetobutylicum* are described below.

1.3.2.2.1 ANTISENSE RNA-MEDIATED DOWNREGULATION OF THE σ^{32}-MEDIATED STRESS RESPONSE IN *E. COLI*

The σ^{32}-mediated stress response in *E. coli* is induced by ethanol or heat shock, and by over-expression of recombinant protein. Accumulation of σ^{32} results in the production of a number of chaperone proteins and proteases, however increased proteolytic activity can reduce the yield of recombinant protein. Therefore, in order to optimise recombinant protein production by *E. coli,* it may be desirable to downregulate the σ^{32}-mediated stress response.

Antisense RNA has been used to downregulate σ^{32} expression in *E. coli,* with the aim of enhancing production of the recombinant protein, organophosphorus hydrolase (Srivastava *et al.,* 2000). A 284-nucleotide antisense RNA was designed to basepair with the 5' region of the σ^{32} mRNA encompassing the ribosome-binding site, and was expressed *in vivo* from a *trc* promoter on a multicopy plasmid. Northern blot analysis revealed that σ^{32} mRNA levels were dramatically reduced in antisense RNA-expressing cultures compared with the control culture, 5-20 minutes after induction of antisense RNA. Downregulation of the σ^{32}-mediated stress response was studied during production of the recombinant protein, organophosphorus hydrolase (OHP). Surprisingly the amount of OHP produced in the presence of σ^{32} antisense RNA was only two thirds of the amount produced in the control culture. However, as both OHP and σ^{32} antisense RNA were expressed from multicopy plasmids, it was suggested that the reduced OHP production might be due to a transcriptional limitation, arising from competition for RNA polymerase. Even though the yield of OHP was reduced, there was a 3-fold increase in biologically active OHP in the presence of σ^{32} antisense RNA. The specific mechanisms for the reduced OHP level and increased OHP activity are not known, as many σ^{32}-regulated proteins in *E. coli* may have contributed to this phenomenon. In summary, this study demonstrates the use of antisense RNA to suppress expression of a global regulatory protein in *E. coli* and enhance specific activity of a recombinant protein product (Srivastava *et al.,* 2000).

1.3.2.2.2   ANTISENSE RNA-MEDIATED DOWNREGULATION OF BUTYRATE PRODUCTION BY *CLOSTRIDIUM ACETOBUTYLICUM*

Clostridium acetobutylicum is a gram-positive, spore-forming, obligate anaerobe that produces acids (acetate and butyrate) and solvents (ethanol, acetone and butanol) by fermenting a variety of sugars. This organism was used was used to produce acetone and butanol up until the 1950s, when the petrochemical process became economically superior. Research in recent years, has focused on optimising solventogenic clostridia for solvent production with the aim of reviving the industrial fermentation process (Desai and Papoutsakis, 1999).

The effectiveness of antisense RNA in redirecting *Clostridium acetobutylicum* central carbon metabolism to optimise solvent production has been investigated (Desai and Papoutsakis, 1999). Specifically, antisense RNA was employed to downregulate expression of the phosphotransbutyrylase gene (*ptb*) and the butyrate kinase gene (*buk*), which are responsible for butyrate formation in *Clostridium acetobutylicum*. Butyrate levels are thought to influence solvent production by *Clostridium acetobutylicum*, therefore downregulation of Ptb and Buk was expected to have a significant impact on primary metabolism. Two plasmids constructs were developed to express antisense RNA targeted against either the *buk* gene or the *ptb* gene. Both antisense RNA oligonucleotides were designed to basepair with the 5' end of the target mRNA, in the region of the ribosome binding site. The impact of putative *buk* antisense RNA and putative *ptb* antisense RNA on enzyme levels and product formation in *Clostridium acetobutylicum* was evaluated. In addition, fermentation data was used for metabolic flux analysis to examine the effect of reduced levels of acid formation enzymes on the central carbon fluxes.

The research has many analogies with this thesis, including the experimental approach taken and the target pathway for downregulation by antisense RNA. The pathway for butyrate formation in *Clostridium acetobutylicum* is comprised of two reactions, which are similar to the two steps in the acetate production pathway of *E. coli*. In the first step butyryl CoA is converted to butyryl phosphate by phosphotransbutyrylase (Ptb), and in the second step, butyryl phosphate is converted to butyrate by butyrate kinase. The genes *ptb* and *buk* form an operon, however they are organised in the order *ptb-buk*, whereas the analogous genes for acetate production in *E. coli* are organised in the reverse order, *ackA-pta*, in an operon (described in more detail in section 4.2.3).

Cultures of *Clostridium acetobutylicum* expressing putative *buk* antisense RNA exhibited

significantly lower peak levels of Ptb and Buk compared to the control strain. Cultures expressing putative *ptb* antisense RNA also exhibited lower levels of Ptb and Buk compared to the control, and higher peak levels of the enzyme lactate dehydrogenase, which converts pyruvate to lactate. As the enzymes *ptb* and *buk* are cotranscribed, it was expected that expression of antisense RNA targeting one of the genes might reduce expression of both. However, increased lactate dehydrogenase activity in the putative *ptb*-expressing culture was an unexpected result.

Analysis of the product formation profiles of both antisense RNA-expressing cultures revealed that even though Ptb and Buk levels were significantly lower compared to the control culture, butyrate production was not reduced. In fact, the peak butyrate concentration of the *buk*-antisense RNA expressing culture was ~35% higher than in the control culture. These results imply that flux through the butyrate formation pathway is not tightly controlled by enzyme levels (Desai and Papoutsakis, 1999). Although butyrate production was not reduced in the antisense RNA-expressing cultures, the pattern of solvent production was altered in both strains. In cultures expressing putative *buk* antisense RNA, acetone and butanol were detected earlier and accumulated to higher final concentrations than in the control culture. In contrast, cultures expressing putative *ptb* antisense RNA, exhibited much lower solvent production than the control culture, which was compensated for by a ~100-fold increase in lactate production. The increased lactate production was assumed to be due to probable elevated levels of the lactate precursors, pyruvate and NADH. This research demonstrates that antisense RNA can be used to downregulate specific protein production and manipulate the primary metabolism of *Clostridium acetobutylicum*, but often with unexpected outcomes.

Subsequently, metabolic flux analysis was used to compare the impact of *buk* gene inactivation and antisense RNA-mediated *buk* downregulation on the central carbon flux distribution in *Clostridium acetobutylicum* (Desai et al., 1999). Results revealed that both strategies led to increased flux to butanol and acetone production. The patterns indicated by flux analysis suggested the possibility of butyryl-phosphate as an inducer of solventogenesis.

1.3.2.2.3 ANTISENSE RNA-MEDIATED DOWNREGULATION OF ACETATE PRODUCTION BY *E. COLI*

At the beginning of this research thesis (in 2001), use of antisense RNA to downregulate enzymes of the acetate production pathway in *E. coli* had not been investigated. However, a recent publication (Kim and Cha, 2003) describes antisense RNA-mediated downregulation of the acetate production pathway, with the specific goal of enhancing recombinant protein production by *E. coli*. Three plasmid constructs were developed to

41

express antisense RNA targeted against the *pta* gene, the *ackA* gene, or both genes simultaneously. The plasmids were introduced into *E. coli* BL21, a low acetate producer, and the effect of antisense RNA expression on acetate production and GFP (green fluorescent protein) production was evaluated.

All shake flask *E. coli* cultures expressing antisense RNA exhibited higher growth rates and final cell densities, and accumulated higher acetate levels than the control strain. However, even though the excreted acetate was not reduced, the antisense RNA-expressing cultures exhibited a 10-20% reduction in *ackA* mRNA and *pta* mRNA in the respective antisense RNA-expressing strains. In addition, Ack and Pta enzyme activity analysis confirmed a 15-25% reduction in enzyme levels. In contrast, shake flask *E. coli* cultures co-expressing GFP and *ackA/pta/ackA-pta* antisense RNA exhibited reduced levels of acetate accumulation compared to the control culture. The dual antisense RNA-expressing culture had the lowest level of acetate accumulation. Furthermore, the antisense RNA-expressing cultures exhibited higher levels of GFP production compared to the control culture. *ackA* antisense RNA-expressing cultures showed a 1.6-fold increase in GFP production compared to the control culture.

To investigate the effect of culture scale-up on antisense RNA regulation of the acetate pathway, *E. coli* producing GFP and expressing *ackA* antisense RNA was cultivated in a 3 L stirred-tank bioreactor. The growth rate was reduced by about 20% compared to the control culture producing GFP. In addition, the pattern of acetate accumulation was altered by expression of *ackA* antisense RNA. The control culture accumulated acetate rapidly through growth phase, with a peak concentration of 3.36 mM, and then reconsumed it during early stationary phase, even though residual glucose levels were high. In contrast, the *ackA* antisense RNA-expressing culture showed a slower but steady increase in acetate accumulation until the end of the culture, with a final concentration of 2.69 mM. No acetate reconsumption was evident, which may be due to interference from *ackA* antisense RNA expression. GFP production was increased about 2-fold in the antisense RNA-regulated culture, compared to the control. These results suggest that even a small decrease in target gene expression using antisense RNA can have a big impact on cellular metabolism and in particular recombinant protein expression.

The key differences between the above study and this research thesis are:

- **_E. coli_ strains:** _E. coli_ B (BL21) used in the study of Kim and Cha (2003) is a low acetate producer. In contrast, _E. coli_ K-12 (MG1655) used in this research thesis is a high acetate producer (van de Walle and Shiloach, 1998). The strain-specific differences in acetate production between _E. coli_ B and K derivatives have been attributed to differences in the expression levels of key metabolic genes involved in acetate production and consumption (Phue and Shiloach, 2004). Therefore, it is interesting to study the effect of _ackA_ and _pta_ antisense RNA expression in a high acetate producing _E. coli_ strain.

- **Promoters for antisense RNA expression:** Kim and Cha (2003) used the relatively weak _ackA_ constitutive promoter for expression of antisense RNA oligonucleotides. The research described in this thesis uses the strong _trc_ and _tac_ promoters for conditional expression of _ackA_ and _pta_ antisense RNA.

- **Enzyme analysis:** Kim and Cha (2003) analysed Pta and AckA enzyme activity levels at mid-log phase during fermentation. This study evaluates Pta and AckA enzyme activity levels periodically over a 24 h time course, allowing a more detailed analysis of the effect of antisense RNA on target protein expression.

- **Organic acid analysis:** Kim and Cha (2003) focused on analysing acetate production. However, in order to determine the effectiveness of antisense RNA in redirecting central carbon metabolism, this study monitored the concentration of a range of organic acids in the culture medium, including pyruvate, lactate, succinate and acetate.

- **Metabolic flux analysis:** this is the first study to use metabolic flux analysis to examine the effect of antisense targeted against _ackA_ and _pta_ on the central carbon flux distribution in _E. coli_.

1.4 SPECIFIC AIMS OF PHD THESIS

The overall goal of this research thesis is to determine the effectiveness of antisense RNA in suppressing the expression of target enzymes and redirecting the central carbon metabolism of *E. coli*. Specifically, it was attempted to downregulate the expression of phosphotransacetylase and acetate kinase, which form the primary acetate production pathway in *E. coli,* and use a combination of physiological characterisation and metabolic flux analysis to examine the effect of *pta* and *ackA* antisense RNA on central carbon metabolism.

During the course of this research, three plasmid constructs were developed to produce antisense RNA targeted against either *ackA* mRNA or *pta* mRNA. Two *ackA* antisense RNA constructs were generated: one was developed from the expression vector pTrc99A, which was also used to generate the *pta* antisense construct, and one was developed from the expression vector pMMB66EH, which is compatible with pTrc99A and therefore facilitates co-expression of *ackA* and *pta* antisense RNA. Plasmid constructs were introduced into *E. coli* MG1655 for antisense RNA expression studies.

The effectiveness of putative *pta* and *ackA* antisense RNA in suppressing expression of phosphotransacetylase and acetate kinase was evaluated by monitoring the enzyme activity levels, and the effect on organic acid production by *E. coli* was examined by monitoring the concentration of acetate and other organic acids present in the culture medium. In addition, fermentation data was used for metabolic flux analysis, which predicts the intracellular flux distribution, and therefore gives a more detailed insight into the effect of antisense RNA on *E. coli* metabolism.

This thesis discusses the research that was carried out to achieve the overall goal, and is presented in chapters, which are described below.

- **Chapter 2** describes the materials and methods used during the course of the research, which included molecular biology techniques for DNA recombination, batch fermentation and HPLC.
- **Chapter 3** discusses the initial shake-flask studies performed with *E. coli* MG1655 to optimise the growth conditions and experimental procedures for physiological characterisation.
- **Chapter 4** discusses the construction of a series of plasmids to express antisense RNA targeted against *E. coli* MG1655 phosphotransacetylase and acetate kinase.
- **Chapter 5** discusses the shake flask and bioreactor experiments that were

performed in order to determine the effect of putative *pta* and *ackA* antisense RNA on growth, enzyme levels, and organic acid production by *E. coli* MG1655.

- **Chapter 6** discusses the results of metabolic flux analysis, which was used to examine the impact of putative *pta* and *ackA* antisense RNA on carbon flow through *E. coli* central metabolism.

- **Chapter 7** summarises the work as a whole, draws conclusions and suggests future work to explore further the results presented in this thesis.

Antisense RNA is a flexible and still relatively novel tool for metabolic engineering. Consequently, if it can be successfully applied in this research to suppress expression of target enzymes and redirect *E. coli* central carbon metabolism, then it might encourage further use of antisense RNA for partial gene inactivation in advanced metabolic engineering strategies.

CHAPTER 2

MATERIALS AND METHODS

2.1   MATERIALS

Chemicals, media components and enzymes were supplied by Sigma-Aldrich (www.sigma-aldrich.com), Oxoid (www.oxoid.co.uk), Invitrogen (www.invitrogen.com), Qiagen (www.qiagen.com), and New England Biolabs (www.neb.com). Double distilled water (equivalent of) was produced using an Elga Option 4 water purifier (www.elga.co.uk). Media and buffers were sterilized by autoclaving for 20 min at 121°C, or filtering through a 0.2 μm sterile syringe filter (www.millipore.com).

2.2   BACTERIAL STRAINS AND PLASMIDS

The bacterial strains and plasmids used in this study are listed in Table 2.1.

2.2.1   *E. COLI* STRAINS

E. coli MG1655 is a K12 strain and was selected for antisense RNA expression studies due to the availability of it's complete genome sequence (Blattner et al., 1997).

E. coli TOP10, supplied by Invitrogen, was used as a cloning host for pCR2.1-TOPO-derived plasmids.

E. coli DH5*a* was used as a routine cloning host (Woodcock et al., 1989).

2.2.2   PLASMIDS

pTrc99A and pMMB66EH were used to develop antisense RNA expressing-plasmids. pTrc99A (Amann et al., 1988) is a 4.2 kb plasmid which carries the pBR322 origin of replication. It provides high-level expression via a strong *trc* promoter upstream of the multiple cloning site, *rrnB* terminator downstream of the multiple cloning site, and *lacI*^{q} for *lacI*^{q} mediated repression. A plasmid encoded β-lactamase confers resistance to ampicillin.

pMMB66EH is an 8.8 kb plasmid containing the RSF1010 replicon. This plasmid is a member of the IncQ incompatibility group, characterised by small size, low copy number and a broad host range among gram-negative bacteria (Morales et al., 1990). It possesses the strong *tac* promoter upstream of the multiple cloning site, *rrnB* terminator downstream of the multiple cloning site, and *lacI*^{q} for *lacI*^{q} mediated repression. A plasmid encoded β-lactamase confers resistance to ampicillin.

The *tac* promoter is a hybrid of the *trp* and *lac* UV5 promoters and was originally constructed in the early 1980's (de Boer H.A. *et al.*, 1983). Transcription from the promoter is induced by addition of 1mM IPTG. The *trc* promoter is derived from the *tac* promoter by the addition of 1 bp between the -35 and -10 consensus sequences, making the distance 17 bp. It was anticipated that this alteration would generate a stronger promoter, however the resulting *trc* promoter has only 90% activity of the original *tac* promoter (Brosius J. *et al.*, 1985).

Contrasting replication mechanisms in pTrc99A and pMMB66EH facilitate co-existence in *E. coli*, allowing construction of a dual antisense RNA-expressing strain. pCR2.1-TOPO (Invitrogen) was used for direct capture of *Taq* polymerase-amplified PCR products. pUC4K was used as a template for PCR-amplification of an aminoglycoside 3'-phosphotransferase (*kan*), which confers resistance to kanamycin. Plasmids pQR438-pQR446 were constructed during this study and are described in chapters 4-6.

Table 2.1   Bacterial strains and plasmids

Bacterial strain or plasmid	Relevant characteristic(s)[a]	Reference/Source
Strain		
E. coli MG1655	*F-, λ-, ilvG-, rfb-50, rph-1.*	(Blattner *et al.*, 1997)
E. coli DH5α	*F-, λ -, thi-1, supE44, hsdR17, recA1, gyrA96, endA1, relA1, deoR, Δ(lacIZYA - argF)*	(Woodcock *et al.*, 1989)
E. coli TOP 10		Invitrogen
Plasmid		
pTrc99A	Amp^r; *trc* promoter; *lac* I^q; pBR322 ori	(Amann *et al.*, 1988)
pMMB66EH	Amp^r; *tac* promoter; *lac* I^q; RSF1010 ori	(Furste *et al.*, 1986)
pUC4K	Amp^r, Kan^r; pBR322 ori	(Taylor and Rose, 1988)
pCR2.1-TOPO	Amp^r, Kan^r, pUC ori	Invitrogen
pQR438	Amp^r, Kan^r; pUC ori, antisense *pta*	This study
pQR439	Amp^r; *trc* promoter; *lac* I^q; pBR322 ori; antisense *pta*	This study
pQR440	Amp^r, Kan^r; pUC ori, antisense *ackA*	This study
pQR441	Amp^r; *trc* promoter; *lac* I^q; pBR322 ori; antisense *ackA*	This study
pQR444	Amp^r, Kan^r; pUC ori, *kan*	This study
pQR445	Kan^r; *tac* promoter; *lac* I^q; RSF1010 ori	This study
pQR446	Kan^r; *tac* promoter; *lac* I^q; RSF1010 ori; antisense *ackA*	This study

[a] Plasmid components are described in Chapter 4, Table 4.1.

2.3 MOLECULAR BIOLOGY

2.3.1 PREPARATION OF BUFFERS AND SOLUTIONS

(i)   Ethidium Bromide

A stock solution of 10 mg ml^{-1} was prepared and stored in a foil-covered bottle at room temperature.

(ii)   Gel loading buffer

A 6X stock solution was prepared containing 1 mg ml^{-1} bromophenol blue, 40%(v/v) sucrose and 0.1 M Na$_2$EDTA, and stored at room temperature.

(iii)   Lysozyme

A stock solution was prepared containing 10 mg ml^{-1} lysozyme in sterile TE buffer, and stored at -20 °C.

(iv)   Pronase

A stock solution was prepared containing 10 mg ml^{-1} Pronase in sterile TE buffer, incubated at 37 °C for 2 h to destroy any endogenous DNAases, and stored at -20°C.

(v)   RNAase A

A stock solution was prepared containing 10 mg ml^{-1} ribonuclease A in sterile TE buffer, boiled for 15 min to remove any trace DNAase activity, and stored at -20 °C.

(vi)   TBE buffer

A 10X stock was prepared by dissolving 54 g Trizma Base, 27.5 g Boric acid and 3.75 g Na$_2$EDTA in a final volume of 1 L. The solution was stored at room temperature.

(vii)   TE buffer

A solution containing 10 mM Tris-HCl (pH 7.5) and 1mM Na$_2$EDTA was prepared, and stored at room temperature.

(viii)   X-Gal

A stock solution of 40 mg ml^{-1} X-Gal in dimethylformamide was prepared, and stored in a foil-covered bottle at -20°C.

2.3.2 DNA PREPARATION

2.3.2.1 PREPARATION OF CHROMOSOMAL DNA

Chromosomal DNA was isolated from cultures of *E. coli* MG1655, grown overnight in 50 ml nutrient broth, as follows. Bacterial cells were harvested by centrifugation (9,000 rpm, 10 min), before being resuspended in 5 ml TE buffer. Lysozyme was then added to a final concentration of 50 µg ml^{-1}, and the solution incubated at 37°C for 15 min. Lysis was induced by the addition of SDS to a final concentration of 1%, followed by gentle mixing by inversion 4-6 times. Pronase and RNAase were added to final concentrations of 50 µg ml^{-1} and 20 µg ml^{-1} respectively, the solution was mixed as before, and incubated at 37°C for 2 h. Following incubation, 0.5 ml of 5 M NaCl was added, mixed by inversion, and 10 ml ethanol pipetted on to the surface of the lysate. A sterile glass rod was used to spool the DNA precipitate that collected at the interface. The DNA was then transferred to a sterile container and left to dissolve in 10 ml TE buffer. At this point, the DNA solution was frozen at -20°C.

Upon thawing, the DNA solution was gently mixed to, before testing for purity via agarose gel electrophoresis.

2.3.2.2 PREPARATION OF PLASMID DNA

Plasmid DNA was isolated from small-scale cultures of *E. coli* grown overnight in 5 ml selective nutrient broth using Miniprep preparative kits (Qiagen), according to manufacturer's instructions. Plasmid DNA was eluted into 50 µl buffer EB (10 mM Tris-HCl, pH 8.5), and stored at -20°C.

Plasmid DNA was isolated from larger scale cultures grown overnight in 50 ml selective nutrient broth using Midiprep preparative kits (Qiagen), according to manufacturer's instructions. Plasmid DNA was eluted 1 ml TE buffer (10 mM Tris-HCl (pH 7.5), 1mM Na$_2$EDTA), and stored at -20°C.

2.3.3 ENZYMATIC MANIPULATIONS

2.3.3.1 RESTRICTION DIGESTS

Digestion of plasmid DNA with restriction enzymes was performed using enzymes and buffers supplied by New England Biolabs. When using the enzymes *Bam*HI and *Pvu*I, BSA was added to a final concentration of 100 µg ml^{-1}. Typically 10 µl plasmid DNA

(prepared as above) was digested in a total volume of 20 µl, comprising 1 µl restriction enzyme, 2 µl 10X restriction buffer, and 7 µl TE buffer. The solution was incubated at 37°C for 2 h. Digested DNA was analysed by agarose gel electrophoresis.

2.3.3.2   LIGATION

DNA fragments were ligated into plasmid vectors using enzymes and buffers supplied by New England Biolabs. A typical reaction was performed in a total volume of 100 µl, comprising 30 µl linearised plasmid, 30 µl DNA insert, 10 µl 10X ligation buffer, 3 µl T4 DNA ligase and 27 µl TE buffer. The reaction was mixed gently and incubated at 16°C overnight. Subsequently, an aliquot of competent *E. coli* was transformed with 20-100 µl ligation mixture (refer to section 2.4.2).

The TOPO TA cloning system (Invitrogen) was used for direct capture of *Taq* polymerase-amplified PCR products. The reaction comprised 1 µl PCR product, 1 µl salt solution, 1µl pCR2.1-TOPO and 3µl sterile water. Ligation was performed by mixing the components gently and incubating at room temperature for 30 min. An aliquot of competent *E. coli* TOP10 (Invitrogen) was transformed with 3 µl of ligation reaction (refer to section 2.4.2).

2.3.4   ELECTROPHORESIS

2.3.4.1   ELECTROPHORESIS OF DNA IN AGAROSE GELS

Agarose gel electrophoresis was performed using 1, 1.5 or 2% (w/v) agarose, in TBE buffer. Gels were prepared by dissolving agarose powder in TBE by boiling, then cooling the molten agarose and adding ethidium bromide to a final concentration of 0.5 µg ml^{-1}, before pouring the gel into a casting tray containing a comb of the required size to form sample wells. Once the gel was set, the comb was removed and the gel was fully submerged in TBE buffer. Electrophoresis was performed at 100 volts for 30 -90 min. When complete, gels were visualised using a short wave UV light transilluminator in conjunction with a UVI Tec CCD digital camera, linked to a PC operating the UVBand software package. Digital images were saved in TIF format.

2.3.4.2   ISOLATION OF DNA FROM AGAROSE GELS

DNA fragments were isolated from agarose gels using a QIAquick Gel Extraction Kit (Qiagen), according to manufacturer's instructions. DNA bands were visualised using a

UV light transilluminator, before being excised from the agarose gel using a clean scalpel and the DNA isolated. DNA was eluted into 30 µl buffer EB (10 mM Tris-HCl, pH 8.5) and stored at -20°C.

2.3.5 POLYMERASE CHAIN REACTION (PCR)

PCR was used to amplify sequences from plasmid DNA and *E. coli* chromosomal DNA. Reactions were performed in a Hybaid Omnigene thermal cycler (www.hybaid.co.uk), with enzymes and buffers supplied by Quiagen. A typical thermal cycle is shown in table 2.2

PCR reactions were performed in a total volume of 50 µl, comprising 1 unit *Taq* polymerase, 10 µl dNTP (0.2 mM), 1 µl forward primer (30 µM), 1 µl reverse primer (30 µM), 5 µl *Taq* polymerase buffer (containing 1.5 mM MgCl), 5 µl Q solution, 26 µl sterile water, and 1 µl template DNA. Primers (synthesised by Qiagen), are detailed in table 2.3, which highlights the restriction sites incorporated to facilitate directional cloning of PCR products.

Table 2.2 PCR Program

Stage	Temperature (°C)	Time (min)	Repetition (cycles)
Denaturation	95	4	1
Denaturation	94	0.5	
Primer Annealing	55 - 63	0.5 – 1.5	30
Elongation	72	0.5	
Elongation	72	20	1

Table 2.3 PCR Primers

Primer Name	Oligonucleotide sequence (5'-3')	Restriction Site Incorporated
ackA f. p.	GCAAGCTTTATCAATTATAGGTACT	*Bam*HI
ackA r. p.	CGCTTAAGTAGTATTAACGATAAAG	*Eco*RI
pta f. p.	GCAAGCTTCGAAAGAGGATAAACCG	*Hind*III
pta r. p.	CGCTTAAGTGGAAGAGTTCGCACGC	*Eco*RI
kan f. p.	GCCGATCGGTCGACCTGCAGGGGGGGGGGGGGCGCTGA	*Pvu*I
kan r. p.	GCCGATCGGCAGGGGGGGGGGGGGGAAGCCACGTTGTGT	*Pvu*I

2.3.6   DNA SEQUENCING

DNA sequencing was performed by the DNA Sequencing Service, Wolfson Institute for Biomedical Research, University College London (www.ucl.ac.uk/WIBR). DNA concentration was analysed by agarose gel electrophoresis, and provided for sequencing at 150-300 ng/µl. Sequencing results were analysed using freeware downloadable from the following websites: pDraw32, http://medlem.spray.se/acaclone; BioEdit, www.mbio.ncsu.edu/BioEdit/bioedit.html.

2.4   *E. COLI* TRANSFORMATION

2.4.1   PREPARATION OF CHEMICALLY COMPETENT *E. COLI*

Chemically competent *coli* MG1655 and DH5α cells were prepared as follows. A freshly streaked nutrient agar plate of the strain to be made competent was used to inoculate 10 ml sterile nutrient broth in a universal bottle, and grown overnight at 37°C. The 10 ml culture was then used to inoculate 200 ml nutrient broth supplemented with 20 mM $MgCl_2$ in a 1 L shake flask, which had been pre-warmed to 37°C. The culture was grown in an orbital shaker (37°C , 200 rpm) until A_{600} of ~0.6 was reached. Subsequently, the culture was chilled on ice before harvesting the cells by centrifugation (9,000 rpm, 5 min, 4°C) in a Sorvall centrifuge. The cell pellet was resuspended in 5 ml ice cold 75 mM calcium chloride, 15% (v/v) glycerol. 500 µl aliquots of competent cell suspension were stored at -80°C ready for use. Transformation efficiency was tested with the high copy number plasmid pUC19 (Yanisch-Perron *et al.*, 1983).

2.4.2   TRANSFORMATION OF COMPETENT *E. COLI* CELLS

Transformation of competent *E. coli* by plasmid DNA was performed as follows. 2 µl plasmid DNA, or up to 50 µl ligation reaction, was added to a 500 µl aliquot of chemically competent *E. coli*, mixed gently and incubated on ice for 45 min. The cells were heat-shocked at 37°C for 5 min, before adding to 5 ml nutrient broth and incubating (37°C, 200 rpm) for 1 h. Transformants were selected by plating 100 µl transformation broth onto nutrient agar plates supplemented with appropriate antibiotics.

Transformation of pCR2.1-TOPO into One-Shot Chemically Competent *E. coli* TOP10 (Invitrogen) was performed according to manufacturer's instructions. Transformants were selected by plating 100 µl transformation broth onto selective nutrient agar plates, coated with 40 µl X-gal (40 mg ml^{-1}) to facilitate blue-white colour screening.

2.5 *E. COLI* CULTURES

2.5.1 MAINTENANCE OF BACTERIAL STRAINS

E. coli strains were maintained as 20% glycerol stocks. Cell stocks were prepared from selective nutrient agar plates by resuspending the colonies in 3 ml 20% glycerol using a sterile glass rod before harvesting the suspension with a sterile pipette. Alternatively, *E. coli* culture in selective nutrient broth was combined with an equal volume of 40% sterile glycerol. Cell suspensions were stored as 1 ml aliquots, at -80°C

2.5.2 MEDIA

E. coli growth media and media supplements are detailed in Table 4. For strain development, *E. coli* cultures were grown in nutrient broth (Oxoid Nutrient Broth No. 2) or on nutrient agar (Oxoid Nutrient agar) at 37°C. Liquid cultures were incubated in an orbital shaker (New Brunswick Scientific). Antisense RNA expression studies were performed with M9 minimal media (refer to Table 2.4) (Miller, 1972). M9 salts were prepared as a 10X stock solution, autoclaved and stored at room temperature. Glucose was prepared as a 10X stock, autoclaved and stored at room temperature. Calcium and magnesium salts were prepared as a 100X stock, autoclaved and stored at room temperature. The trace element solution was prepared as a 4,000X concentrated stock solution, autoclaved and stored at room temperature. Uracil was prepared as a 100X stock solution, filter sterilised and stored at -20°C. Thymidine was prepared as a 1,000X stock solution, filter sterilised and stored at -20°C.

Plasmid-harbouring strains were maintained by supplementing with appropriate antibiotics. Stock solutions of 50 mg ml^{-1} ampicillin (sodium salt) and 50 mg ml^{-1} kanamycin sulphate were prepared, filter sterilised and stored at -20°C. Ampicillin was used at a working concentration of 100 - 500 µg ml^{-1}, according to plasmid copy number. Kanamycin was used at a working concentration of 10 µg ml^{-1}.

Induction of antisense RNA was achieved by addition of Isopropyl β-D-thiogalactopyranoside (IPTG) to a final concentration of 1 mM. A 100 mM stock solution of IPTG was prepared, filter sterilised and stored at 20°C.

Table 2.4   *E. coli* Growth Medium and Media Supplements

Component	Stock Concentration (g L^{-1})	Working Concentration (g L^{-1})
Nutrient Agar (Oxoid)	-	28
Nutrient Broth No. 2 (Oxoid)	-	25
M9 salts		
$Na_2PO_4.12H_2O$	152	15.2
KH_2PO_4	30	3
NaCl	5	0.5
NH_4Cl	10	1
Calcium/Magnesium salts		
$CaCl_2$	1.47	0.0147
$MgSO_4.7H_2O$	24.6	0.246
Glucose	100	10
Trace element solution		
$FeCl_3.6H_2O$	2.7	6.75×10^{-4}
$ZnCl_2.4H_2O$	0.2	5×10^{-5}
$CoCl.6H_2O$	0.2	5×10^{-5}
$NaMoO_4.2H_2O$	0.2	5×10^{-5}
$CaCl_2.2H_2O$	0.1	2.5×10^{-5}
$CuCl_2.6H_2O$	0.13	3.25×10^{-5}
H_3BO_3	0.05	1.25×10^{-5}
Conc. HCl		2.5×10-^{3}
Strain-specific supplements		
Uracil	2	0.02
Thymidine	5	0.005
Antibiotics		
Ampicillin	50	0.1 – 0.5
Kanamycin	50	0.01
Inducer		
IPTG	100 mM	1 mM

2.5.3 SHAKE-FLASK EXPERIMENTS

2.5.3.1 SHAKE-FLASK CULTURES

Shake-flask cultures were prepared from a single colony on a fresh, selective nutrient agar plate. Biomass from the colony was used to inoculate 25 ml glucose minimal media (refer to section 2.5.2) in a 100 ml flask and grown overnight in an orbital shaker (37°C, 200 rpm). The pre-culture was transferred to 225 ml fresh glucose minimal media in a 2 L baffled flask and incubated in an orbital shaker (37°C, 200 rpm), for 24 h.

2.5.3.2 SAMPLING PROCEDURE, ANTISENSE RNA EXPRESSION AND ANALYSIS OF PLASMID STABILITY

5 ml samples were taken from shake flask cultures at 1 h intervals and placed on ice prior to analysis. Duplicate A_{600} readings of culture broth were performed immediately. The remaining broth was pipetted into 3 x 1 ml aliquots and microfuged (5 min, 14,000 rpm). Supernatant was transferred into clean eppendorf tubes and stored at -20°C for subsequent analysis of residual glucose and organic acid concentrations. Cell pellets were stored at -80°C for enzyme activity analysis.

Expression of antisense RNA was induced in early/mid exponential growth phase (A_{600} 1.0 – 1.5) by addition of IPTG to a final concentration of 1 mM.

Plasmid stability was evaluated after 24 h growth by preparing two-fold serial dilutions of culture broth in saline, and plating 100 µl on selective and non-selective nutrient agar. Following overnight growth at 37°C, cell counts from selective and non-selective plates were determined.

2.5.4 BATCH FERMENTATION

2.5.4.1 FERMENTATION EQUIPMENT

Batch fermentations were performed in an Adaptive 2 L stirred-tank bioreactor (working volume 1 L), shown in Figure 2.1. The vessel consisted of a glass tank with a stainless steel head-plate containing ports for probes and additions, and a top-driven turbine. On-line monitoring and control of temperature, pH and impeller speed was performed by the Bioview software package (Adaptive). pH was maintained at 7.0 by automatic addition of 2M NaOH or 2M H_3PO_4 using a peristaltic pump. Temperature was maintained at 37°C by a heating element and cooling coils in the fermenter vessel. Process data was recorded every 2 min.

2.5.4.2 EXHAUST GAS ANALYSIS

The concentrations of CO_2, O_2, and N_2 in the inlet and exhaust gases were measured by mass spectrometry. Raw data was transferred into the computer of the fermenter digital control system, where derived variables (i.e. OUR, CER, RQ) were automatically calculated and stored. The formulas used to calculate OUR, CER and RQ were as follows:

Oxygen Uptake Rate:

$$OUR = \frac{F_1}{V_0 V_m}\left[X_{O2}^1 - \frac{\left(1 - X_{O2}^1 - X_{CO2}^1\right)}{\left(1 - X_{O2}^0 - X_{CO2}^0\right)}X_{O2}^0\right] x60 x1000$$

Carbon Dioxide Evolution Rate:

$$CPR = \frac{F_1}{V_0 V_m}\left[X_{CO2}^0 x\frac{\left(1 - X_{O2}^1 - X_{CO2}^1\right)}{\left(1 - X_{O2}^0 - X_{CO2}^0\right)} - X_{CO2}^1\right] x60 x1000$$

Respiratory Quotient:

$$RQ = \frac{CPR}{OUR}$$

Where F_1 = air flow rate (L/min)

V_0 = working volume liquid phase (L)

V_m = molar volume of gas (22.4 L/mol)

X_y^1 = mol fraction gas y at inlet

X_y^0 = mol fraction gas y at outlet

2.5.4.3   FERMENTER STERILISATION AND SET-UP

Sterilisation and set-up was performed one day prior to inoculation. The fermenter vessel, containing 790 ml M9 salt solution (42 mM $Na_2HPO_4.12H_2O$, 22 mM KH_2PO_4, 9 mM NaCl, 19 mM NH_4Cl) and fitted with pH and dissolved oxygen (DOT) electrodes, was sterilised by autoclaving at 121°C, 15 psi for a minimum of 20 min. Ancillary vessels for addition of acid, base, media components and inoculum were autoclaved along with the fermentor. The fermenter was set-up as follows. pH and DOT probes were connected and a temperature probe and heating element inserted into ports in the fermenter head plate. Ancillary vessels were connected aseptically to addition ports, before priming the acid and base lines. Cold water was connected to the condenser and to cooling coils running through the fermenter vessel. Compressed air was connected to the fermenter sparge line, via a 0.2 µm filter. The motor was attached to the turbine by a connection on the fermenter head plate. Following set-up of the fermenter, the remaining sterile media components and antibiotics were added aseptically, via an addition port.

2.5.4.4   INOCULUM PREPARATION AND CULTURE CONDITIONS

Inoculum cultures were prepared from a single colony on a fresh, selective nutrient agar plate. Typically, biomass from a colony was used to inoculate 10 ml selective glucose minimal media (refer to section 2.5.2) in a 50 ml falcon tube and grown for ~5 h in an orbital shaker (37°C, 200 rpm). This culture was used to inoculate 90 ml fresh selective glucose minimal media in a 250 ml flask and incubated overnight in an orbital shaker (37°C, 200 rpm). The A_{600} of the resulting 100 ml pre-culture was determined and the culture diluted in fresh media to give 100 ml of culture with an A_{600} of ~2.0. This was used to inoculate 900 ml fresh media in the 2 L fermenter. Fermentation was performed at temperature 37°C, pH 7.0, airflow rate 1 vvm, agitation rate 800 rpm, for a total of 24 h.

2.5.4.5   SAMPLING PROCEDURE, ANTISENSE RNA EXPRESSION AND ANALYSIS OF PLASMID STABILITY

Aseptic sampling was carried out via a sample port and line controlled by a 20 ml syringe. A 5 ml discard sample was taken before each 5 ml sample taken for analysis. Samples were taken from the fermenter at 1 h intervals and placed on ice prior to analysis. Duplicate A_{600} readings of culture broth were performed immediately. The remaining broth was pipetted into 3 x 1 ml aliquots and microfuged (5 min, 14,000 rpm). Supernatant was transferred into clean eppendorf tubes and stored at -20°C for subsequent analysis of residual glucose and organic acid concentrations. Cell pellets were stored at -80°C for enzyme activity analysis.

Expression of antisense RNA was induced in early/mid exponential growth phase (A_{600} 1.0 – 1.5) by addition of IPTG to a final concentration of 1 mM. Polypropylene glycol (PPG) was added manually when required, using a needle and syringe, to prevent excess foaming in the fermentor.

Plasmid stability was evaluated after 24 h growth by preparing two-fold serial dilutions of culture broth in saline, and plating 100 µl on selective and non-selective nutrient agar. Following overnight growth at 37°C, cell counts from selective and non-selective plates were determined.
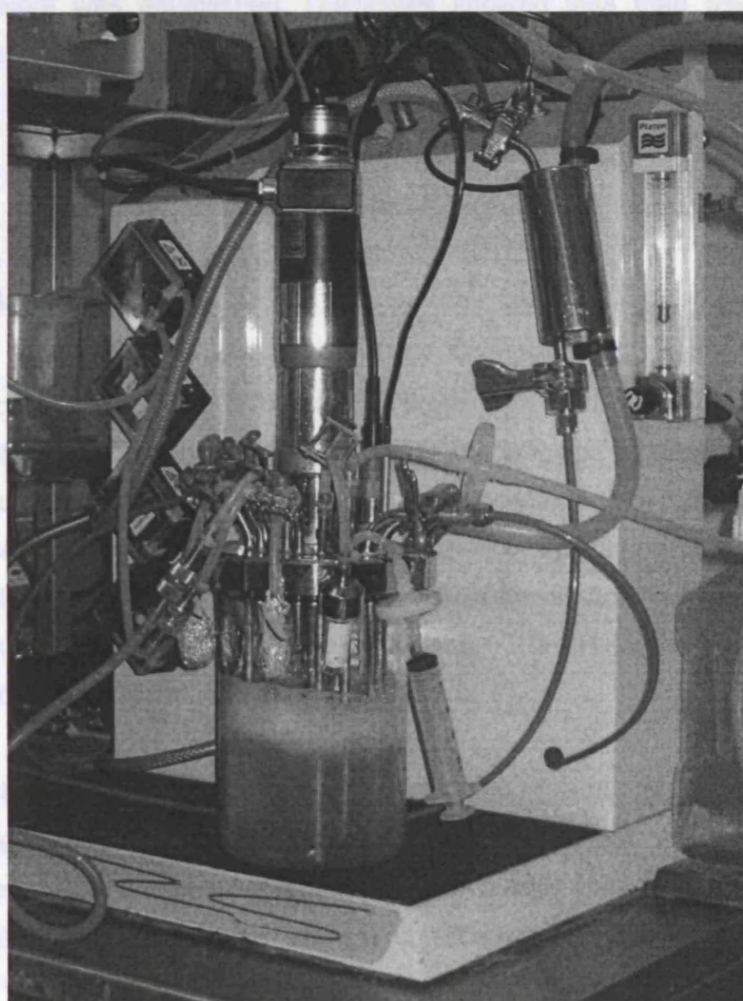
Figure 2.1 Adaptive 2 L fermenter used for bioreactor experiments. The vessel consisted of a glass tank with a stainless steel head-plate containing ports for probes and additions, and a top-driven turbine. Control of temperature, pH and impeller speed was achieved via digital computer control. pH was maintained at 7.0 by automatic addition of 2M NaOH or 2M H_3PO_4 using a peristaltic pump. Temperature was maintained at 37°C by a heating element and cooling coils in the fermenter vessel.

2.6   FERMENTATION ANALYSIS

2.6.1   BIOMASS

Cell growth was monitored by A_{600} of culture broth, against a blank of sterile culture medium. A correlation between A_{600} and dry cell weight (dcw) was determined as follows. Duplicate 20 ml samples of culture broth were taken at mid- log (6 h) and stationary phase (24 h) and pelleted by centrifugation (15 min, 3,000 rpm) in pre-weighed, pre-dried centrifuge tubes. The supernatant was discarded, before drying the pellets at 90°C until a stable dry weight was established. Duplicates showed less than 5% variation. The following correlation was generated for *E. coli* MG1655 grown in glucose minimal media:

$$1 \text{ Unit } A_{600} = 0.3 \text{ g L}^{-1} \text{ dcw}$$

2.6.2   GLUCOSE

Residual glucose in clarified fermentation broth was measured using a previously described method (Dubois *et al.*, 1956). The assay involves oxidation of the aldehyde functional group present in glucose and simultaneous reduction of 3,5-dinitrosalicylic acid (DNS) to 3-amino,5-nitrosalicylic acid, under alkaline conditions. Assay reagent was prepared by dissolving 16 g NaOH and 10 g dinitrosalicylic acid in ~300 ml dH_2O. Then 300 g sodium potassium tartrate was dissolved in ~300 dH_2O, the two solutions were combined, and dH_2O was added to a final volume of 1 L.

50μl of filtered sample or standard was added to 100μl of assay reagent (16 g L^{-1} sodium hydroxide, 10g L^{-1} dinitro-salicylic acid and 300 g L^{-1} sodium potassium tartrate prepared in dH_2O). The mixture was incubated at 100°C for 5 min, cooled on ice, and quenched with 1 ml water. The A_{540} of each sample or standard was then measured against a blank, which was generated with dH_2O in place of sample or standard. The standard curve is shown in Figure 2.2.

The chart shows a linear plot of OD 540 versus Glucose Concentration, mM, with the fitted equation:

$$y = 0.0497x - 0.0328$$
$$R^2 = 0.9985$$
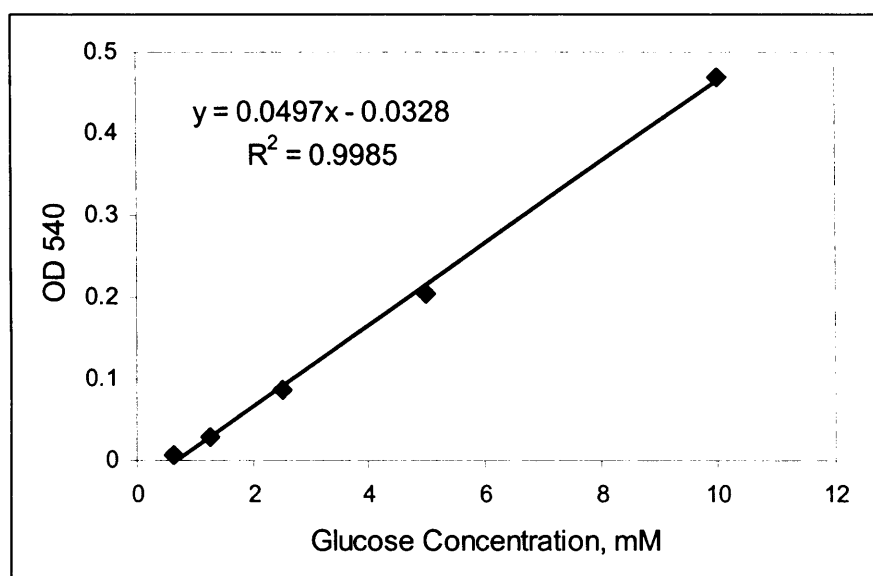
Figure 2.2   Glucose standard curve, generated with 2-fold serial dilutions of 10 mM glucose.

2.6.3 PHOSPHATE

Phosphate concentration in clarified fermentation broth was measured using a previously described method (Baykov *et al.*, 1988). Assay reagent was prepared by adding 60 ml conc. sulphuric acid to 300 ml dH₂O and cooling to room temperature, before supplementing with 0.44 g malachite green. On the day of use 2.5 ml of 7.5% ammonium molybdate and 0.2 ml of 11% Tween-20 was added to 10 ml of the dye solution. The assay was performed by mixing one volume of the assay reagent with four volumes of filtered sample or standard and incubating at room temperature for 10 min.

The A_{630} of each sample or standard was then measured against a blank, which was generated with dH₂O in place of sample or standard. The standard curve is shown in Figure 2.3.
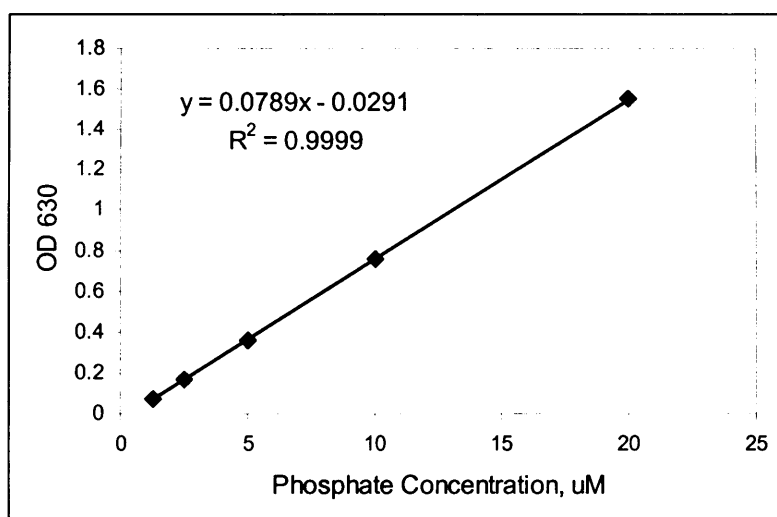
Figure 2.3 Phosphate standard curve, generated with 2-fold serial dilutions of 20 µM sodium phosphate.

2.6.4 ORGANIC ACID

Organic acids in clarified fermentation broth were measured by high performance liquid chromatography (Dionex, www.dionex.com). The Chromeleon software package (Dionex) was used for peak integration and quantitation.

20 µl of filtered sample or standard was analyzed on an Aminex HPX-87H organic acids column with 5 mM sulphuric acid at a flow rate of 0.6 ml min^{-1} and a column temperature of 60°C. The organic acids were detected at 215 nm using a UV detector. Standards of α-ketoglutarate, pyruvate, succinate, lactate, formate and acetate were used to quantify sample peaks. Figure 2.4 shows the relative elution times of the standard compounds. Standard curves are shown in Figure 2.5, A-C.

A sample of sterile culture media identified that uracil, thymidine and IPTG were the only media components and supplements detectable by this method.
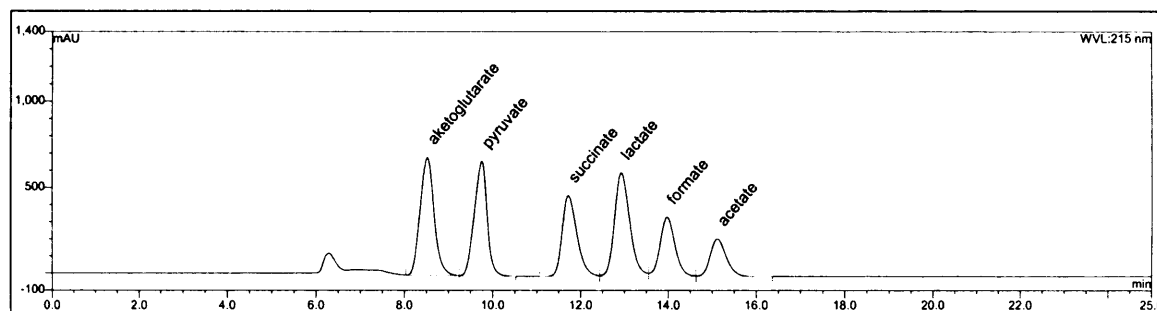
Figure 2.4 A typical chromatogram showing the relative elution times of α-ketoglutarate, pyruvate, succinate, lactate, fumarate, formate and acetate. The peaks represent 10 mM concentrations of αketoglutarate and pyruvate, and 100 mM concentrations of succinate, lactate, formate and acetate.
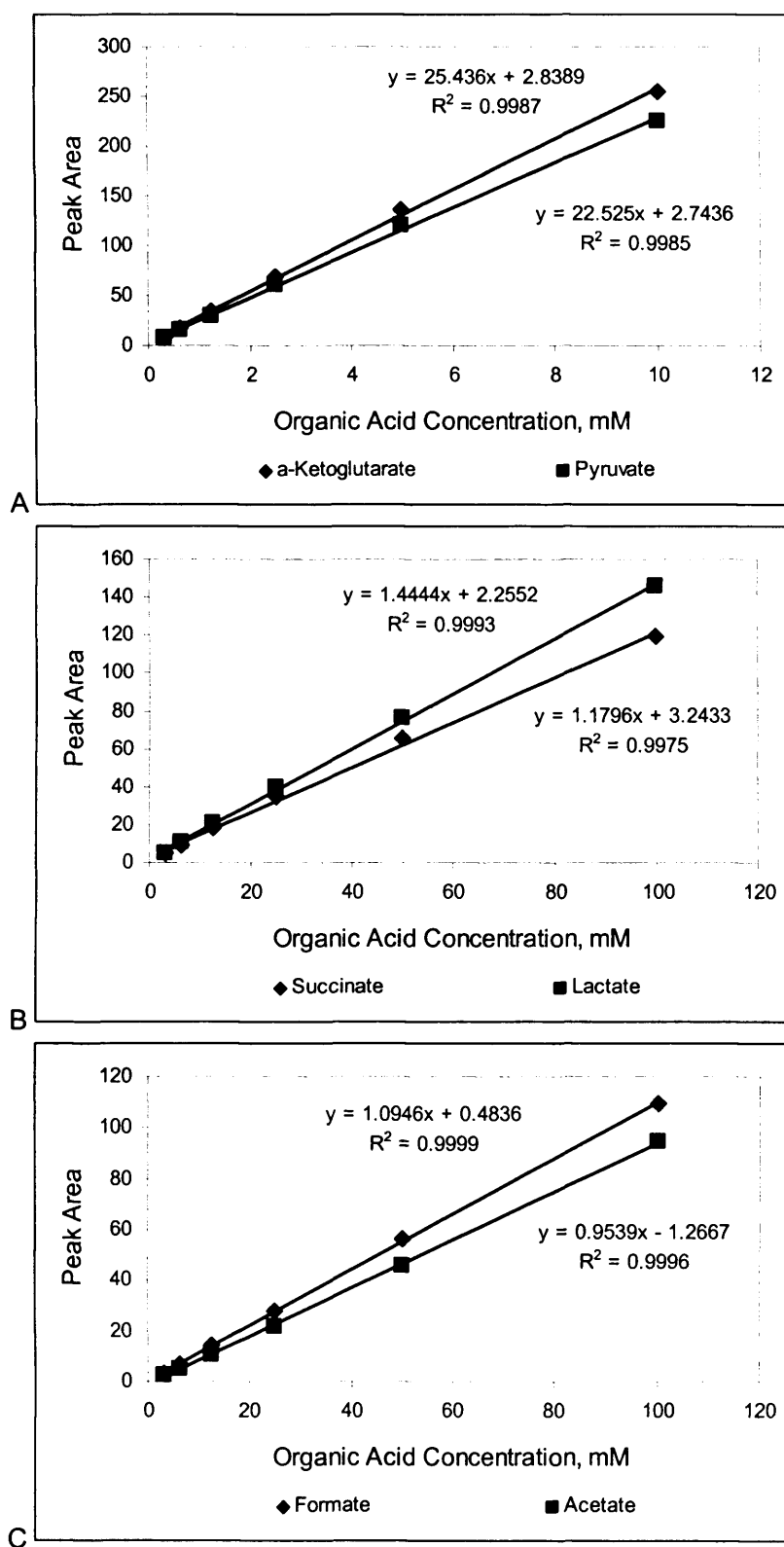
Figure 2.5 Organic acid standard curves generated by 2-fold serial dilutions of 10 mM α-ketoglutarate and pyruvate (A), 100 mM succinate and lactate (B), and 100 mM formate and acetate (C).

2.6.4.1   IDENTIFICATION OF FUMARATE PEAK

To identify an unknown peak on sample chromatograms a range of compounds, including malate, citrate, fumarate and acetoin were tested. The elution time of fumarate closely matched that of the unidentified peak. To confirm that the identity of the sample peak was fumarate, 5 units of fumarase, which converts fumarate to malate, was added to 500 μl supernatant and analysed by HPLC. The putative fumarate peak was reduced by approx. 50%, shown in Figure 2.6, which positively confirmed its identity. A fumarate standard curve, shown in Figure 2.7 was used for quantification.
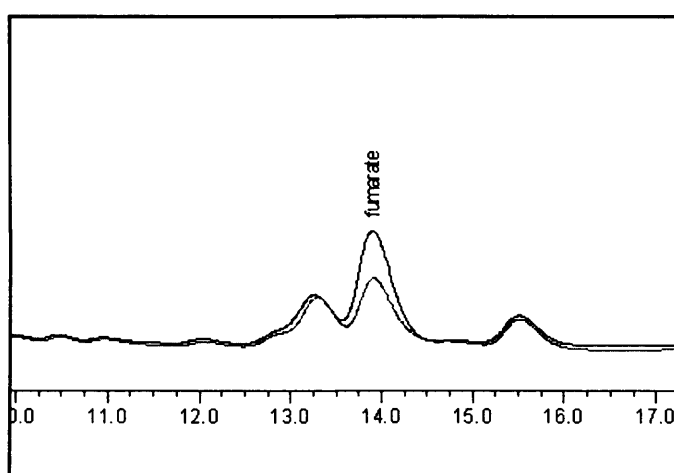
Figure 2.6   Chromatogram showing fumarate peak in clarified fermentation broth. The peak is reduced by approx. 50% after the addition of fumarase, which converts fumarate to malate.
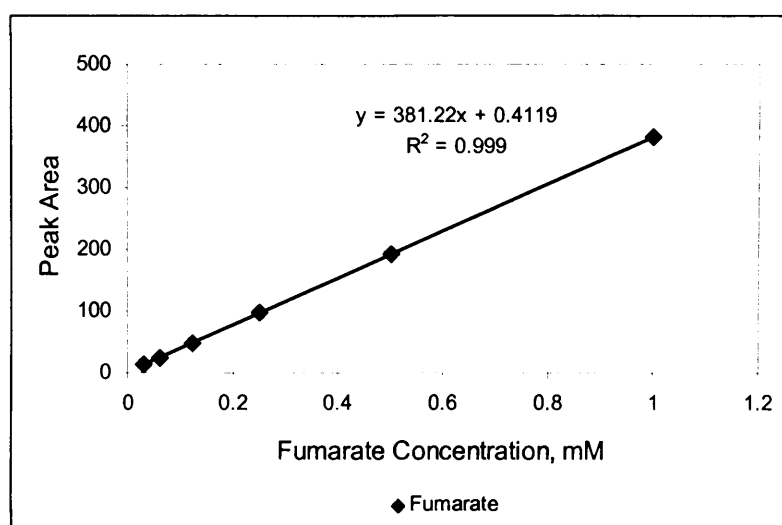
Figure 2.7   Fumarate standard curve generated with 2-fold serial dilutions of 1 mM fumarate.

2.6.5   TOTAL PROTEIN

Total cellular protein was measured using a previously described method (Bradford, 1976). The principle of the assay is based on the absorbance shift from 465 – 595 nm that occurs when coomassie blue binds to proteins in acidic solution.

2.6.5.1   SAMPLE PREPARATION

Crude cell extracts for analysis were prepared as follows. Cell pellets, harvested from 1 ml fermentation broth, were washed twice with 0.5 ml washing buffer (10 mM sodium phosphate, pH 7.5; 10 mM magnesium chloride, 1 mM EDTA) before resuspending in 0.5 ml of the same buffer. Subsequently, the cells were disrupted by sonication (5 cycles of 10 s on, 10 s off, 6 microns) whilst immersed in an ice bath. Cell debris was pelleted by centrifugation (10 min, 14,000 rpm, 4°C) and the extracts recovered into clean 1.5 ml tubes. Extracts were placed on ice prior to analysis.

2.6.5.2   ASSAY PROCEDURE

The assay was performed by mixing 20 μl sample/standard with 1 ml Bio-Rad solution (diluted 1 in 5 with dH_2O), and incubating at room temperature for 5 min. The absorbance at 595 nm was measured and used to calculate total protein from the standard curve.
A standard curve, shown in Figure 2.8, was generated with 2-fold serial dilutions of bovine serum albumin (BSA).

y = 1.4111x - 0.0077
R^2 = 0.9989
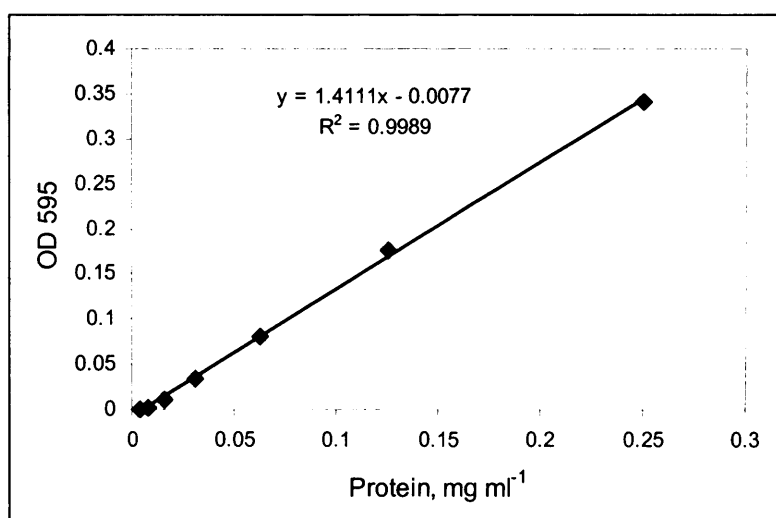
Figure 2.8 Total protein standard curve, generated with 2-fold serial dilutions of bovine serum albumin.

2.6.6 PHOSPHOTRANSACETYLASE & ACETATE KINASE ENZYME ACTIVITY

The activity of phosphotransacetylase and acetate kinase were measured in the forward direction (towards acetyl CoA) using a previously described method (Brown *et al.*, 1977). The coupled reactions for each assay are shown below. β-NADH formation was measured at 340 nm in a Biomate 3 spectrophotometer (Thermospectronic).

Phosphotransacetylase:

Phosphotransacetylase

Acetyl phosphate $+$ Co A $\longleftrightarrow$ Acetyl Co A $+$ P

Malate dehydrogenase

Malate $+$ NAD $\longleftrightarrow$ Oxaloacetate $+$ NADH

Citrate synthase

Oxaloacetate $+$ Acetyl Co A $\longleftrightarrow$ Citrate $+$ Co A

Acetate Kinase:

Acetate Kinase

Acetate $+$ ATP $\longleftrightarrow$ Acetyl phosphate $+$ ADP

Phosphotransacetylase

Acetyl phosphate $+$ Co A $\longleftrightarrow$ Acetyl Co A $+$ P

Malate dehydrogenase

Malate $+$ NAD $\longleftrightarrow$ Oxaloacetate $+$ NADH

Citrate synthase

Oxaloacetate $+$ Acetyl Co A $\longleftrightarrow$ Citrate $+$ Co A
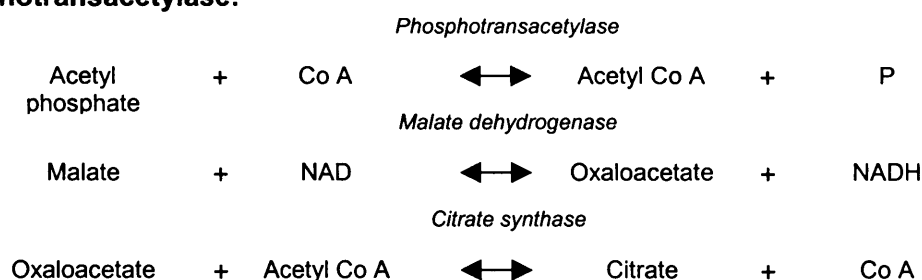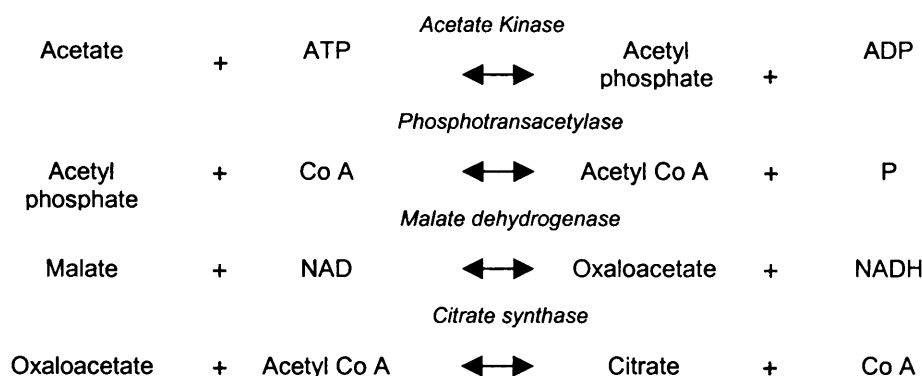
2.6.6.1 ASSAY REAGENTS

The reagents for phosphotransacetylase and acetate kinase enzyme activity assays are detailed in table 2.5 and table 2.6. A 10X assay buffer was prepared with Tris-HCl pH 8.0, $MgCl_2$ and malate, and stored at 4°C. Coupling enzymes were purchased as ammonium sulphate suspensions and stored at 4°C. The remaining components were prepared as concentrated stocks and stored in aliquots at -20°C. The reagents were thawed and combined immediately prior to sample analysis as several of the reagents degrade rapidly.

Table 2.5   Reagents for phosphotransacetylase enzyme activity assays

Reagent	Stock Conc., mM (unless otherwise stated)	Working Conc., mM (unless otherwise stated)
Buffer		
Tris-HCl pH 8.0	500	50
Magnesium Chloride	50	5
L-Malate	100	10
Intermediates		
Co Enzyme A	50	1
Nicotinamide Adenine Dinucleotide (NAD)	100	10
Coupling Enzymes		
Citrate Synthase (porcine heart)	1.5 Units μl^{-1}	10 Units ml^{-1}
Malate Dehydrogenase (porcine heart)	5 Units μl^{-1}	10 Units ml^{-1}
Substrate		
Acetyl Phosphate	1000	10

Table 2.6   Reagents for acetate kinase enzyme activity assays

Reagent	Stock Conc., mM (unless otherwise stated)	Working Conc., mM (unless otherwise stated)
Buffer		
Tris-HCl pH 8.3	500	50
Magnesium Chloride	50	5
L-Malate	100	10
Intermediates		
Co Enzyme A	50	1
Nicotinamide Adenine Dinucleotide (NAD)	100	10
Adenosine triphosphate (ATP)	600	1
Coupling Enzymes		
Citrate Synthase (porcine heart)	1.5 Units μl^{-1}	10 Units ml^{-1}
Malate Dehydrogenase (porcine heart)	5 Units μl^{-1}	10 Units ml^{-1}
Phosphotransacetylase (Methanosarcina thermophila)	1 Unit μl^{-1}	1 Unit ml^{-1}
Substrate		
Sodium Acetate	1000	300

2.6.6.2 SAMPLE PREPARATION

Crude cell extracts were prepared as described in section 2.6.5.1 and assayed immediately for enzyme activity.

2.6.6.3 ENZYME ACTIVITY MEASUREMENT AND ANALYSIS

Enzyme activity assays were performed at room temperature, in quartz cuvettes with a 1 ml volume and 1 cm path length. Total assay volume was 1 ml, consisting of 100 μl cell extract and 900 μl assay mix.

For each sample, assay reagents were mixed gently in the cuvette and incubated at room temperature for 2 min to allow the NADH-forming reaction to reach equilibrium. 100 μl cell extract was then added and mixed by gentle inversion, before placing the cuvette in the spectrophotometer and measuring the change in A_{340} as a function of time. The maximum slope was recorded. A control of purified enzyme was run with each assay. Samples were assayed in duplicate.

To determine enzyme activity from the maximum slope the following equation was used:

Units of Enzyme Activity = (Maximum slope/ 6.22)*10

where 6.22 is the molar extinction coefficient of NADH at 340 nm.

One unit of enzyme activity is defined as that amount of enzyme which catalyses the formation of 1 μmole of NADH per min, per ml of cell extract. Specific activity is expressed as units per mg of protein.

2.7 CALCULATIONS

2.7.1 SPECIFIC GROWTH RATE

The specific growth rate for batch cultures was calculated by plotting a scatter graph of time vs. $\ln(OD_{600})$, and using Microsoft Excel to draw a line of best fit through the data points corresponding to exponential growth phase. The gradient of the line was calculated by Excel, and quoted as the specific growth rate of the culture. Standard error of the growth rate was calculated using the 'LINEST' function in Excel.

2.7.2 SUBSTRATE UPTAKE / PRODUCT FORMATION RATES

The substrate uptake and product formation rates were calculated by plotting a scatter graph of time vs. substrate concentration and using Excel to draw a line of best fit through the data points. The gradient of the line, which corresponded to the substrate uptake or product formation rate, was calculated by Excel. Standard error of the line was calculated using the 'LINEST' function in Excel.

CHAPTER 3

E. COLI MG1655
GROWTH STUDIES

3.1 SUMMARY

This chapter describes growth studies that were conducted with *E. coli* MG1655 prior to the main body of experimentation. *E. coli* MG1655 was selected for use in this research due to availability of the complete genome sequence for the strain (Blattner *et al.*, 1997), which was useful for antisense RNA design and metabolic modelling.

The objective of the growth studies was to optimise media composition and inoculation regime for shake flask experiments. Several studies were performed, however four time-course analyses form the basis of this chapter. The first study compared growth of *E. coli* MG1655 in M9 minimal media, a well-established defined media, with growth in nutrient broth. The second study examined the effect of plasmid pTrc99A on growth rate of the host cell. The third study aimed to determine the effect of uracil and thymidine supplements on growth of *E. coli* MG1655 in minimal media. The fourth study optimised the inoculum regime for shake flask fermentations and analysed glucose uptake and acetate excretion from the strain.

3.2 BACKGROUND

3.2.1 *E. COLI* PHYSIOLOGY

E. coli is a member of the family Enterobacteriaceae (Neidhardt *et al.*, 1987). It is a Gram-negative bacteria, whose cells are rod-shaped and approximately 2 µm long and 1 µm in diameter (Voet and Voet, 1995). In nature *E. coli* can be found colonising the lower gut of animals and as a facultative anaerobe, survives when released into the environment, allowing widespread dissemination to new hosts. Pathogenic strains are responsible for infections of the enteric, urinary, pulmonary and nervous systems. For many years now this small microbe has been the preferred model organism in biochemical genetics, molecular biology and biotechnology (Blattner *et al.*, 1997). It is widely used for microbiological research because it is easily accessible, not highly virulent and grows readily on defined media (Neidhardt *et al.*, 1987).

E. coli can synthesise their constituents from a single organic compound and a few minerals. They exhibit very efficient energy expenditure, only synthesising what they require. The richer array of nutrients available the faster they grow (Neidhardt *et al.*, 1987). *E. coli* have evolved a complex set of control mechanisms that sense the external and internal milieu, which operates very fast and allows them to adapt to a constantly changing environment. This is expected from organisms that must compete with others for their food source. Demands from selective pressure for efficiency and adaptability have resulted in a complex regulatory network. Many proteins have not only an enzymatic or controlling function but also regulate their own synthesis (Neidhardt *et al.*, 1987).

3.2.2 INDUSTRIAL *E. COLI* FERMENTATION

E. coli is extensively used in the biotechnology industry as a host for recombinant protein production. There are several advantages of using *E. coli* for this purpose. Firstly, it has a rapid growth rate, which results in efficient production of biomass. Secondly, there is extensive understanding of its genetics and physiology, which allows for directed pathway modification. In addition, there are more genetic engineering tools and procedures available for *E. coli* than for any other organism (Blanch and Clark, 1996). However, there are also disadvantages of using *E. coli*. These are largely involved with the expression of eukaryotic proteins. *E. coli* does not readily glycosylate proteins or form disulphide bonds, which are post-translational modifications performed by eukaryotic cells. Also, eukaryotic proteins overproduced in *E. coli* typically form inclusion bodies

74

which require solubilization and subsequent refolding of the resultant protein. This is a complicated procedure, and in most cases the recover of biologically active proteins is incomplete (Blanch and Clark, 1996). Another problems is that *E. coli* does not normally secrete proteins, although new strategies have been developed to achieve secretion, which will ease product isolation. Another factor to be considered is the removal of endotoxins, which need to be removed from food and health-care products (Blanch and Clark, 1996).

3.2.3 *E. COLI* MG1655

E. coli was the first organism to be selected as a candidate for whole-genome sequencing (Blattner *et al.*, 1997). MG1655 was chosen as the strain to sequence because it has been maintained as a wild-type strain with minimal genetic manipulation (Blattner *et al.*, 1997). The genome of *E. coli* consists of 4,639,221 bp of circular duplex DNA. Protein-coding genes account for 87.8% of the genome, 0.8% encodes stable RNAs and 0.7% consists of non-coding repeats, leaving ~11% for regulatory and other functions (Blattner *et al.*, 1997). The annotated genome sequence (accession number U00096) is available at the National Centre for Biotechnology Information (NCBI) through Entrez Genomes division, and GenBank (Blattner *et al.*, 1997).

E. coli MG1655 is a derivative of the Lederberg strain W1485, which arose from the original *E. coli* K-12 strain after treatment with UV light (Jensen, 1993). It has been used as a genetic background for characterising the phenotypes of several RNA polymerase mutations, for studies on the control of ribosome synthesis, as the host for a collection of Tn10 insertions to facilitate genetic mapping, for total genome sequencing, and as a control strain in many experiments involving DNA replication of *E. coli* growing without thymidine (Molina *et al.*, 1998).

3.3 COMPARISON OF CELL GROWTH IN M9 MINIMAL MEDIA AND NUTRIENT BROTH

3.3.1 OBJECTIVE

The objective of this study was to compare the growth kinetics of *E. coli* MG1655 in M9 minimal media and nutrient broth.

3.3.2 EXPERIMENTAL CONDITIONS

The experimental conditions for this study are shown in Table 3.1.

Table 3.1   Experimental conditions for comparing cell growth in M9 minimal media and nutrient broth.

Strain	*E. coli* MG1655
Media	a) M9 minimal media, 4 g L^{-1} glucose b) Nutrient broth
Growth mode	Batch, 2 L shake flask (250 ml working volume)
Inoculum	1 ml glycerol cell stock
Temperature	37°C
Shaker rpm	200
Sampling times, hours	0, 1, 2, 3, 4, 5, 6, 7, 8 and 24.
Experimental duplication	Each media was tested independently two times

3.3.3 RESULTS AND DISCUSSION

The growth of *E. coli* MG1655 in M9 minimal media and nutrient broth was compared in shake-flask cultures over a 24 h time-course. The profiles of OD_{600} are shown in Figure 3.1. Maximum specific growth rates and maximum OD_{600} are shown in Table 3.2. The results show that maximum specific growth rate is more than two-fold higher in cultures grown in nutrient media compared to M9 minimal media. This difference was expected due to the presence of complex ready-made nutrients such as amino acids in nutrient broth, which the cells can quickly utilise. In contrast, when cultured in M9 minimal media the cells must synthesise all their constituents from glucose, ammonia and a few minerals, resulting in a slower growth rate.
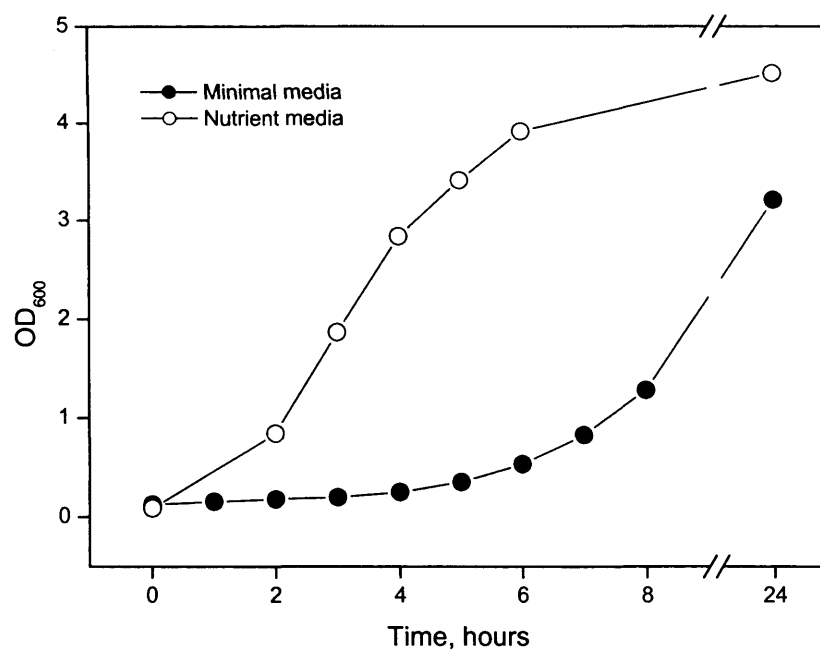
Figure 3.1 Time-course profiles of cell growth for *E. coli* MG1655 cultured in a) glucose minimal media, and b) nutrient broth. Recombinant cells were grown in 2 L baffled flasks containing 250 ml medium at 37°C, 200 rpm. Duplicate analyses were performed for each sample; average values of the duplicates are reported.

Table 3.2 Maximum specific growth rates and maximum OD_{600} from growth studies of *E. coli* MG1655 in M9 minimal media and nutrient broth

Media	$\mu_{max}(h^{-1})$	Maximum OD_{600}
M9 Minimal Media	0.43	3.2
Nutrient broth	1.1	4.5

3.4 EFFECT OF PLASMID PTRC99A ON GROWTH OF *E. COLI* MG1655

3.4.1 OBJECTIVE

The objective of this study was to determine if plasmid pTrc99A, to be used for antisense RNA expression, caused a reduction in growth of *E. coli* MG1655 cultured in M9 minimal media.

3.4.2 EXPERIMENTAL CONDITIONS

The experimental conditions for this study are shown in Table 3.3.

Table 3.3   Experimental conditions for testing the effect of plasmid pTrc99A on the growth of *E. coli* MG1655.

Strains	*E. coli* MG1655, *E. coli* MG1655(pTrc99A)
Media	M9 minimal media, 4 g L^{-1} glucose, 100 µg ml^{-1} ampicillin*
Growth mode	Batch, 2 L shake flask (250 ml working volume)
Inoculum	10 ml overnight culture, constructed from 10^{-4} dilution of glycerol cell stock.
Temperature	37°C
Shaker rpm	200
Sampling times, hours	0, 2, 4, 6, 8 and 24.
Experimental duplication	Each media was tested independently two times

* For plasmid-harbouring strain

3.4.3 RESULTS AND DISCUSSION

The effect of plasmid pTrc99A on growth of *E. coli* MG1655 in M9 minimal media was studied in 2 L shake-flasks. The profiles of OD_{600} are shown in Figure 3.2. Maximum specific growth rates and maximum OD_{600} are shown in Table 3.4. Results show that maximum specific growth rate of the host cell is not impaired by the presence of plasmid pTrc99A. Colony counts from selective and non-selective nutrient agar plates indicated that the plasmid was stably maintained in the host cell over 24 h (data not shown).
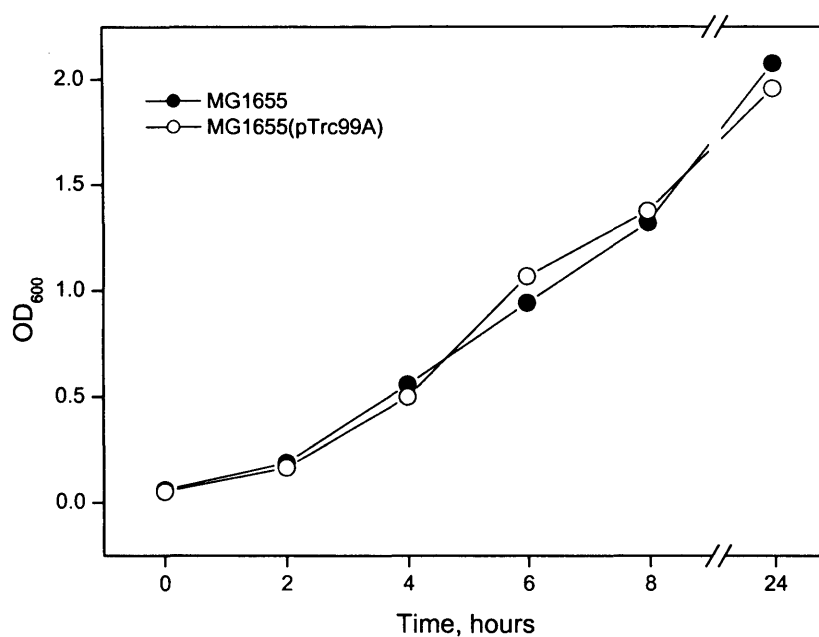
Figure 3.2 Time-course profiles of cell growth for *E. coli* MG1655 and *E. coli* MG1655 (pTrc99A). Recombinant cells were cultured in 2 L baffled flasks containing 250 ml M9 medium with 0.4% (wt/vol) glucose at 37°C, 200 rpm. Duplicate analyses were performed for each sample; average values of the duplicates are reported.

Table 3.4 Maximum specific growth rates and maximum OD_{600} from growth studies of *E. coli* MG1655 and *E. coli* MG1655(pTrc99A) in 2 L shake flasks.

Strain	$\mu_{max}(h^{-1})$	Maximum OD_{600}
E. coli MG1655	0.56	2.1
E. coli MG1655(pTc99A)	0.57	2.0

3.5 EFFECT OF URACIL AND THYMIDINE SUPPLEMENTS ON GROWTH OF *E. COLI* MG1655 IN M9 MINIMAL MEDIA

3.5.1 OBJECTIVE

The objective of this study was to determine if uracil and thymidine supplements increase the growth rate of *E. coli* MG1655 in M9 minimal media. Uracil is a pyrimidine base that is incorporated into RNA and thymidine is a nucleoside that is incorporated into DNA. Both are essential for cell growth and replication. It has previously been reported that *E. coli* MG1655 may require uracil and thymidine supplements in minimal media for optimal growth (Jensen, 1993; Molina *et al.*, 1998).

3.5.2 EXPERIMENTAL CONDITIONS

The experimental conditions for this study are shown in Table 3.5.

Table 3.5 Experimental conditions for testing the effect of uracil and thymidine supplements on growth of *E. coli* MG1655 in M9 minimal media.

Strain	*E. coli* MG1655(pTrc99A)
Media	M9 minimal media, 5 g L^{-1} glucose, trace element mix, 100 µg ml^{-1} ampicillin. Uracil was added at 20 µg ml^{-1} and thymidine at 5 µg ml^{-1}.
Growth mode	Batch, 2 L shake flask (250 ml working volume)
Inoculum	10 ml starter culture, constructed from 10^{-4} dilution of glycerol cell stock.
Temperature	37°C
Shaker rpm	200
Sampling times, hours	0, 1, 2, 3, 4, 5, 6, 7, 8, 9, 10 and 24.

3.5.3 RESULTS AND DISCUSSION

The results of Jensen (1993) showed that the growth of *E. coli* MG1655 in minimal media was 10 to 15% higher in the presence of uracil than in the absence of exogenous pyrimidines. Their investigation concluded that *E. coli* K-12 strains MG1655 and W3110 starve for pyrimidine in minimal media due to a suboptimal content of the pyrimidine biosynthetic enzyme orotate phosphoribosyltransferase (*pyrE*). This defect is caused by

80

a frameshift mutation in the *rph-pyrE* operon (Jensen, 1993).

Molina *et al.* (1998) reported that *E. coli* MG1655 has a partial Thy- phenotype and requires 5 µg ml^{-1} thymidine for optimal cell growth. Thy- strains do not have impaired growth rates, but chromosome replication time is affected resulting in changes in DNA-to-mass ratio and cell composition.

The effect of uracil (20 µg ml $^{-1}$) and/or thymidine (5 µg ml $^{-1}$) on growth of *E. coli* MG1655 in M9 minimal media was studied in 2 L shake-flasks. Time-course profiles of OD$_{600}$ are shown in Figure 3.3 and maximum specific growth rates are compared in Table 3.6. The results show a 15% increase in maximum specific growth rate of *E. coli* MG1655 cultured in M9 minimal media supplemented with 20 µg ml $^{-1}$ uracil, compared to the same strain grown without uracil addition. As expected, thymidine addition to M9 minimal media does not result in a noticeable increase in maximum specific growth rate, but will be included in M9 minimal media for future experiments to ensure optimal cell growth. Our results agree with the findings of Jensen (1993) and Molina *et al.* (1998).

Increasing the supplement concentrations two-fold (40 µg ml^{-1} uracil, 10 µg ml^{-1} thymidine) resulted in no further increase in growth rate (data not shown).

Table 3.6   Maximum growth rates of *E. coli* MG1655 grown in M9 minimal media with uracil and/or thymidine supplements.

Supplement(s)	μ_{max} (h^{-1})
No supplements	0.71
20 µg ml^{-1} uracil	0.82
5 µg ml^{-1} thymidine	0.73
20 µg ml^{-1} uracil + 5 µg ml^{-1} thymidine	0.81
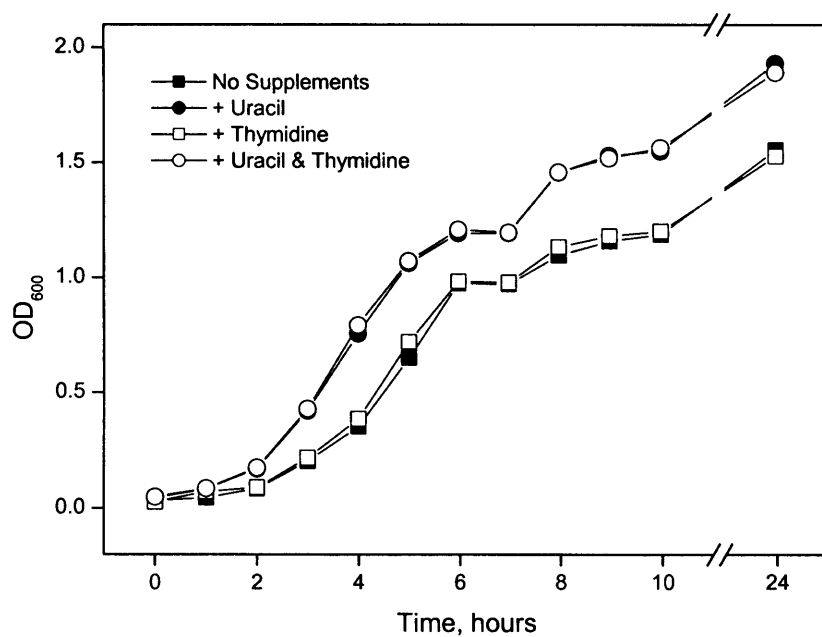
Figure 3.3 Time-course profiles of cell growth for *E. coli* MG1655 harbouring pTrc99A. Recombinant cells were cultures in 2 L baffled flasks containing 250 ml M9 medium with 0.5% (wt/vol) glucose at 37°C, 200 rpm. The effect of uracil and thymidine on cell growth was tested by supplementing individual *E. coli* cultures with a) 20 µg ml^{-1} uracil, b) 5 µg ml^{-1} thymidine and c) 20 µg ml^{-1} uracil and 5 µg ml^{-1} thymidine. The growth of these cultures was compared with the growth of *E. coli* without uracil or thymidine supplements.

3.6 OPTIMISATION OF SHAKE-FLASK FERMENTATION PROCEDURES

3.6.1 OBJECTIVE

The objective of this study was to optimise the procedures for shake flask fermentation with respect to media composition and an inoculation regime.

3.6.2 EXPERIMENTAL CONDITIONS

The experimental conditions for this study are shown in Table 3.7.

Table 3.7 Experimental conditions for optimising shake-flask fermentations

Strain	*E. coli* MG1655(pTrc99A)
Media	M9 minimal media, 10 g L^{-1} glucose, trace element mix, 20 µg ml^{-1} uracil, 5 µg ml^{-1} thymidine, 100 µg ml^{-1} ampicillin..
Growth mode	Batch, 2 L shake flask (250 ml total working volume)
Inoculum	10% (v/v) overnight culture, inoculated from a colony on a fresh selective nutrient agar plate.
Temperature	37°C
Shaker rpm	200
Sampling times, hours	0, 1, 2, 3, 4, 5, 6, 7, 8, and 24.

3.6.3 RESULTS AND DISCUSSION

The results presented here show an 'optimised' shake-flask fermentation of *E. coli* MG1655(pTrc99A) cultured in M9 minimal media. Figure 3.4 shows a profile of growth, glucose uptake and acetate excretion under the above conditions. These conditions were formulated by a series of experiments to shorten the lag phase, capture the exponential phase within the working day and ensure glucose was not limiting for the duration of the fermentation.
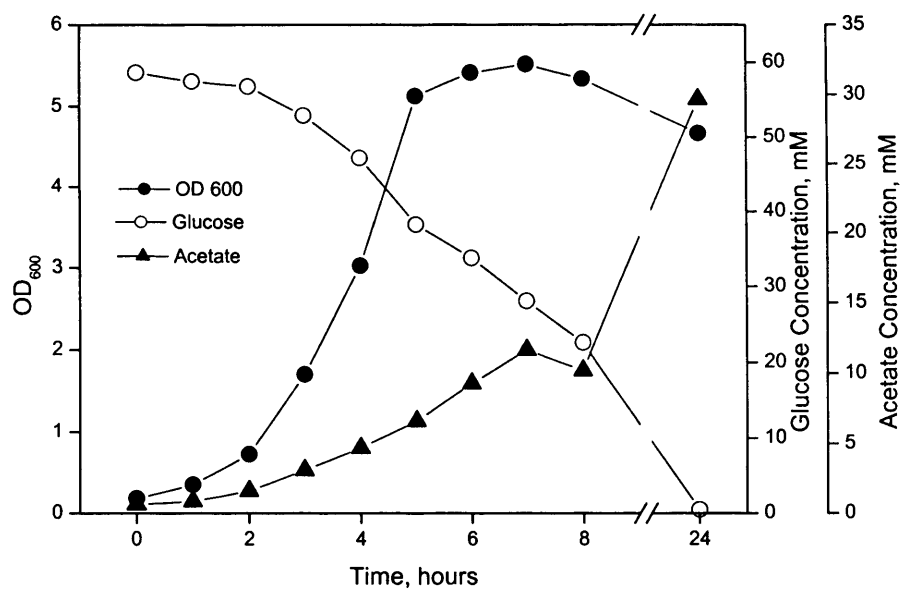
Figure 3.4 Time-course profile of cell growth, residual glucose concentration and acetate concentration in *E. coli* MG1655 harbouring pTrc99A. Recombinant cells were cultured in a 2 L baffled flask containing 250 ml of M9 medium with 1% (wt/vol) glucose at 37°C, 200 rpm. Duplicate analyses were performed for each sample; average values of the duplicates are reported.

3.7   DISCUSSION AND CONCLUSIONS

This chapter described the shake flask studies that were performed in order to optimise growth of *E. coli* MG1655 in glucose minimal media. Four experiments were performed, which investigated: A) the maximum specific growth rate and biomass levels that were achieved in nutrient broth compared with glucose minimal media; B) the impact of empty expression vector pTrc99A on cell growth rate; C) the effect of strain-specific supplements uracil and thymidine on maximum specific growth rate; and D) optimisation of general shake-flask fermentation procedures.

The results from these studies showed that the presence of expression vector pTrc99A did not impair cell growth. Furthermore, the addition of 20 µg ml^{-1} uracil to M9 minimal media increased the maximum cell growth rate by 15%. In addition, it was established that inoculating shake flask cultures with a 10% (v/v) overnight culture, instead of directly from a glycerol cell stock, shortened the lag phase and enabled the exponential growth phase to be analysed during the working day. Finally, the concentration of glucose added to M9 minimal media was increased from 5 g L^{-1} to 10 g L^{-1} to ensure that glucose was not limiting throughout the fermentation. It was important to ensure that glucose in the culture medium was not depleted during the course of a 24 h fermentation, because in the absence of another carbon source it is likely that *E. coli* would re-consume excreted acetate from the culture medium. Under these conditions, it would be difficult to establish the total amount of acetate that was produced by *E. coli* in each experiment. Reconsumption of acetate would also alter the flow of carbon through central metabolism and lower the cell growth rate.

The minimal media used in this research comprised 10 g L^{-1} glucose as a carbon source and 1 g L^{-1} ammonium chloride as a nitrogen source. Due to the composition of *E. coli* cells, and the ratio of carbon to nitrogen in the minimal media, it was established that ammonium chloride would be depleted before glucose. Therefore, nitrogen availability would limit the maximum cell density that could be achieved by *E. coli* cultures in this study. It would be possible to increase the concentration of ammonium chloride, along with the concentration of calcium and magnesium salts if it was required to grow *E. coli* to a high cell density, however for the purposes of this study that was not necessary.

Subsequent physiological studies in this research, which are presented in Chapter 5, were conducted using the media composition and cultivation procedures that were determined by the experiments described in this chapter.

CHAPTER 4

GENETIC ENGINEERING
E. COLI MG1655 TO EXPRESS ANTISENSE RNA
TARGETED AGAINST PHOSPHOTRANSACETYLASE
AND ACETATE KINASE

4.1 SUMMARY

In *E. coli*, the majority of acetate is produced via the *ackA-pta* pathway. It is comprised of two enzyme-catalysed reactions, which convert acetyl CoA into acetate. In the first step, acetyl CoA is converted to acetyl phosphate by phosphotransacetylase (*pta*) and in the second step, acetyl phosphate is converted to acetate by acetate kinase (*ackA*). Inactivating the *ackA-pta* pathway in *E. coli* abolishes production of the intermediary compound acetyl phosphate, which has been implicated in a range of important cellular functions (refer to section 1.1.1). Furthermore, *ackA-pta* deletion mutant's exhibit reduced growth rates in glucose-supplemented media. Therefore, this research proposed to use antisense RNA as a flexible metabolic engineering tool to partially downregulate expression of the *pta* and *ackA* genes, and study the effects on *E. coli* central metabolism before and after induction of antisense RNA.

This chapter describes the development of *E. coli* strains to express antisense RNA targeted against phosphotransacetylase and acetate kinase. The expression vector pTrc99A was used to develop two plasmids, one with inducible expression of *pta* antisense RNA and one with inducible expression of *ackA* antisense RNA. In addition, the expression vector pMMB66EH, which is compatible with pTrc99A-derived plasmids, was used to construct a second plasmid with inducible expression of *ackA* antisense RNA. The plasmids were designed to facilitate individual expression of *pta* and *ackA* antisense RNA, and co-expression of antisense RNA targeted against both the *pta* and *ackA* genes simultaneously.

Antisense RNA oligonucleotides were designed to basepair with a short region (~200 nucleotides) of the target mRNA, encompassing the ribosome binding site and translation initiation site. This strategy aims to block ribosome binding and prevent translation of the target mRNA, and is generally thought to be the most effective in suppressing expression of target genes. Gene fragments for antisense RNA expression were placed under the control of the inducible *trc* and *tac* promoters on the pTrc99A and pMMB66EH plasmids respectively. This allowed conditional expression of antisense RNA during *E. coli* fermentation by addition of IPTG to the culture medium.

4.2 BACKGROUND

The acetate kinase (*ackA*) and phosphotransacetylase (*pta*) genes from *E. coli* have been cloned and sequenced, and were found to encode proteins of 400 and 714 amino acids respectively (Kakuda *et al.*, 1994; Matsuyama *et al.*, 1989; Yamamoto-Otake *et al.*, 1990). In the following pages the *ackA* and *pta* genes, mRNA transcripts and corresponding proteins are described, and the targets for antisense RNA binding are highlighted.

4.2.1 THE *ACKA-PTA* OPERON IN *E. COLI*

In *E. coli,* the genes *ackA* and *pta* are organised in the order *ackA-pta* in an operon (Kakuda *et al.*, 1994), which is illustrated in Figure 4.1. Two mRNA transcripts of different sizes are produced from the operon. The largest is a 3,700-nucleotide transcript, which is produced from the first promoter (P$_1$), and encompasses both the acetate kinase and phosphotransacetylase genes. The smaller transcript, which is 2,300 nucleotides long, is produced from the second promoter (P$_2$). It encodes only the phosphotransacetylase gene. The *ackA* and *pta* genes are regarded as constitutively expressed, although the fine structures and regulation of the two promoters remain largely unknown. Putative Shine-Dalgarno sequences have been identified in both genes and are highlighted in Figure 4.1.
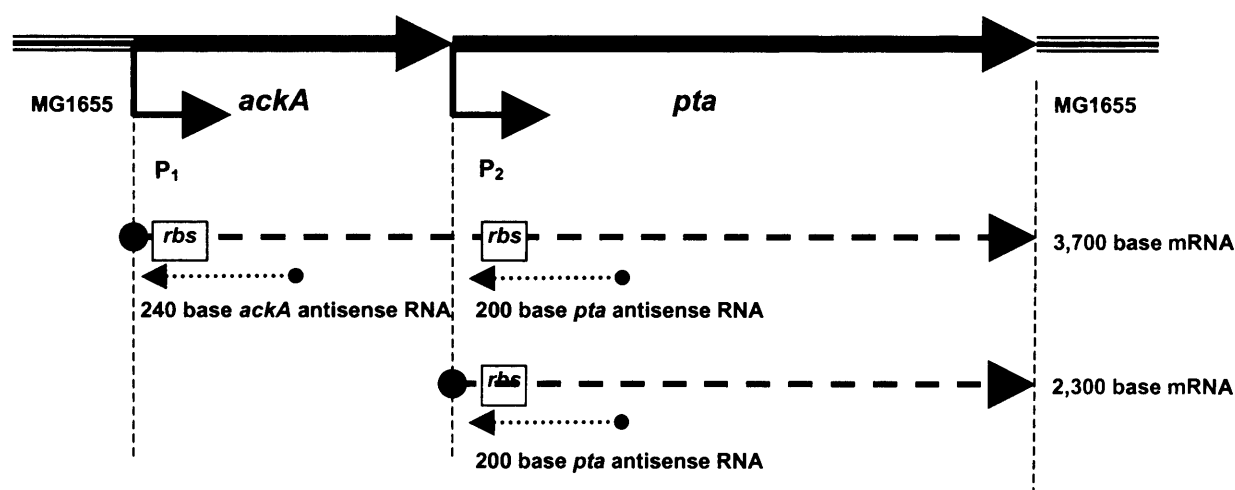
Figure 4.1 Structure of the *ackA-pta* operon (not drawn to scale). Two mRNA transcripts of different sizes are produced: a 3,700 nt mRNA transcribed from both the *ackA* and *pta* genes; and a 2,300 nt mRNA transcribed from just the *pta* gene. Antisense RNA oligonucleotides have been designed to basepair with a region encompassing the putative ribosome binding site and translation initiation site on the *ackA* and *pta* mRNA targets, as illustrated above.

88

4.2.2 PHOSPHOTRANSACETYLASE (EC 2.3.1.8)

E. coli phosphotransacetylase is a 77 kD enzyme which catalyses the reversible conversion of acetyl CoA to acetyl phosphate (Kakuda *et al.*, 1994), (Figure 4.2). It has been purified from *E. coli* B and shown to be an allosteric enzyme which is activated by pyruvate and inhibited mainly by NADH (Shimizu *et al.*, 1969; Suzuki, 1969). ADP and ATP also inhibit the enzyme, but their inhibitory strengths were found to be only one-quarter and one-tenth of NADH, respectively.

Structural analysis of the 714 amino acid *E. coli* phosphotransacetylase protein revealed that it contains a 350 amino acid fragment that is not required for phosphotransacetylase activity (Galperin and Grishin, 2000). Phosphotransacetylases from most other organisms consist of approximately 350 amino acid residues, corresponding to the C-terminal part of the *E. coli* enzyme. Sequence analysis of the additional N-terminal fragment from *E. coli* phosphotransacetylase revealed its similarity with the enzymes dethiobiotin synthetase, cobyrinic acid a,c-diamide synthase CobB, cobyric acid synthase CobQ and MinD, an ATPase involved in regulation of bacterial cell division (Galperin and Grishin, 2000). However, mutations in a possible ATPase sequence in the N-terminal fragment of *E. coli* phosphotransacetylase mean that it is most likely to be devoid of catalytic activity. Therefore, the function of this N-terminal domain was suggested to be regulation of phosphotransacetylase activity, possibly in response to the intracellular ATP level.

4.2.3 ACETATE KINASE (EC 2.7.2.1)

E. coli acetate kinase is a 40 kDa protein, comprising 400 amino acids, which catalyses the reversible conversion of acetyl phosphate to acetate (Fox and Roseman, 1986a), (Figure 4.2). *ackA* mutants still excrete acetate, therefore It is likely that acetyl phosphate can undergo non-enzymatic hydrolysis, which occurs rapidly at 37°C, and form acetate even in the absence of acetate kinase (Brown *et al.*, 1977).
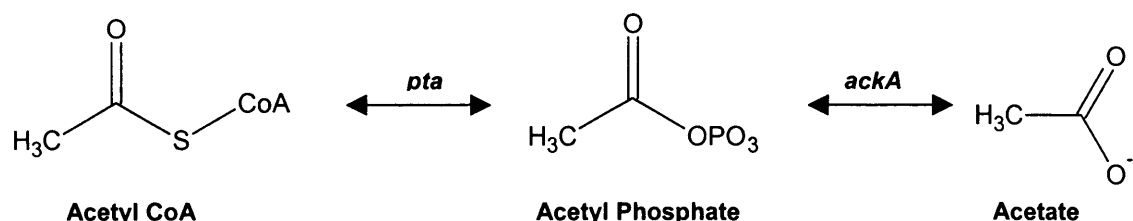
Figure 4.2 The *ackA-pta* pathway in *E. coli*.

4.3 PLASMID CONSTRUCTION

In total, seven novel plasmids were constructed in this work. Four intermediary plasmids (pQR438, pQR440, pQR444, pQR445) were developed in order to produce a *pta* antisense RNA expression vector (pQR439), and two *ackA* antisense RNA expression vectors (pQR441, pQR446). The component parts of the plasmids are listed and described in Table 4.1.

Table 4.1   Plasmid component definitions

Plasmid Component	Description
P$_{trc}$	*trc* promoter
P$_{tac}$	*tac* promoter
mcs	Multiple cloning site
rrnBT$_1$T$_2$	Transcription termination signal
pBR322 ori	Origin of plasmid replication from plasmid pBR322: Includes all genes and sites necessary for a plasmid to replicate in *E. coli*.
RSF 1010 ori	Origin of plasmid replication from plasmid RSF 1010: Includes all genes and sites necessary for a plasmid to replicate in *E. coli*.
pUC ori	Origin of plasmid replication from plasmid pUC: Includes all genes and sites necessary for a plasmid to replicate in *E. coli*.
lac I^q	*lac* I^q repressor for strong inhibition of transcription from the *trc* or *tac* promoters in the absence of inducer, i.e. 1 mM IPTG
antisense *pta*	DNA fragment of the *pta* gene
antisense *ackA*	DNA fragment of the *ackA* gene
Amp^r	Ampicillin resistant
Kan^r	Kanamycin resistant

4.3.1 DEVELOPMENT OF A CONSTRUCT FOR *PTA* ANTISENSE RNA EXPRESSION

4.3.1.1 PQR439

Plasmid pQR439 was developed to express antisense RNA targeted against *E. coli* MG1655 *pta* mRNA. Using *E. coli* MG1655 chromosomal DNA as a template, a 200 bp fragment of the 2,141 bp *pta* gene, encompassing the putative ribosome binding site and extending into the open reading frame, was amplified by PCR (Figure 4.3). The PCR primers were designed to introduce restriction sites at the 5' and 3' ends of the amplified gene fragment, to facilitate cloning of the PCR product into expression vector pTrc99A in an antisense orientation. The forward primer (5'-GCAAGCTTCGAAAGAGGATAAACCG-3') introduced a *Hind*III restriction site onto the 5' end of the *pta* gene fragment, and the reverse primer (5'-CGCTTAAGTGGAAGAGTTCGCACGC-3') introduced an *Eco*RI restriction site onto the 3' end of the *pta* gene fragment. In total, the PCR product was 216 bp in length.

To ensure there was no significant chance of *pta* antisense RNA binding to other mRNAs transcribed from the *E. coli* genome, the antisense strand of the *pta* gene fragment was screened against the complete genome sequence of *E. coli* MG1655 using the BLASTn homology search (available at www.ncbi.nlm.nih.gov/BLAST/). The results showed that the *pta* gene fragment had no significant homology with any other areas of the *E. coli* MG1655 genome.
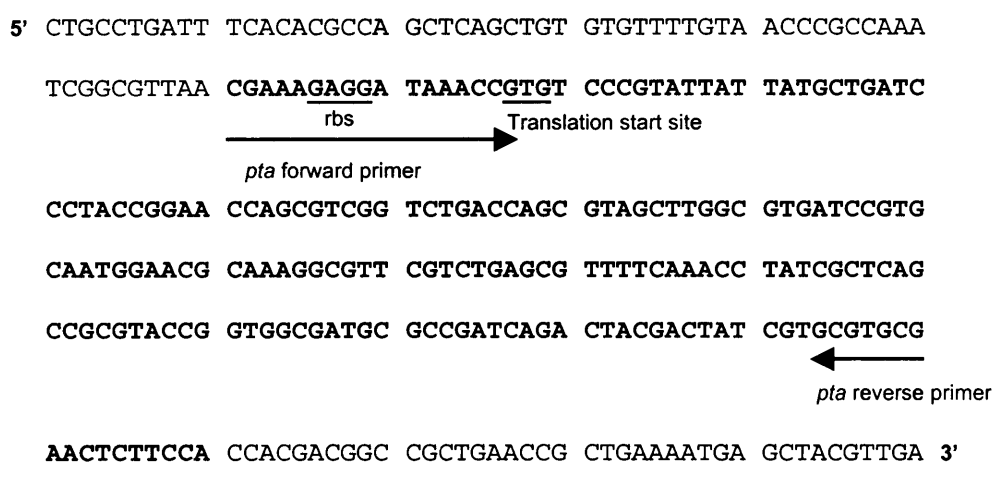
Figure 4.3 Partial DNA sequence of the *E. coli* MG1655 *pta* gene. The 200 bp gene fragment amplified by PCR is highlighted in bold, and the location for primer binding is shown, in relation to the *pta* ribosome-binding site and translation start site.

The PCR-amplified *pta* gene fragment was ligated into cloning vector pCR2.1-TOPO, forming pQR438. *E. coli* TOP10 was transformed with the ligation mixture. Colonies of *E. coli* TOP10 harbouring pQR438 were identified by antibiotic selection and blue-white colour screening, followed by restriction analysis of the purified plasmid. In addition, a section of plasmid pQR438, encompassing the DNA insert, was sequenced to ensure that the plasmid contained the correct DNA insert i.e. the *pta* gene fragment.

Subsequently, the *pta* gene fragment was excised from pQR438 by *Eco*RI/*Hind*III double digestion and gel purified, prior to ligating in antisense orientation into the multiple cloning site of expression vector pTrc99A, forming pQR439 (Figure 4.5). The ligation mixture was used to transform *E. coli* DH5*α*. Restriction analysis of isolated pQR439 was performed to confirm presence of the *pta* gene fragment (Figure 4.4). *E. coli* MG1655 was transformed with pQR439 for *pta* antisense RNA expression studies.
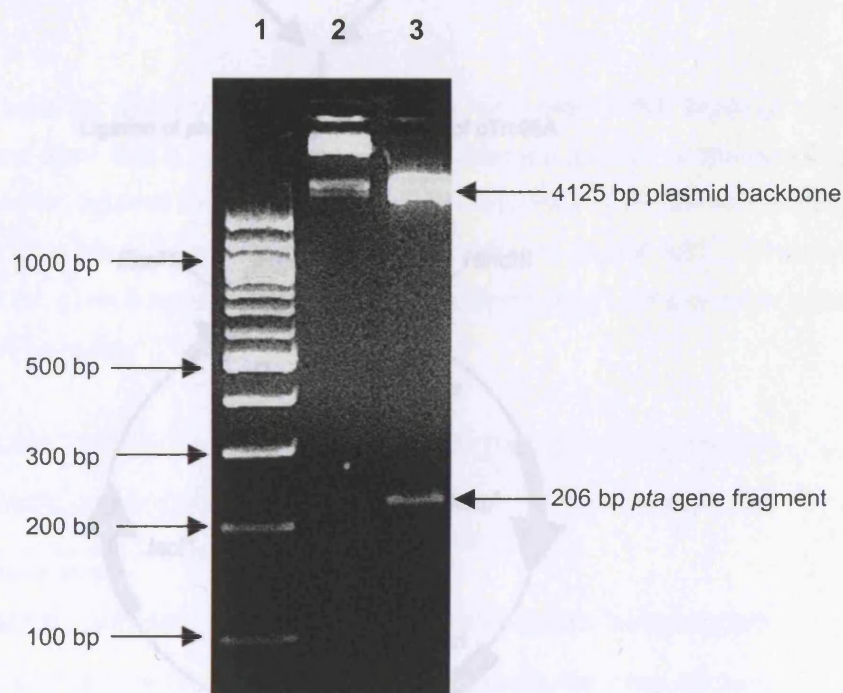
Figure 4.4 TBE agarose gel (2%) of pQR439 following *Eco*RI/*Hind*III digestion. Lane 1, 100 bp ladder comprising DNA fragments of 100, 200, 300, 400, 500, 517, 600, 700, 800, 900, 1000, 1200 and 1517 bp; Lane 2, pQR439 undigested; Lane 3, pQR439 digested with *Eco*RI and *Hind*III. Agarose gel electrophoresis was performed at 100 v for approximately 1 h (as described in Materials and Methods) and visualised under UV light.
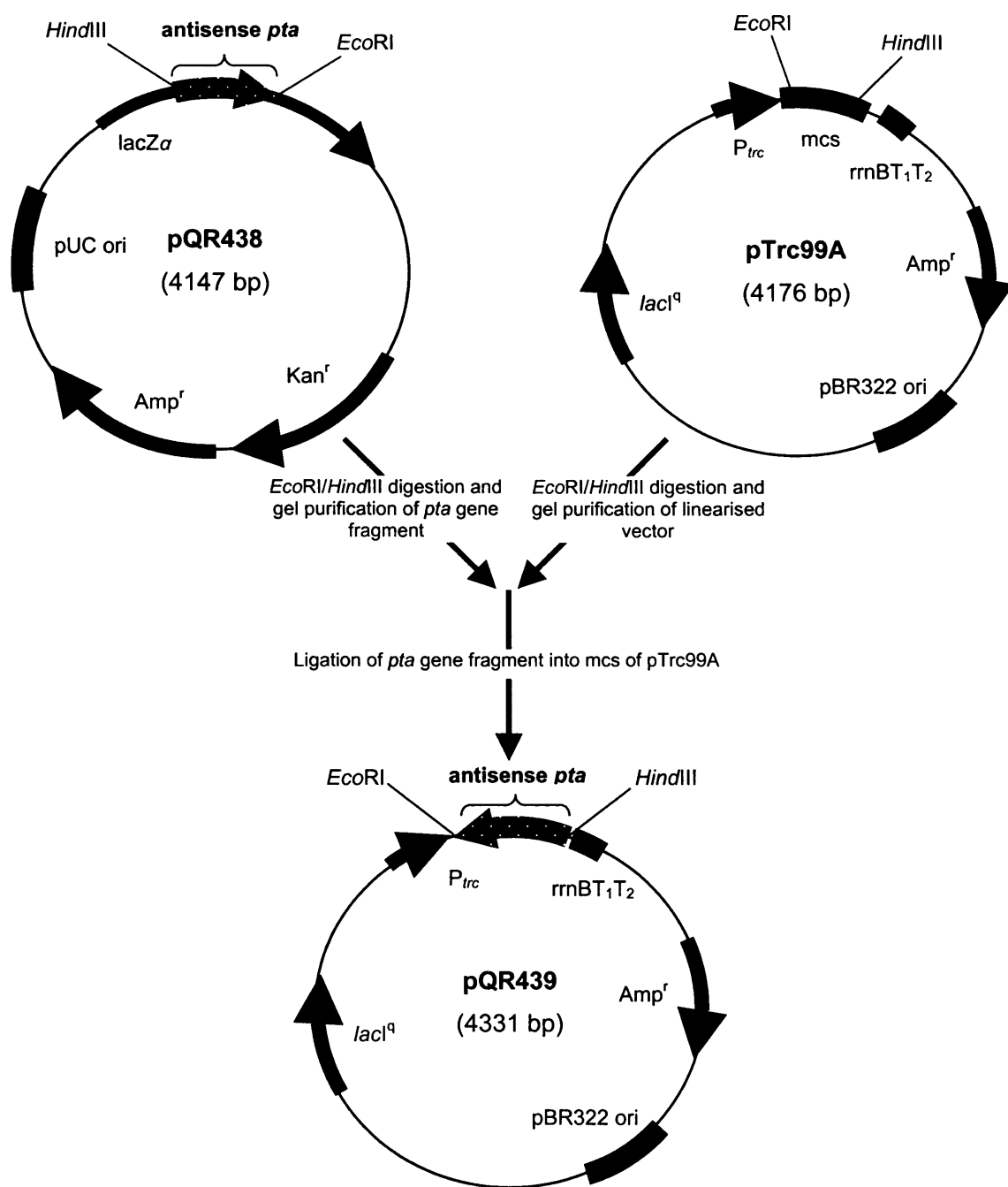
Figure 4.5 Construction of plasmid pQR439, designed to express antisense RNA targeted against the *E. coli* MG1655 *pta* gene. Relevant restriction sites are shown. Genes and plasmids are not drawn to scale.

4.3.2 DEVELOPMENT OF CONSTRUCTS FOR *ACKA* ANTISENSE RNA EXPRESSION

4.3.2.1 PQR441

Plasmid pQR441 was developed to express antisense RNA targeted against *E. coli* MG1655 *ackA* mRNA. Using *E. coli* MG1655 chromosomal DNA as a template, a 240 bp fragment of the 1202 bp *ackA* gene, encompassing the putative ribosome binding site and extending into the open reading frame, was amplified by PCR. The PRC primers were designed to introduce restriction sites at the 5' and 3' ends of the amplified gene fragment, to facilitate cloning of the PCR product into expression vector pTrc99A in an antisense orientation. The forward primer (5'-GC<u>AAGCTT</u>TATCAATTATAGGTACT-3') introduced a *Bam*HI restriction site onto the 5' end of the *ackA* gene fragment, and the reverse primer (5'-CG<u>CTTAAG</u>TAGTATTAACGATAAAG-3') introduced an *Eco*RI restriction site onto the 3' end of the *ackA* gene fragment. In total, the PCR product was 256 bp in length.

To ensure there was no significant chance of *ackA* antisense RNA binding to other mRNAs transcribed from the *E. coli* genome, the antisense strand of the *ackA* gene fragment was screened against the complete genome sequence of *E. coli* MG1655 using the BLASTn homology search (available at www.ncbi.nlm.nih.gov/BLAST/). The results showed that the *ackA* gene fragment had no significant homology with any other areas of the *E. coli* MG1655 genome.
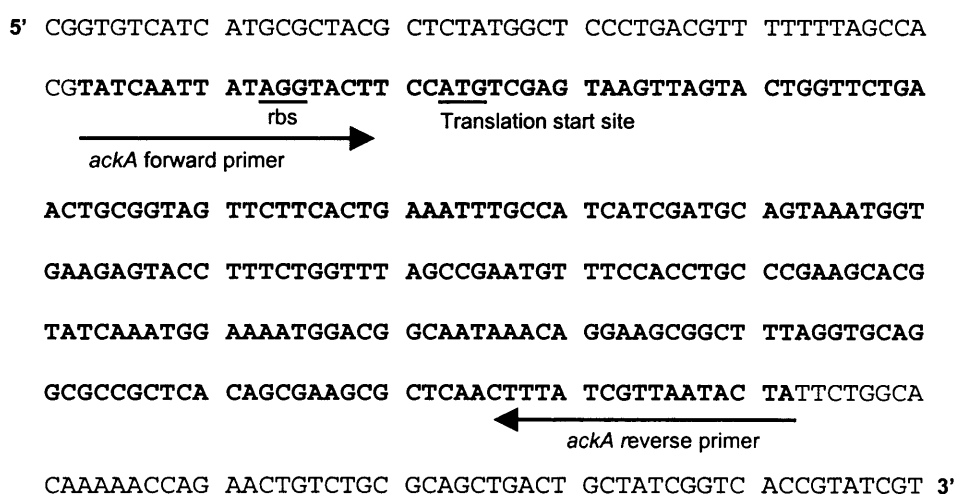
Figure 4.6 Partial DNA sequence of the *E. coli* MG1655 *ackA* gene. The 240 bp gene fragment amplified by PCR is highlighted in bold, and the location for primer binding is shown in relation to the *ackA* ribosome-binding site and translation start site.

The PCR-amplified *ackA* gene fragment was ligated into cloning vector pCR2.1-TOPO forming pQR440. *E. coli* TOP10 was transformed with the ligation mixture. Colonies of *E. coli* TOP10 harbouring pQR440 were identified by antibiotic selection and blue-white colour screening, followed by restriction analysis of the purified plasmid. In addition, a section of plasmid pQR440, encompassing the DNA insert, was sequenced to ensure that the plasmid contained the correct DNA insert, i.e. the *ackA* gene fragment.

Subsequently, the *ackA* gene fragment was excised from pQR440 by *Eco*RI/*Bam*HI double digestion and gel purified, prior to ligating in antisense orientation into the multiple cloning site of expression vector pTrc99A, forming pQR441 (Figure 4.8). The ligation mixture was used to transform *E. coli* DH5*a*. Restriction analysis of isolated pQR441 was performed to confirm presence of the *ackA* gene fragment (Figure 4.7). *E. coli* MG1655 was transformed with pQR441 for *ackA* antisense RNA expression studies.
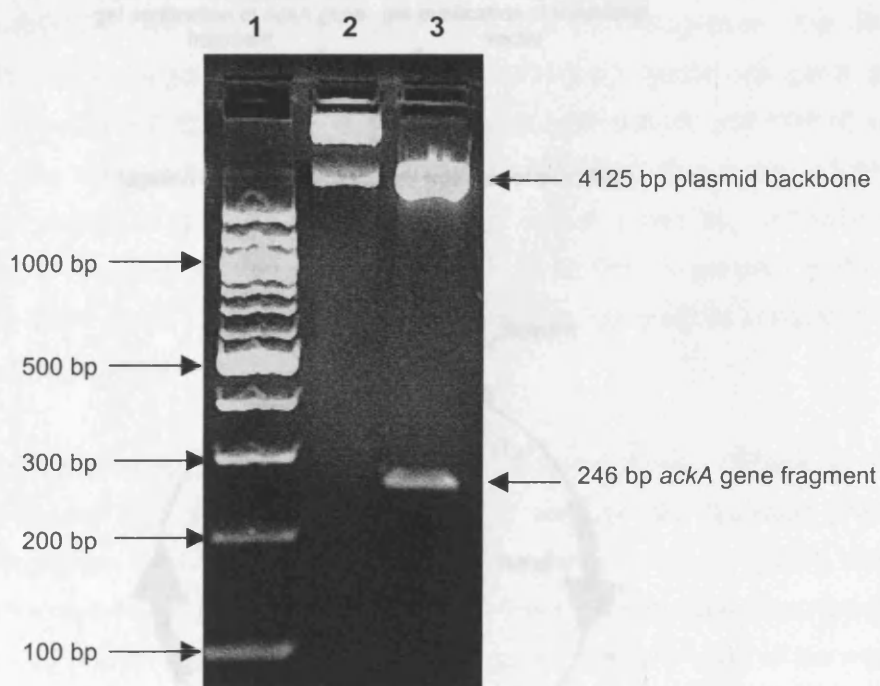
Figure 4.7   TBE agarose gel (2%) of pQR441 following *Eco*RI/*Bam*HI digestion. Lane 1, 100 bp ladder comprising DNA fragments of 100, 200, 300, 400, 500, 517, 600, 700, 800, 900, 1000, 1200 and 1517 bp; Lane 2, pQR441 undigested; Lane 3, pQR441 digested with *Eco*RI and *Bam*HI. Agarose gel electrophoresis was performed at 100 v for approximately 1 h (as described in Materials and Methods) and visualised under UV light.
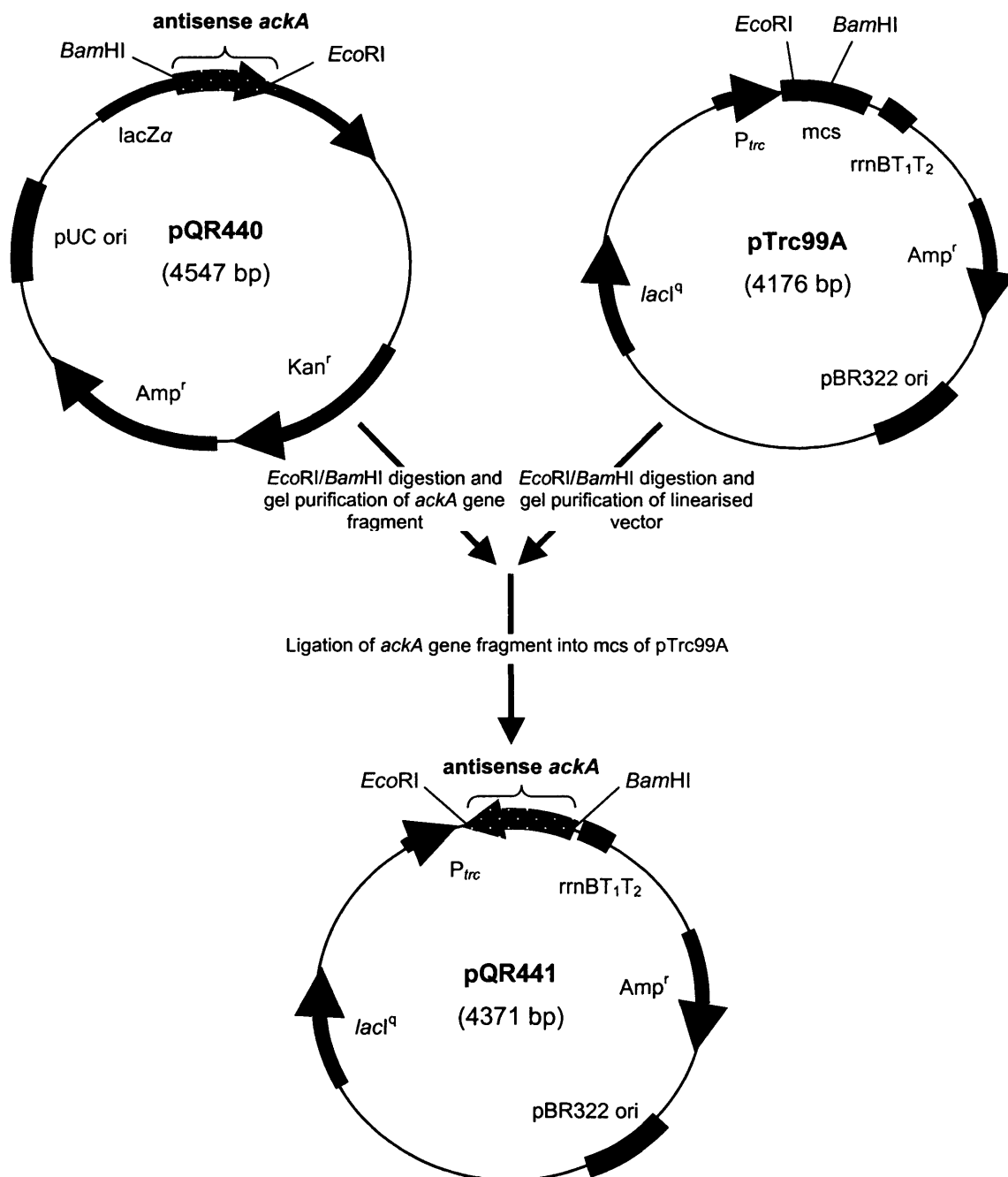
Figure 4.8 Construction of plasmid pQR441, designed to express antisense RNA targeted against the *E. coli* MG1655 *ackA* gene. Relevant restriction sites are shown. Genes and plasmids are not drawn to scale.

4.3.2.2   pQR445

Plasmid pQR445 was developed from pMMB66EH to provide a vector for antisense RNA expression, which can stably coexist in *E. coli* with pTrc99A-derived vectors, and has a different antibiotic selection marker. Both pTrc99A and pMMB66EH possess the β-lactamase gene which confers resistance to ampicillin, therefore it was decided to clone an aminoglycoside 3'-phosphotransferase gene, which confers resistance to kanamycin, into a unique *Pvu*I restriction site in the β-lactamase gene of pMMB66EH to abolish ampicillin resistance and introduce kanamycin resistance (Figure 4.11).

Using plasmid pUC4K as a template, a 1250 bp DNA fragment containing the 815 bp aminoglycoside 3'-phosphotransferase gene, which confers resistance to kanamycin, was amplified by PCR. PCR primers were designed to introduce *Pvu*I restriction sites at the 5' and 3' ends of the PCR product (PCR primer sequences: forward primer, 5'-GCCGATCGGTCGACCTGCAGGGGGGGGGGGGGGCGCTGA-3'; reverse primer, 5'-GCCGATCGGCAGGGGGGGGGGGGGGAAGCCACGTTGTGT-3'). Altogether, the PCR product was 1266 bp in length. The PCR-amplified kanamycin resistance gene was ligated into cloning vector pCR2.1-TOPO, forming plasmid pQR444. *E. coli* TOP10 was transformed with the ligation mixture. Colonies of *E. coli* TOP10 harbouring pQR444 were identified by antibiotic selection and blue-white colour screening, followed by restriction analysis of the purified fragment. In addition, a section of plasmid pQR444, encompassing the DNA insert was sequenced to ensure that the plasmid contained the correct DNA insert i.e. the kanamycin resistance gene.

Subsequently, the kanamycin resistance gene was excised from pQR444 in two fragments of 559 bp and 697 bp (due to an internal *Pvu*I site) by *Pvu*I digestion (Figure 4.9). The gene fragments were gel purified and then combined, prior to ligating into a unique *Pvu*I site located in the open reading frame of the ampicillin resistance gene in pMMB66EH, forming pQR445 (Figure 4.11). The ligation mixture was used to transform *E. coli* DH5α and colonies harbouring pQR445 were selected by plating on 10 μg ml^{-1} kanamycin. Plasmid pQR445 was then isolated, and the identity confirmed by restriction analysis. It proved difficult to achieve a sufficiently high yield and purity of plasmid pQR445 using the Qiagen Mini/Midiprep Kits, so pQR445 was purified on a caesium chloride gradient, by Dr John Ward. Restriction analysis of pQR445 confirmed presence of the kanamycin resistance gene, excised in two fragments from the 8.8 kb plasmid backbone by *Pvu*I digestion (Figure 4.10). *E. coli* MG1655 was transformed with pQR445 to generate a control strain for antisense RNA expression studies.
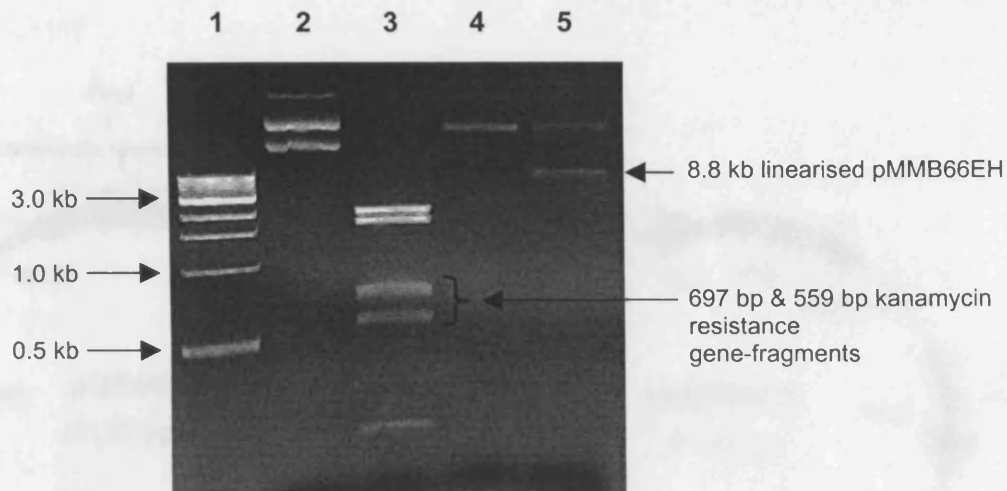
Figure 4.9 TBE agarose gel (1%) of pQR444 and pMMB66EH, following *Pvu*I digestion. Lane 1, 1 kb ladder comprising DNA fragments of 0.5, 1, 1.5, 2, 3, 4, 5, 6, 8 and 10 kb; Lane 2, pQR444 undigested; Lane 3, pQR444 digested with *Pvu*I; Lane 4, pMMB66EH undigested; Lane 5, pMMB66EH digested with *Pvu*I. Agarose gel electrophoresis was performed at 100 v, for approximately 1 h (as described in Materials and Methods) and visualised under UV light.
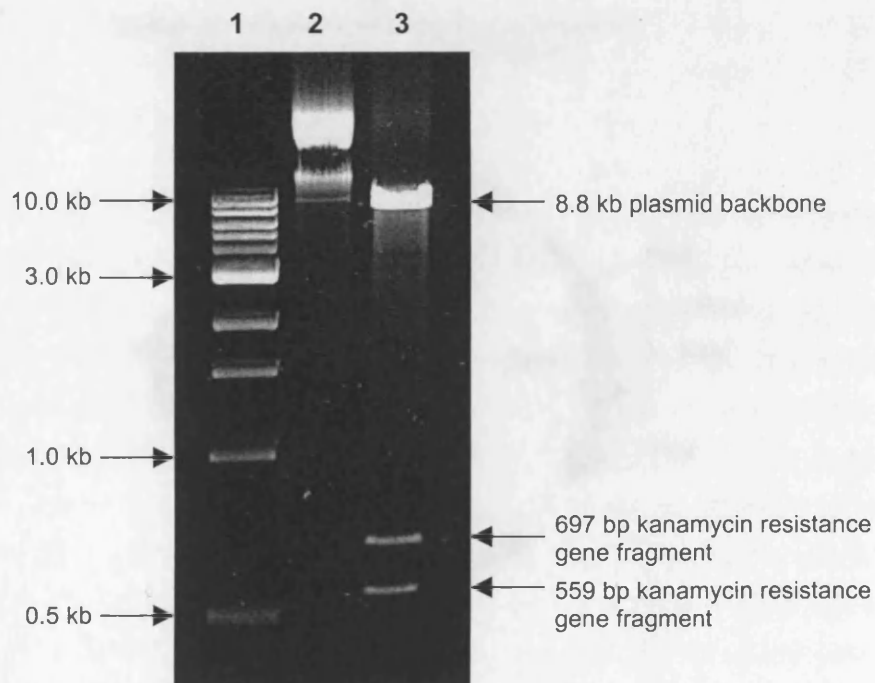
Figure 4.10 TBE agarose gel (1%) of pQR445 following *Pvu*I digestion. Lane 1, 1 kb ladder comprising DNA fragments of 0.5, 1, 1.5, 2, 3, 4, 5, 6, 8 and 10 kb; Lane 2, pQR445 undigested; Lane 3, pQR445 digested with *Pvu*I. Agarose gel electrophoresis was performed at 100 v, for approximately 1 h (as described in Materials and Methods) and visualised under UV light.
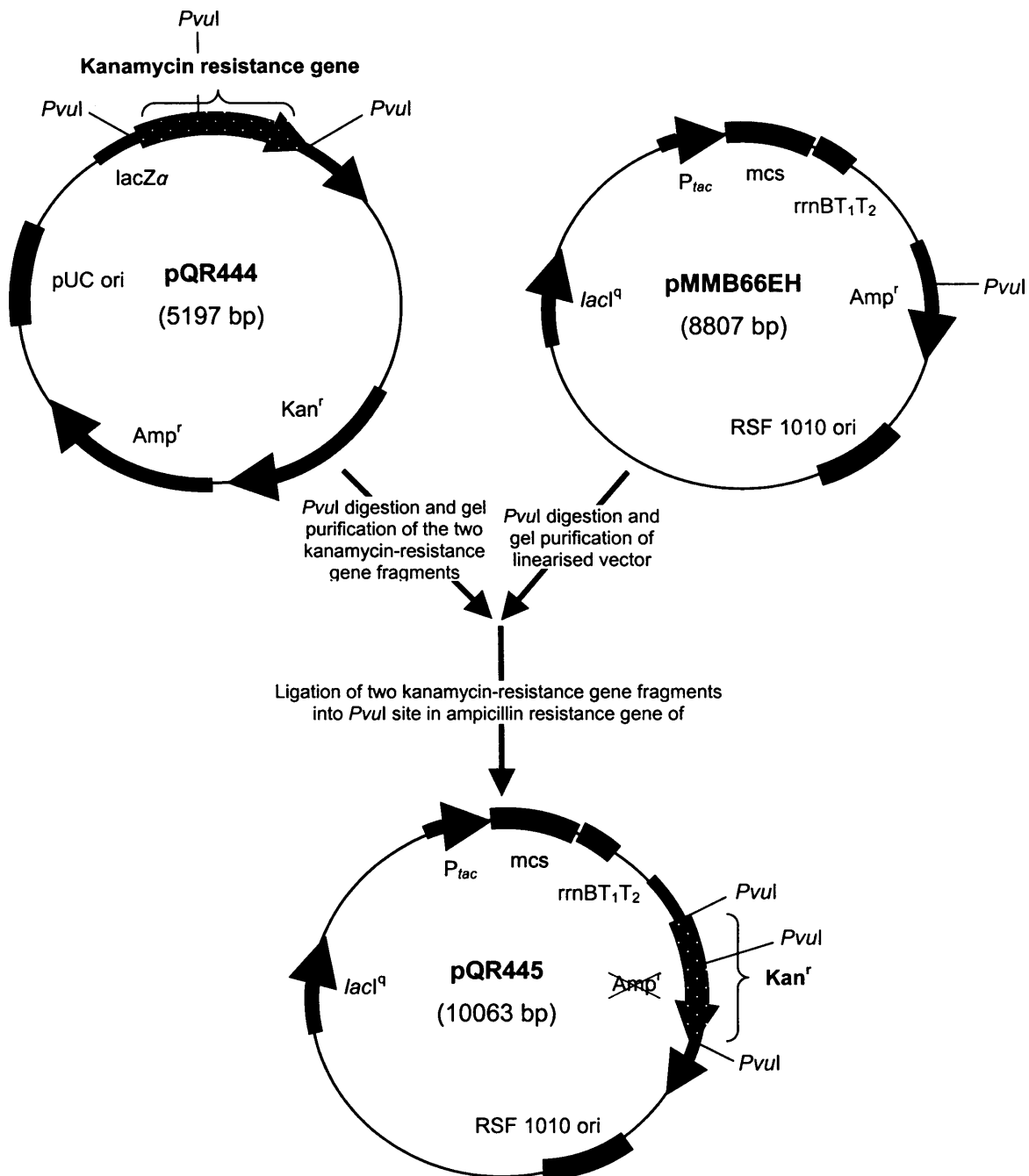
Figure 4.11 Construction of plasmid pQR445, developed from pMMB66EH to provide a vector for antisense RNA expression, which can stably coexist in *E. coli* with pTrc99A-derived vectors, and has a different selection marker (kanamycin). Relevant restriction sites are shown. Genes and plasmids are not drawn to scale.

4.3.2.3 PQR446

Plasmid pQR446 was designed to express antisense RNA targeted against *E. coli* MG1655 *ackA* mRNA. It was developed from pQR445 to enable co-expression of *pta* antisense RNA (from pQR439) and *ackA* antisense RNA (from pQR446) in *E. coli* MG1655. The same *ackA* gene fragment used to construct pQR441 (for details refer to section 4.3.2.1) was incorporated into pQR445 to generate pQR446.

The *ackA* gene fragment was excised from pQR440 by *Eco*RI/*Bam*HI double digestion and gel purified, prior to ligating in antisense orientation into the multiple cloning site of expression vector pQR445, forming pQR446 (Figure 4.13). The ligation mixture was used to transform *E. coli* DH5α, which resulted in a number of unusually slow growing colonies on selective nutrient agar. Five colonies were picked and cultured in nutrient broth, and the plasmid DNA was purified for analysis. However, due to the low concentration of the resulting plasmid DNA preparations, a restriction analysis was inconclusive. The problems with purification of pQR445 and pQR446 are likely to be due to the low copy number of the parent plasmid, pMMB66EH. Low copy number plasmids are known to be more difficult to work with and are not frequently used for laboratory work. Plasmid pMMB66EH was chosen to work with in this research because it is compatible with pTrc99A, in contrast to many other expression vectors, which are not.

Instead of restriction analysis, it was decided to use PCR to detect the *ackA* gene fragment in the five individual plasmid preparations of putative pQR446. The original primers, used to amplify the *ackA* gene fragment from *E. coli* MG1655 chromosomal DNA, were used for these PCR reactions. Negative and positive control PCRs were performed, with no template in the reaction, and with *E. coli* MG1655 chromosomal DNA as a template, respectively. The results, shown in Figure 4.12, indicate that the *ackA* gene fragment is present in all five plasmid preparations of putative pQR446. It is possible that the plasmid preparations could have been contaminated with chromosomal DNA, which would give the same results. However, subsequent analysis of a larger scale preparation of putative pQR446 confirmed the presence of a plasmid of the correct size. In addition, *E. coli* MG1655 transformed with pQR446 is resistant to kanamycin, but has different physiological properties from *E. coli* MG1655(pQR445). Specifically, pQR446 has a much lower growth rate. The physiological characterisation of *E. coli* MG1655(pQR446) is examined in detail in Chapter 6.
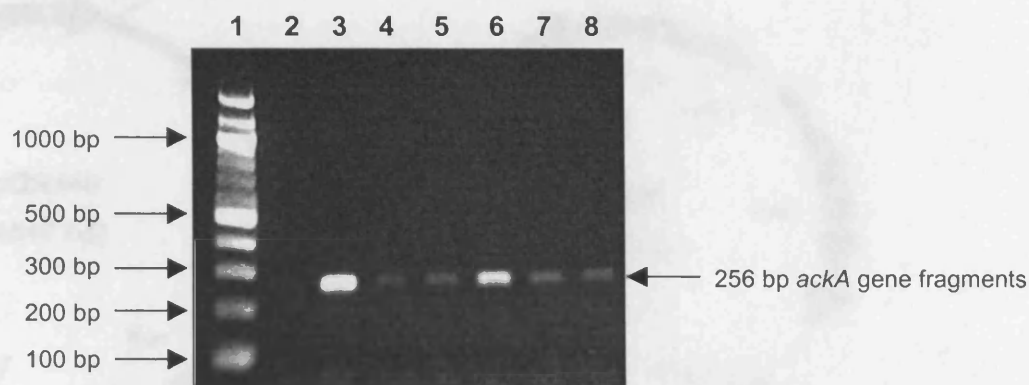
Figure 4.12 TBE agarose gel (1.5%) of PCR reactions, designed to amplify the *ackA* gene fragment from pQR446. Lane 1, 100 bp ladder comprising DNA fragments of 100, 200, 300, 400, 500, 517, 600, 700, 800, 900, 1000, 1200 and 1517 bp; Lane 2, negative control using no template in the reaction; Lane 3, positive control using MG1655 chromosomal DNA as a template for the reaction; Lanes 4-8 PCR reactions using pQR446 as the template and the original primers designed to amplify the *ackA* gene fragment. Agarose gel electrophoresis was performed at 100 v for approximately 1 h (as described in Materials and Methods) and visualised under UV light.
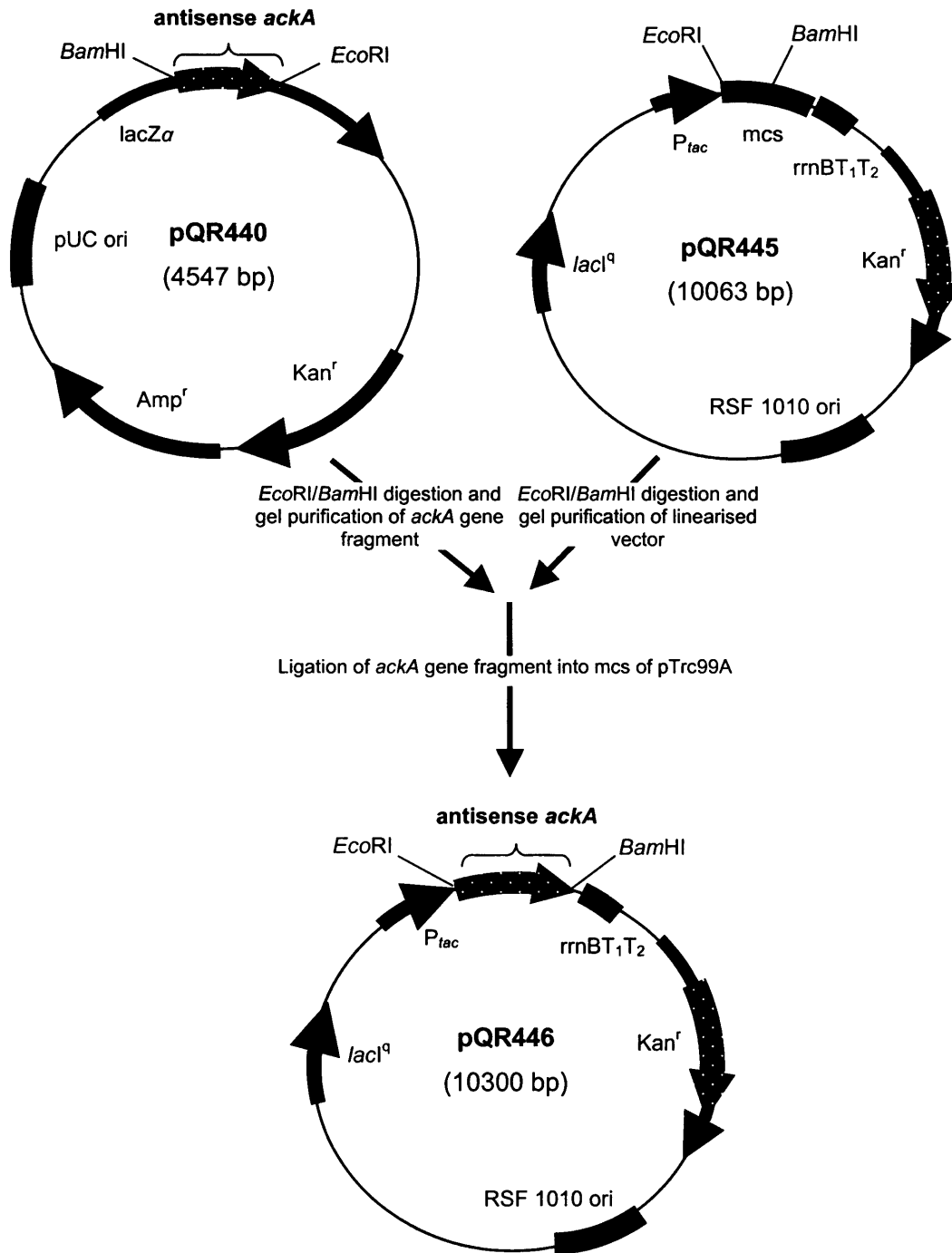
Figure 4.13 Construction of plasmid pQR446, designed to express antisense RNA targeted against the *ackA* gene. Relevant restriction sites are shown. Genes and plasmids are not drawn to scale.

4.4   RECOMBINANT *E. COLI* STRAINS

Table 4.2 describes the *E. coli* strains that were developed and characterised during this research. These include control strains, which comprise *E. coli* MG1655 containing just the empty expression vectors, and antisense RNA-expressing strains, which comprise *E. coli* MG1655 harbouring the antisense RNA constructs previously described in this chapter.

Table 4.2   Recombinant *E. coli* Strains

Strain Name	Plasmid(s)	Description
E. coli MG1655(pTrc99A)	pTrc99A	Control for *E. coli* strains harbouring a plasmid derived from pTrc99A.
E. coli MG1655(pQR439)	pQR439	*E. coli* with pTrc99A-derived plasmid that expresses antisense RNA targeted against phosphotransacetylase
E. coli MG1655(pQR441)	pQR441	*E. coli* with pTrc99A-derived plasmid that expresses antisense RNA targeted against acetate kinase
E. coli MG1655(pQR445)	pQR445	Control for *E. coli* strains harbouring a plasmid derived from pQR445
E. coli MG1655(pQR446)	pQR446	*E. coli* with pQR445-derived plasmid that expresses antisense RNA targeted against acetate kinase
E. coli MG1655(pTrc99A/pQR445)	pTrc99A & pQR445	Control for *E. coli* strain harbouring two plasmids, one derived from pTrc99A and one from pQR445
E. coli MG1655(pQR439/pQR446)	pQR439 & pQR446	*E. coli* with a pTrc99A-derived plasmid that expresses antisense RNA targeted against phosphotransacetylase and pQR445-derived plasmid that expresses antisense RNA targeted against acetate kinase

4.4.1 DUAL-PLASMID HARBOURING STRAINS

4.4.1.1 *E. COLI* MG1655(pTrc99A/pQR445)

E. coli MG1655(pTrc99A/pQR445) was developed as a plasmid control strain for *E. coli* MG1655(pQR439/pQR446) (see section 4.4.1.2). *E. coli* MG1655 was transformed with pTrc99A and pQR445 simultaneously, and plated on selective nutrient agar plates containing 10 µg ml^{-1} kanamycin and 500 µg ml^{-1} ampicillin to select for double transformants. Figure 4.14 shows plasmids pTrc99A and pQR445 isolated from MG1655(pTrc99A/pQR445) and linearised by *Eco*RI digestion. The observed difference in the band intensities of pQR445 and pTrc99A is due to the difference in copy number between these two plasmids. pTrc99A, which is a derivative of pBR322, has an average copy number of ~50-80 plasmids/cell, depending on the media and cell growth phase (Lin-Chao and Bremer, 1986). In contrast, pMMB66EH, which is a derivative of RSF1010, has a lower average copy number of ~10-15 plasmids/cell (Morales et al., 1990).
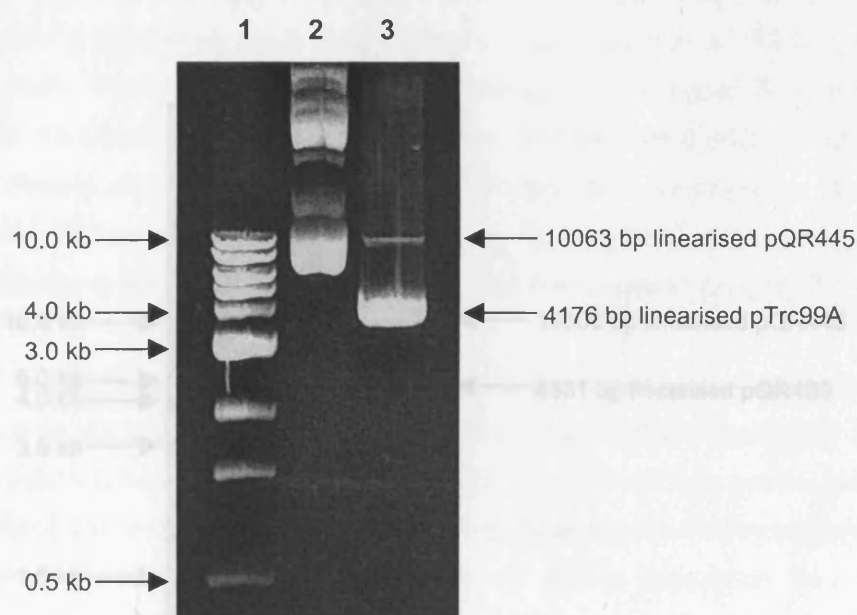
Figure 4.14 TBE Agarose gel (1%) of pTrc99A and pQR445, isolated from a culture of *E. coli* MG1655(pTrc99A/pQR445) and linearised by *Eco*RI digestion. Lane 1, 1 kb ladder comprising DNA fragments of 0.5, 1, 1.5, 2, 3, 4, 5. 6. 8. 10 kb; Lane 2, pTrc99A and pQR445 undigested; Lane 3, pTrc99A and pQR445 digested with *Eco*RI. Agarose gel electrophoresis was performed at 100 v for approximately 1 h (as described in Materials and Methods) and visualised under UV light.

## 4.4.1.2   *E. COLI* MG1655(PQR439/PQR446)

E. coli MG1655(pQR439/pQR446) was developed to express antisense RNA targeted against both the *pta* and *ackA* genes. Competent *E. coli* MG1655 transformed with pQR439 and pQR446 simultaneously did not result in any colonies on selective nutrient agar, therefore *E. coli* MG1655(pQR439/pQR446) was developed by preparing competent *E. coli* MG1655(pQR439), and transforming an aliquot of these with pQR446. Cell counts of MG1655(pQR439/pQR446) grown on selective and non-selective nutrient agar revealed that 10 μg ml^{-1} kanamycin and 500 μg ml^{-1} ampicillin stably maintained both plasmids in *E. coli* MG1655.

Plasmids pQR439 and pQR446 isolated from MG1655(pQR439/pQR446) and linearised by *Eco*RI digestion, are shown in Figure 4.15. As mentioned in the previous section, the observed difference in band intensities for pQR439 and pQR446 is due to the difference in the copy numbers of these two plasmids. It is possible that the discrepancy in copy number will affect the level of antisense RNA expressed from these plasmids. This is discussed further in the following section (section 4.5).
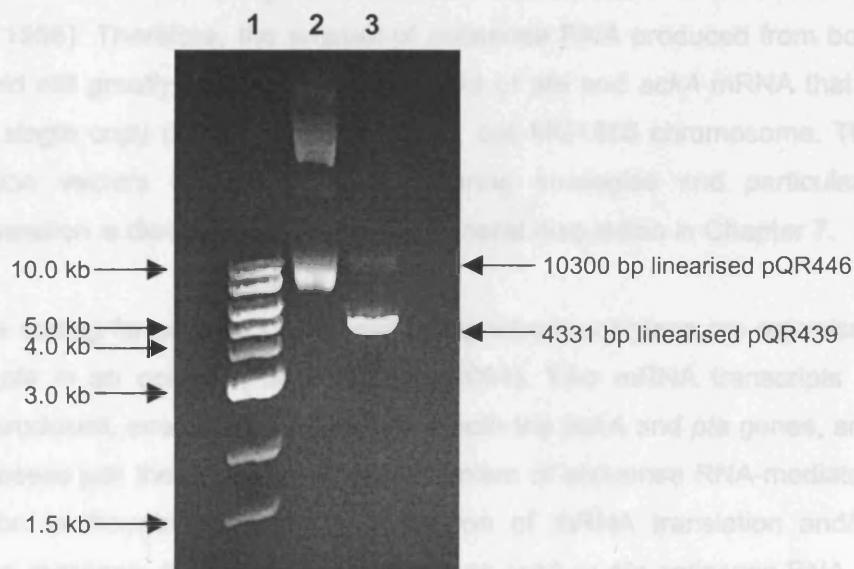
Figure 4.15 TBE Agarose gel (1%) of pQR439 and pQR446, isolated from a culture of *E. coli* MG1655(pQR439/pQR446) and linearised by *Eco*RI digestion. Lane 1, 1 kb ladder comprising DNA fragments of 0.5, 1, 1.5, 2, 3, 4, 5. 6. 8. 10 kb; Lane 2, pQR439 and pQR446 undigested; Lane 3, pQR439 and pQR446 digested with *Eco*RI. Agarose gel electrophoresis was performed at 100 v for approximately 1 h (as described in Materials and Methods) and visualised under UV light.

4.5 DISCUSSION AND CONCLUSIONS

This chapter described the construction of seven novel plasmids, which were generated using molecular biology techniques for DNA recombination. Four intermediary plasmids (pQR438, pQR440, pQR444, pQR445) were constructed in order to produce a *pta* antisense RNA expression vector (pQR439), and two *ackA* antisense RNA expression vectors (pQR441, pQR446). *E. coli* MG1655 was transformed with the individual plasmids, and with combinations of compatible plasmids, to generate seven recombinant strains for antisense RNA expression studies.

The novel plasmids that were constructed in this research were derived from the expression vectors pTrc99A and pMMB66EH. pTrc99A is a relatively high copy number plasmid, with an average copy number of ~50-80 plasmids/cell (Lin-Chao and Bremer, 1986). In contrast, pMMB66EH is a relatively low copy number plasmid, with an average copy number of ~10-15 plasmids/cell (Morales et al., 1990). The difference in plasmid copy number may potentially affect the relative amount of antisense RNA produced from the constructs derived from each plasmid-type. However, the promoters used for antisense RNA expression are the strong *trc* and *tac* promoters (Amann et al., 1988; Lin-Chao and Bremer, 1986). Therefore, the amount of antisense RNA produced from both plasmid types should still greatly out-number the amount of *pta* and *ackA* mRNA that is produced from the single copy of each gene on the *E. coli* MG1655 chromosome. The choice of expression vectors for metabolic engineering strategies and particularly antisense RNA expression is discussed further in the general discussion in Chapter 7.

In *E. coli,* the genes coding for acetate kinase and phosphotransacetylase are organised in the order *ackA-pta* in an operon (Kakuda et al., 1994). Two mRNA transcripts of different sizes are produced, one which encompasses both the *ackA* and *pta* genes, and one which encompasses just the *pta* gene. The mechanism of antisense RNA-mediated gene downregulation is thought to involve suppression of mRNA translation and/or destabilisation of the message, therefore binding of either *ackA* or *pta* antisense RNA to the dual message could potentially affect the expression of both genes. This was evaluated by examining the enzyme levels of both phosphotransacetylase and acetate kinase in all the strains that were characterised in this study. The results are discussed in the following chapter (Chapter 5).

Factors to consider, which might affect the suppression of *pta* and *ackA* gene expression by antisense RNA are: 1) the stability of the antisense RNA products in *E. coli*; 2) the rate of antisense RNA binding to the target mRNA; and 3) the half-life of

phosphotransacetylase and acetate kinase proteins. This information is not known, however it may be possible to gain some insight into the half-life of phosphotransacetylase and acetate kinase by the experiments that were performed in this study.

Analysis of the recombinant *E. coli* strains involved physiological characterisation, which is described in the following chapter (Chapter 5), and metabolic flux analysis, which is described in Chapter 6.

CHAPTER 5

IMPACT OF PUTATIVE ANTISENSE RNA EXPRESSION ON GROWTH AND ORGANIC ACID PRODUCTION BY *E. COLI* MG1655

5.1 SUMMARY

The objective of this study was to determine the impact of putative *pta* and *ackA* antisense RNA on growth, enzyme levels and organic acid production by *E. coli* MG1655. Four novel *E. coli* strains were constructed to express antisense RNA targeted against phosphotransacetylase mRNA and/or acetate kinase mRNA, as described in the previous chapter (Chapter 4). This chapter describes the physiological effect of putative antisense RNA expression, as determined by shake flask and bioreactor experiments. Growth, enzyme levels and organic acid production were evaluated in the antisense RNA-expressing cultures and compared with those of the control cultures, which harboured the parent plasmids.

It was hypothesised that putative *pta/ackA* antisense RNA would partially suppress expression of phosphotransacetylase and acetate kinase, and result in reduced acetate production by *E. coli* MG1655. Previous studies with mutant *E. coli* strains have indicated that in the absence of the *ackA-pta* pathway, excess carbon flux in central metabolism is re-directed towards lactate production (Chang et al., 1999; Diaz-Ricci et al., 1991). The aim of this study was to determine the effectiveness of antisense RNA in suppressing expression of phosphotransacetylase and acetate kinase, and re-directing carbon flow in *E. coli* central metabolism.

Shake flask and bioreactor experiments showed that expression of putative *pta* antisense RNA from plasmid pQR439 resulted in ~40% reduction in phosphotransacetylase levels in *E. coli* MG1655 compared to the control culture, and a ~10-15% decrease in total acetate accumulation. Furthermore, *E. coli* MG1655(pQR439) showed ~2-fold increase in lactate production compared to the control. Expression of putative *ackA* antisense RNA from plasmid pQR441 resulted in ~40% reduction in acetate kinase and ~50-60% reduction in phosphotransacetylase levels in *E. coli* MG1655. However, acetate accumulation was still only reduced by ~12-20% in the antisense RNA-regulated cultures, compared to the control culture. In contrast, expression of putative *ackA* antisense RNA from plasmid pQR446 led to severe growth retardation, reduced acetate production and dramatically increased lactate production in *E. coli* MG1655. However, the control culture harbouring the parent plasmid for this set of experiments had lower enzyme levels and acetate production than the control culture for the previous sets of experiments, which suggested that some component of the parent plasmid, pQR445, might interfere with acetate production by *E. coli* MG1655.

Simultaneous expression of *pta* & *ackA* antisense RNA from plasmids pQR439 and pQR446 respectively, achieved ~40% reduction in phosphotransacetylase levels compared to the control culture harbouring the parent plasmids. The levels of acetate kinase were also reduced in this culture, compared to the parent strain, and no growth retardation was observed. Furthermore, total acetate accumulation was reduced by up to ~28%, compared to the control culture. However the control culture, *E. coli* MG1655(pTrc99A/pQR445) exhibited ~40% lower levels of acetate accumulation compared to the original control culture *E. coli* MG1655(pTrc99A). This again suggested that the presence of plasmid pQR445 lead to reduced acetate production by *E. coli* MG1655. In conclusion, the fermentation results indicated that *pta* and/ or *ackA* antisense RNA partially suppressed expression of phosphotransacetylase and acetate kinase in *E. coli* MG1655, resulting in decreased levels of acetate formation and redirection of carbon flux to lactate production.

5.2 IMPACT OF PUTATIVE *PTA* ANTISENSE RNA ON GROWTH AND PRODUCTION FORMATION

5.2.1 CONSTRUCTION OF *E. COLI* MG1655(PQR439)

Plasmid pQR439 was constructed to express a 200-nucleotide *pta* antisense RNA molecule, complementary to the 5' region of *pta* mRNA encompassing the ribosome-binding site and translation initiation site. *E. coli* K-12 strain MG1655 was transformed with plasmid pQR439, as described in Materials and Methods, and the identities of ampicillin-resistant transformants as *E. coli* MG1655(pQR439) were verified by plasmid isolation and restriction analysis (see section 4.3.1.1). *E. coli* MG1655(pQR439) cultured on selective nutrient agar exhibited growth characteristics that were typical of *E. coli* MG1655.

In the following pages, shake flask and bioreactor experiments to evaluate the impact of putative *pta* antisense RNA on growth and product formation are described. *E. coli* MG1655 harbouring the parent plasmid, pTrc99A, was used as a control strain for these studies. *E. coli* MG1655(pQR439) was studied under 'uninduced' conditions, i.e. no IPTG was added to the culture medium, and under 'induced' conditions, in which IPTG (1mM) was added to the culture medium at early-mid log phase (after 3 hours growth). All the plasmids were stably maintained throughout the 24 hour study.

Under uninduced conditions, expression of *pta* antisense RNA from the *trc* promoter on plasmid pQR439 should be repressed. However, there may be 'leaky' expression of *pta* antisense RNA from the uninduced plasmid. Therefore, comparing the profiles of the uninduced culture of *E. coli* MG1655(pQR439) with the plasmid control culture should indicate how well expression of antisense RNA from this construct is regulated.

5.2.2   SHAKE FLASK ANALYSIS OF *E. COLI* MG1655(PQR439)

The objective of this study was to determine the effect of *pta* antisense RNA expression on growth and acetate production by *E. coli* MG1655 in shake flask culture, prior to a more detailed study in controlled bioreactors. Two *E. coli* strains were used in this study: *E. coli* MG1655(pQR439), generated to express antisense RNA targeted against phosphotransacetylase; and *E. coli* MG1655(pTrc99A), a control strain harbouring the parent plasmid. Experimental conditions for the shake flask experiments are detailed in Table 5.1, and the results are presented and discussed in the following pages.

Table 5.1   Experimental conditions for testing the effect of putative *pta* antisense RNA in shake flask experiments

Strains	*E. coli* MG1655(pQR439) (see Table 2.1) *E. coli* MG1655(pTrc99A) (see Table 2.1)
Media	M9 minimal media, 10 g L^{-1} glucose, trace element mix, 20 µg ml^{-1} uracil, 5 µg ml^{-1} thymidine, 100 µg ml^{-1} ampicillin. (see Table 2.4)
Growth Mode	Batch, 2 L shake flask (250 ml total working volume)
Temperature	37°C
Shaker Speed	200 rpm
Sampling Times	0, 1, 2, 3, 4, 5, 6, 7, 8, and 24 h
IPTG Addition Time	3 h

5.2.2.1   GROWTH AND GLUCOSE UPTAKE BY *E. COLI* MG1655(PQR439)

The impact of putatively produced *pta* antisense RNA on maximum biomass concentration (expressed as OD_{600}), growth rate and glucose uptake rate is summarised in Table 5.2. Time course profiles of cell density and residual glucose concentration are shown in Figure 5.1. Overall, the results indicated that growth and glucose uptake were comparable in all three cultures. During the exponential growth phase, the cell densities in the induced and uninduced cultures of *E. coli* MG1655(pQR439) were lower than in the control culture. However, all the cultures achieved a similar final biomass concentration after 24 h growth. Glucose was depleted at similar rates for all three cultures.

Table 5.2   Summary of substrate uptake and biomass formation in shake flask experiments

Fermentation characteristic	MG1655(pTrc99A)	MG1655(pQR439) uninduced	MG1655(pQR439) induced
	(control)	(antisense *pta*)	(antisense *pta*)
Max. OD_{600}[a]	5.5 ± 0.1	5.3 ± 0.02	5.4 ± 0.02
Growth Rate (h^{-1})[b]	0.51 ± 0.08	0.55 ± 0.03	0.54 ± 0.03
Glucose Uptake Rate $(mM\ h^{-1})$[b]	6.1 ± 0.5	4.7 ± 0.2	5.3 ± 0.5

[a] Mean ± standard error of the mean.

[b] Rate established over the range 2-6 hours after inoculation (± standard error).
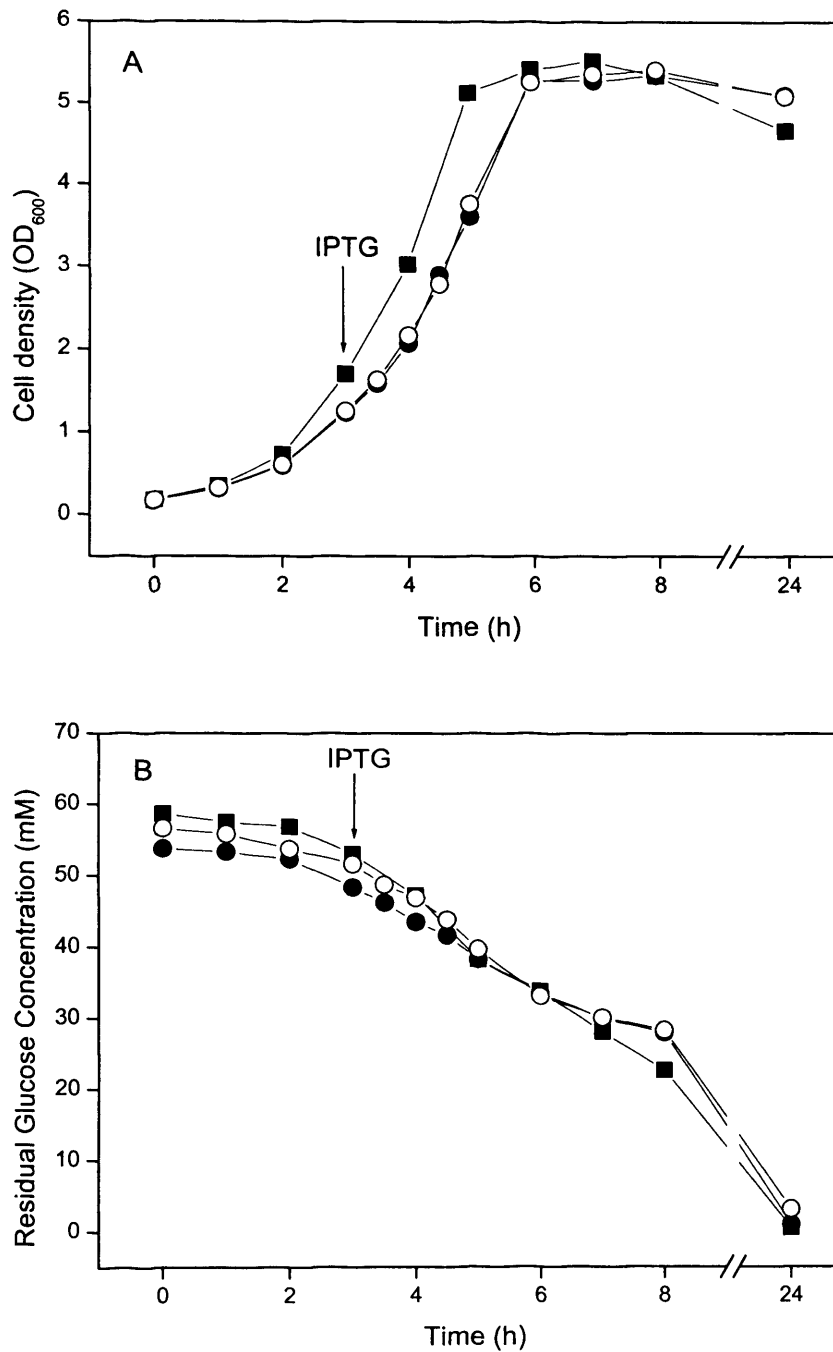
Figure 5.1 Time-course profiles of (A) cell growth and (B) residual glucose concentration in E. coli MG1655 harbouring pTrc99A (■), pQR439 uninduced (●), and pQR439 induced (○). Recombinant cells were cultured in 2 L baffled shake flasks containing 250 ml of M9 medium with 1% (wt/vol) glucose at 37°C and shaken at 200 rpm. The arrow indicates the point of induction with 1 mM IPTG. Duplicate analyses were performed for each sample; average values of the duplicates are shown.

5.2.2.2   ORGANIC ACID PRODUCTION BY *E. COLI* MG1655(PQR439)

As previously discussed in Chapter 1 (section 1.2.3.2), *E. coli* grown with glucose under aerobic conditions produces acetate as the main by-product of fermentation. However, under anaerobic conditions, ethanol, formate, succinate and lactate are often produced, in addition to acetate (Clark, 1989). The fermentative pathways leading to succinate, lactate and ethanol formation play an important role in regenerating NAD^+ in the absence of oxidative phosphorylation, as shown in Figure 1.2. In this study, it was hypothesised that reducing the carbon flow to acetate might result in re-channelling of carbon to some of these other by-products, even under aerobic conditions. Furthermore, although pyruvate is not typically excreted by *E. coli*, some previous studies have observed pyruvate excretion in *pta* mutant strains (Chang et al., 1999; Diaz-Ricci et al., 1991; Kakuda et al., 1994). Therefore, the concentrations of acetate, pyruvate, succinate, lactate and ethanol in the culture medium were examined in all the physiological studies that are presented in this chapter. Formate was not produced by any of the *E. coli* cultures that were studied. This was expected because pyruvate formate lyase, which converts pyruvate to formate, is only expressed under anaerobic conditions. It is extremely sensitive to molecular oxygen, which causes irreversible inactivation due to peptide bond cleavage of one of the protein subunits (Becker et al., 1999; Knappe and Sawers, 1990).

The impact of putatively produced *pta* antisense RNA on organic acid production by *E. coli* MG1655 in shake flask culture is summarised in the following pages. Results showed that there was negligible difference in the production of pyruvate, lactate, succinate or ethanol by *E. coli* MG1655(pQR439) compared to the control culture (Table 5.3 A). However, acetate production was reduced in both the induced and uninduced cultures of *E. coli* MG1655(pQR439), compared to the control culture.

The peak acetate concentration was reduced by ~30% in the induced culture of *E. coli* MG1655(pQR439), and by ~23% in the uninduced culture of *E. coli* MG1655(pQR439), compared to the control culture (Table 5.3 A). Furthermore, the acetate production rates were also lower in these cultures during exponential growth phase (Table 5.3 B), and the total amount of acetate produced (mmoles) per 100 mmoles of glucose consumed followed the same trend (Table 5.3 C). These initial results are promising and suggest that production of acetate in *E. coli* MG1655 is reduced by expression of putative *pta* antisense RNA.

Time course profiles of acetate accumulation are shown in Figure 5.2. All the cultures exhibited peak acetate levels after 24 hours growth. The peak acetate levels were more than 2-fold higher than the acetate levels after 8 hours growth, which suggests that during stationary phase all the cultures continued to metabolise glucose and produce acetate.

During mid-late exponential growth phase, the acetate levels are slightly lower in both the induced and uninduced cultures of *E. coli* MG1655(pQR439), compared to the control culture. This may have been due to lower biomass levels during this time. However, after 24 hours growth, the biomass levels were comparable in all three cultures, but there was lower levels of acetate in both the induced and uninduced cultures of *E. coli* MG1655(pQR439). The similarity in profiles of the induced and uninduced cultures of *E. coli* MG1655(pQR439) suggests that putative *pta* antisense RNA was expressed from pQR439 even under repressed conditions. This will be discussed further in light of the bioreactor experiments.

Figure 5.2 Time course profiles of acetate concentration in *E. coli* MG1655 harbouring pTrc99A (■), pQR439 uninduced (●), and pQR439 induced (o). Recombinant cells were cultured in 2 L baffled shake flasks containing 250 ml of M9 medium with 1% (wt/vol) glucose at 37°C and shaken at 200 rpm. The arrow indicates the point of induction with 1 mM IPTG.

Table 5.3

Summary of organic acid production in shake flask experiments: (A) Peak Product Concentration, (B) Production Rate, and (C) mmoles produced per 100 mmoles of glucose consumed.

A

Peak Product Concentration (mM)	MG1655(pTrc99A)	MG1655(pQR439) uninduced	MG1655(pQR439) induced
	(control)	(antisense *pta*)	(antisense *pta*)
Acetate	30	23	21
Pyruvate	2	< 1	1
Lactate	1	2	< 1
Succinate	3	3	2
Ethanol	<1	< 1	< 1

B

Production Rate (mM h^{-1})[a]	MG1655(pTrc99A)	MG1655(pQR439) uninduced	MG1655(pQR439) induced
	(control)	(antisense *pta*)	(antisense *pta*)
Acetate	1.9 ± 0.1	1.2 ± 0.05	1.3 ± 0.05

[a] Rate established over the range 2-6 hours after inoculation (± standard error).

C

mmoles produced / 100 mmoles glucose consumed	MG1655(pTrc99A)	MG1655(pQR439) uninduced	MG1655(pQR439) induced
	(control)	(antisense *pta*)	(antisense *pta*)
Acetate	50	42	39

5.2.3 ANALYSIS OF *E. COLI* MG1655(PQR439) IN A CONTROLLED BIOREACTOR

The objective of this study was to determine the effect of *pta* antisense RNA expression on growth, enzyme levels and organic acid production by *E. coli* MG1655, cultured in a controlled bioreactor. Two *E. coli* strains were used in this study: *E. coli* MG1655(pQR439), generated to express antisense RNA targeted against phosphotransacetylase; and *E. coli* MG1655(pTrc99A), a control strain harbouring the parent plasmid. Experimental conditions for the bioreactor experiments are detailed in Table 5.4, and the results are presented and discussed in the following pages.

Table 5.4 Experimental conditions for testing the effect of putative *pta* antisense RNA in bioreactor experiments

Strains	*E. coli* MG1655(pQR439) (see Table 2.1) *E. coli* MG1655(pTrc99A) (see Table 2.1)
Media	M9 minimal media, 10 g L^{-1} glucose, trace element mix, 20 $\mu g \, ml^{-1}$ uracil, 5 $\mu g \, ml^{-1}$ thymidine, 100 $\mu g \, ml^{-1}$ ampicillin. (see Table 2.4)
Growth Mode	Batch, 2 L bioreactor (1 L working volume), pH control
Temperature	37°C
Agitation Speed	800 rpm
Air Flow Rate	1 vvm
Sampling Times	0, 1, 2, 3, 4, 5, 6, 7, 8, and 24 h
IPTG Addition Time	3 h

5.2.3.1   OPTIMISATION OF AERATION CONDITIONS FOR BIOREACTOR EXPERIMENTS

Prior to the first bioreactor experiment, the airflow rate and rate of agitation in the fermentor vessel were optimised to ensure that the *E. coli* cultures would remain fully aerated during the course of a 24-hour long fermentation. A culture of the control strain, *E. coli* MG1655(pTrc99A), was used to establish the optimum conditions.

Initially the airflow rate was set at 0.5 vvm, and the agitation rate at 500 rpm. By monitoring the %DOT (dissolved oxygen tension) in the culture, it was apparent that the available oxygen in the culture was depleted rapidly. Therefore, the airflow rate and agitation rate were increased in a step-wise fashion up to 1 vvm and 800 rpm respectively. At these levels, the %DOT in a culture of *E. coli* MG1655(pTrc99A) remained above 60% for the duration of a 24 hour fermentation (Figure 5.3 A). These parameters were kept constant for all of the bioreactor experiments that are presented in this chapter.

Time course profiles of %DOT, carbon dioxide production rate (CPR) and oxygen uptake rate (OUR), for a culture of *E. coli* MG1655(pTrc99A), are shown in Figure 5.3. Oxygen was utilised and carbon dioxide was produced rapidly, and at the same rate, for the first 6 hours of the fermentation, which corresponded to exponential growth phase on glucose. The subsequent sharp peak at ~6h corresponded to depletion of ammonium chloride, which is the nitrogen source in M9 minimal media. Hence, nitrogen depletion coincides with the onset of stationary phase in the culture (data not shown). The effect of nitrogen depletion on the levels of acetate produced by *E. coli* will be discussed at the end of this chapter in section 5.5. Off-gas profiles for all bioreactor experiments in this chapter were recorded, and showed little variation from these profiles.
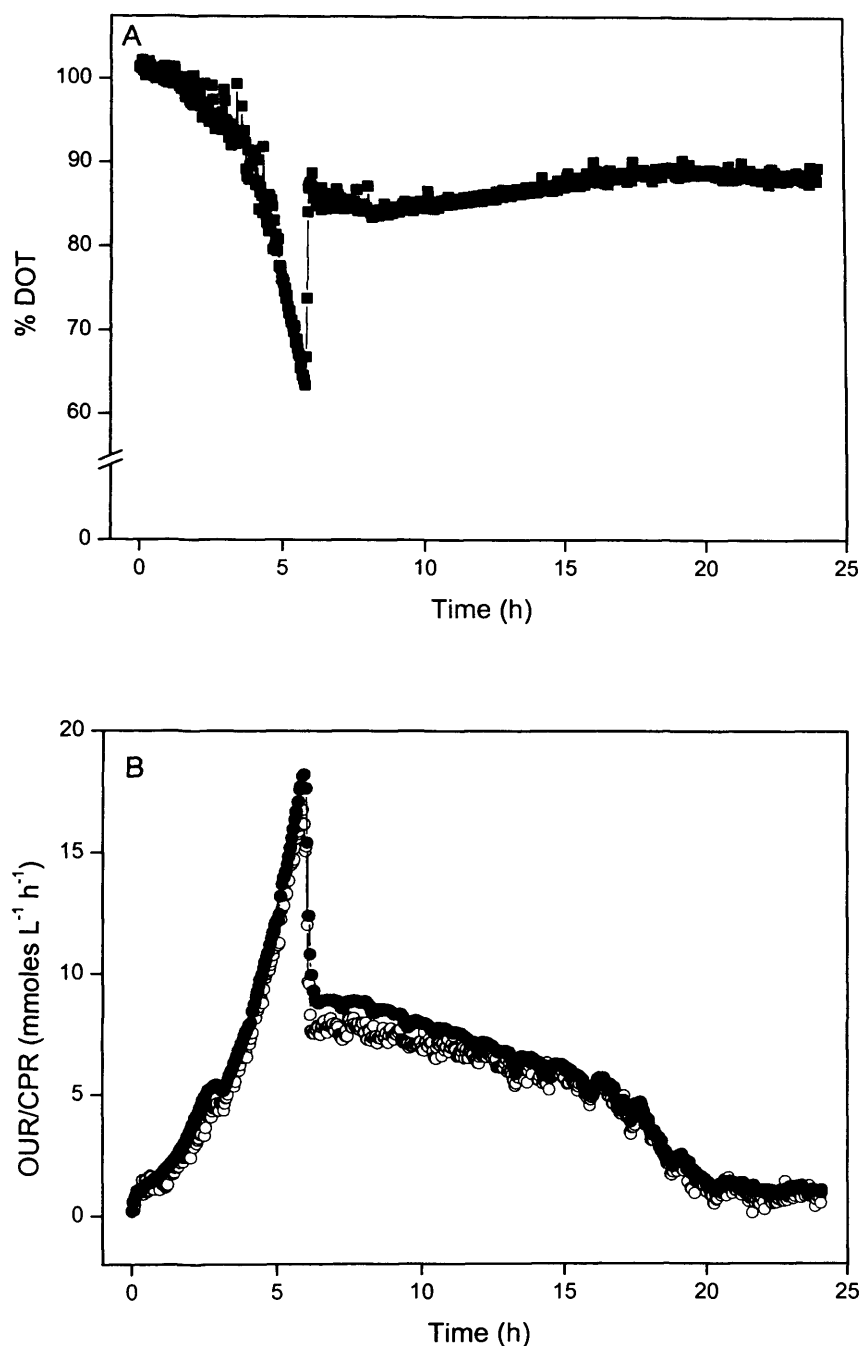
Figure 5.3 Time course profiles of (A) % DOT (■), and (B) OUR (o) and CPR (●), in *E. coli* MG1655 harbouring pTrc99A. Recombinant cells were cultured in a 2 L baffled fermenter containing 1 L of M9 medium with 1% (wt/vol) glucose at 37°C. The airflow rate was set at 1 vvm and the rate of agitation was set at 800 rpm, to ensure the culture was fully aerated. The sharp peak that can be seen on both graphs at ~6 h corresponds to depletion of ammonium chloride, the nitrogen source in M9 minimal media. This was determined experimentally (data not shown).

5.2.3.2 GROWTH AND GLUCOSE UPTAKE BY *E. COLI* MG1655(PQR439)

The impact of putatively produced *pta* antisense RNA on maximum biomass concentration (expressed as OD_{600}), growth rate and glucose uptake rate is summarised in Table 5.5. Time-course profiles of cell density and residual glucose concentration are shown in Figure 5.4. Overall, the results indicated that growth and glucose uptake were comparable in all three cultures, which agrees with previous observations of these strains in shake flask culture (see section 5.2.2.1). However, the maximum OD_{600} of both the induced and uninduced cultures of *E. coli* MG1655(pQR439) were slightly higher than the control culture. This may have been due to small variations in the media composition, which allowed these cultures to accumulate slightly more biomass. Glucose was depleted at similar rates for all three cultures.

Table 5.5 Summary of substrate uptake and biomass formation in bioreactor experiments

Fermentation characteristic	MG1655(pTrc99A)	MG1655(pQR439) uninduced	MG1655(pQR439) induced
	(control)	(antisense *pta*)	(antisense *pta*)
Max. OD_{600}[a]	5.5 ± 0.1	6.6 ± 0.09	5.8 ± 0.09
Growth Rate (h^{-1})[b]	0.49 ± 0.03	0.54 ± 0.007	0.55 ± 0.02
Glucose Uptake Rate $(mM\ h^{-1})$[b]	5.0 ± 0.5	5.2 ± 0.9	4.5 ± 0.6

[a] Mean ± standard error of the mean.

[b] Rate established over the range 2-6 hours after inoculation (± standard error).
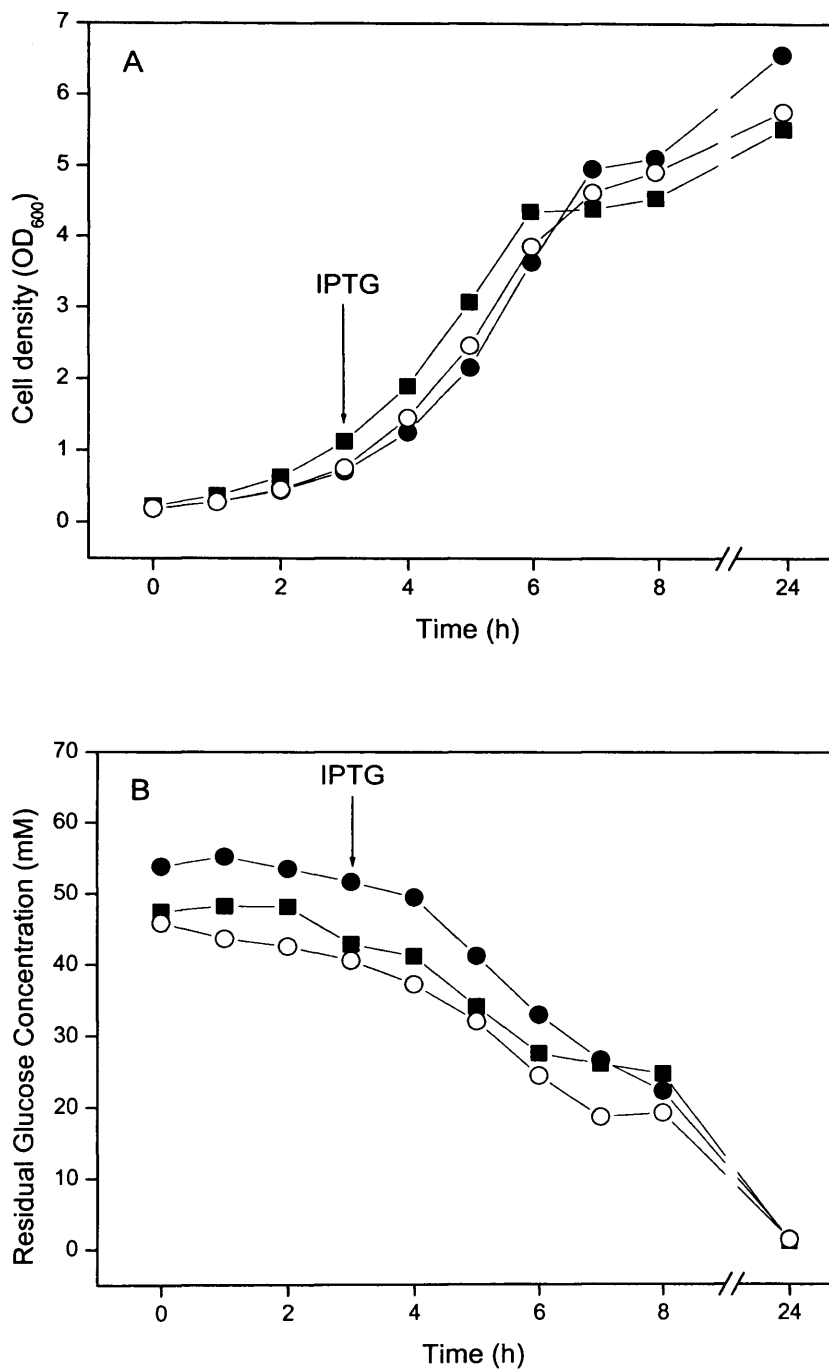
Figure 5.4 Time-course profiles of (A) cell growth and (B) residual glucose concentration in *E. coli* MG1655 harbouring pTrc99A (■), pQR439 uninduced (●), and pQR439 induced (○). Recombinant cells were cultured in a 2 L baffled fermenter containing 1 L of M9 medium with 1% (wt/vol) glucose at 37°C. The arrow indicates the point of induction with 1 mM IPTG. Duplicate analyses were performed for each sample; average values of the duplicates are reported.

5.2.3.3   ENZYME ACTIVITY LEVELS IN *E. COLI* MG1655(PQR439)

The impact of putatively produced *pta* antisense RNA on the levels of phosphotransacetylase and acetate kinase in *E. coli* MG1655 was evaluated by examining the specific enzyme activities (Figure 5.5). Time course profiles of phosphotransacetylase specific activity showed that both the induced and uninduced cultures of *E. coli* MG1655(pQR439) had reduced levels of phosphotransacetylase compared to the control culture. After 24h growth, the level of phosphotransacetylase in the induced culture of *E. coli* MG1655(pQR439) was ~40% lower than the control culture. These results indicate that putative *pta* antisense RNA partially suppressed expression of phosphotransacetylase in *E. coli* MG1655. In addition, the results confirmed that phosphotransacetylase levels were reduced in the uninduced culture of *E. coli* MG1655(pQR439), which suggests that putative *pta* antisense RNA was expressed even under repressed conditions. This will be discussed further in section 5.5 at the end of this chapter, and in Chapter 7.

The levels of acetate kinase in both the induced and uninduced cultures of *E. coli* MG1655 were comparable with the control culture. This indicates that putative *pta* antisense RNA does not affect expression of acetate kinase in *E. coli* MG1655.

It is notable that the error margin was highest in the enzyme activity assays from the earliest fermentation samples, due to a low cell density in the samples of culture broth. This explains the variation in specific activities immediately after fermenter inoculation.
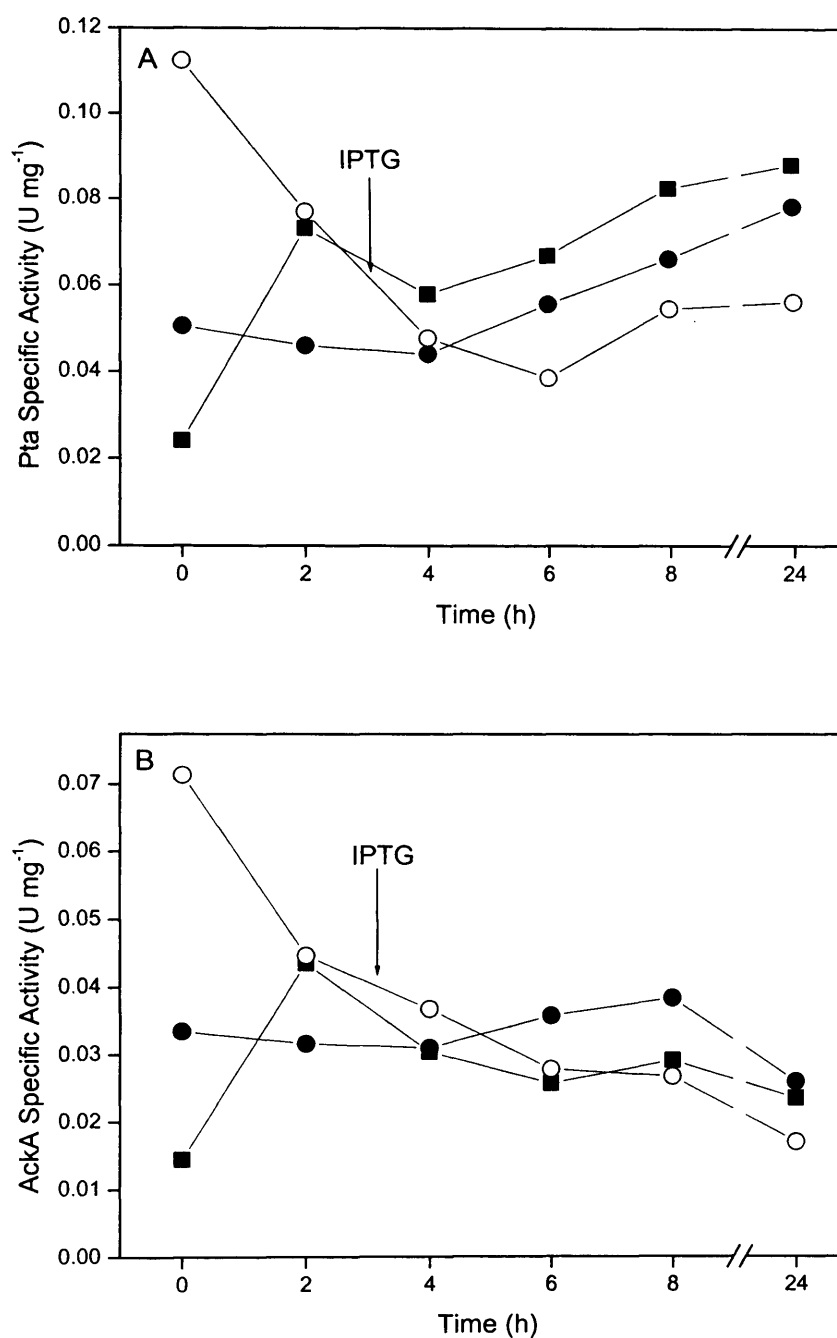
Figure 5.5 Time-course profiles of specific enzyme activity for (A) phosphotransacetylase and (B) acetate kinase in *E. coli* MG1655 harbouring pTrc99A (■), pQR439 uninduced (●), and pQR439 induced (○). Recombinant cells were cultured in a 2 L baffled fermenter containing 1 L of M9 medium with 1% (wt/vol) glucose at 37°C. The arrow indicates the point of induction with 1 mM IPTG. Duplicate analyses were performed for each sample; average values of the duplicates are reported.

5.2.3.4   ORGANIC ACID PRODUCTION BY *E. COLI* MG1655(PQR439)

The impact of putatively expressed *pta* antisense RNA on organic acid production by *E. coli* MG1655 cultured under controlled conditions is summarised in the following pages. Results showed that there was negligible difference in the production of pyruvate, succinate or ethanol by *E. coli* MG1655(pQR439) compared to the control culture (Table 5.6 A). However, differences in the production of acetate and lactate were observed.

The peak acetate concentration in the induced culture of *E. coli* MG1655(pQR439) was reduced by ~15% compared to the control culture. This is not as big a reduction in peak acetate levels as was observed in the shake flask study. However, the control culture accumulated less acetate in the bioreactor experiments compared to the shake flask experiments, which may account for the difference. The induced cultures of *E. coli* MG1655(pQR439) actually produced equivalent amounts of acetate in shake flask culture and under controlled conditions in a bioreactor.

Time course profiles of acetate concentration (Figure 5.6 A) showed that both the induced and uninduced cultures of *E. coli* MG1655(pQR439) accumulated lower levels of acetate during exponential growth phase, compared to the control culture. This trend closely resembles the biomass profiles of the cultures, and is consistent with the results obtained from the shake flask studies (see section 5.2.2.2). The total amounts of acetate produced (mmoles) per 100 mmoles of glucose consumed (Table 5.6 C) confirmed that the control culture produced the most acetate, followed by the uninduced culture of *E. coli* MG1655(pQR439), and then the induced culture of *E. coli* MG1655(pQR439). Taken together, these results indicate that putative *pta* antisense RNA results in partial suppression of phosphotransacetylase, which leads to reduced carbon flow to acetate in *E. coli* MG1655.

Surprisingly, all the bioreactor cultures accumulated lactate after 24 h growth. This was unexpected in the control culture, as lactate is not typically produced by *E. coli* under aerobic conditions. The fermentative lactate dehydrogenase (*ldhA*), which coverts pyruvate to lactate, is usually induced by low pH under anaerobic conditions (Bunch et al., 1997; Ruijun et al., 2001). However, lactate dehydrogenase is present in substantial basal levels under all conditions, and is allosterically activated by its substrate, pyruvate. Therefore, Ruijun et al. (2001) proposed that increased sugar metabolism indirectly induces expression of lactate dehydrogenase. In this study, lactate may have been produced in the control culture as a consequence of the excess glucose that was present in the media after depletion of the nitrogen source. Under these conditions, glucose was

taken up and metabolised by *E. coli*, but not used for biomass generation. Therefore, it is feasible that metabolites at the end of the glycolytic pathway, such as pyruvate, may have accumulated, causing increased expression of lactate dehydrogenase and subsequent production of lactate. Time course profiles of lactate concentration (Figure 5.6 B) confirmed that lactate was produced during stationary phase.

The timing of lactate production by the induced and uninduced cultures of *E. coli* MG1655(pQR439) was similar to the control culture. However, the peak lactate levels were ~2-fold higher than the control culture. The amounts of lactate produced (mmoles) per 100 mmoles of glucose consumed (Table 5.6 C) confirmed that the induced culture of *E. coli* MG1655(pQR439) produced the most lactate, followed by the uninduced culture of *E. coli* MG1655(pQR439), and then the control culture. These results suggest that expression of putative *pta* antisense RNA leads to reduced carbon flow to acetate and increased carbon flow to lactate.

Re-direction of carbon flow from acetate production to lactate production has previously been observed in mutant *E. coli* strains defective in phosphotransacetylase (Chang et al., 1999; Diaz-Ricci et al., 1991). The probable mechanism for the alteration in carbon flux involves the build up of acetyl CoA, which is the substrate for phosphotransacetylase. Increased levels of acetyl CoA inhibit activity of the pyruvate dehydrogenase enzyme, which leads to a build up of pyruvate in the cell, and as previously described, pyruvate has been shown to increase expression of the lactate dehydrogenase enzyme (Bunch et al., 1997). Hence, excess pyruvate is converted to lactate, which accumulates in the culture medium. Studies have shown that reducing the level of acetyl CoA in *pta* mutant strains effectively diminishes lactate production by the culture (Chang et al., 1999; Diaz-Ricci et al., 1991).

In this study, it is notable that the greatest differences in lactate production occur during stationary phase. Therefore, it would be interesting to analyse the pattern of lactate and acetate accumulation in more detail during this period, to determine whether they accumulate rapidly during early stationary phase, or more gradually. It would also be interesting to see whether reduced carbon flow to acetate in cultures of *E. coli* expressing putative *pta* antisense RNA, occurs at the same time as increased carbon flow to lactate.
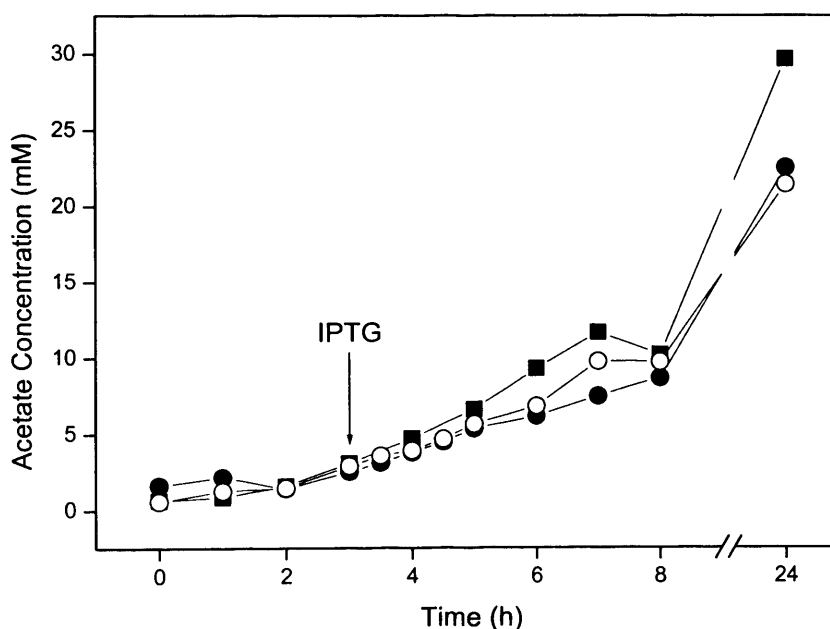
A
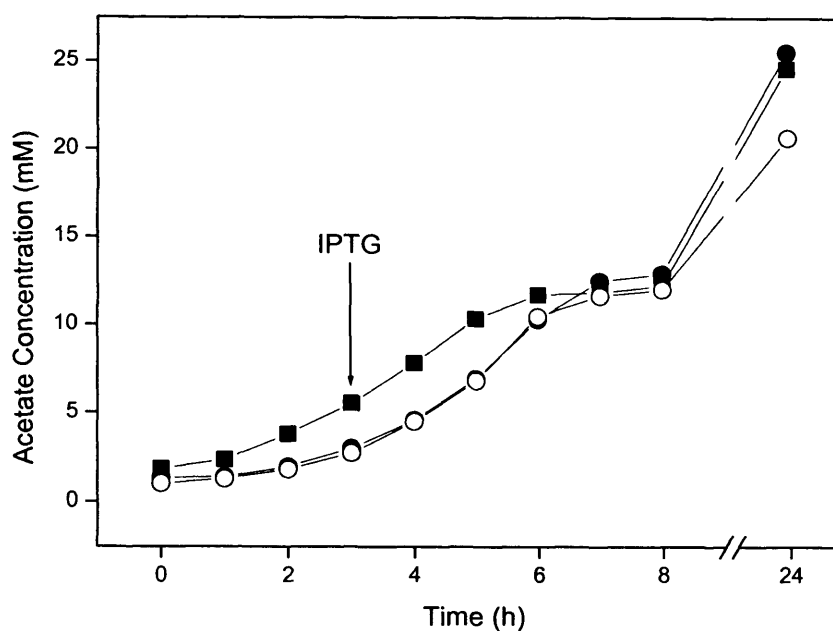
B

Figure 5.6 Time-course profiles of (A) acetate concentration and (B) lactate concentration in *E. coli* MG1655 harbouring pTrc99A (■), pQR439 uninduced (●), and pQR439 induced (○). Recombinant cells were cultured in a 2 L baffled fermenter containing 1 L of M9 medium with 1% (wt/vol) glucose at 37°C. The arrows indicate the point of induction with 1 mM IPTG.

Table 5.6

Summary of organic acid production in bioreactor experiments: (A) Peak Product Concentration, (B) Production Rate, and (C) mmoles produced per 100 mmoles of glucose consumed.

A

Peak Product Concentration (mM)	MG1655(pTrc99A)	MG1655(pQR439) uninduced	MG1655(pQR439) induced
	(control)	(antisense *pta*)	(antisense *pta*)
Acetate	25	26	21
Pyruvate	2	< 1	< 1
Lactate	6	12	13
Succinate	1	1	2
Ethanol	< 1	< 1	< 1

B

Production Rate (mM h^{-1})[a]	MG1655(pTrc99A)	MG1655(pQR439) uninduced	MG1655(pQR439) induced
	(control)	(antisense *pta*)	(antisense *pta*)
Acetate	2.0 ± 0.1	2.1 ± 0.3	2.1 ± 0.3
Lactate	0.0	0.0	0.3 ± 0.08

[a] Rate established over the range 2-6 hours after inoculation (± standard error).

C

mmoles produced / 100 mmoles glucose consumed	MG1655(pTrc99A)	MG1655(pQR439) uninduced	MG1655(pQR439) induced
	(control)	(antisense *pta*)	(antisense *pta*)
Acetate	49	46	44
Lactate	12	23	30

5.3 IMPACT OF PUTATIVE *ACKA* ANTISENSE RNA ON GROWTH AND PRODUCT FORMATION

5.3.1 CONSTRUCTION OF *E. COLI* MG1655(PQR441)

Plasmid pQR441 was constructed to express a 240-nucleotide *ackA* antisense RNA molecule, complementary to the 5' region of *ackA* mRNA encompassing the ribosome-binding site and translation initiation site. *E. coli* K-12 strain MG1655 was transformed with plasmid pQR441, as described in Materials and Methods, and the identities of ampicillin-resistant transformants as *E. coli* MG1655(pQR441) were verified by plasmid isolation and restriction analysis (see section 4.3.2.1).

Due to the fact that *E. coli* MG1655(pQR441) exhibited normal growth characteristics on nutrient agar and in nutrient broth, it was decided not to perform shake flask studies of the strain, and proceed directly to cultivation under controlled conditions in a fermenter. In the following pages, bioreactor experiments to evaluate the impact of putative *ackA* antisense RNA are described. *E. coli* MG1655 harbouring the parent plasmid, pTrc99A, was used as a control strain for these studies. *E. coli* MG1655(pQR441) was studied under 'uninduced' conditions, i.e. no IPTG was added to the culture medium, and under induced conditions, in which IPTG (1mM) was added to the culture medium at early-mid log phase (after 3 hours growth). All the plasmids were stably maintained throughout the 24 hour study.

5.3.2   ANALYSIS OF E. COLI MG1655(PQR441) IN A CONTROLLED BIOREACTOR

The objective of this study was to determine the effect of *ackA* antisense RNA expression on growth, enzyme levels and organic acid production by E. coli MG1655, cultured in a controlled bioreactor. Two E. coli strains were used in this study: E. coli MG1655(pQR441), constructed to express antisense RNA targeted against acetate kinase; and E. coli MG1655(pTrc99A), a control strain harbouring the parent plasmid. Experimental conditions for the bioreactor experiments are detailed in Table 5.7, and the results are presented and discussed in the following pages.

Table 5.7   Experimental conditions for testing the effect of putative *ackA* antisense RNA in bioreactor experiments

Strains	E. coli MG1655(pTrc99A) (see Table 2.1) E. coli MG1655(pQR441) (see Table 2.1)
Media	M9 minimal media, 10 g L^{-1} glucose, trace element mix, 20 $\mu g\ ml^{-1}$ uracil, 5 $\mu g\ ml^{-1}$ thymidine, 100 $\mu g\ ml^{-1}$ ampicillin. (see Table 2.4)
Growth Mode	Batch, 2 L bioreactor (1 L working volume)
Temperature	37°C
Agitation Speed	800 rpm
Air Flow Rate	1 vvm
Sampling Times, hours	0, 1, 2, 3, 4, 5, 6, 7, 8, and 24.
IPTG Addition Time, hours	3

5.3.2.1   GROWTH AND GLUCOSE UPTAKE BY *E. COLI* MG1655(PQR441)

The impact of putatively produced *ackA* antisense RNA on maximum biomass concentration (expressed as OD_{600}), growth rate and glucose uptake rate is summarised in Table 5.8. Overall, the results indicated that the growth and glucose uptake were comparable in all three cultures. The maximum OD_{600} of the induced culture of *E. coli* MG1655(pQR441) was slightly higher than the control culture. This may have been due to a small variation in the media composition. Time course profiles of cell density and residual glucose concentration (Figure 5.7) show that the biomass production and depletion of glucose are comparable in all three cultures for the duration of the 24 hour fermentation.

Table 5.8   Summary of substrate uptake and biomass formation in bioreactor experiments

Fermentation characteristic	MG1655(pTrc99A)	MG1655(pQR441) uninduced	MG1655(pQR441) induced
	(control)	(antisense *ackA*)	(antisense *ackA*)
Max. OD_{600}[a]	5.5 ± 0.1	5.5 ± 0.005	6.0 ± 0.1
Growth Rate (h^{-1})[b]	0.49 ± 0.03	0.53 ± 0.01	0.53 ± 0.03
Glucose Uptake Rate $(mM\ h^{-1})$[b]	5.3 ± 0.6	3.8 ± 0.9	5.2 ± 0.4

[a] Mean ± standard error of the mean

[b] Rate established over the range 2-6 hours after inoculation (± standard error).
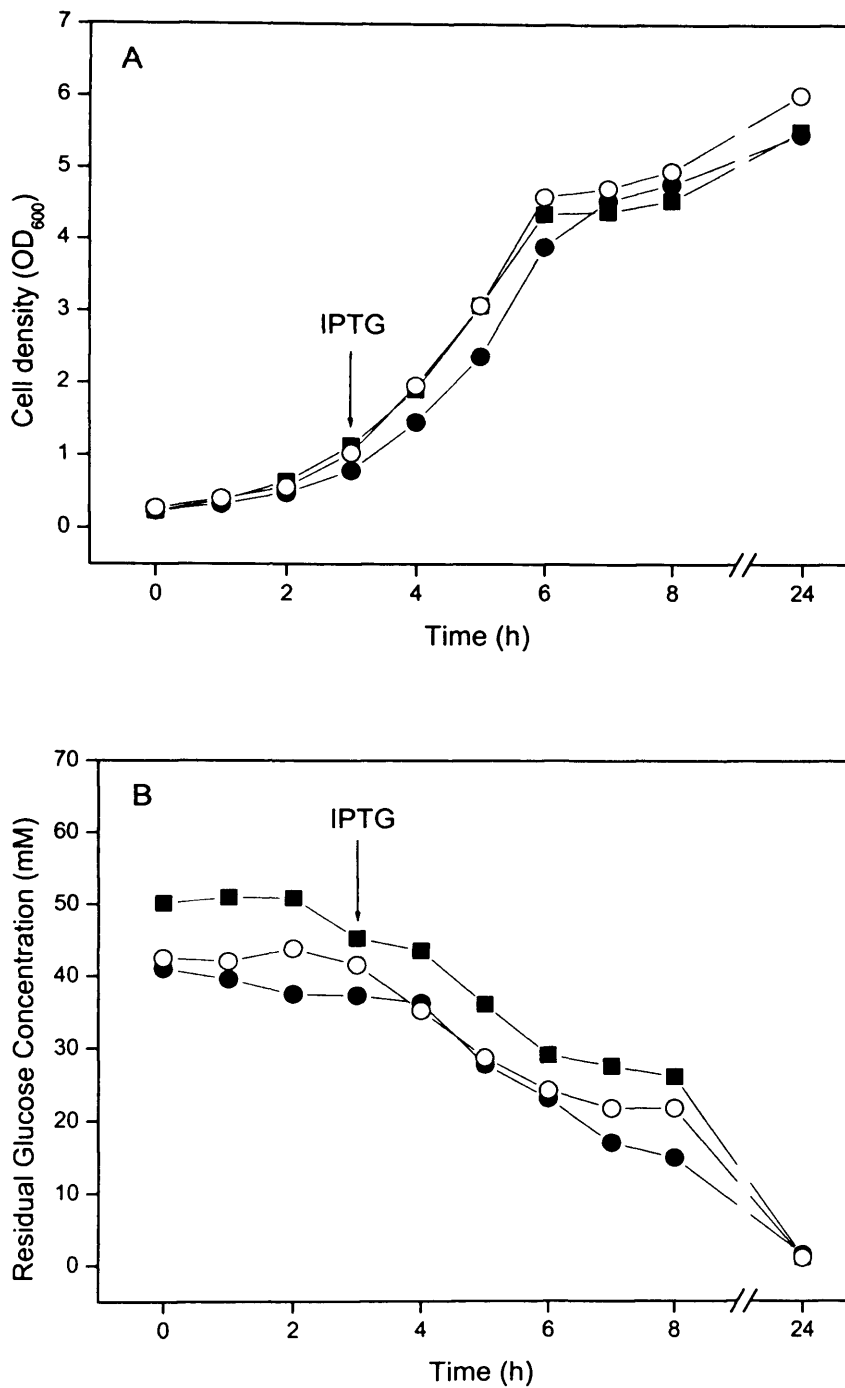
Figure 5.7 Time-course profiles of (A) cell growth and (B) residual glucose concentration in *E. coli* MG1655 harbouring pTrc99A (■), pQR441 uninduced (●), and pQR441 induced (○). Recombinant cells were cultured in a 2 L baffled fermenter containing 1 L of M9 medium with 1% (wt/vol) glucose at 37°C. The arrow indicates the point of induction with 1 mM IPTG. Duplicate analyses were performed for each sample; average values of the duplicates are shown.

5.3.2.2   ENZYME ACTIVITY LEVELS IN E. COLI MG1655(PQR441)

The impact of putatively produced *ackA* antisense RNA on phosphotransacetylase and acetate kinase specific enzyme activity is shown in Figure 5.8. Time course profiles of acetate kinase specific activity indicated that both the induced and uninduced cultures of *E. coli* MG1655(pQR441) had reduced levels of acetate kinase compared to the control culture. After 24 hours of growth, the level of acetate kinase in the induced culture of *E. coli* MG1655(pQR441) was ~40% lower than the control culture. These results indicated that putative *ackA* antisense RNA partially suppressed expression of acetate kinase in *E. coli* MG1655. Furthermore, the results indicated that putative *ackA* antisense RNA was expressed from the uninduced culture of *E. coli* MG1655(pQR441). This was expected due to the fact that plasmid pQR441 was derived from the same parent plasmid as pQR439 (i.e. pTrc99A), which also showed probable leaky expression of antisense RNA from the *trc* promoter.

Time course profiles of phosphotransacetylase activity indicated that both the induced and uninduced cultures of *E. coli* MG1655(pQR441) had reduced levels of phosphotransacetylase compared to the control culture. After 24 hours of growth, the levels of phosphotransacetylase in the induced and uninduced cultures of *E. coli* MG1655(pQR441) were ~50-60% lower than the control culture. These results suggest that putative *ackA* antisense RNA indirectly suppressed the expression of phosphotransacetylase in *E. coli* MG1655. This effect was anticipated because the genes for phosphotransacetylase and acetate kinase are co-transcribed (see section 4.2.1).
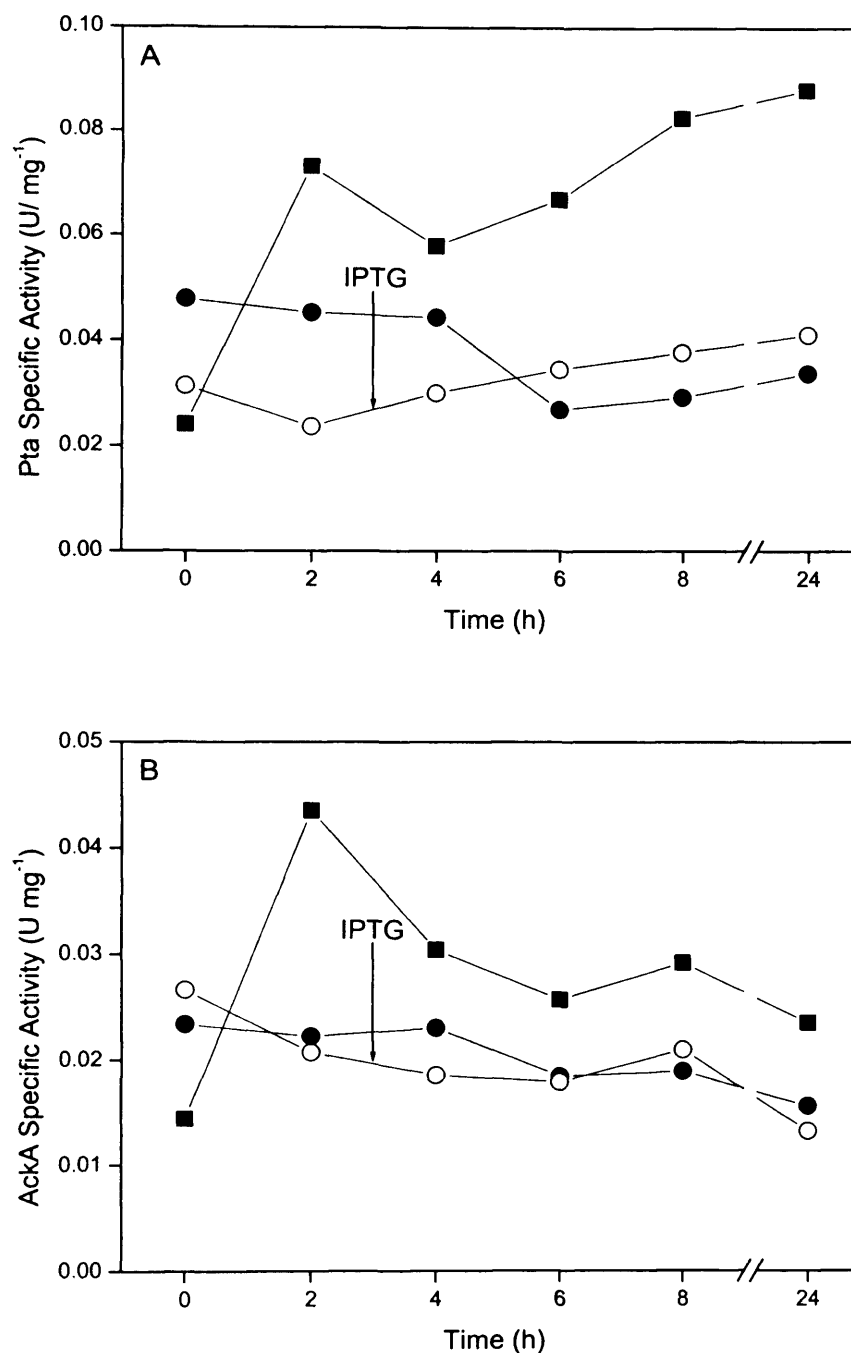
Figure 5.8 Time-course profiles of specific enzyme activity for (A) phosphotransacetylase and (B) acetate kinase in E. coli MG1655 harbouring pTrc99A (■), pQR441 uninduced (●), and pQR441 induced (○). Recombinant cells were cultured in a 2 L baffled fermenter containing 1 L of M9 medium with 1% (wt/vol) glucose at 37°C. The arrow indicates the point of induction with 1 mM IPTG. Duplicate analyses were performed for each sample; average values of the duplicates are shown.

5.3.2.3   ORGANIC ACID PRODUCTION BY E. COLI MG1655(PQR441)

The impact of putatively expressed *ackA* antisense RNA on organic acid production is summarised in the following pages. Results showed that there was negligible difference in the production of pyruvate, succinate or ethanol by the induced or uninduced cultures of *E. coli* MG1655(pQR441) compared to the control culture (Table 5.9 A). However, differences in the production of acetate and lactate were observed.

The peak acetate concentration was reduced by ~12-20% in the induced and uninduced cultures of *E. coli* MG1655(pQR441), compared to the control culture. Furthermore, the peak level of acetate in the induced culture of *E. coli* MG1655(pQR441) was comparable to the peak level in the induced culture of *E. coli* MG1655(pQR439) (as shown in section 5.2.3.4). These results indicate that no additional reduction in carbon flow to acetate was achieved by suppressing expression of acetate kinase in addition to phosphotransacetylase. This was expected due to the fact that the reaction that is catalysed by acetate kinase (i.e. conversion of acetyl phosphate to acetate) can occur rapidly by non-enzyme hydrolysis at 37°C (Brown et al., 1977).

Time course profiles of acetate concentration (Figure 5.9 A) showed that both the induced and uninduced cultures of *E. coli* MG1655(pQR441) accumulated slightly higher levels of acetate during mid-late exponential phase and early stationary phase, compared to the control culture. However, the final acetate levels in both the induced and uninduced cultures of *E. coli* MG1655(pQR441) were slightly lower than the control culture. Total amounts of acetate produced (mmoles) per 100 mmoles of glucose consumed (Table 5.9 C) revealed that both the induced and uninduced cultures of *E. coli* MG1655(pQR441) produced equivalent amounts of acetate as the control culture. These results are unexpected and do not reflect the reduced levels of phosphotransacetylase and acetate kinase observed in the cultures expressing putative *ackA* antisense RNA.

The peak lactate level in the uninduced culture of *E. coli* MG1655(pQR441) was ~2-fold higher than the control culture (Table 5.9 A). This increase in lactate production was also observed in the uninduced culture of *E. coli* MG1655(pQR439) (as shown in section 5.2.3.4.). However, the peak lactate concentration in the induced culture of *E. coli* MG1655(pQR441) was ~2-fold lower than the control culture, which was unexpected. Time course profiles of lactate concentration (Figure 5.9 B) showed that the levels of lactate were low in all three cultures up until stationary phase, which was expected due to the results of the previous study with *E. coli* MG1655(pQR439). However, after 24 hours of growth the induced culture of *E. coli* MG1655(pQR441) exhibited a reduced level of

lactate compared to the control culture, whereas the uninduced culture of *E. coli* MG1655(pQR441) exhibited an increased level of lactate, compared to the control culture. The amounts of lactate produced (mmoles) per 100 mmoles of glucose consumed (Table 5.9 C) reflected this trend.

In conclusion, the results of this study indicate that expression of putative *ackA* antisense RNA in *E. coli* MG1655 suppresses expression of phosphotransacetylase and acetate kinase, but does not greatly reduce carbon flow to acetate. The impact of putative expression of *ackA* antisense RNA from plasmid pQR441 (derived from pTrc99A) is compared with expression of putative *ackA* antisense RNA from plasmid pQR446 (derived from pMMB66EH), in the following section (section 5.3.6).
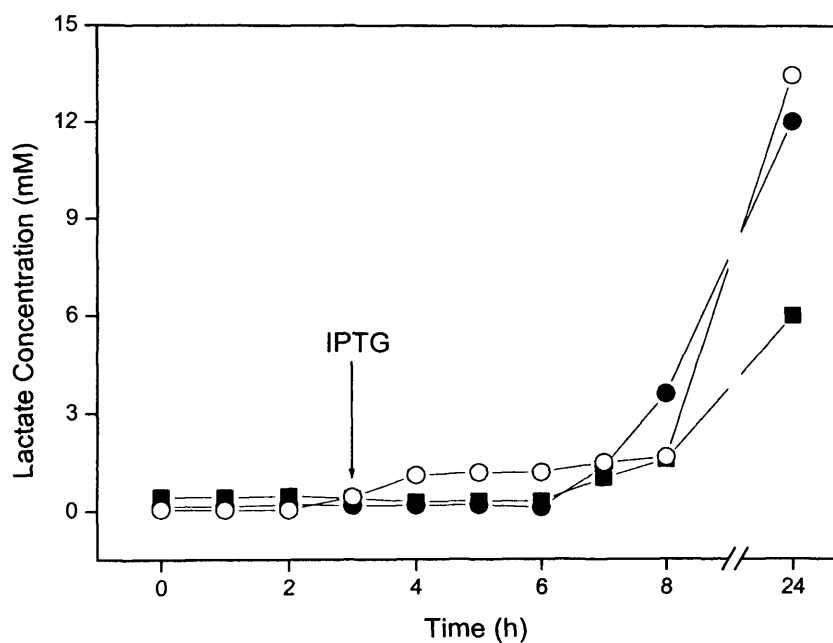
A
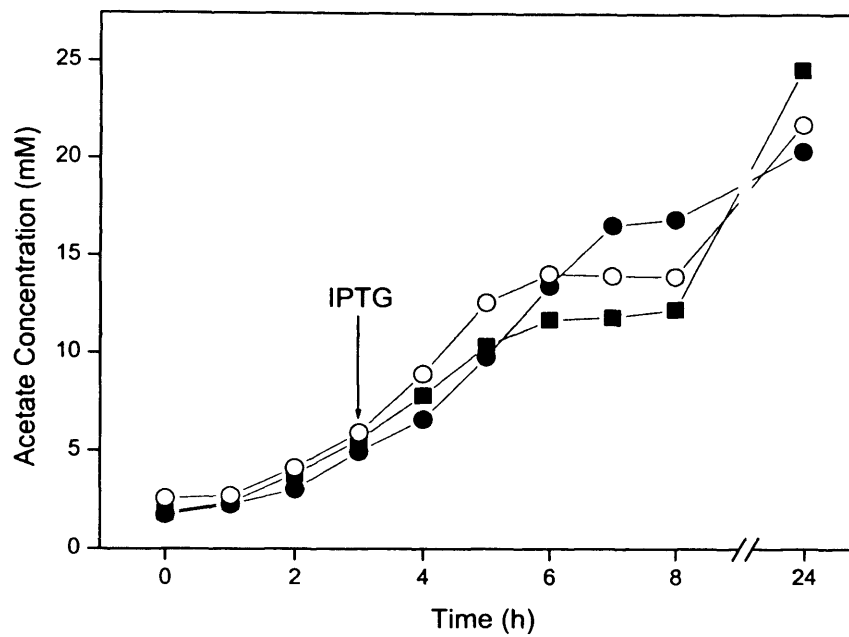
B
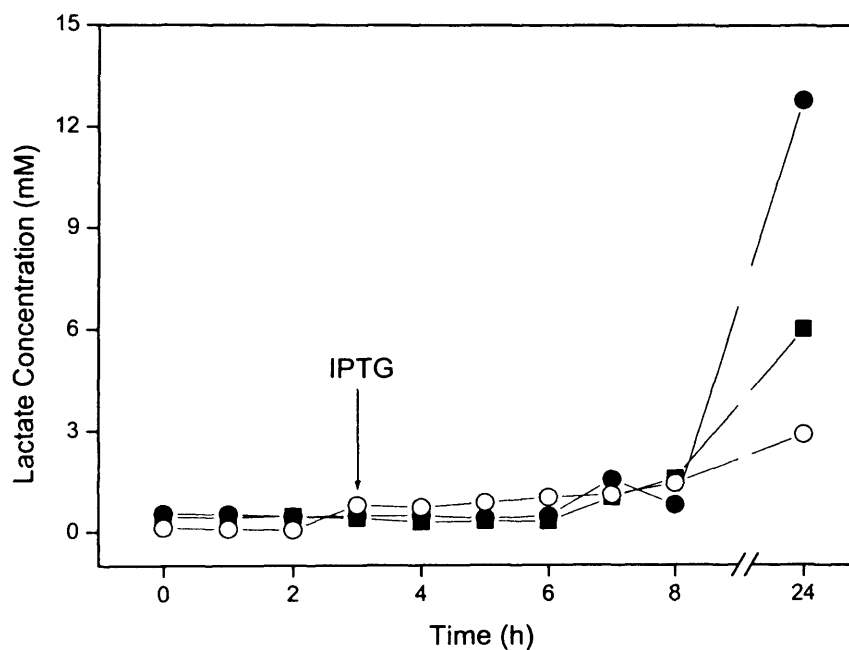
Figure 5.9 Time-course profiles of (A) acetate concentration and (B) lactate concentration in *E. coli* MG1655 harbouring pTrc99A (■), pQR441 uninduced (●), and pQR441 induced (o). Recombinant cells were cultured in a 2 L baffled fermenter containing 1 L of M9 medium with 1% (wt/vol) glucose at 37°C. The arrows indicate the point of induction with 1 mM IPTG.

Table 5.9

Summary of organic acid production in bioreactor experiments: (A) Peak Product Concentration, (B) Production Rate, and (C) mmoles produced per 100 mmoles of glucose consumed.

A

Peak Product Concentration (mM)	MG1655(pTrc99A)	MG1655(pQR441) uninduced	MG1655(pQR441) induced
	(control)	(antisense *ackA*)	(antisense *ackA*)
Acetate	25	20	22
Pyruvate	2	< 1	<1
Lactate	6	13	3
Succinate	1	1	< 1
Ethanol	< 1	< 1	< 1

B

Production Rate (mM h^{-1})[a]	MG1655(pTrc99A)	MG1655(pQR441) uninduced	MG1655(pQR441) induced
	(control)	(antisense *ackA*)	(antisense *ackA*)
Acetate	2.1 ± 0.1	2.6 ± 0.3	2.7 ± 0.2
Lactate	0.0	0.0	0.2 ± 0.07

[a] Rate established over the range 2-6 hours after inoculation (± standard error).

C

mmoles produced / 100 mmoles glucose consumed	MG1655(pTrc99A)	MG1655(pQR441) uninduced	MG1655(pQR441) induced
	(control)	(antisense *ackA*)	(antisense *ackA*)
Acetate	47	47	46
Lactate	11	31	7

5.3.3   CONSTRUCTION OF *E. COLI* MG1655(PQR445)

Plasmid pQR445 was constructed from pMMB66EH to provide a vector for antisense RNA expression, which can stably coexist in *E. coli* with pTrc99A-derived vectors, and has a different antibiotic selection marker. Both pTrc99A and pMMB66EH possess the β-lactamase gene, which confers resistance to ampicillin. Therefore, an aminoglycoside 3'-phosphotransferase gene, which confers resistance to kanamycin, was cloned into the open reading frame of the β-lactamase gene, abolishing ampicillin resistance and introducing kanamycin resistance (see section 4.3.2.2). *E. coli* K-12 strain MG1655 was transformed with plasmid pQR445, as described in Materials and Methods, and the identities of kanamycin-resistant transformants as *E. coli* MG1655(pQR445) were verified by plasmid isolation and restriction analysis. *E. coli* MG1655(pQR445) cultured on selective nutrient agar exhibited growth characteristics that were typical of *E. coli* MG1655.

5.3.4   CONSTRUCTION OF *E. COLI* MG1655(PQR446)

Plasmid pQR446 was constructed from pQR445 to express a 240-nucleotide *ackA* antisense RNA molecule, complementary to the 5' region of *ackA* mRNA encompassing the ribosome-binding site and translation initiation site. The *ackA* gene fragment in plasmid pQR446 is identical to the *ackA* gene fragment in plasmid pQR441. The purpose of developing pQR446 was to create a plasmid that expresses putative *ackA* antisense RNA, which can stably coexist in *E. coli* MG1655 with pQR439 (putative *pta* antisense RNA expression vector). *E. coli* K-12 strain MG1655 was transformed with plasmid pQR446, as described in Materials and Methods. The identities of the kanamycin-resistant transformants as *E. coli* MG1655(pQR446) were verified by plasmid isolation and PCR-amplification of the *ackA* gene fragment (see section 4.3.2.3).

E. coli MG1655(pQR446) exhibited growth patterns that were uncharacteristic of the parent strain. Colonies of *E. coli* MG1655(pQR446) cultured on selective nutrient agar were unusually small, indicating a slow growth rate. In addition, the segregational stability of plasmid pQR446 in the host cell was initially low. However, passaging the strain several times on selective nutrient agar led to increased stability of pQR446 in *E. coli* MG1655(pQR446). Plasmid maintenance was monitored as described in Materials and Methods (Chapter 2).

In the following pages, shake flask experiments to determine the growth and plasmid stability of *E. coli* MG1655(pQR445) and *E. coli* MG1655(pQR446) are described. In addition, bioreactor experiments to evaluate the impact of putative *ackA* antisense RNA from pQR446 are discussed. *E. coli* MG1655 harbouring the parent plasmid, pQR445, was used as a control strain for the studies. *E. coli* MG1655(pQR446) was studied under 'uninduced' conditions, i.e. no IPTG was added to the culture medium, and under induced conditions, in which IPTG (1mM) was added to the culture medium at early-mid log phase (after 3 hours growth). Under uninduced conditions, expression of *ackA* antisense RNA from the *tac* promoter on plasmid pQR446 should be repressed. However, the reduced growth rate of uninduced *E. coli* MG1655(pQR446) on selective nutrient agar indicated that there was basal expression of *ackA* antisense RNA from the plasmid.

5.3.5 GROWTH AND PLASMID-STABILITY STUDIES OF *E. COLI* MG1655(PQR445) & *E. COLI* MG1655(PQR446)

5.3.5.1 SHAKE-FLASK GROWTH STUDY OF *E. COLI* MG1655(PQR445)

E. coli MG1655(pQR445) is a plasmid control strain for experiments involving putative *ackA* antisense RNA expression from plasmid pQR446. *E. coli* MG1655 harbouring plasmid pQR445 exhibited typical growth characteristics of the host strain when cultured on selective nutrient agar. However, it was decided to perform a shake flask study of *E. coli* MG1655(pQR445) to examine the growth profile and to evaluate plasmid stability after 24 hours growth, prior to cultivation of the strain in a controlled bioreactor. Experimental conditions for the shake flask study are shown in Table 5.10, and the results are presented and discussed below.

Table 5.10 Experimental conditions for examining the growth and plasmid stability of *E. coli* MG1655(pQR445)

Strain	*E. coli* MG1655(pQR445) (see Table 2.1)
Media	M9 minimal media, 10 g L^{-1} glucose, trace element mix, 20 $\mu g\ ml^{-1}$ uracil, 5 $\mu g\ ml^{-1}$ thymidine, 10 $\mu g\ ml^{-1}$ kanamycin. (see Table 2.4)
Growth Mode	Batch, 2 L shake flask (250 ml total working volume)
Temperature	37°C
Shaker Speed	200 rpm
Sampling Times	0, 1, 2, 3, 4, 5, 6, 7, 8, and 24 h

A time course profile of cell density for *E. coli* MG1655(pQR445) is shown in Figure 5.10. Results show that the growth characteristics of *E. coli* MG1655(pQR445) are comparable with *E. coli* MG1655(pTrc99A), which was the original control strain used in this study (see section 5.2.2.1). Analysis of the plasmid stability of *E. coli* MG1655(pQR445) after 24 h growth indicated that there was no decrease in plasmid-harbouring cells in the population.
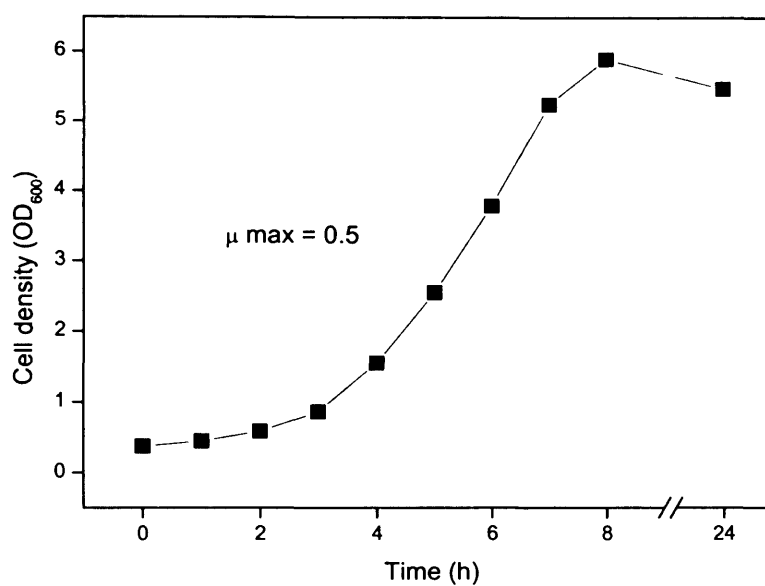
Figure 5.10 A time-course profile of cell growth for *E. coli* MG1655(pQR445). Recombinant cells were cultured in 2 L baffled shake flasks containing 250 ml of M9 medium with 1% (wt/vol) glucose at 37°C and shaken at 200 rpm. Duplicate analyses were performed for each sample; average values of the duplicates are shown.

5.3.5.2 PLASMID STABILITY STUDY OF *E. COLI* MG1655(PQR446) IN NUTRIENT BROTH AND M9 MINIMAL MEDIA

Due to the initial instability of plasmid pQR446 in host cell *E. coli* MG1655, it was decided to examine the proportion of plasmid-containing cells at several time-points throughout the course of a 24 h shake flask fermentation. The study was conducted in both nutrient broth and M9 minimal media, to determine whether the media composition affected plasmid stability. Experimental conditions for the shake flask study are shown in Table 5.11.

Table 5.11 Experimental conditions for examining the plasmid stability of *E. coli* MG1655(pQR446) in nutrient broth and M9 minimal media

Strain	*E. coli* MG1655(pQR446) (see Table 2.1)
Media	Nutrient agar, 10 µg ml^{-1} kanamycin. M9 minimal media agar, 10 µg ml^{-1} kanamycin (see Table 2.4)
Growth Mode	Batch, 250 ml shake flask (50 ml total working volume)
Temperature	37°C
Shaker Speed	200 rpm
Sampling Times	0, 2, 4, 6, and 24 h

The results showed plasmid stability was high at all points tested during the 24 h culture, and no discernible difference was detected between cultures grown in nutrient broth or M9 minimal media (data not shown).

5.3.5.3   SHAKE FLASK GROWTH STUDY OF *E. COLI* MG1655(PQR446)

Following the observation that plasmid pQR446 was stably maintained in a population of *E. coli* MG1655(pQR446) for 24 h, it was decided to study the growth kinetics in shake flask culture, prior to fermentation in a controlled bioreactor. Experimental conditions for the shake flask study are shown in Table 5.12, and the results are presented and discussed below.

Table 5.12   Experimental conditions for examining the growth and plasmid stability of *E. coli* MG1655(pQR446)

Strain	*E. coli* MG1655(pQR446) (see Table 2.1)
Media	M9 minimal media, 10 g L^{-1} glucose, trace element mix, 20 µg ml^{-1} uracil, 5 µg ml^{-1} thymidine, 10 µg ml^{-1} kanamycin. (see Table 2.4)
Growth Mode	Batch, 500 ml shake flask (100 ml total working volume)
Temperature	37°C
Shaker Speed	200 rpm
Sampling Times	0, 1, 2, 3, 4, 5, 6, 7, 8, 9, 10, 11, 12 and 24 h

A time course profile of cell density for *E. coli* MG1655(pQR446) grown in shake flask culture is shown in Figure 5.11. The growth rate and maximum cell density of the culture were reduced by ~45% and ~60% respectively, compared to the plasmid control strain grown in shake flask culture (see section 5.3.5.1). These results indicate that a dramatic alteration in the physiology of *E. coli* MG1655 was brought about by the presence of plasmid pQR446. This is discussed further in light of the bioreactor experiments in the following section (5.3.6).
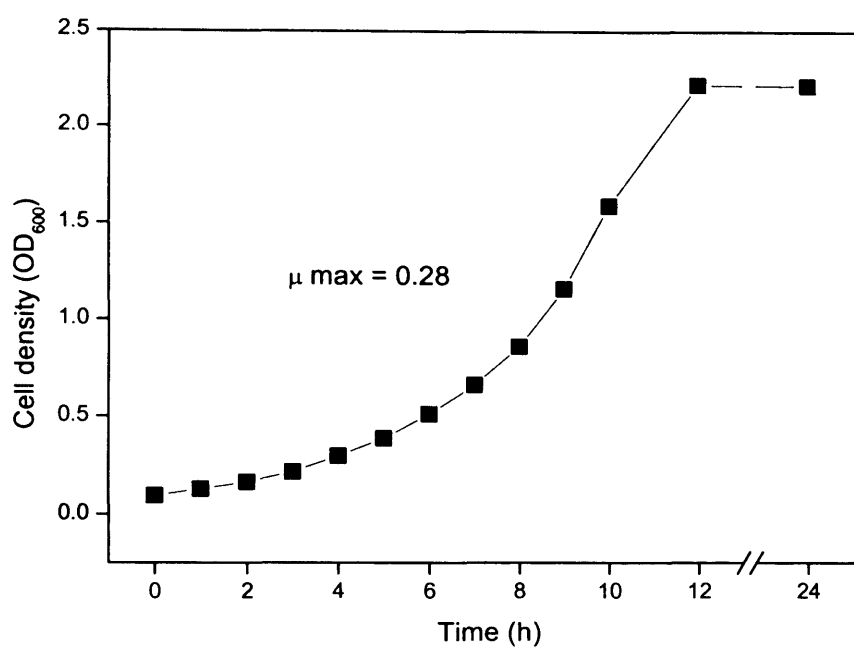
Figure 5.11 A time-course profile of cell growth for *E. coli* MG1655(pQR446). Recombinant cells were cultured in a 500 ml shake flasks containing 100 ml of M9 medium with 1% (wt/vol) glucose at 37°C and shaken at 200 rpm. Duplicate analyses were performed for each sample; average values of the duplicates are shown.

5.3.6 ANALYSIS OF *E. COLI* MG1655(PQR446) IN A CONTROLLED BIOREACTOR

The objective of this study was to determine the impact of putative *ackA* antisense RNA, expressed from plasmid pQR446, on growth, enzyme levels and organic acid production by *E. coli* MG1655 cultured in a controlled bioreactor. Two *E. coli* strains were used in this study: *E. coli* MG1655(pQR446), generated to express antisense RNA targeted against acetate kinase; and *E. coli* MG1655(pQR445), a control strain harbouring the parent plasmid. Experimental conditions for the bioreactor experiments are detailed in Table 5.13, and the results are presented and discussed in the following pages.

Table 5.13 Experimental conditions for testing the effect of putative *ackA* antisense RNA in bioreactor experiments

Strains	*E. coli* MG1655(pQR445) (see Table 2.1) *E. coli* MG1655(pQR446) (see Table 2.1)
Media	M9 minimal media, 10 g L^{-1} glucose, trace element mix, 20 µg ml^{-1} uracil, 5 µg ml^{-1} thymidine, 10 µg ml^{-1} kanamycin. (see Table 2.4)
Growth Mode	Batch, 2 L bioreactor (1 L working volume)
Temperature	37°C
Agitation Speed	800 rpm
Air Flow Rate	1 vvm
Sampling Times	0, 1, 2, 3, 4, 5, 6, 7, 8, 9, 10 and 24 h
IPTG Addition Time	3 h

5.3.6.1 GROWTH AND GLUCOSE UPTAKE BY *E. COLI* MG1655(PQR446)

The impact of putatively produced *ackA* antisense RNA from plasmid pQR446 on maximum biomass concentration (expressed as OD_{600}), growth rate and glucose uptake rate is summarised in Table 5.14. The maximum OD_{600} of the induced and uninduced cultures of *E. coli* MG1655(pQR446) were reduced by ~48% and ~38% respectively, compared to the control culture. Furthermore, growth rates of the induced and uninduced cultures of *E. coli* MG1655(pQR446) were reduced by ~65% and ~ 54% respectively, compared to the control culture. These results are dramatically different to those obtained from the study of putative *ackA* antisense RNA expression from plasmid pQR441 (see section 5.3.2.1).

Time course profiles of cell density and residual glucose concentration are shown in Figure 5.12. The cell densities of both the induced and uninduced cultures of *E. coli* MG1655(pQR446) were much lower than the control culture for the duration of the 24 h fermentation. However, the results show that glucose is depleted at a comparable rate in all three cultures for the first eight hours of growth, and is almost competed depleted in both the induced and uninduced culture of *E. coli* MG1655(pQR446) after 10 hours growth. These observations suggest that *E. coli* MG1655(pQR446) is metabolising glucose rapidly and utilising it for production of another compound rather than converting it to biomass, as in the control culture.

Table 5.14 Summary of substrate uptake and biomass formation in bioreactor experiments

Fermentation characteristic	MG1655(pQR445)	MG1655(pQR446) uninduced	MG1655(pQR446) induced
	(control)	(antisense *ackA*)	(antisense *ackA*)
Max. OD_{600}[a]	6.5 ± 0.05	4.0 ± 0.01	3.4 ± 0.02
Growth Rate (h^{-1})[b]	0.63 ± 0.03	0.28 ± 0.01	0.22 ± 0.01
Glucose Uptake Rate $(mM\ h^{-1})$[b]	5.2 ± 0.7	2.3 ± 0.3	1.1 ± 0.7

[a] Mean ± standard error of the mean.

[b] Rate established over the range 0-4 hours after inoculation (± standard error).

147
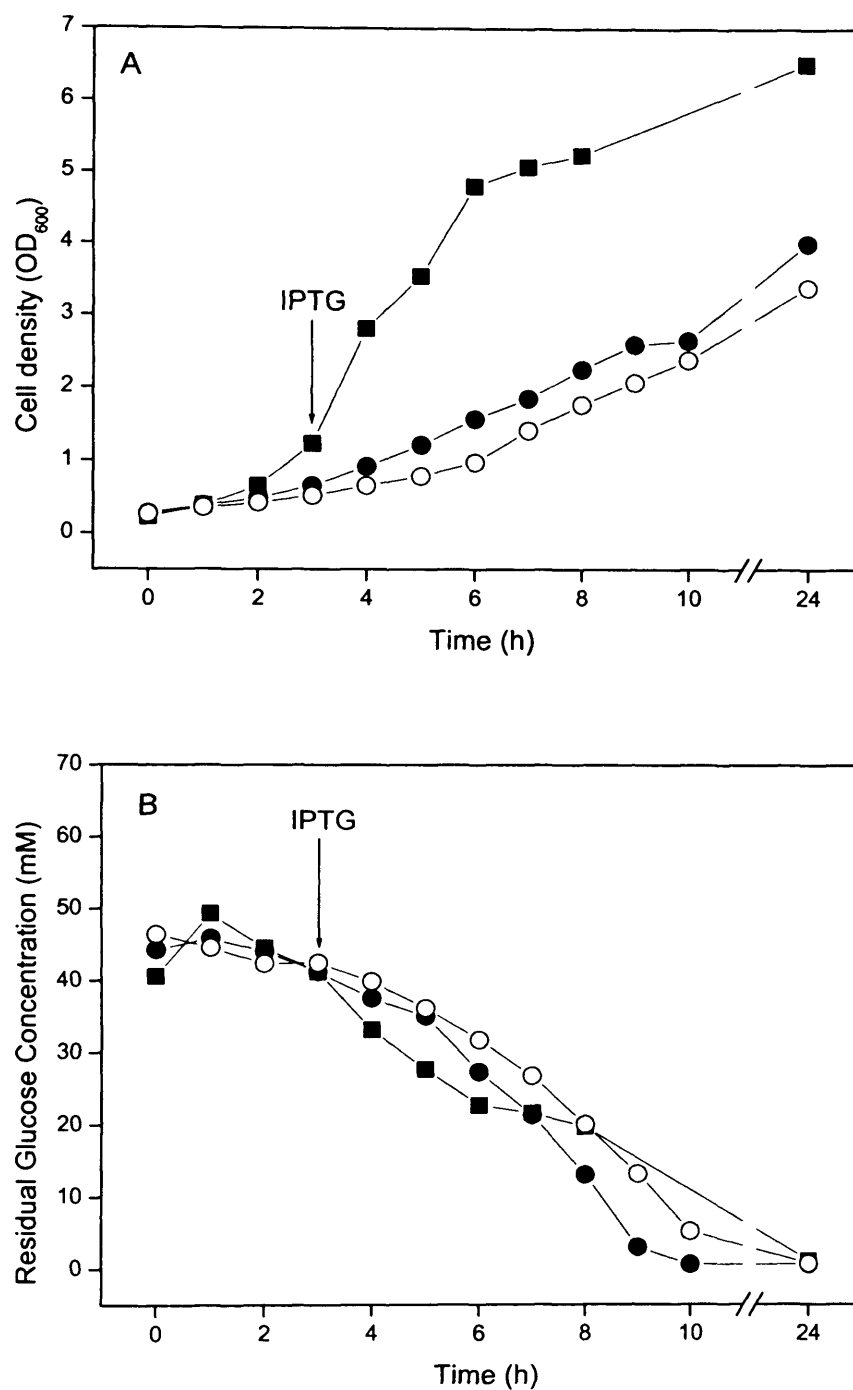
Figure 5.12 Time-course profiles of (A) cell growth and (B) residual glucose concentration in *E. coli* MG1655 harbouring pQR445 (■), pQR446 uninduced (●), and pQR446 induced (○). Recombinant cells were cultured in a 2 L baffled fermenter containing 1 L of M9 medium with 1% (wt/vol) glucose at 37°C. The arrow indicates the point of induction with 1 mM IPTG. Duplicate analyses were performed for each sample; average values of the duplicates are shown.

5.3.6.2   ENZYME ACTIVITY LEVELS IN *E. COLI* MG1655(PQR446)

The impact of putatively produced *ackA* antisense RNA from plasmid pQR446 on phosphotransacetylase and acetate kinase specific enzyme activity is shown in Figure 5.13. The time course profiles of acetate kinase activity indicated that both the induced and uninduced cultures of *E. coli* MG1655(pQR446) had elevated levels of acetate kinase compared to the control culture. After 24 h growth, the level of acetate kinase in the induced and uninduced cultures of *E. coli* MG1655(pQR446) was ~3-fold higher than the control culture. However, it is notable that the levels of acetate kinase in this control culture were ~60% lower than the acetate kinase levels in the original plasmid control culture, *E. coli* MG1655(pTrc99A) (see section 5.3.2.2). Furthermore, the time course profiles of phosphotransacetylase activity indicated that both the induced and uninduced cultures of *E. coli* MG1655(pQR446) also had elevated levels of phosphotransacetylase compared to the control culture. Again, the levels of phosphotransacetylase in this control culture were ~80% lower than the phosphotransacetylase levels in the original plasmid control culture, *E. coli* MG1655(pTrc99A) (see section 5.3.2.2).

These results were unexpected and are difficult to explain. The presence of plasmid pQR445 in *E. coli* MG1655 seems to result in reduced levels of both acetate kinase and phosphotransacetylase. This may be due to the interaction of a component that is encoded by plasmid pQR445 with the *E. coli* MG1655 chromosomal DNA. It would be interesting to compare the enzyme activities in the host cell with this control strain. In addition, microarray analysis could be used to investigate the effect of pQR445 presence on global gene expression in *E. coli* MG1655.
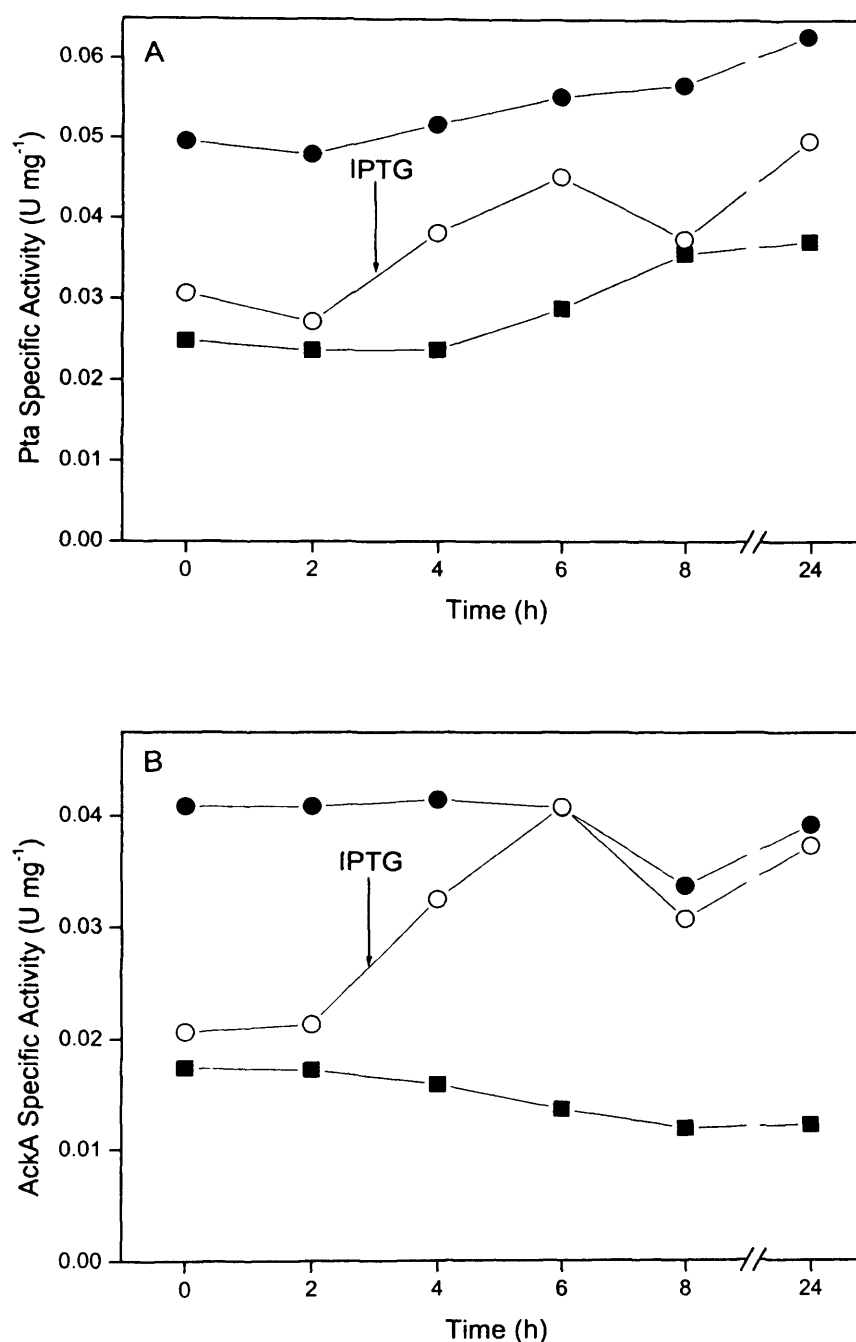
Figure 5.13 Time-course profiles of specific enzyme activity for (A) phosphotransacetylase and (B) acetate kinase in *E. coli* MG1655 harbouring pQR445 (■), pQR446 uninduced (●), and pQR446 induced (○). Recombinant cells were cultured in a 2 L baffled fermenter containing 1 L of M9 medium with 1% (wt/vol) glucose at 37°C. The arrow indicates the point of induction with 1 mM IPTG. Duplicate analyses were performed for each sample; average values of the duplicates are shown.

5.3.6.3   ORGANIC ACID PRODUCTION BY *E. COLI* MG1655(PQR446)

The impact of putatively produced *ackA* antisense RNA on organic acid production is summarised in the following pages. Results showed that there was negligible difference in the production of pyruvate, succinate or ethanol by the induced or uninduced cultures of *E. coli* MG1655(pQR446) compared to the control culture. However, dramatic differences in the production of acetate and lactate were observed.

Time course profiles of acetate concentration (Figure 5.14) showed that during exponential growth phase and early stationary phase, acetate accumulation in both the induced and uninduced cultures of *E. coli* MG1655(pQR446) was greatly reduced compared to the control culture. This trend is reflected in the initial acetate production rates (Table 5.15 B). However, the final acetate levels were comparable in all three cultures. The peak acetate concentration exhibited by the control culture, *E. coli* MG1655(pQR445), was ~45% lower than the peak acetate concentration in the original control culture, *E. coli* MG1655(pTrc99A) (see section 5.3.2.3). This observation is consistent with the lower levels of phosphotransacetylase and acetate kinase in *E. coli* MG1655(pQR445) compared to *E. coli* MG1655(pTrc99A). Overall, these results are very interesting, and suggest that putative expression of *ackA* antisense RNA from pQR446 greatly reduced acetate production by *E. coli* MG1655. However, it is difficult to separate the probable effects of the parent plasmid with the effects of putative *ackA* antisense RNA. Further investigation is required to determine how the presence of control plasmid pQR445 affects acetate production by *E. coli* MG1655.

Cultures of *E. coli* MG1655(pQR446) exhibited peak lactate levels that were ~6-7-fold higher than the control culture. The amounts of lactate produced (mmoles) per 100 mmoles of glucose consumed agree with this trend (Table 5.15 C). Time course profiles of lactate accumulation (Figure 5.14) showed that lactate was produced by both the induced and uninduced cultures of *E. coli* MG1655(pQR446) right from the start of growth in the fermenter, which is strikingly different from the lactate production pattern that has been observed in all the other cultures studied during this research. The timing of lactate production by the control culture *E. coli* MG1655(pQR445) followed the same trend as all the previous cultures studied i.e. lactate was only produced during stationary phase (Figure 5.14).

The high levels of lactate that were produced by the slow-growing *E. coli* MG1655(pQR446) indicate that lactate dehydrogenase was expressed at high levels in these cultures. This would agree with a study by Bunch et al. (1997), which showed that

151

E. coli cultures expressing high levels of lactate dehydrogenase grew very poorly, especially in minimal medium. Growth inhibition was thought to be due to depletion of the intracellular pyruvate pool. The cause of probable increased levels of lactate dehydrogenase in *E. coli* MG1655(pQR446) may have been accumulation of intracellular pyruvate due to inhibition of the pyruvate dehydrogenase complex by elevated levels of acetyl CoA, as previously discussed in section 5.2.3.4. However, the phosphotransacetylase and acetate kinase levels in *E. coli* MG1655(pQR446) were not reduced to such an extent that high levels of acetyl CoA would have been expected to accumulate. Therefore, it is likely that additional, more complex factors are involved. The results of this study are discussed further in section 5.5 at the end of the chapter.

A
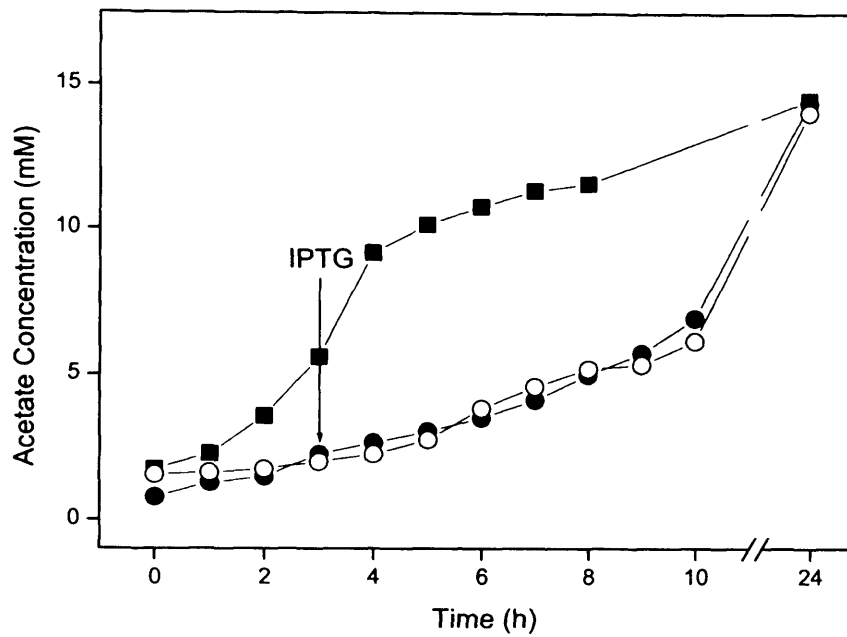
B
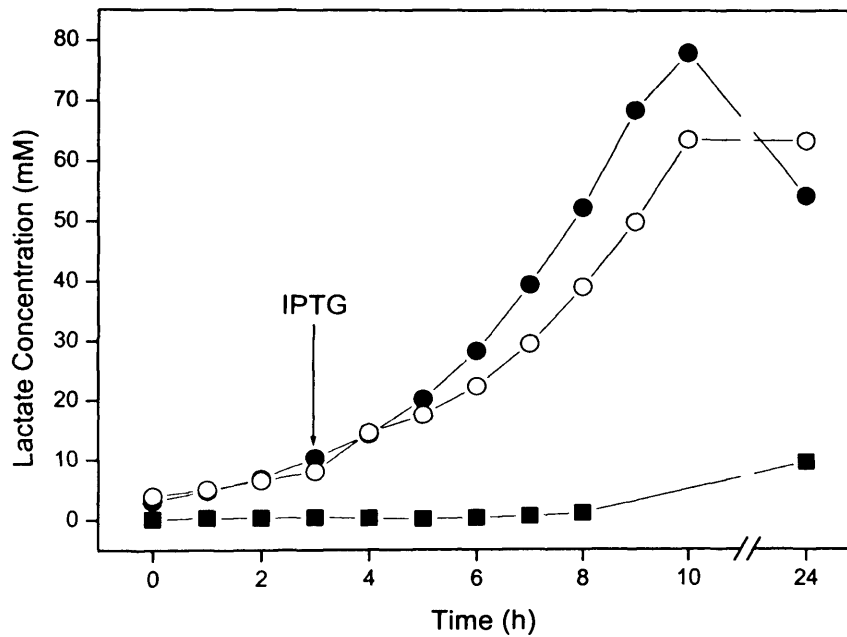
Figure 5.14 Time-course profiles of (A) acetate concentration and (B) lactate concentration in *E. coli* MG1655 harbouring pQR445 (■), pQR446 uninduced (●), and pQR446 induced (○). Recombinant cells were cultured in a 2 L baffled fermenter containing 1 L of M9 medium with 1% (wt/vol) glucose at 37°C. The arrow indicates the point of induction with 1 mM IPTG.

Table 5.15

Summary of organic acid production in bioreactor experiments: (A) Peak Product Concentration, (B) Production Rate, and (C) mmoles produced per 100 mmoles of glucose consumed.

A

Peak Product Concentration (mM)	MG1655(pQR445)	MG1655(pQR446) uninduced	MG1655(pQR446) induced
	(control)	(antisense *ackA*)	(antisense *ackA*)
Acetate	14	14	14
Pyruvate	< 1	< 1	< 1
Lactate	9	54	63
Succinate	< 1	< 1	< 1
Ethanol	< 1	< 1	< 1

B

Production Rate (mM h^{-1})[a]	MG1655(pQR445)	MG1655(pQR446) uninduced	MG1655(pQR446) induced
	(control)	(antisense *ackA*)	(antisense *ackA*)
Acetate	1.8 ± 0.3	0.5 ± 0.05	0.0
Lactate	0.0	2.8 ± 0.3	2.4 ± 0.6

[a] Rate established over the range 0-4 hours after inoculation (± standard error).

C

mmoles produced / 100 mmoles glucose consumed	MG1655(pQR445)	MG1655(pQR446) uninduced	MG1655(pQR446) induced
	(control)	(antisense *ackA*)	(antisense *ackA*)
Acetate	32	31	27
Lactate	24	117	130

5.4 IMPACT OF PUTATIVE *PTA* & *ACKA* ANTISENSE RNA ON GROWTH AND PRODUCT FORMATION

5.4.1 CONSTRUCTION OF *E. COLI* MG1655(PQR439/PQR446)

E. coli MG1655(pQR439/pQR446) was constructed to co-express putative *pta* and *ackA* antisense RNA in *E. coli*. Construction of plasmids pQR439 and pQR446 have previously been summarised in sections 5.2.1 and 5.3.4 respectively.

Simultaneous transformation of *E. coli* MG1655 with pQR439 and pQR446 resulted in no ampicillin-kanamycin resistant transformants. Therefore, plasmids pRQ439 and pQR446 were transformed into *E. coli* MG1655 in several stages. First, *E. coli* MG1655 was transformed with pQR439, and competent *E. coli* MG1655(pQR439) cells were prepared. Then, *E. coli* MG1655(pQR439) was transformed with pQR446. Initially, many colonies grew on nutrient agar supplemented with 15 μg ml^{-1} kanamycin and 100 μg ml^{-1} ampicillin. However, re-streaking of individual colonies from the transformation plate on to selective nutrient agar resulted in an unexpectedly small number of colonies, which were short lived and could not easily be sub-cultured if the plate was more than a few days old. Subsequent analysis of the cells by plating on nutrient agar containing either ampicillin or kanamycin, and by analysis of isolated plasmid DNA, revealed that pQR439 was being 'lost' from the strain. Therefore, it was decided to increase the concentration of ampicillin from 100 μg ml^{-1} to 500 μg ml^{-1} to increase the selection pressure for maintenance of pQR439 in *E. coli* MG1655(pQR439/pQR446). This higher level of ampicillin was successful in maintaining pQR439 in *E. coli* MG1655(pQR439/pQR446), without inhibiting growth of the strain (data not shown). The identities of ampicillin-kanamycin resistant colonies were confirmed by plasmid isolation and restriction analysis (see section 4.4.1.2). All experiments with *E. coli* MG1655(pQR439/pQR446) were initiated by culturing cells, from a glycerol stock stored at -80°C, on selective nutrient agar as individual colonies, and then immediately sub-culturing them in selective liquid media.

E. coli MG1655(pQR439/pQR446) cultured on selective nutrient agar exhibited growth characteristics that were typical of the host strain. In the following pages, bioreactor experiments to determine the impact of putative *pta* and *ackA* antisense RNA are described. *E. coli* MG1655 harbouring the parent plasmids, pTrc99A & pQR445, was used as a control strain for these studies. *E. coli* MG1655(pQR439/pQR446) was studied under 'uninduced' conditions, i.e. no IPTG was added to the culture medium, and under induced condition, in which IPTG (1 mM) was added to the culture medium. Two time points were selected for IPTG addition: immediately after fermenter inoculation (0 h); and

early-mid log phase (after 3 hours growth). Under uninduced conditions, expression of *pta* & *ackA* antisense RNA should be repressed. However, previous studies of *E. coli* MG1655(pQR439) (section 5.2) and *E. coli* MG1655(pQR446) (section 5.3) indicated that high levels of antisense RNA were expressed even under repressed conditions.

5.4.2 ANALYSIS OF *E. COLI* MG1655(PQR439/PQR446) IN A CONTROLLED BIOREACTOR

The objectives of this study were to determine (A) the effect of co-expression of *pta* & *ackA* antisense RNA on growth, enzyme levels and organic acid production by *E. coli* MG1655, and (B) whether induction of antisense RNA at the start of fermentation results in greater suppression of the target enzymes, compared to induction in early-mid log phase. Two *E. coli* strains were used in this study: *E. coli* MG1655(pQR439/pQR446), developed to co-express antisense RNA targeted against phosphotransacetylase and acetate kinase; and *E. coli* MG1655(pTrc99A/pQR445), a control strain harbouring the parent plasmids. All the plasmids were stably maintained throughout the 24 hour study. Experimental conditions for the bioreactor experiments are detailed in Table 5.16, and the results are presented and discussed in the following pages.

Table 5.16 Experimental conditions for testing the effect of putative *ackA* & *pta* antisense RNA in bioreactor experiments

Strains	*E. coli* MG1655(pQR439/pQR446) (see Table 2.1) *E. coli* MG1655(pTrc99A/pQR445) (see Table 2.1)
Media	M9 minimal media, 10 g L^{-1} glucose, trace element mix, 20 μg ml^{-1} uracil, 5 μg ml^{-1} thymidine, 10 μg ml^{-1} kanamycin, 500 μg ml^{-1} ampicillin. (see Table 2.4)
Growth Mode	Batch, 2 L bioreactor (1 L working volume)
Temperature	37°C
Agitation Speed	800 rpm
Air Flow Rate	1 vvm
Sampling Times	0, 1, 2, 3, 4, 5, 6, 7, 8, and 24 h
IPTG Addition Time	3 h

5.4.2.1   GROWTH AND GLUCOSE UPTAKE BY *E. COLI* MG1655(PQR439/PQR446)

The impact of putatively expressed *pta* and *ackA* antisense RNA on maximum biomass concentration (expressed as OD_{600}), growth rate and glucose uptake rate is summarised in Table 5.17. Time course profiles of cell density and residual glucose concentration are shown in Figure 5.15. Overall, the results indicated that growth and glucose uptake were comparable in all three cultures, and were typical of the host cell. These results were unexpected due to the impaired growth rate and reduced biomass levels that were observed in cultures of *E. coli* MG1655 harbouring the single plasmid pQR446 (see section 5.3.4.1).

Table 5.17   Summary of substrate uptake and biomass formation in bioreactor experiments

Fermentation characteristic	MG1655 (pTrc99A/pQR445)	MG1655 (pQR439/pQR446) uninduced	MG1655 (pQR439/pQR446) induced at 0 h	MG1655 (pQR439/pQR446) induced at 3 h
	(control)	(antisense *pta* & *ackA*)	(antisense *pta* & *ackA*)	(antisense *pta* & *ackA*)
Max. OD_{600}[a]	5.1 ± 0.03	5.1 ± 0.03	5.7 ± 0.09	4.7 ± 0.07
Growth Rate (h^{-1})[b]	0.48 ± 0.04	0.47 ± 0.04	0.49 ± 0.06	0.45 ± 0.04
Glucose Uptake Rate $(mM\ h^{-1})$[b]	6.1 ± 0.5	5.9 ± 0.9	4.9 ± 0.7	6.0 ± 0.8

[a] Mean ± standard error of the mean.

[b] Rate established over the range 2-6 hours after inoculation (± standard error).
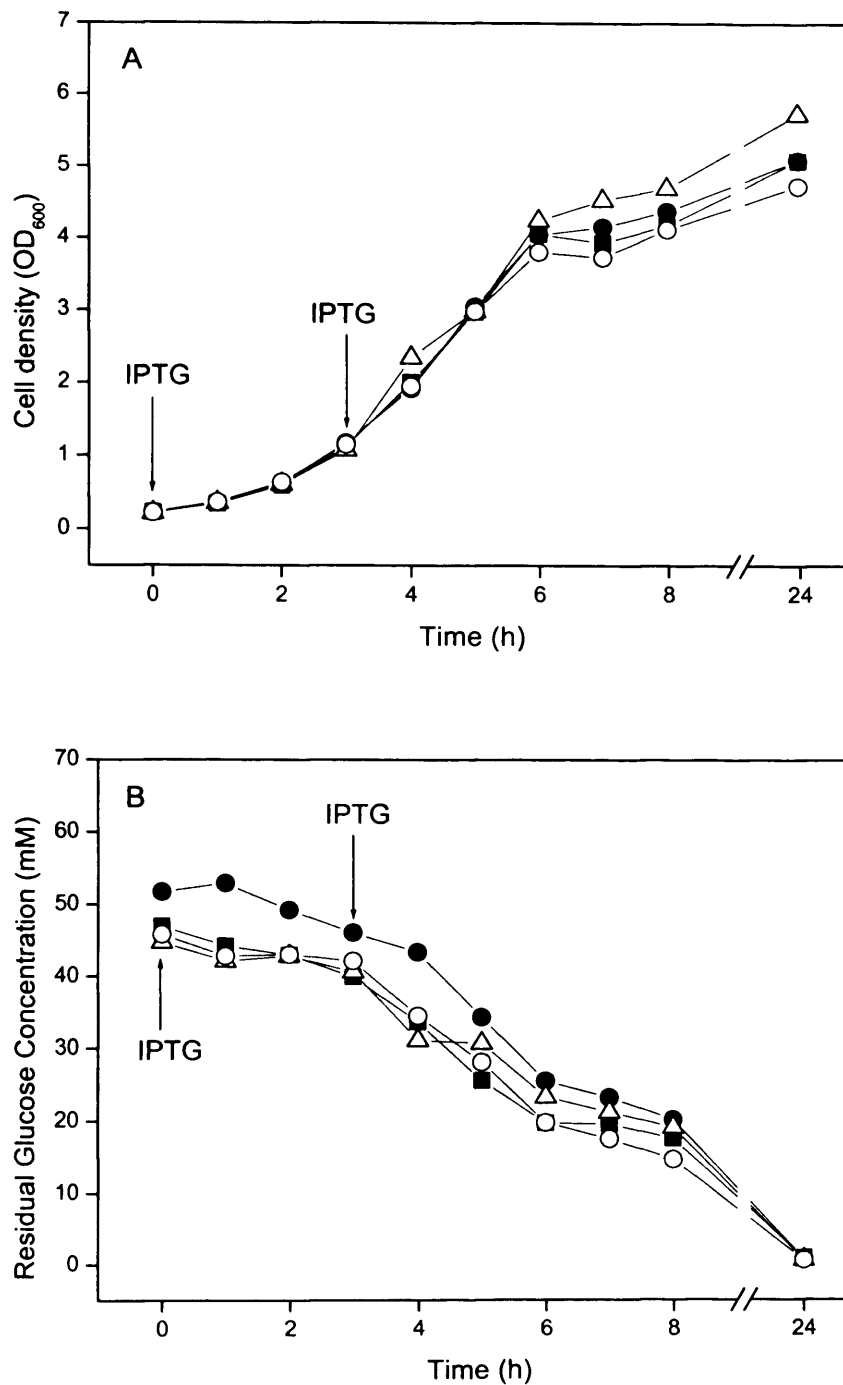
Figure 5.15 Time-course profiles of (A) cell growth and (B) residual glucose concentration in *E. coli* MG1655 harbouring pTrc99A & pQR445 (■), pQR439 & pQR446 uninduced (●), pQR439 & pQR446 induced at the point of fermenter inoculation (△), and pQR439 & pQR446 induced 3 h after inoculation (○). Recombinant cells were cultured in a 2 L baffled fermenter containing 1 L of M9 medium with 1% (wt/vol) glucose at 37°C. Arrows indicate the points of induction with 1 mM IPTG. Duplicate analyses were performed for each sample; average values of the duplicates are shown.

5.4.2.2   ENZYME ACTIVITY LEVELS IN *E. COLI* MG1655(PQR439/PQR446)

The impact of putatively produced *pta* and *ackA* antisense RNA on phosphotransacetylase and acetate kinase specific enzyme activity is shown in Figure 5.16.

Time course profiles of phosphotransacetylase activity revealed that the control culture, *E. coli* MG1655(pTrc99A/pQR445) exhibited comparable levels with *E. coli* MG1655 harbouring the single plasmid pTrc99A, which were higher than the levels in *E. coli* MG1655 harbouring only plasmid pQR445. Furthermore, the profiles of acetate kinase activity also reflected this trend, i.e. *E. coli* MG1655(pTrc99A/pQR445) exhibited comparable acetate kinase levels with *E. coli* MG1655 harbouring the single plasmid pTrc99A, which were higher than *E. coli* MG1655 harbouring only plasmid pQR445.

Results showed that the culture of *E. coli* MG1655(pQR439/pQR446) that was induced immediately after fermenter inoculation had reduced levels of both phosphotransacetylase and acetate kinase, compared to the control culture. *E. coli* MG1655(pQR439/pQR446) that was induced after 3 hours growth also had slightly reduced levels of phosphotransacetylase compared to the control culture, and exhibited levels of both phosphotransacetylase and acetate kinase that were similar to the culture of *E. coli* MG1655 harbouring only the single pQR439 plasmid.

In this study, the levels of phosphotransacetylase and acetate kinase in the uninduced culture of *E. coli* MG1655(pQR439/pQR446) were comparable with the control culture. These results suggest that putative expression of *pta* & *ackA* antisense RNA in *E. coli* MG1655 leads to partial suppression of phosphotransacetylase and acetate kinase. Whilst the effect was more pronounced in *E. coli* MG1655(pQR439/pQR446) induced at the start of fermentation, the overall enzyme suppression achieved did not exceed the enzyme suppression achieved with individual expression of putative *pta* (see section 5.2) or *ackA* (see section 5.3) antisense RNA.
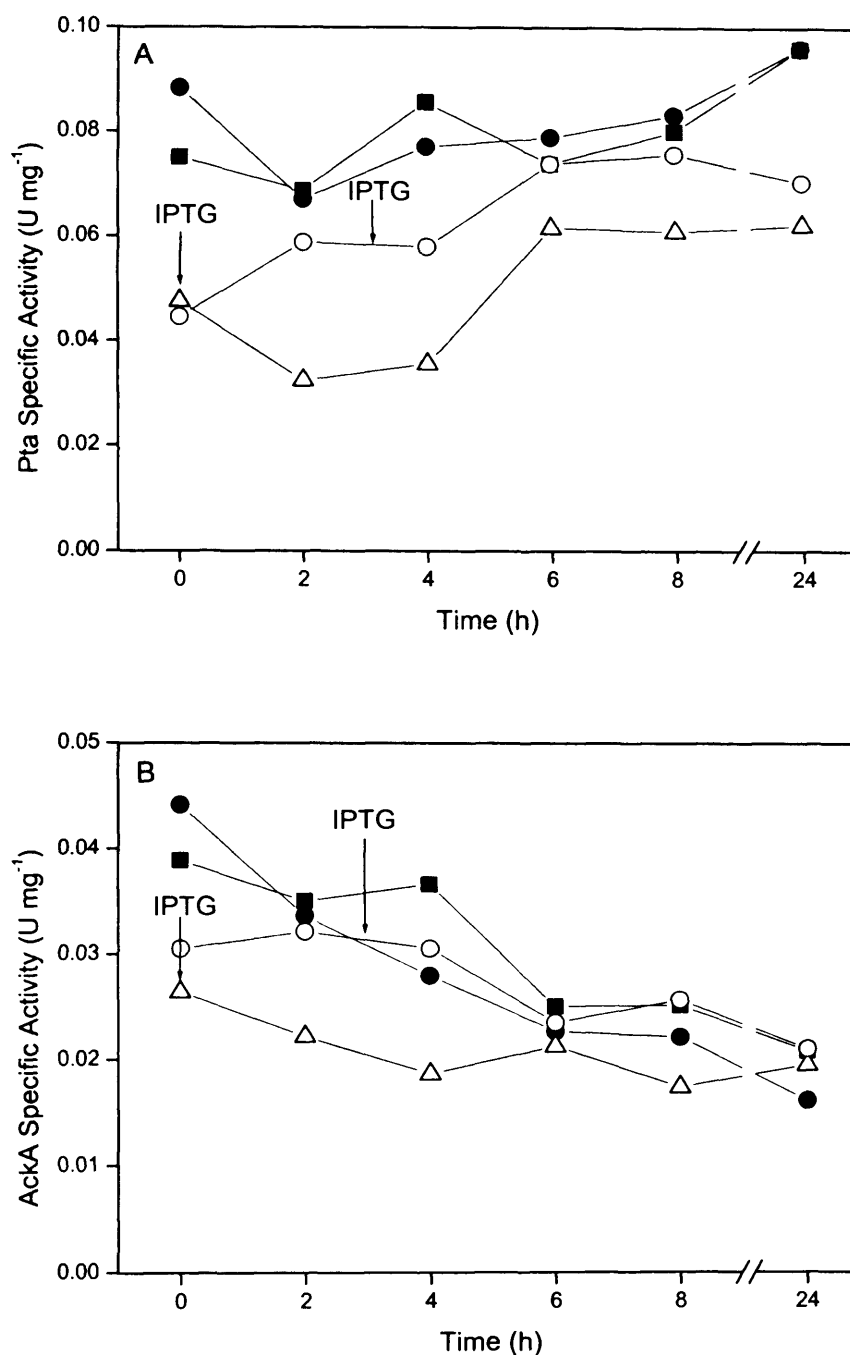
Figure 5.16 Time-course profiles of specific enzyme activity for (A) phosphotransacetylase and (B) acetate kinase in *E. coli* MG1655 harbouring pTrc99A & pQR445 (■), pQR439 & pQR446 uninduced (●), pQR439 & pQR446 induced at the point of fermenter inoculation (Δ), and pQR439 & pQR446 induced 3 h after inoculation (○). Recombinant cells were cultured in a 2 L baffled fermenter containing 1 L of M9 medium with 1% (wt/vol) glucose at 37°C. The arrow indicates the point of induction with 1 mM IPTG. Duplicate analyses were performed for each sample; average values of the duplicates are shown.

5.4.2.3   ORGANIC ACID PRODUCTION BY *E. COLI* MG1655(PQR439/PQR446)

The impact of putatively produced *pta* and *ackA* antisense RNA on organic acid production is summarised in the following pages. Results showed that there was negligible difference in the production of pyruvate, succinate or ethanol in any of the cultures studied. However, differences in the production of acetate and lactate were observed.

The peak acetate levels in all the cultures of *E. coli* MG1655(pQR439/pQR446) and in the control culture, *E. coli* MG1655(pTrc99A/pQR445), were reduced by ~40% compared to *E. coli* MG1655 harbouring the single control plasmid, pTrc99A (as shown in section 5.2.3.4). However, these lower peak acetate levels were comparable with the peak acetate levels in *E. coli* MG1655 harbouring either pQR445 or pQR446 (as shown in section 5.3.6.3). Therefore, these results suggest that the presence of plasmid pQR445 or pQR446 in the dual plasmid-harbouring strains is having an impact on acetate production by the cultures.

Time course profiles of acetate accumulation (Figure 5.17 A) show that the acetate levels in all the cultures were roughly the same up until early-mid log phase. After this point there is some variation between the cultures, with *E. coli* MG1655(pQR439/pQR446) induced at 0 h accumulating the highest levels of acetate during mid-late exponential growth phase and into early stationary phase. After 24 hours growth, all the cultures exhibited comparable levels of acetate, apart from the culture of *E. coli* MG1655(pQR439/pQR446) induced at 3 h, which exhibited a slightly lower level. The total amounts of acetate produced (mmoles) per 100 mmoles of glucose consumed reflected this trend (Table 5.18 C).

The peak level of lactate in the control culture, *E. coli* MG1655(pTrc99A/pQR445), was comparable with the culture of *coli* MG1655 harbouring the single plasmid pQR445. In fact, the amounts of lactate produced per 100 mmoles of glucose consumed were identical in *E. coli* MG1655(pTrc99A/pQR445) and *E. coli* MG1655(pQR445). The peak lactate levels in all the cultures of *E. coli* MG1655(pQR439/pQR446) were comparable, and were ~50% lower than the control culture. This trend was also reflected by the amounts of lactate produced per 100 mmoles of glucose consumed, (Table 5.18 C). Time course profiles of lactate production (Figure 5.17 B) showed that lactate levels were low in all the cultures during exponential growth phase, increasing into early stationary phase and peaking after 24 h in late stationary phase. This pattern was typical of *E. coli* MG1655 harbouring pTrc99A, pQR439 or pR445, but was not typical of pQR446.

In conclusion, the results of this study show that the dual plasmid-harbouring strains possess some characteristics of both of the strains harbouring the individual plasmids. Cultures of *E. coli* MG1655(pTrc99A/pQR445) resembled *E. coli* MG1655(pTrc99A) in biomass production and enzyme levels, however the acetate and lactate levels were more similar to *E. coli* MG1655(pQR445). Cultures of *E. coli* MG1655(pQR439/pQR446) resembled *E. coli* MG1655(pQR439) in biomass production, enzyme levels, and lactate accumulation, however the levels of acetate accumulation were more similar to *E. coli* MG1655(pQR446).

It is difficult to separate the effects of putative antisense RNA expression from the probable effects of the pMMB66EH-derived constructs (i.e. pQR445 and pQR446) on *E. coli* MG1655 metabolism. However, it would be interesting to study these constructs further and determine the mechanism of acetate reduction in *E. coli* MG1655 harbouring the pMMB66EH-derived constructs.

A
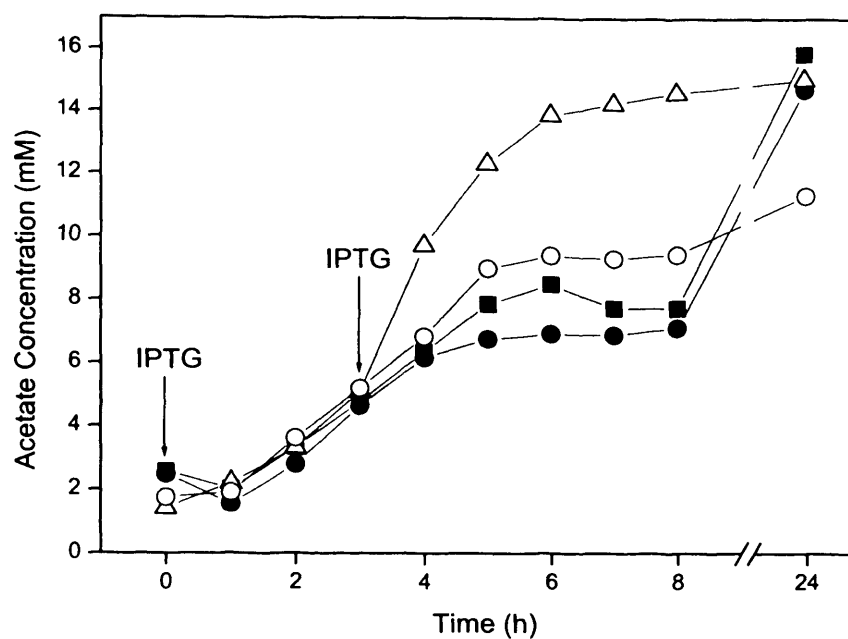
B
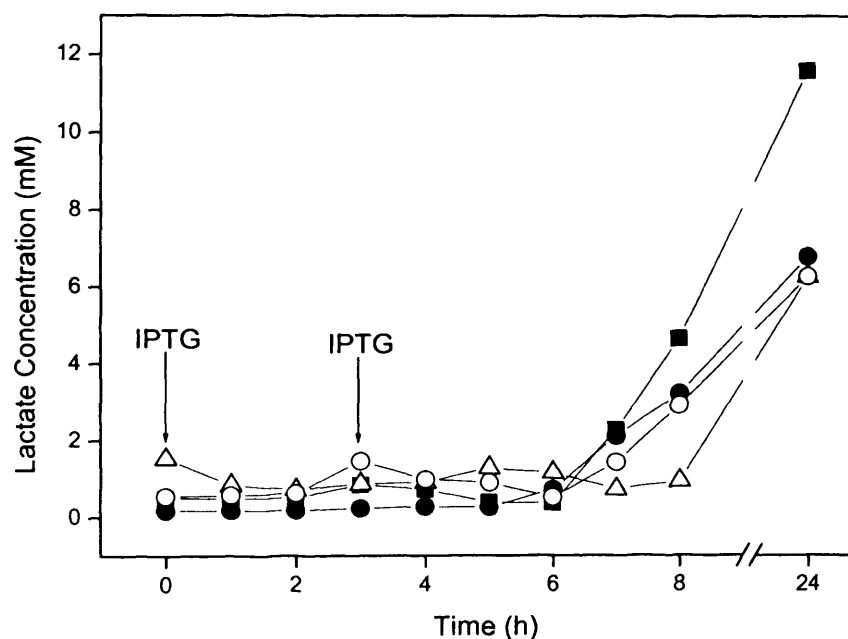
Figure 5.17 Time-course profiles of (A) acetate concentration and (B) lactate concentration in *E. coli* MG1655 harbouring pTrc99A & pQR445 (■), pQR439 & pQR446 uninduced (●), pQR439 & pQR446 induced at the point of fermenter inoculation (△), and pQR439 & pQR446 induced 3 h after inoculation (○). Recombinant cells were cultured in a 2 L baffled fermenter containing 1 L of M9 medium with 1% (wt/vol) glucose at 37°C. The arrows indicate the points of induction with 1 mM IPTG.

Table 5.18

Summary of organic acid production in bioreactor experiments: (A) Peak Product Concentration, (B) Production Rate, and (C) mmoles produced per 100 mmoles of glucose consumed.

A

Peak Product Concentration (mM)	MG1655 (pTrc99A/pQR445)	MG1655 (pQR439/pQR446) uninduced	MG1655 (pQR439/pQR446) induced at 0 h	MG1655 (pQR439/pQR446) induced at 3 h
	(control)	(antisense *pta* & *ackA*)	(antisense *pta* & *ackA*)	(antisense *pta* & *ackA*)
Acetate	16	15	15	11
Pyruvate	< 1	< 1	< 1	< 1
Lactate	12	7	6	6
Succinate	< 1	< 1	< 1	< 1
Ethanol	< 1	< 1	< 1	< 1

B

Production Rate (mM h⁻¹)	MG1655 (pTrc99A/pQR445)	MG1655 (pQR439/pQR446) uninduced	MG1655 (pQR439/pQR446) induced at 0 h	MG1655 (pQR439/pQR446) induced at 3 h
	(control)	(antisense *pta* & *ackA*)	(antisense *pta* & *ackA*)	(antisense *pta* & *ackA*)
Acetate	1.3 ± 0.1	1.0 ± 0.2	2.8 ± 0.3	1.5 ± 0.1
Lactate	0.0	0.1 ± 0.05	0.1 ± 0.04	0.0

[a] Rate established over the range 2-6 hours after inoculation ($\pm$ standard error).

C

mmoles produced / 100 mmoles glucose consumed	MG1655 (pTrc99A/pQR445)	MG1655 (pQR439/pQR446) uninduced	MG1655 (pQR439/pQR446) induced at 0 h	MG1655 (pQR439/pQR446) induced at 3 h
	(control)	(antisense *pta* & *ackA*)	(antisense *pta* & *ackA*)	(antisense *pta* & *ackA*)
Acetate	29	24	31	21
Lactate	24	13	11	13

5.5   DISCUSSION AND CONCLUSIONS

This chapter discussed the physiological characterisation of four recombinant *E. coli* strains that were constructed to express putative antisense RNA targeted against phosphotransacetylase and acetate kinase in *E. coli* MG1655. It was hypothesised that expression of these putative antisense RNA molecules would suppress expression of their target enzymes and reduce acetate accumulation in the culture medium. Recombinant *E. coli* strains were cultured in shake flasks and 2 L controlled bioreactors to evaluate the impact of putative antisense RNA expression on growth kinetics, enzyme levels and organic acid production. Some of the interesting aspects of these studies are discussed further in this section.

Results of the bioreactor experiments showed that expression of putative *pta* antisense RNA from a pTrc99A-derived construct (pQR439) was able to reduce the total acetate accumulation by ~15%, compared to the control culture. Lactate accumulation was increased by ~50% in this culture (as shown in section 5.2.3.4). Putative expression of *ackA* antisense RNA from a pTrc99A-derived construct (pQR441) also resulted in reduced total acetate accumulation compared to the control culture. However, the proportion of acetate that was produced from the metabolised glucose was not reduced in this culture. Lactate accumulation was not increased in this culture either (as shown in section 5.3.2.3).

Putative expression of *ackA* antisense RNA from a pMMB66EH-derived construct (pQR446) resulted in dramatically altered growth and product formation by *E. coli* MG1655 (as shown in section 5.3.6). However as previously discussed, the reduced levels of acetate in cultures of *E. coli* MG1655 harbouring plasmid pQR446 may have been due to a plasmid-mediated affect. This conclusion was based on the fact that cultures of *E. coli* MG1655 harbouring the parent plasmid (pQR445) exhibited reduced levels of acetate compared to the original control culture, *E. coli* MG1655(pTrc99A), and the other cultures studied in this research. The possible mechanism that caused reduced acetate production by pQR445 might involve the interaction of a plasmid-encoded molecule with the *E. coli* MG1655 chromosomal DNA. Such a molecule may have directly inhibited expression of phosphotransacetylase and/or acetate kinase at the level of transcription or translation, or may have inhibited activity of the phosphotransacetylase and/or acetate kinase enzymes by binding to them and either altering their conformation or blocking access to their active site. This would agree with the reduced enzyme activity levels that were exhibited by *E. coli* MG1655(pQR445). To examine this further, it would

be necessary to compare the enzyme activity levels and acetate accumulation in cultures of E. coli MG1655(pQR445) with cultures of E. coli MG1655 harbouring the parent plasmid pMMB66EH, and with the empty host cell.

Surprisingly, the enzyme activity levels of phosphotransacetylase and acetate kinase were higher in cultures of E. coli MG1655 harbouring plasmid pQR446, compared to E. coli MG1655 harbouring the parent plasmid, pQR445. This suggests that the region of plasmid pQR445 that was disrupted in constructing pQR446 (i.e. the multiple cloning site) may have been responsible for mediating the reduction in acetate production by the host cell. However, this seems unlikely due to the nature of the region. It consists of a series of restriction sites for cloning in heterologous gene fragments. Analysis of the sequence similarity of this region with E. coli MG1655 chromosomal DNA may give an indication of the likelihood of this possibility. Furthermore, results suggest that the impaired growth rate, reduced levels of acetate production and very high levels of lactate production by E. coli MG1655 harbouring pQR446 (described in section 5.3.6.3) may have been due to a combination of putative ackA antisense RNA and plasmid-mediated effects.

Kim and Cha (2003) also attempted to reduce acetate production by E. coli using antisense RNA (see section 1.3.2.2.3). The key difference in their study was the E. coli strain they investigated, which was the low-acetate producer BL21. As previously discussed in Chapter 1, a recent study has shown that the glyoxylate shunt and acetyl CoA synthetase (Figure 1.1) are active when E. coli BL21 is grown on glucose (Phue and Shiloach, 2004). This allows the cells to utilise carbon in the central pathways more efficiently, and excrete less as acetate. In contrast, the glyoxylate shunt and acetyl CoA synthetase are inactive in high-acetate producing K-12 strains, when grown on glucose. Kim and Cha (2003) found that in shake flask culture, E. coli BL21 expressing a) pta antisense RNA, b) ackA antisense RNA, and c) pta and ackA antisense RNA all accumulated slightly higher levels of acetate compared to the control culture. However, when recombinant protein (GFP: green fluorescent protein) was co-expressed with the antisense RNA molecules in E. coli BL21, ~15-20% reduction in peak acetate levels was achieved. Lactate accumulation was not reported in this study. Overall, the study achieved a similar reduction in acetate production using antisense RNA as was found in this research, despite the probable differences in acetate metabolism in the two strains.

In glucose minimal media, mutant E. coli strains defective in phosphotransacetylase and acetate kinase typically exhibit reduced growth rates (15-30%) and very low levels of acetate production. In the absence of phosphotransacetylase, it is assumed that acetate is produced by pyruvate oxidase, which converts pyruvate directly to acetate (as

described in Chapter 1). The reduced acetate excretion is compensated for by increased excretion of pyruvate and/or lactate in these cultures, during the exponential growth phase (Chang et al., 1999; Contiero et al., 2000; Diaz-Ricci et al., 1991; Hahm et al., 1994; Kakuda et al., 1994). The antisense-regulated strains that were constructed in this study have similar phenotypes as the mutant *E. coli* strains with defective phosphotransacetylase and acetate kinase. However, to examine the effects of putative *pta* and *ackA* antisense RNA in *E. coli* MG1655 further, it would be necessary to isolate and quantify the levels of antisense RNA and target mRNA that are present in the recombinant *E. coli* strains. Although, studies have shown that the level of a specific mRNA does not always correlate with the level of its corresponding protein (Lee et al., 2003; Mehra et al., 2003). Therefore, measurement of enzyme activity levels and product formation provides a better gauge of the impact of antisense RNA on metabolism.

In the majority of cultures in this study, ammonium chloride was depleted after ~6 hours growth. However, glucose was still present in excess amounts after this time. Therefore, it is likely that the high levels of acetate that accumulated after 24 hours growth were a consequence of the excess glucose that was present after biomass production had ceased. It would be interesting to study the effect of increasing the initial concentration of ammonium chloride on the final acetate levels in these cultures. Alternatively, the effect of using ammonium hydroxide as an alkali in the pH buffering system for the fermentations could be investigated. This would provide a secondary nitrogen source, which may lead to increased carbon flow to biomass production and lower carbon flow to acetate.

In order to investigate the effects of *pta* and *ackA* antisense RNA expression further, the fermentation results presented in this chapter have been used for metabolic flux analysis of the recombinant *E. coli* strains. This approach used the specific growth rate, specific glucose uptake rate and specific product formation rates to calculate the intracellular flux distribution for each *E. coli* strain. The results are presented in the following chapter (Chapter 6).

CHAPTER 6

METABOLIC FLUX ANALYSIS OF *E. COLI* MG1655 EXPRESSING ANTISENSE RNA

6.1   SUMMARY

A quantitative description of metabolism is of fundamental importance for analysing the impact of genetic or environmental perturbations on carbon flow through the *E. coli* metabolic network. This chapter describes the use of metabolic flux analysis to investigate the impact of reduced acetate production on carbon flow through the central metabolic pathways of *E. coli* MG1655. Metabolic flux analysis was the approach chosen for this study due to its simplicity. It requires only information about metabolic reaction stoichiometry, metabolic requirements for growth, and the measurement of a few strain-specific parameters. Enzyme kinetic data, which is difficult to obtain, is not required for metabolic flux analysis.

In this study, the computer software *FluxAnalyzer* V.4.1 was used in conjunction with a pre-determined metabolic reaction network of *E. coli* central metabolism, to perform metabolic flux analysis. The aim of the study was to provide a more detailed insight into the effect of *pta* and *ackA* antisense RNA on *E. coli* MG1655 metabolism and complement the results from physiological studies presented in the previous chapter (Chapter 5). Substrate uptake and product formation profiles, from the physiological studies in Chapter 5, were used to calculate specific substrate uptake and product formation fluxes for each strain. These external measured fluxes were used to determine the intracellular flux distribution of each strain at steady state. A pseudo-steady state was assumed during the different phases of fermentation where all the measured variables were changing at a constant rate (Stephanopoulos et al., 1998).

Results from metabolic flux analysis revealed that putative *ackA* antisense RNA, expressed from plasmid pQR446 had the greatest impact on carbon flux through *E. coli* MG1655 central metabolism. These results were not surprising as the physiological characteristics of this strain were dramatically altered compared to the control strain. Specifically, the induced culture of *E. coli* MG1655(pQR446) exhibited reduced fluxes through the pentose phosphate pathway and the TCA cycle, and a reduced specific growth rate compared to the control culture.

6.2 BACKGROUND

A quantitative description of metabolism and the ability to engineer metabolic change are important for achieving specific bioprocessing goals, and for developing our fundamental understanding of cell biology. For example, analysing the metabolism in an organism can provide useful information to help optimise strains for the production of metabolites and therapeutics, and to assess the metabolic consequences of genetic alterations. Hence, quantitative analysis of metabolism is of fundamental and practical importance (Edwards et al., 1999).

There are four main approaches to modelling metabolic pathways, which are 1) kinetic modelling, 2) biochemical systems theory, 3) metabolic control analysis, and 4) metabolic flux analysis. Attempts at kinetic modelling of metabolism have been hampered by the requirement for extensive and explicit enzyme kinetics. Furthermore, enzyme analysis is usually performed *in vitro*, which may not be representative of the conditions existing inside the cell. The human red blood cell is the only system for which sufficient enzyme kinetics are available, and a full dynamic model has been developed (Lee and Palsson, 1991). In general, comprehensive kinetic information is not available for some pathways in microbial cells. However, a small kinetic model of *E. coli* central carbon metabolism has been developed, which is capable of describing the dynamic behaviour of metabolites in the central pathways with regard to amino acid synthesis (Chassagnole et al., 2002). Biochemical systems theory identifies the enzymes in a metabolic pathway that have a significant influence on the overall pathway flux (Savageau, 1970). However, this approach is quite complicated mathematically because it incorporates non-linear elements into the model. Metabolic control analysis has been used for investigating metabolic regulation at steady state (Heinrich and Rapoport, 1974; Kacser and Burns, 1973). This analysis can be useful for small systems, but tends not to be predictive for environments that differ largely from the original operating point. Metabolic flux analysis is the most user-friendly approach for modelling metabolism. This is the approach chosen for this thesis and is described in more detail in the following section.

6.2.1 METABOLIC FLUX ANALYSIS

Metabolic flux analysis (MFA) is a mathematical method, which is used to evaluate the flow of carbon through a steady-state metabolic network. It is based on the fundamental law of mass conservation, and only requires information about metabolic reaction stoichiometry, metabolic requirements for growth, and the measurement of a few strain-specific parameters (Edwards et al., 2002; Edwards et al., 1999; Varma and Palsson,

1994). Kinetic information, which is difficult to obtain, is not necessary for metabolic flux analysis.

MFA is performed by using a stoichiometric model to represent the reactions in a metabolic network. A pseudo-steady state can be assumed because metabolic transients are typically rapid compared to cellular growth rates and environmental changes. The consequence of this assumption is that all the metabolic fluxes leading to formation and degradation of any given metabolite must balance, represented by the flux balance equation

$$S \cdot v = b \qquad\qquad (1)$$

where S is a matrix containing the stoichiometry of the metabolic reactions, v is a vector of the 'n' reaction rates, and b is a vector containing the net metabolite uptake by the cell (Stephanopoulos et al., 1998). Equation (1) is typically underdetermined as the number of reactions in a given metabolic network normally exceeds the number of metabolites. The number of reactions minus the number of metabolites in a network specifies the number of degrees of freedom. If for example, there were 10 degrees of freedom in a network, then 10 measured fluxes would be required in order to determine a unique solution for the intracellular flux distribution. If, in this example, 10 measured fluxes could not be determined experimentally, a linear optimisation algorithm could be used to optimise the intracellular flux distribution for a certain objective (e.g. maximising biomass production) (Varma and Palsson, 1994).

The outcome of MFA is a metabolic flux map, which shows the biochemical reactions included in the model along with an estimation of the steady state rate (i.e. the flux) at which each reaction in the diagram occurs. Such maps contain useful information about the contribution of specific pathways to the overall processes of substrate utilisation and product formation. However, the real value lies in the differences that are observed when flux maps obtained from different strains or under different conditions are compared with one another. Through these comparisons, the impact of genetic and environmental perturbations can be examined, and the importance of specific pathways accurately described. In addition to quantification of pathway fluxes, MFA can also be used for: 1) identification of branch point control, 2) identification of alternative pathways, and 3) calculation of maximum theoretical yields (Holms, 1999; Stephanopoulos et al., 1998).

The reliance of metabolic flux analysis on reaction stoichiometry is its greatest strength but can also be its greatest weakness. This is because flux distributions within the cell

are ultimately determined by the kinetics properties of cellular enzymes, expression of these enzymes, and regulatory mechanisms within the cell. MFA does not incorporate this additional information, which limits its ability to describe cellular metabolism accurately.

6.2.1.1   METABOLIC FLUX ANALYSIS OF *E. COLI*

Metabolic flux analysis has been widely used to study *E. coli* metabolism. Therefore, four examples from the literature have been selected and are discussed below in chronological order. The first example used MFA to study the central metabolic pathways of *E. coli*, grown under a range of different conditions in batch culture. Specifically, the efficiency of carbon conversion to biomass, and the excretion of acetate by *E. coli* ML308 were examined. Results showed that carbon compounds that feed into phosphorylated parts of the central pathways are converted to biomass more efficiently than carbon compounds that feed into non-phosphorylated pathways. In addition, MFA indicated that acetate excretion by *E. coli* is a consequence of the uptake rate of the primary carbon source, and is used by the cell to balance the flux to CO_2 and energy generation with the fluxes to biosynthesis and growth (Holms, 1986).

The second example used MFA to predict cell growth and by-product secretion in chemostat cultures of *E. coli* W3110. Strain-specific parameters, such as the maximum oxygen uptake rate and maximum glucose uptake rate for *E. coli* W3110 were experimentally determined and used to constrain the stoichiometric model of central metabolism. The internal flux distributions were then calculated by using linear optimisation, with the objective of maximising biomass production. Linear optimisation is a mathematical method, which calculates the unknown fluxes by determining the optimum flux distribution that would achieve a certain objective. Results from the study showed that by specifying a glucose uptake rate, the model was capable of quantitatively predicting the optimal growth rate, oxygen uptake rate and by-product secretion rates in chemostat experiments (Varma and Palsson, 1994). These results indicate that the objective set for linear optimisation (i.e. to maximise biomass production) is valid, and gives a good approximation of carbon flow through the *E. coli* metabolic network.

The third example is a theoretical study, which was based on a comprehensive flux model of *E. coli* metabolism. The model aimed to include all known reactions in the *E. coli* metabolic network, including those compiled in the Kyoto Encyclopaedia of Genes and Genomes (KEGG, 1999, website http://www.genome.ad.jp/kegg/). Due to the size of the model, linear optimisation, with the objective of maximising biomass, was used to

calculate the flux distributions. The aim of the study was to determine the smallest gene set capable of maximising biomass production on glucose, and then investigate the maximum number of gene deletions from this gene set that still maintains a specified level of biomass production. The model predicted that 202 intracellular reactions (out of 400 reactions in the model) were required to sustain maximum biomass production. These included glycolytic reactions, the pentose phosphate pathway, the TCA cycle, the respiratory reactions and other anabolic and catabolic routes necessary for optimal growth. From this set of reactions, the model predicted that only 18 gene deletions would render the network incapable of growth (Burgard and Maranas, 2001). This study is interesting and contributes to our understanding of the crucial reactions and pathways that are necessary to support growth.

The final example is a recent theoretical study of a comprehensive flux model of the *E. coli* metabolic network, which was originally developed by the group of Palsson (Edwards et al., 2001; Edwards and Palsson, 2000). The flux model was generated by 'reconstructing' the metabolic network of *E. coli* MG1655 from the annotated genome sequence. In the recent study using this model, the overall organisation of flux in the *E. coli* metabolic network was investigated under different growth conditions. Results showed that flux distribution in the *E. coli* metabolic network is highly uneven. Furthermore, the study indicated that most metabolic reactions have low fluxes, and the overall activity of metabolism is dominated by several reactions with very high fluxes i.e. the reactions in central metabolism. Fluxes, mainly within the high-flux backbone, are reorganised by *E. coli* in response to changes in growth conditions (Almaas et al., 2004).

Evident in these examples of metabolic flux analysis is the trend towards developing larger and more comprehensive flux models. This is desirable in terms of the overall goal of simulating cellular activity *in silico*, however comprehensive models of metabolism are not always required. As the final example demonstrated, the majority of carbon flux is concentrated in a high-flux backbone, in the central metabolic pathways. Therefore, a smaller flux model of central metabolism can be effectively used for many investigative studies. In the work presented here, a small model of *E. coli* central metabolism was used to study the flow of carbon to acetate and other organic acids in *E. coli* MG1655 expressing antisense RNA targeted against phosphotransacetylase and acetate kinase. The aim of the study was to determine the effectiveness of antisense RNA in redirecting carbon flux in *E. coli* central metabolism.

174

6.3 MATERIALS AND METHODS

6.3.1 *E. COLI* FERMENTATIONS

The fermentation data used for metabolic flux analysis in this study was obtained from bioreactor experiments described in Chapter 5. Materials and methods for fermentation procedures are detailed in Chapter 2.

Briefly, batch fermentations of *E. coli* MG1655 harbouring recombinant plasmids were performed in a 2 L bioreactor (1 L working volume). Cultures were grown in selective M9 minimal media supplemented with 10 g L^{-1} glucose and a trace element solution (see section 2.5.2). Fermentations were maintained at 37°C, pH 7.0, airflow rate of 1 vvm, and impeller agitation rate of 800 rpm. These aeration conditions maintained a DOT of >60% throughout the 24 h fermentation. Two molar phosphoric acid and two molar sodium hydroxide were used to control pH.

Each fermentation was prepared in the same manner and run under the same conditions. A 10 ml culture was inoculated using a colony from a fresh selective nutrient agar plate, and incubated at 37°C, 200 rpm for ~6 hours. The entire 10 ml culture was then used to inoculate 90 ml sterile media, and incubated at 37°C, 200 rpm overnight. The resulting 100 ml pre-culture was then used to inoculate 900 ml sterile media in the fermenter to bring the working volume to 1 L. Ten samples were aseptically removed from the fermenter over the course of the 24 h fermentation. The cell density (OD_{600}) was determined, then the sample was immediately centrifuged and the supernatant was removed from the solids, and stored at -20°C for analysis. The cell pellet was stored at -80°C for analysis. The concentrations of residual glucose and organic acids in the supernatant samples were determined by colorimetric assay and HPLC, as described in section 2.6.

6.3.2 DATA PREPARATION FOR METABOLIC FLUX ANALYSIS

After the fermentation data was collected and analysed, the external fluxes (i.e. growth rate, specific glucose uptake rate and specific organic acid production rates) were calculated in order to perform metabolic flux analysis. Three steps were used to calculate the external fluxes: 1) partitioning of the fermentation data into phases of linear change, 2) calculation of the slope for each measured variable in each phase, and 3) conversion into specific flux units (mM h^{-1} g DCW^{-1}) to account for biomass variations. There are different ways of calculating the external fluxes for metabolic flux analysis, however this

method suited the data that was obtained in this study, and was also used to examine the impact of antisense RNA expression in the study of Desai and Papoutsakis (1999).

The first step was to plot the fermentation data (biomass, residual glucose concentration and organic acid concentration) on a single graph, and partition the data into phases where all variables are changing linearly. The plotted data helped to determine where to partition the data into phases. For example, one phase boundary would be at the change from exponential growth into stationary phase. The slope of the biomass changes at this point, therefore the biomass variable is not changing linearly. Examples of how data was partitioned into phases are shown in the following sections. The phases are indicated in roman numerals above the graphs. The second step was to calculate the slope of the line (mM h^{-1}) for each variable in each phase. Finally, to account for variations in biomass, the specific flux for each variable at the mid-point of each phase was calculated. The resulting specific flux units were millimolar per hour per gram of dry cell weight (mM h^{-1} g DCW^{-1}). Metabolic flux analysis was performed for each phase, using the measured extracellular fluxes as inputs for the calculation. Comparisons were then made between the internal flux distributions of different phases in a fermentation, and comparable phases in different fermentations.

6.3.3   METABOLIC FLUX ANALYSIS

In this study, MFA was performed using the computer programme FluxAnalyzer V. 4.1, which was developed specifically for flux and pathway analysis in metabolic networks by Steffen Klamt (Max-Planck-Institute for Dynamics of Complex Technical Systems, Magdeburg, Germany; http://www.mpi-magdeburg.mpg.de/projects/fluxanalyzer; E-mail: Klamt@mpi-magdeburg.mpg.de). This software is freely available for scientific purposes, and requires Mathwork's MATLAB software for operation.

A metabolic model of *E. coli* central metabolism, that was developed by Steffen Klamt (see contact details above) and provided with the FluxAnalyzer software, was used for metabolic flux analysis in this study. Figure 6.1 shows a diagram of the *E. coli* metabolic network as it appears in the Flux Analyzer programme. The grey boxes beside each reaction arrow are for the display of flux values. The model is composed of 106 reactions, (see Appendix 1) including glycolysis, the TCA cycle, pentose phosphate cycle, oxidative phosphorylation and pathways for amino acid biosynthesis. There are 89 internal (balanced) metabolites (abbreviations and full names of each metabolite are listed in Appendix 2). Consequently, the model has 17 degrees of freedom, which means that 17 fluxes must be specified in order to determine the intracellular flux distribution.

The 17 fluxes that were used as inputs to calculate the intracellular flux distributions in this study include measured extracellular fluxes and fluxes that can be set to 0.00, to constrain the model (see Table 6.1). The fluxes set to 0.00 include uptake fluxes of carbon compounds that are not present in the media and cannot therefore be taken up into the cell, reactions that we can assume are not occurring under the fermentation conditions, and some reverse reactions. Futile cycles and linearly dependent reactions (i.e. coupled reactions such as the interconversion of cofactors, or reversible reactions in central metabolism) cannot be included in flux balance models as the linear algebra used to calculate the intracellular flux distributions cannot resolve these reactions. Such reactions will simply cancel each other out (Stephanopoulos et al., 1998). Due to technical problems with the measurement of carbon dioxide evolution and oxygen uptake in some of the bioreactor experiments, the CPR and OUR have not been used as inputs for metabolic flux analysis. Instead they are left as 'unknown' and are calculated by MFA, along with the intracellular flux distribution.

Table 6.1   Set of fluxes used to constrain the stoichiometric model and calculate intracellular flux distributions.

Measured extracellular fluxes	Fluxes set to 0.00 to constrain the model
1. μ (specific growth rate)	1. Glucose uptake (non-PTS)
2. Glucose uptake rate	2. Gluconate uptake
3. Acetate production rate	3. Glycerol uptake
4. Lactate production rate	4. 6-phosphogluconate : 2 keto-3-desoxy-6-phosphogluconate
5. Formate production rate	5. Isocitrate : glyoxylate
6. Ethanol production rate	6. NADH : NADPH
7. Succinate production rate	7. Fructose-1,6-bisphosphate : Fructose-6-phosphate
	8. Oxaloacetate : Phosphoenolpyruvate
	9. Pyruvate : Phosphoenolpyruvate
	10. Fumarate : Succinate

Figure 6.1 *E. coli* metabolic reaction network. External metabolites are shown in boxes. The grey boxes are used to display fluxes. Measured extracellular fluxes are inputted into the appropriate boxes, and used to calculate the unknown internal fluxes.

6.4   SENSITIVITY ANALYSIS OF THE *E. COLI* METABOLIC NETWORK

The results of metabolic flux analysis are only as accurate as the experimentally measured rates that are used as inputs for the flux calculation. To analyse the effect of variability in the measured input fluxes on the calculated output fluxes, a sensitivity analysis was performed. The input data-set used for the sensitivity analysis was from the control culture *E. coli* MG1655(pTrc99A), Phase II (see section 6.5.1). Sensitivity analysis was performed by calculating the internal flux distribution for a high and low value of each measured input flux, and determining the maximum variability on the output fluxes. The high values corresponded to the mean flux value plus standard error, and the low values corresponded to the mean flux value minus standard error. Results of the sensitivity analysis are reported in Table 6.2.

The results showed that variability in the measured glucose uptake rate leads to the greatest variation in the calculated output fluxes in central metabolism. The standard error on the measured glucose uptake rate was ± 6 %. However, this small variation led to up to 13 % variation in calculated oxygen uptake rates and carbon dioxide production rates, up to 16 % variation in calculated fluxes through glycolysis and up to 20 % variation in calculated fluxes through the TCA cycle. These variations are quite high and should be taken in consideration when comparing metabolic flux distributions and extrapolating differences between different flux maps. In contrast, the error margin on the specific growth rate and the acetate production rate did not have such a great effect on the variability of the calculated output fluxes.

Table 6.2 Sensitivity analysis of *E. coli* MG1655(pTrc99A) Phase II.

	Reaction 1: μ		Reaction 6: Glc_PTS_up		Reaction 14: Ac_ex	
	HIGH	LOW	HIGH	LOW	HIGH	LOW
MEASURED INPUT FLUXES						
Reaction 1: μ (0.49 ± 0.03)	**0.52**	**0.46**	0.49	0.49	0.49	0.49
Reaction 6: Glc_PTS_up (8.5 ± 0.5)	8.5	8.5	**9.0**	**8.0**	8.5	8.5
Reaction 12: Lac_ex (0)	0	0	0	0	0	0
Reaction 14: Ac_ex (3.6 ± 0.1)	3.6	3.6	3.6	3.6	**3.7**	**3.5**
CALCULATED OUTPUT FLUXES						
Reaction 2: O2_up :	21.1	23.7	25.4	19.4	22.2	22.6
Reaction 3: N_up :	5.7	5.0	5.3	5.3	5.3	5.3
Reaction 4: CO2_ex :	22.4	24.9	26.6	20.6	23.4	23.8
Reaction 5: S_up :	0.1	0.1	0.1	0.1	0.1	0.1
Reaction 7: Glc_ATP_up :	0	0	0	0	0	0
Reaction 8: Succ_ex :	0	0	0	0	0	0
Reaction 9: Glyc_up :	0	0	0	0	0	0
Reaction 10: Glyc::Glyc3P :	0	0	0	0	0	0
Reaction 11: DHAP::Glyc3P :	0.07	0.07	0.07	0.07	0.07	0.07
Reaction 13: Eth_ex :	0	0	0	0	0	0
Reaction 15: Glucn_up :	0	0	0	0	0	0
Reaction 16: Form_ex :	0	0	0	0	0	0
Reaction 17: G6P::F6P :	6.3	7.5	8.0	5.8	6.8	7.0
Reaction 18: F16P::F6P :	0	0	0	0	0	0
Reaction 19: F6P::F16P :	7.3	7.8	8.3	6.9	7.5	7.6
Reaction 20: F16P::T3P :	7.3	7.8	8.3	6.9	7.5	7.6
Reaction 21: DHAP::G3P :	7.3	7.7	8.2	6.8	7.5	7.5
Reaction 22: G3P::DPG :	15.1	15.6	16.5	14.1	15.3	15.4
Reaction 23: DPG::3PG :	15.1	15.6	16.5	14.1	15.3	15.4
Reaction 24: 3PG::2PG :	14.1	14.8	15.7	13.3	14.4	14.5
Reaction 25: 2PG::PEP :	14.1	14.8	15.7	13.3	14.4	14.5
Reaction 26: PEP::PYR :	3.7	4.5	4.8	3.4	4.1	4.1
Reaction 27: Pyr::PEP :	0	0	0	0	0	0
Reaction 28: PYR::AcCoA :	10.6	11.6	12.3	9.9	11.1	11.1
Reaction 29: AcCoA::Cit :	5.4	6.6	7.2	4.8	5.9	6.2

Reaction						
Reaction 30: Cit::ICit :	5.4	6.6	7.2	4.8	5.9	6.2
Reaction 31: ICit::alKG :	5.4	6.6	7.2	4.8	5.9	6.2
Reaction 32: alKG::SuccCoA :	4.8	6.1	6.7	4.3	5.3	5.6
Reaction 33: SuccCoA::Succ :	4.5	5.9	6.4	4.0	5.1	5.3
Reaction 34: Succ::Fum :	4.8	6.1	6.7	4.3	5.3	5.6
Reaction 35: Fum::Succ :	0	0	0	0	0	0
Reaction 36: Fum::Mal :	5.4	6.6	7.2	4.8	5.9	6.1
Reaction 37: Mal::OxA :	5.4	6.6	7.2	4.8	5.9	6.1
Reaction 38: ICit::Glyox :	0	0	0	0	0	0
Reaction 39: Glyox::Mal :	0	0	0	0	0	0
Reaction 40: G6P::PGlac :	2.1	1.0	0.9	2.1	1.6	1.5
Reaction 41: AcCoA::Adh :	0	0	0	0	0	0
Reaction 42: Adh::Eth :	0	0	0	0	0	0
Reaction 43: PGlac::PGluc :	2.1	1.0	0.9	2.1	1.6	1.5
Reaction 44: Glucn::PGluc :	0	0	0	0	0	0
Reaction 45: PGluc::RI5P :	2.1	1.0	0.9	2.1	1.6	1.5
Reaction 46: RI5P::X5P :	1.1	0.3	0.3	1.1	0.7	0.6
Reaction 47: RI5P::R5P :	1.1	0.6	0.7	1.1	0.9	0.8
Reaction 48: Transket1 :	0.6	0.3	0.2	0.6	0.5	0.4
Reaction 49: Transaldo :	0.4	0.06	0.04	0.4	0.3	0.2
Reaction 50: Transket2 :	0.6	0.3	0.2	0.6	0.5	0.4
Reaction 51: PGluc::KetoPGluc :	0	0	0	0	0	0
Reaction 52: KetoPGluc::G3P_Pyr :	0	0	0	0	0	0
Reaction 53: OxA::PEP :	0	0	0	0	0	0
Reaction 54: PEP::OxA :	1.5	1.4	1.4	1.4	1.4	1.4
Reaction 55: AcCoA::AcP :	3.3	3.3	3.3	3.3	3.4	3.2
Reaction 56: AcP::Ac :	3.3	3.3	3.3	3.3	3.4	3.2
Reaction 57: Pyr::Form :	0	0	0	0	0	0
Reaction 58: Pyr::Lac :	0	0	0	0	0	0

181

6.5   RESULTS OF METABOLIC FLUX ANALYSIS

6.5.1   METABOLIC FLUX ANALYSIS OF *E. COLI* MG1655(PQR439)

Metabolic flux analysis was performed to examine the impact of reduced acetate production on carbon fluxes in *E. coli* MG1655(pQR439) expressing putative *pta* antisense RNA. The results were compared with the carbon fluxes in the plasmid control strain, *E. coli* MG1655(pTrc99A). The first step was to examine the substrate and product concentration profiles for each strain, and partition the data into phases of approximately linear change. Profiles for *E. coli* MG1655(pTrc99A) and *E. coli* MG1655(pRQ439) induced are shown in Figure 6.2. The data was partitioned into four phases, which are labelled at the top of each graph in roman numerals. Specific external fluxes were then determined at the mid-point of each phase of interest and used to calculate the intracellular flux distribution (Table 6.3). In this study, MFA was not performed for phase I or phase IV. This was due to the fact that in phase I, which corresponded to early exponential growth phase, the biomass levels were low, the cells were adjusting to conditions in the fermenter, and there was some variations in the measurements of residual glucose concentration during this time. In phase IV, which corresponded to stationary phase, there were not enough data points to establish the rates of substrate uptake and product formation.

Phase II corresponded to mid-late exponential growth phase in both the control culture, *E. coli* MG1655(pTrc99A), and *E. coli* MG1655(pQR439) expressing putative *pta* antisense RNA. Metabolic flux analysis showed that the intracellular flux distributions were comparable in both cultures during this time. This is not surprising given the similar substrate utilisation and product formation patterns for these cultures (as described in Chapter 5, section 5.2.3). Phase III corresponded to early stationary phase in both the control cultures. Once again, due to similar physiological profiles, MFA revealed very similar flux distributions for the control culture and the culture of *E. coli* MG1655(pQR439) expressing putative *pta* antisense RNA. Therefore, due to the greatest differences occurring during stationary phase, this approach was not able to provide additional insight into the effect of putative *pta* antisense RNA on carbon flow through central metabolism.

The results from metabolic flux analysis of *E. coli* MG1655(pQR441) and *E. coli* MG1655(pTrc99A/pQR439) also showed no noticeable differences in the flux distributions during the phases were there was sufficient data to perform MFA. Therefore, the results of these studies are not described further.

Figure 6.2 Time course profiles of biomass (●), residual glucose (○), acetate concentration (▲) and lactate concentration (△) in (A) *E. coli* MG1655(pTrc99A) and (B) *E. coli* MG1655(pQR439) induced. The data is partitioned into four phases where the rate of change of each variable is approximately linear.

Table 6.3 Measured input fluxes and calculated output fluxes for *E. coli* MG1655(pTrc99A) and *E. coli* MG1655(pQR439) induced for phases II and III.

	E. coli MG1655(pTrc99A)		*E. coli* MG1655 (pQR439) induced	
	Phase II	Phase III	Phase II	Phase III
INPUTS				
Reaction 1: μ	0.49	0.02	0.55	0.12
Reaction 6: Glc_PTS_up	8.5	0.6	9.7	1.5
Reaction 12: Lac_ex	0	0.5	0.7	0.2
Reaction 14: Ac_ex	3.6	0.2	4.8	0.6
OUTPUTS				
Reaction 2: O2_up :	22.4	0.6	22.3	1.8
Reaction 3: N_up :	5.3	0.2	6.0	1.8
Reaction 4: CO2_ex :	23.6	0.6	28.7	2.1
Reaction 5: S_up :	0.1	0.01	0.1	0.08
Reaction 7: Glc_ATP_up :	0	0	0	0
Reaction 8: Succ_ex :	0	0	0	0
Reaction 9: Glyc_up :	0	0	0	0
Reaction 10: Glyc::Glyc3P :	0	0	0	0
Reaction 11: DHAP::Glyc3P :	0.1	0.01	0.1	0.02
Reaction 13: Eth_ex :	0	0	0	0
Reaction 15: Glucn_up :	0	0	0	0
Reaction 16: Form_ex :	0	0	0	0
Reaction 17: G6P::F6P :	6.9	0.4	7.1	0.4
Reaction 18: F16P::F6P :	0	0	0	0
Reaction 19: F6P::F16P :	7.6	0.5	8.4	1.0
Reaction 20: F16P::T3P :	7.6	0.4	8.4	1.0
Reaction 21: DHAP::G3P :	7.5	0.5	8.3	0.9
Reaction 22: G3P::DPG :	15.3	1.0	17.2	2.3
Reaction 23: DPG::3PG :	15.3	1.0	17.2	2.3
Reaction 24: 3PG::2PG :	14.5	1.0	16.3	2.1
Reaction 25: 2PG::PEP :	14.5	1.0	16.3	2.1
Reaction 26: PEP::PYR :	4.1	0.3	4.5	0.1
Reaction 27: Pyr::PEP :	0	0	0	0

Reaction 28: PYR::AcCoA :	11.1	0.3	11.8	1.1
Reaction 29: AcCoA::Cit :	6.0	0.03	5.4	0.2
Reaction 30: Cit::ICit :	6.0	0.09	5.4	0.2
Reaction 31: ICit::alKG :	6.0	0.09	5.4	0.2
Reaction 32: alKG::SuccCoA :	5.5	0.07	4.7	0.01
Reaction 33: SuccCoA::Succ :	5.2	0.06	4.4	0.06
Reaction 34: Succ::Fum :	5.5	0.07	4.7	0.01
Reaction 35: Fum::Succ :	0	0	0	0
Reaction 36: Fum::Mal :	6.0	0.09	5.3	0.1
Reaction 37: Mal::OxA :	6.0	0.08	5.3	0.1
Reaction 38: ICit::Glyox :	0	0	0	0
Reaction 39: Glyox::Mal :	0	0	0	0
Reaction 40: G6P::PGlac :	1.5	0.1	2.4	1.1
Reaction 41: AcCoA::Adh :	0	0	0	0
Reaction 42: Adh::Eth :	0	0	0	0
Reaction 43: PGlac::PGluc :	1.5	0.1	2.4	1.1
Reaction 44: Glucn::PGluc :	0	0	0	0
Reaction 45: PGluc::RI5P :	1.5	0.1	2.4	1.1
Reaction 46: RI5P::X5P :	0.7	0.08	1.2	0.6
Reaction 47: RI5P::R5P :	0.9	0.06	1.2	0.5
Reaction 48: Transket1 :	0.4	0.05	0.8	0.3
Reaction 49: Transaldo :	0.4	0.04	0.7	0.3
Reaction 50: Transket2 :	0.2	0.05	0.5	0.3
Reaction 51: PGluc::KetoPGluc :	0	0	0	0
Reaction 52: KetoPGluc::G3P_Pyr :	0	0	0	0
Reaction 53: OxA::PEP :	0	0	0	0
Reaction 54: PEP::OxA :	1.4	0.06	1.6	0.4
Reaction 55: AcCoA::AcP :	3.3	0.2	4.5	0.5
Reaction 56: AcP::Ac :	3.3	0.2	4.5	0.5
Reaction 57: Pyr::Form :	0	0	0	0
Reaction 58: Pyr::Lac :	0	0.5	0.7	0.2

6.5.2 METABOLIC FLUX ANALYSIS OF *E. COLI* MG1655(PQR446)

Metabolic flux analysis was performed to assess the impact of the dramatically altered physiology of *E. coli* MG1655(pRQ446) expressing putative *ackA* antisense RNA (see Chapter 5, section 5.3.6), on carbon fluxes through the central metabolic pathways. The results were compared with the carbon fluxes in the plasmid control strain, *E. coli* MG1655(pQR445). Fluxes were calculated as previously described in section 6.4.1, and are displayed in Table 6.4. The partitioned profiles of substrate uptake and product formation are shown in Figure 6.3.

The control culture, *E. coli* MG1655(pQR445), and the induced culture of *E. coli* MG1655(pQR446), exhibited very different substrate uptake and product formation patterns, therefore the linear phases in the two cultures are not directly comparable. However, comparisons have been made as far as possible and are discussed below. Metabolic flux analysis was not performed for phase IV due to the small number of data points in this phase.

Phase I corresponded to exponential growth phase in the control culture and early exponential growth phase in the induced culture of *E. coli* MG1655(pQR446). Metabolic flux analysis revealed that the specific fluxes through glycolysis were similar for both cultures, however *E. coli* MG1655(pQR446) exhibited lower specific fluxes through the pentose phosphate pathway and through the TCA cycle (Figure 6.4), which is presumably due to the lower rate of biomass production and therefore the reduced requirement for production of NADPH. The most notable difference involves the flow of carbon to lactate and acetate in these cultures.

Phase II corresponded to late exponential growth phase/transition phase in the control culture *E. coli* MG1655(pQR445), and mid-exponential growth phase in *E. coli* MG1655(pQR446) induced. Metabolic flux analysis revealed that the specific fluxes through glycolysis were ~4-fold higher in the induced culture of *E. coli* MG1655(pQR446) compared to the control culture. In addition, the specific fluxes through the pentose phosphate pathway were ~3-fold lower in the induced culture of *E. coli* MG1655(pQR446) compared to the control culture. The specific fluxes through the TCA cycle were similar for both cultures. These results confirm that glucose is being utilised primarily for lactate production in the induced culture of *E. coli* MG1655(pQR446) at the expense of biomass production. The results are illustrated in Figure 6.5.

Phase III corresponded to the transition between exponential growth phase and stationary phase in the control culture, *E. coli* MG1655(pQR445), and late exponential growth phase in the induced culture of *E. coli* MG1655(pQR446). Metabolic flux analysis revealed low specific fluxes through glycolysis, the pentose phosphate pathway and the TCA cycle in the control culture. This was expected, due to the fact that biomass production was very low during this time. Specific acetate and lactate production fluxes were also low in the control culture in phase III. In contrast, the specific fluxes in phase III through the central metabolic pathways in the induced culture of *E. coli* MG1655(pQR446) were only slightly lower than in phase II. This was expected due to the substrate uptake and product formation patterns during this phase. Flux distributions in these two cultures cannot be directly compared for phase III because the cultures are in different stages of growth.
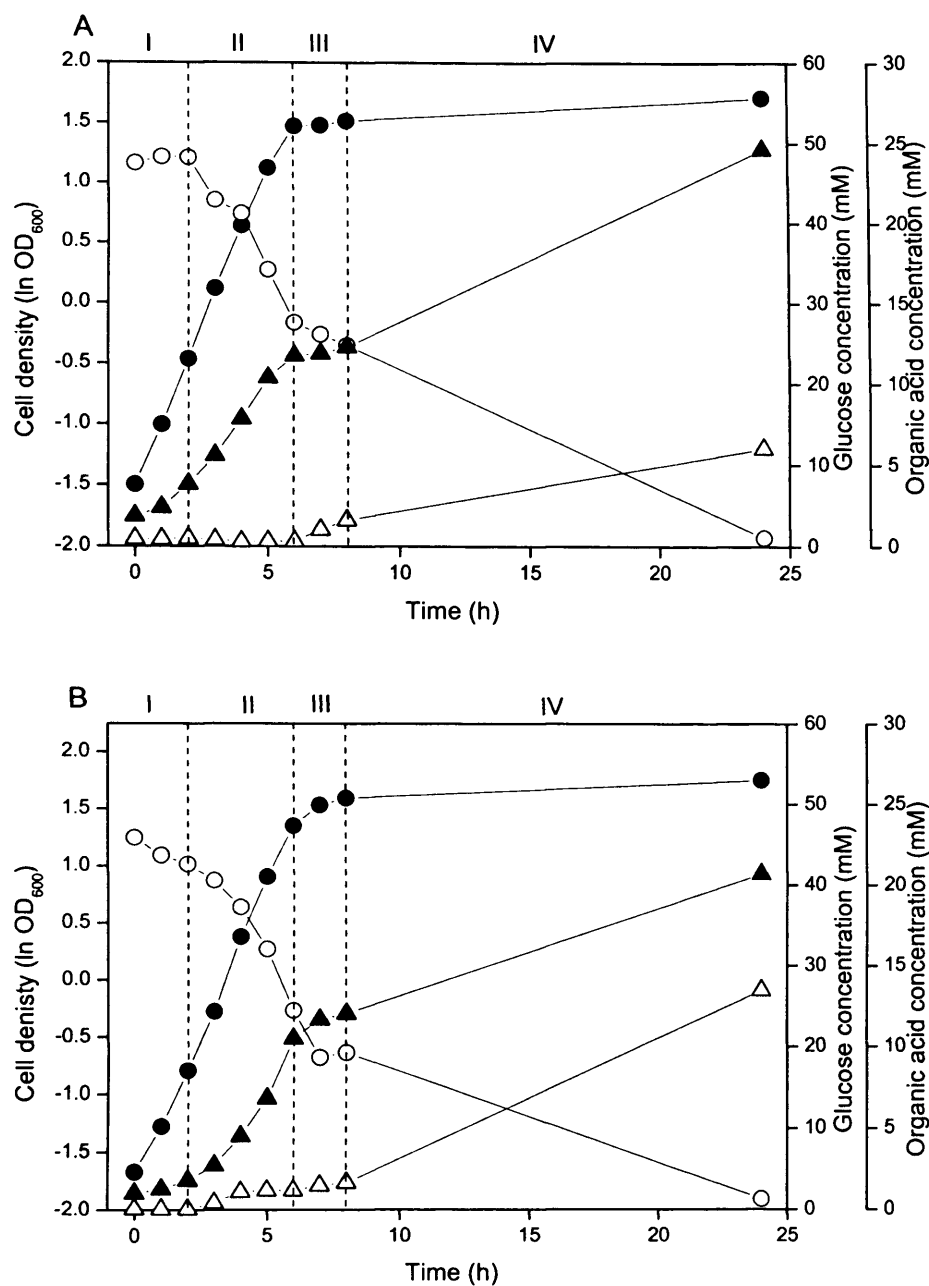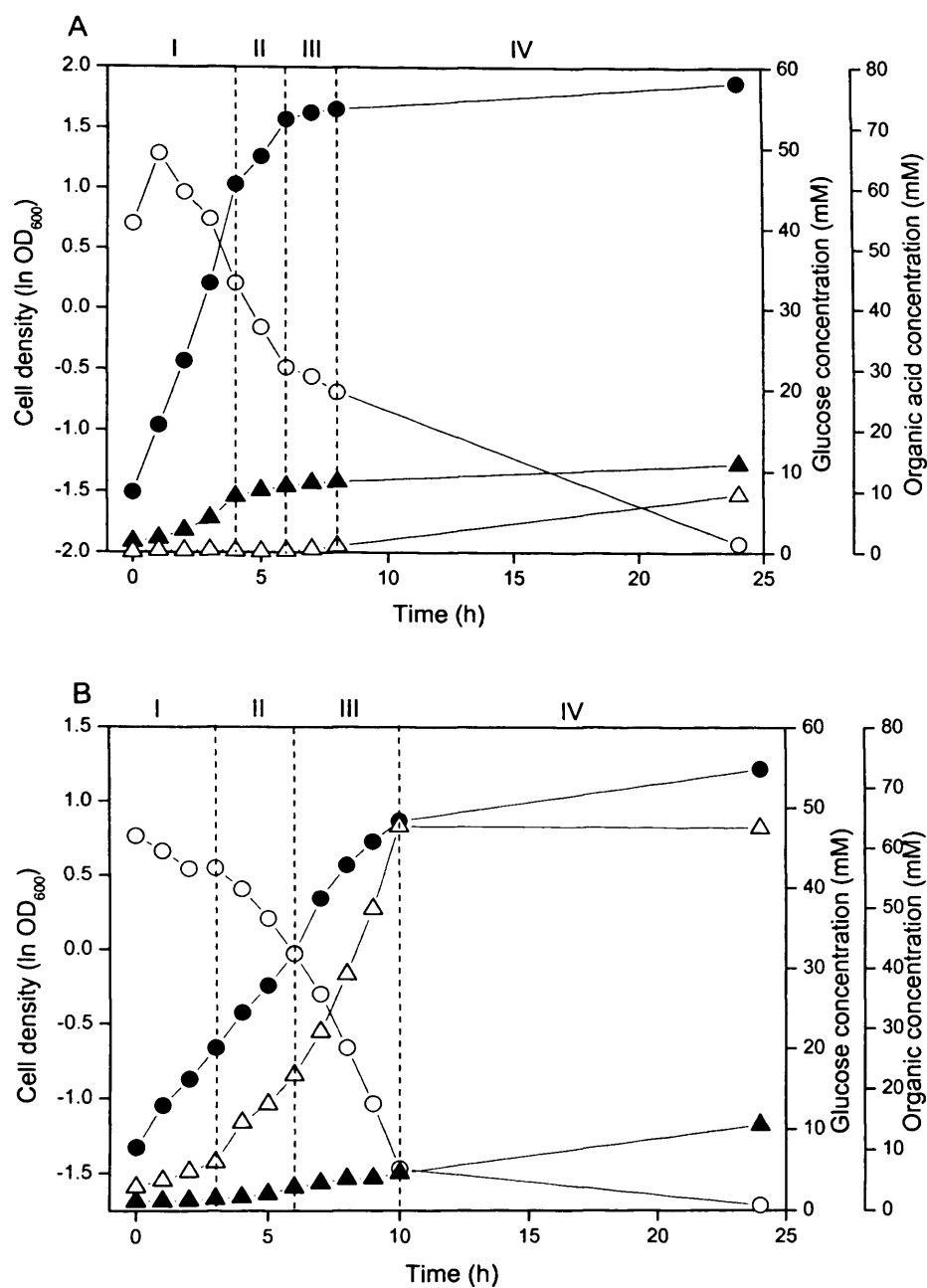
Figure 6.3 Time course profiles of biomass (●), residual glucose (○), acetate concentration (▲) and lactate concentration (△) in (A) *E. coli* MG1655(pQR445) and (B) *E. coli* MG1655(pQR446) induced. The data is partitioned into four phases where the rate of change of each variable is approximately linear.

Table 6.4 Measured input fluxes and calculated output fluxes for *E. coli* MG1655(pQR445) and *E. coli* MG1655(pQR446) induced for phases I, II and III.

	E. coli MG1655(pQR445)			*E. coli* MG1655 (pQR446) induced		
	Phase I	Phase II	Phase III	Phase I	Phase II	Phase III
INPUTS						
Reaction 1: μ	0.63	0.27	0.044	0.22	0.21	0.22
Reaction 6: Glc_PTS_up	11.5	3.9	0.67	9.3	15.1	13.1
Reaction 12: Lac_ex	0.2	0.01	0.26	12.0	21.2	19.5
Reaction 14: Ac_ex	9.4	0.75	0.27	1.3	2.8	1.0
OUTPUTS						
Reaction 2: O2_up :	21.9	10.3	0.8	8.0	12.3	8.6
Reaction 3: N_up :	6.7	2.9	0.5	2.4	2.3	2.4
Reaction 4: CO2_ex :	23.5	11.0	0.8	8.5	12.6	8.2
Reaction 5: S_up :	0.2	0.07	0.01	0.07	0.06	0.06
Reaction 7: Glc_ATP_up :	0	0	0	0	0	0
Reaction 8: Succ_ex :	0	0	0	0	0	0
Reaction 9: Glyc_up :	0	0	0	0	0	0
Reaction 10: Glyc::Glyc3P :	0	0	0	0	0	0
Reaction 11: DHAP::Glyc3P :	0.1	0.04	0.01	0.03	0.03	0.03
Reaction 13: Eth_ex :	0	0	0	0	0	0
Reaction 15: Glucn_up :	0	0	0	0	0	0
Reaction 16: Form_ex :	0	0	0	0	0	0
Reaction 17: G6P::F6P :	7.1	2.9	0.4	8.2	14.7	12.2
Reaction 18: F16P::F6P :	0	0	0	0	0	0
Reaction 19: F6P::F16P :	9.5	3.4	0.5	8.7	14.8	12.7
Reaction 20: F16P::T3P :	9.5	3.3	0.5	8.7	14.0	12.7
Reaction 21: DHAP::G3P :	9.9	3.3	0.5	8.7	14.8	12.6
Reaction 22: G3P::DPG :	20.0	6.8	1.1	17.7	30.0	25.4
Reaction 23: DPG::3PG :	20.0	6.9	1.1	17.7	30.0	25.4
Reaction 24: 3PG::2PG :	18.9	6.4	1.0	17.3	29.2	25.1
Reaction 25: 2PG::PEP :	18.9	6.4	1.0	17.3	29.2	25.1
Reaction 26: PEP::PYR :	5.0	1.5	0.2	7.2	13.3	11.1
Reaction 27: Pyr::PEP :	0	0	0	0	0	0

Reaction						
Reaction 28: PYR::AcCoA :	14.3	4.6	0.5	3.9	6.6	4.0
Reaction 29: AcCoA::Cit :	3.1	3.0	0.08	2.0	3.2	2.4
Reaction 30: Cit::ICit :	3.1	3.0	0.08	2.0	3.2	2.4
Reaction 31: ICit::alKG :	3.1	3.0	0.08	2.0	3.2	2.4
Reaction 32: alKG::SuccCoA :	2.4	2.7	0.08	1.7	2.9	2.1
Reaction 33: SuccCoA::Succ :	2.0	2.5	0.08	1.6	2.8	2.0
Reaction 34: Succ::Fum :	2.4	2.7	0.03	1.7	2.9	2.1
Reaction 35: Fum::Succ :	0	0	0	0	0	0
Reaction 36: Fum::Mal :	3.0	2.9	0.08	1.9	3.1	2.4
Reaction 37: Mal::OxA :	3.0	3.0	0.08	2.0	3.1	2.4
Reaction 38: ICit::Glyox :	0	0	0	0	0	0
Reaction 39: Glyox::Mal :	0	0	0	0	0	0
Reaction 40: G6P::PGlac :	4.3	1.0	0.4	1.0	0.4	0.9
Reaction 41: AcCoA::Adh :	0	0	0	0	0	0
Reaction 42: Adh::Eth :	0	0	0	0	0	0
Reaction 43: PGlac::PGluc :	4.3	1.0	0.4	1.0	0.4	0.9
Reaction 44: Glucn::PGluc :	0	0	0	0	0	0
Reaction 45: PGluc::RI5P :	4.3	1.0	0.4	1.0	0.4	0.7
Reaction 46: RI5P::X5P :	2.4	0.5	0.2	0.5	0.1	0.4
Reaction 47: RI5P::R5P :	1.8	0.5	0.2	0.5	0.3	0.4
Reaction 48: Transket1 :	1.4	0.3	0.1	0.3	0.1	0.3
Reaction 49: Transaldo :	1.1	0.1	0.1	0.2	0.008	0.2
Reaction 50: Transket2 :	1.4	0.3	0.1	0.3	0.1	0.3
Reaction 51: PGluc::KetoPGluc :	0	0	0	0	0	0
Reaction 52: KetoPGluc::G3P_Pyr :	0	0	0	0	0	0
Reaction 53: OxA::PEP :	0	0	0	0	0	0
Reaction 54: PEP::OxA :	1.9	0.8	0.1	0.6	0.6	0.6
Reaction 55: AcCoA::AcP :	9.0	0.6	0.2	1.1	2.7	0.9
Reaction 56: AcP::Ac :	9.0	0.6	0.2	1.1	2.7	0.9
Reaction 57: Pyr::Form :	0	0	0	0	0	0
Reaction 58: Pyr::Lac :	0.2	0.01	0.3	12.0	21.2	19.5
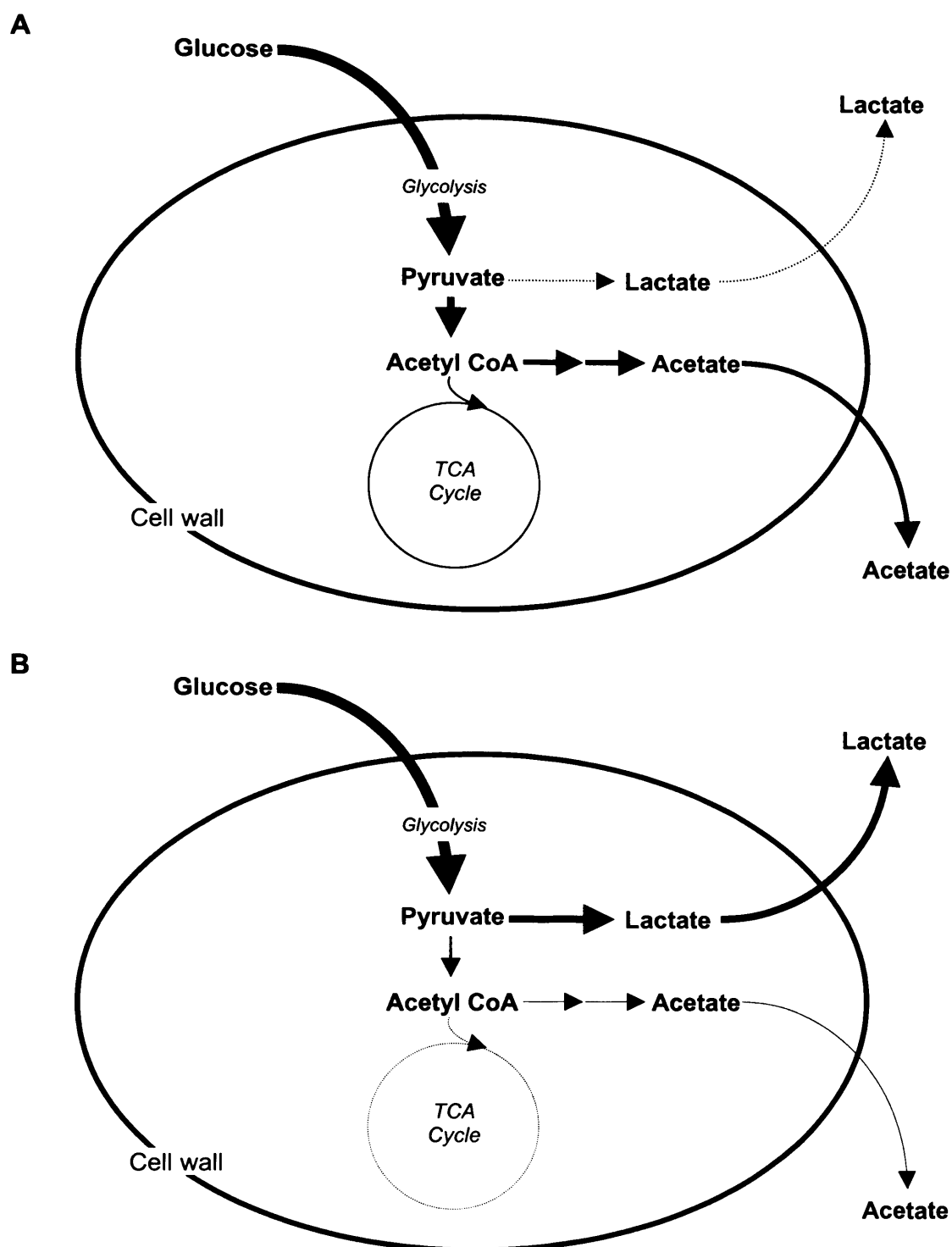
Figure 6.4 Simplified diagram of an *E. coli* cell, showing the differences in carbon flow through the central metabolic pathways during phase I, in cultures of *E. coli* MG1655 harbouring (A) the control plasmid pQR445, and (B) plasmid pQR446 expressing putative *ackA* antisense RNA.
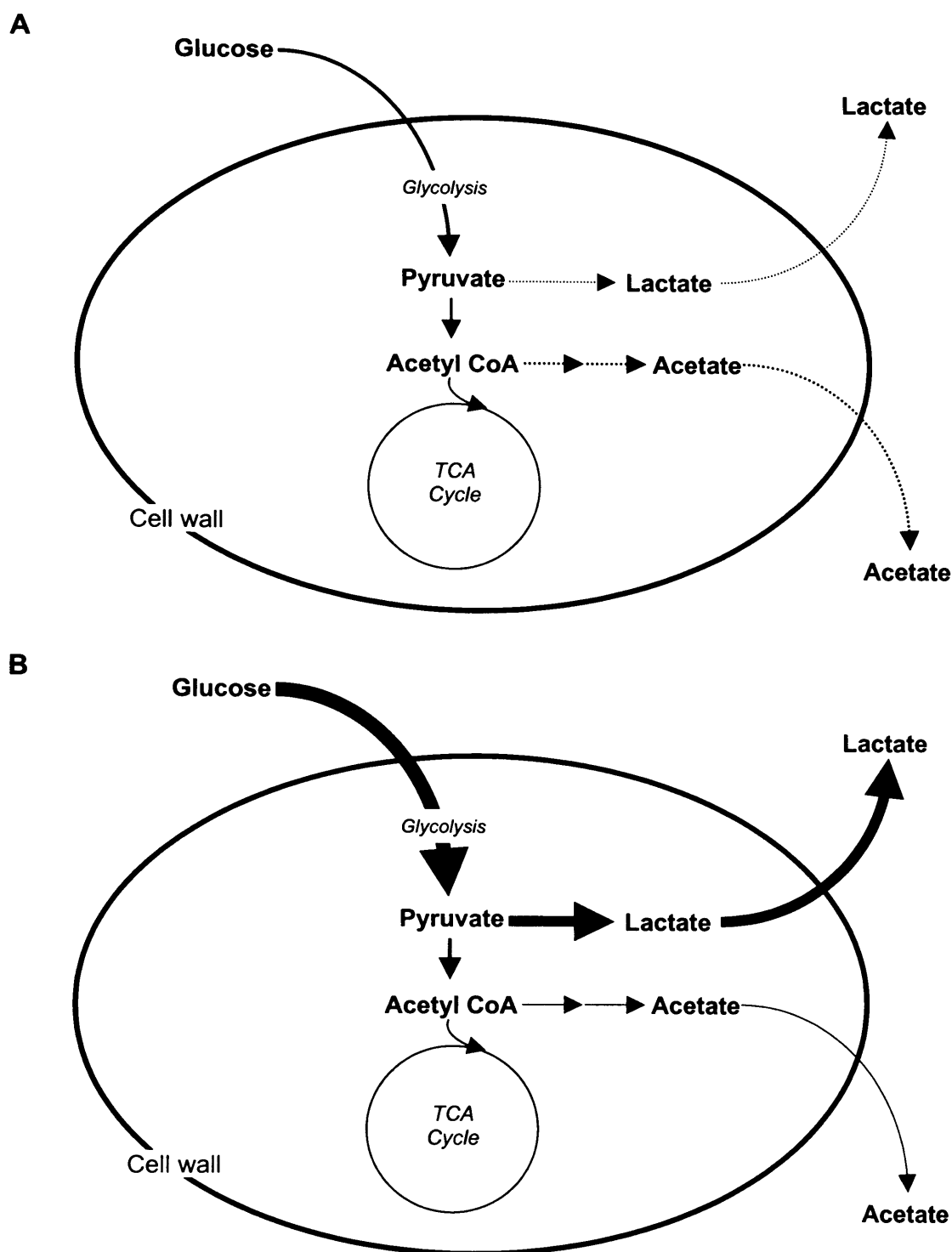
Figure 6.5 Simplified diagram of an *E. coli* cell, showing the differences in carbon flow through the central metabolic pathways during phase II, in cultures of *E. coli* MG1655 harbouring (A) the control plasmid pQR445, and (B) plasmid pQR446 expressing putative *ackA* antisense RNA.

6.6   DISCUSSION AND CONCLUSIONS

This chapter discussed the processes involved in performing metabolic flux analysis to examine the impact of putatively expressed antisense RNA on the carbon fluxes in *E. coli* MG1655. The studies presented in this chapter aimed to provide a more detailed insight into the effect of *pta* and *ackA* antisense RNA on *E. coli* MG1655 metabolism and complement the results from physiological studies presented in the previous chapter (Chapter 5). However, *E. coli* cultures that exhibited similar physiological profiles gave rise to very similar metabolic flux distributions, and only limited information could be gained from these analyses. Therefore, the results from this study suggest that metabolic flux analysis is most suited to analysing the impact of genetic or environmental perturbations that cause a pronounced change in the physiology of the *E. coli* strain. Cultures of *E. coli* MG1655 harbouring pRQ446 exhibited dramatically altered substrate uptake and product formation patterns, compared to the control culture. MFA was able to predict that the changes in growth and by-product secretion in this strain were a consequence of increased flux through the glycolytic pathway, and decreased flux through the pentose phosphate pathway.

Metabolic flux analysis is a useful tool for examining carbon flow through metabolism. However, the incorporation of enzyme data and regulatory information into future metabolic models will enable more detailed and accurate predictions of the dynamic behaviour in cellular metabolism.

CHAPTER 7

DISCUSSION
&
Conclusions

7.1 SUMMARY

This thesis described a metabolic engineering approach that was used to reduce acetate production by *E. coli*. The research involved using antisense RNA as an experimental tool to suppress expression of the enzymes phosphotransacetylase and acetate kinase, which catalyse the conversion of acetyl CoA to acetate in *E. coli*. The challenge was to determine the effectiveness of this antisense RNA strategy in reducing the target enzyme levels, and in re-directing carbon flow through central metabolism.

The research had three main components, each of which represented a phase of the metabolic engineering cycle. The metabolic engineering cycle involves design, modification and subsequent analysis of metabolism for the purpose of strain improvement. The design phase involves proposing genetic modifications to be carried out in order to achieve a specific bioprocessing goal. Modification involves the construction of a novel strain using recombinant DNA technology. Analysis involves characterisation of the resulting strain, which may include physiological studies and metabolic flux analysis. Results from the analytical studies may suggest additional modifications that could be made in order to improve the new strain further, and so the cycle continues (Nielsen, 2001). This research completed a full sequence of the metabolic engineering cycle. Design and construction of recombinant *E. coli* strains expressing putative *pta* and *ackA* antisense RNA was described in Chapter 4. Physiological characterisation of the resulting recombinant *E. coli* strains was described in Chapter 5, and metabolic flux analysis was presented in Chapter 6. This chapter aims to discuss broader aspects of the study and suggest future experiments that could be carried out to further the research.

7.2 EXPRESSION OF ANTISENSE RNA IN *E. COLI*

In this study, the plasmids pTrc99A and pMMB66EH were selected to use for expression of antisense RNA in *E. coli*. One of the reasons that these plasmids were chosen was that they possess the strong promoters, *trc* and *tac*, which make them ideal for high level expression of antisense RNA. This was important because it was anticipated that the artificially designed antisense RNA that was produced *in vivo* would not be very stable in the cell. Therefore, it was thought that if a large excess of antisense RNA was produced, this might compensate for the impact of antisense RNA degradation. An alternative method of overcoming the problem of antisense RNA stability in the cell would have been to incorporate stability control elements such as hairpin structures, on to the ends of the antisense RNA molecules (Carrier and Keasling, 1997; Carrier and Keasling, 1999).

Hairpin structures have been characterised in naturally occurring antisense RNA in *E. coli* and were found to be very important for the longevity of the antisense RNA molecule (Bricker and Belasco, 1999). Stability elements were not incorporated into the antisense RNA molecules in this study, however it would be interesting to investigate whether their presence would increase the stability, and possibly the impact, of *pta* and *ackA* antisense RNA on acetate production by *E. coli.*

Another important feature of the *trc* and *tac* promoters on plasmids pTrc99A and pMMB66EH respectively, is their regulation. Under repressed conditions, an inhibitor molecule, which is produced from the *lacI*^{q} gene present on each plasmid, prevents expression from the *trc* and *tac* promoters. Conditional expression from the *trc* and *tac* promoters is achieved by adding IPTG to the culture medium. In this study, IPTG was added to the culture medium to induce expression of antisense RNA at a selected point mid-way during *E. coli* fermentation. The idea was to examine cellular metabolism before and immediately after enzyme downregulation, which is not possible with the alternative approach of permanent gene inactivation (Datsenko and Wanner, 2000). However, the results from this study indicated that antisense RNA was produced from pTrc99A and pMMB66EH-derived plasmids that were grown under repressed conditions. This was shown in Chapter 5, sections 5.2 – 5.4 by the similarity in enzyme levels and organic acid production in the uninduced and induced cultures of *E. coli* harbouring plasmids that encoded antisense RNA. Therefore, an expression system with tighter control would have been more suitable for this study.

The problem is that the majority of expression vectors that are currently available were originally designed for the purpose of over-expressing heterologous proteins (Baneyx, 1999), and are not ideal for metabolic engineering. Typically, expression vectors are multicopy plasmids that replicate in a relaxed fashion, and are present at 15-60 (e.g. pMB1/ColE1- derived plasmids) or a few hundred copies per cell (e.g. the pUC series of plasmids). They usually possess relatively strong promoters, such as the *trc* or *tac* promoters used in this study, or the T7 promoter which is present on the pET series of vectors (Baneyx, 1999). These characteristics are ideal for achieving a high yield of recombinant protein. However, expression from high copy number plasmids can reduce cell growth due to the metabolic burden placed on the host cell, and strong promoters often have leaky expression of the recombinant products. Numerous researchers have found that these vectors produce significant amounts of protein even when grown under repressed conditions. Therefore, in recent years there has been a move towards developing expression vectors with lower copy numbers and tighter control of expression from the promoter (Anthony et al., 2004; Jones and Keasling, 1998; Warren et al., 2000).

These plasmids are useful for controlled expression of toxic genes, and may be more suitable for expressing products to manipulate cellular metabolism.

An alternative method of expressing antisense RNA *in vivo* would be to incorporate an expression cassette into the *E. coli* genome. This would overcome the problem of plasmid instability because the antisense RNA expression cassette would be replicated along with the rest of the *E. coli* chromosome and segregated at cell division. However, it would be more complicated technically and more time consuming. Furthermore, the amount of antisense RNA produced from one expression cassette inserted in to the genome is likely to be lower than the amount produced from a multicopy plasmid, due to a lower gene dosage. This could possibly be overcome by using a strong promoter or by duplicating the expression cassette so that multiple copies of the antisense RNA product were encoded by the *E. coli* genome. To the best of our knowledge this method has not be attempted for expression of antisense RNA in *E. coli*.

As previously mentioned in Chapter 4, the plasmids used in this study differ significantly in copy number. This was shown in Figure 4.14 by the difference in band intensities of the isolated plasmids, following analysis by agarose gel electrophoresis. Plasmid pTrc99A is a medium-high copy number plasmid, which is present in ~50-80 copies per cell (Lin-Chao and Bremer, 1986), and pMMB66EH is a relatively low copy number plasmid, which is present in ~10-15 copies per cell (Morales et al., 1990). It was hypothesised that the difference in plasmid copy number may affect the total amount of antisense RNA that was produced by each plasmid type, and result in different levels of gene silencing. However, only one copy of each of the target genes is present on the *E. coli* genome, therefore the antisense RNA molecules that are produced should still out-number the target mRNA molecules. In addition, both plasmids possess strong promoters, and therefore it was thought that an excess amount of antisense RNA would be produced by the constructs that were derived from both plasmid types.

In this study, an identical fragment of the *E. coli* acetate kinase gene was cloned in the antisense orientation into both pTrc99A and the pMMB66EH-derivative, pQR445 (see Chapter 4). Comparing the impact of *ackA* antisense RNA in each of the resulting *E. coli* strains should have indicated, whether there was a noticeable difference in the total amount of antisense RNA that was produced from each construct. For example, if the *ackA* antisense RNA expressed from the pMMB66EH-derivative had less of an impact on *E. coli* metabolism than an identical *ackA* antisense RNA expressed from pTrc99A, then it would suggest that the total amount of antisense RNA produced from the former construct was less. These hypothetical results could be confirmed by quantitative

analysis of the antisense RNA produced. However in this study, the recombinant *E. coli* strain expressing putative *ackA* antisense RNA from pQR446 (derived from pMMB66EH, see section 4.3.2.3) had a dramatically altered metabolism compared to the recombinant *E. coli* strain expressing *ackA* antisense RNA from pQR441 (derived from pTrc99A, see section 4.3.2.1). This was highly unexpected, and may have been due to complex interactions between components of the pQR446 plasmid and the *E. coli* genome, as discussed in Chapter 5, section 5.5.

7.3 ACETATE PRODUCTION BY *E. COLI*

As discussed in Chapter 1, it has long been thought that acetate production by *E. coli* is a result of metabolite 'overflow' in central metabolism, and is caused by an imbalance in the rate of carbon uptake into the cell and the rate of carbon utilisation for the production of biomass (Holms, 1986). The imbalance is thought to arise due to a limited capacity of the TCA cycle, leading to accumulation of acetyl CoA and subsequent 'overflow' of carbon flux to acetate (Han et al., 1992; Majewski and Domach, 1989). However, because acetate is relatively toxic to *E. coli*, the reason why *E. coli* has evolved to produce such high amounts under aerobic conditions has remained somewhat of a mystery. One theory is that acetate production allows *E. coli* to maintain a rapid growth rate by balancing the carbon flow, and by generating ATP during the conversion of acetyl phosphate to acetate (Han et al., 1992; Holms, 1986). Another probable function of the acetate production pathway is to generate the pathway intermediate acetyl phosphate, which has been implicated as a phosphate donor in range of cellular reactions (Fox et al., 1986b; Heyde et al., 2000; McCleary and Stock, 1994; Nystrom, 1994; PruB and Wolfe, 1994; Shin and Park, 1995; Wanner and Wilmes-Riesenberg, 1992).

Since the completion of this research, a new study has been published which used mutant strains of *E. coli* and enzyme active site directed inhibitors to investigate the role of acetate production by *E. coli* (El-Mansi, 2004). This study found that the abolition of carbon flux to acetate in *E. coli* ML308 was balanced by excretion of lactate as well as 2-oxoglutarate, isocitrate and citrate. Based on the observations a novel function for the acetate production pathway was proposed, which states that phosphotransacetylase has an anapleurotic function: replenishing the central metabolic pathways with free CoA. As shown in Figure 7.1, the conversion of acetyl CoA to acetyl phosphate liberates free CoA. It was suggested that reduced levels of free CoA in the cell cause a 'bottle-neck' effect at the level of 2-oxoglutarate in the TCA cycle, which is alleviated by the free CoA produced by phosphotransacetylase in the conversion of acetyl CoA to acetyl phosphate. Previously, it has been shown that increasing the intracellular concentration of free CoA

results in a higher yield of central metabolites (San et al., 2002), which lends support to this hypothesis.

In conclusion, it is becoming increasingly clear that abolishing the main acetate production pathway (*ackA-pta* pathway) is detrimental to *E. coli*, and that more advanced strategies are required in order to optimise metabolism for efficient conversion of glucose to biomass. In order to achieve this goal it is likely that a number of reactions would need to be manipulated in both the central metabolic pathways and the glucose phosphotransferase system. As we gain a greater understanding about the interactions of metabolites in the cell and the regulatory mechanisms that govern cellular activity, we will be better equipped to approach the rational optimisation of *E. coli*.

An idea for a future metabolic engineering strategy would be to over-express the enzyme acetyl CoA synthetase in *E. coli*, which is normally repressed during growth on glucose. This enzyme coverts acetate to acetyl CoA, therefore over-expressing this enzyme might allow acetate that has been produced by the *ackA-pta* pathway to be re-channelled back into central metabolism. Another idea would be to reduce expression of the glucose phosphotransferase enzymes using an antisense RNA approach.
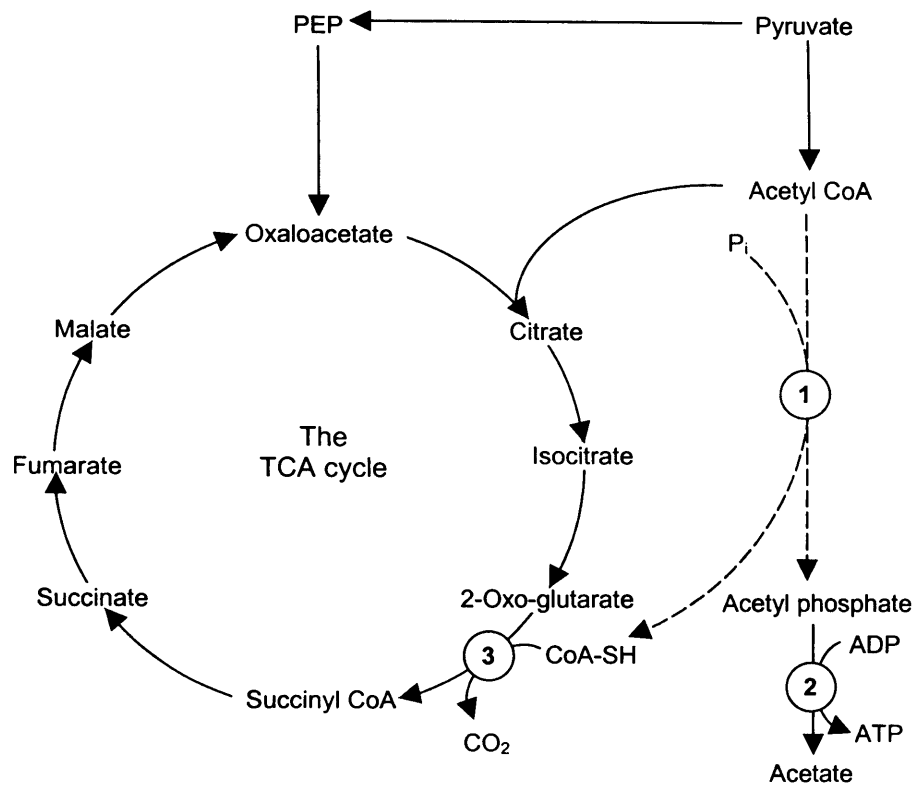
Figure 7.1 Representation of the TCA cycle, highlighting the possible anapleurotic function of phosphotransacetylase (replenishing the central metabolic pathways with free CoA). The arrows with dashed lines show the conversion of acetyl CoA to acetyl phosphate and the generation of free CoA. Key enzymes: 1, phosphotransacetylase; 2, acetate kinase; and 3, 2-oxoglutarate dehydrogenase. The diagram was adapted from El-Mansi (2004).

7.4   CONCLUSIONS

The research presented in this thesis represents a metabolic engineering approach to examine acetate production by *E. coli* MG1655, using antisense RNA technology. The investigation attempted to combine physiological characterisation with metabolic flux analysis to determine the effectiveness of antisense RNA in suppressing expression of enzymes in the acetate production pathway, and redirecting the flow of carbon in *E. coli* central metabolism. To this end, a series of recombinant plasmids were constructed to express putative antisense RNA targeted against phosphotransacetylase and acetate kinase mRNA. The results indicated that the antisense RNA strategy used in this study reduced acetate production by *E. coli* MG1655, and resulted in redirection of carbon flow to lactate production.

This research could be the starting point for further metabolic engineering strategies to manipulate carbon flow through central metabolism using antisense RNA to selectively downregulate the expression of key enzymes involves in by-product formation. Metabolic engineering of organisms for reduced by-product formation is an important issue because many of the organisms used in industry produce large amounts of waste products, which diminishes the efficiency of carbon conversion to biomass and desirable end-products.

Metabolic engineering is a powerful tool that enables the rational design and optimisation of organisms that produce important products in the Biotechnology industry. Each new piece of research contributes to and advances the field of metabolic engineering. With these efforts, the strategies and tools to generate efficient and economical biotechnological processes will increasingly become available.

CHAPTER 8

REFERENCES

Akesson, M., Hagander, P., Axelsson, J. P. (2001) Avoiding acetate accumulation in *E. coli* cultures using feedback control of glucose feeding. Biotechnology and Bioengineering 73, 223-230.

Almaas, E., Kovacs, B., Vicsek, T., Oltvai, Z. N., Barabasi, A. L. (2004) Global organisation of metabolic fluxes in the bacterium *E. coli*. Nature 427, 839-843.

Altuvia, S., Wagner, E. G. H. (2000) Switching on and off with RNA. Proceedings of the National Academy of Science 97, 9824-9826.

Altuvia, S., Weinstein-Fischer, D., Zhang, A., Postow, L., Storz, G. (1997) A small, stable RNA induced by oxidative stress: role as a pleiotropic regulator and antimutator. Cell 90, 43-53.

Altuvia, S., Zhang, A., Argaman, L., Tiwari, A., Storz, G. (1998) The *E. coli* OxyS regulatory RNA represses *fhlA* translation by blocking ribosome binding. EMBO Journal 17, 6069-6075.

Amann, E., Ochs, B., Abel, K. J. (1988) Tightly regulated tac promoter vectors useful for the expression of unfused and fused proteins in Escherichia coli. Gene 69, 301-315.

Anthony, L. C., Suzuki, H., Filutowicz, M. (2004) Tightly regulated vectors for the cloning and expression of toxic genes. Journal of Microbiological Methods 58, 243-250.

Argaman, L., Altuvia, S. (2000) *fhlA* repression by OxyS RNA: Kissing complex formation at two sites results in a stable antisense-target RNA complex. Journal of Molecular Biology 300, 1101-1112.

Aristidou, A. A., San, K. Y., Bennett, G. N. (1994) Modification of central metabolic pathway in *E. coli* to reduce acetate accumulation by heterologous expression of the *Bacillus subtilis* acetolactate synthase gene. Biotechnology and Bioengineering 44, 944-951.

Aristidou, A. A., San, K. Y., Bennett, G. N. (1995) Metabolic engineering of *E. coli* to enhance recombinant protein production through acetate reduction. Biotechnology Progress 11, 475-478.

Aristidou, A. A., San, K. Y., Bennett, G. N. (1999) Metabolic flux analysis of *E. coli* expressing the *Bacillus subtilis* acetolactate synthase in batch and continuous cultures. Biotechnology and Bioengineering 63, 737-749.

Arnold, C. N., McElhanon, J., Lee, A., Leonhart, R., Siegele, D. A. (2001) Global analysis of *E. coli* gene expression during the acetate-induced acid tolerance response. Journal of Bacteriology 183, 2178-2186.

Avignone Rossa, C., White, J., Kuiper, A., Postma, P. W., Bibb, M. and Teixeira de Mattos, M. J. (2002) Carbon flux analysis in antibiotic-producing chemostat cultures of *Streptomyces lividans.* Metabolic Engineering 4, 138-150.

Bailey, J. E. (1991) Towards a science of metabolic engineering. Science 252, 1668-1674.

Baneyx, F. (1999) Recombinant protein expression in *E. coli.* Current Opinion in Biotechnology 10, 421

Baykov, A. A., Evtushenko, O. A., Avaeva, S. M. (1988) A malachite green procedure for orthophosphate determination and its use in alkaline phosphatase-based enzyme immunoassay. Analytical Biochemisty 171, 266-270.

Becker, A., Fritz-Wolf, K., Kabsch, W., Knappe, J., Schultz, S., Volker Wagner, A. F. (1999) Structure and mechanism of the glycyl radical enzyme pyruvate formate-lyase. Nature Structural Biology 6, 969-975.

Berrios-Rivera, S. J., Bennett, G. N., Ka-Yiu, S. (2002) The effect of increasing NADH availability on the redistribution of metabolic fluxes in *Escherichia coli* chemostat cultures. Metabolic Engineering 4, 230-237.

Blanch, H. W., Clark, D. S. (1996) Biochemical Engineering. Marcel Dekker, New York.

Blattner, F. R., Plunkett, G., Bloch, C. A., Perna, N. T., Burland, V., Riley, M., Collado-Vides, J., Glasner, J. D., Rode, C. K., Mayhew, G. F., Gregor, J., Davis, N. W., Kirkpatrick, H. A., Goeden, M. A., Rose, D. J., Mau, B., Shao, Y. (1997) The complete genome sequence of *E. coli* K-12. Science 277, 1453-1462.

Bradford, M. M. (1976) A rapid and sensitive method for the quantitation of microgram quantities of protein utilising the principle of protein-dye binding. Annals of Biochemistry 72, 248-254.

Brantl, S. (2002) Antisense RNA regulation and RNA interference. Biochimica et Biophysica Acta 1575, 15-25.

Brescia, C. C., Kaw, M. K., Sledjeski, D. D. (2004) The DNA binding protein H-NS binds to and alters the stability of RNA *in vitro* and *in vivo*. Journal of Molecular Biology 339, 505-514.

Brescia, C. C., Mikulecky, P. J., Feig, A. L., Sledjeski, D. D. (2003) Identification of the Hfq-binding site on DsrA RNA: Hfq binds without altering DsrA secondary structure. RNA 9, 33-43.

Bricker, A. L., Belasco, J. G. (1999) Importance of a 5' stem-loop for longevity of *papA* mRNA in *E. coli*. Journal of Bacteriology 181, 3587-3590.

Brosius J., Erfle M., Storella J. (1985) Spacing of the -10 and -35 regions in the tac promoter. Effect on its in vivo activity. Journal of Biological Chemistry 260, 3539-3541.

Brown, T. D. K., Jones-Mortimer, M. C., Kornberg, H. L. (1977) The enzymatic interconversion of acetate and acetyl-coenzmye A in *E. coli*. Journal of General Microbiology 102, 327-336.

Bunch, P. K., Mat-Jan, F., Lee, N., Clark, D. P. (1997) The *ldhA* gene encoding the fermentative lactate dehydrogenase of *E. coli*. Microbiology 143, 187-195.

Burgard, A. P., Maranas, C. D. (2001) Probing the performance limits of the *E. coli* metabolic network subject to gene additions or deletions. Biotechnology and Bioengineering 74, 364-375.

Carrier, T. A., Keasling, J. D. (1997) Engineering mRNA stability in *E. coli* by the addition of synthetic hairpins using a 5' cassette system. Biotechnology and Bioengineering 55, 577-580.

Carrier, T. A., Keasling, J. D. (1999) Library of synthetic 5' secondary structures to manipulate mRNA stability in *E. coli*. Biotechnology Progress 15, 58-64.

Chang, D. E., Shin, S., Rhee, J. S., Pan, J. G. (1999) Acetate metabolism in a *pta* mutant of *E. coli* W3110: importance of maintaining acetyl coenzyme A flux for growth and survival. Journal of Bacteriology 181, 6656-6663.

Chassagnole, C., Noisommit-Rizzi, N., Schmid, J. W., Mauch, K., Reuss, M. (2002) Dynamic modelling of the central carbon metabolism of *E. coli*. Biotechnology and Bioengineering 79, 53-73.

Chou, C. H., Bennett, G. N., San, K. Y. (1994b) Effect of modified glucose uptake using genetic engineering techniques on high-level recombinant protein production in *E. coli* dense cultures. Biotechnology and Bioengineering 44, 952-960.

Chou, C. H., Bennett, G. N., San, K. Y. (1994a) Effect of modulated glucose uptake on high-level recombinant protein production in a dense *E. coli* culture. Biotechnology Progress 10, 644-647.

Clark, D. P. (1989) The fermentation pathways of *E. coli*. FEMS Microbiology Reviews 63, 223-234.

Coleman, J., Green, P. J., Inouye, M. (1984) The use of RNAs complementary to specific mRNAs to regulate the expression of individual bacterial genes. Cell 37, 429-436.

Contiero, J., Beatty, C., Kumari, S., de Santi, C. L., Strohl, W. R., Wolfe, A. (2000) Effects of mutations in acetate metabolism on high-cell-density growth of *E. coli*. Journal of Industrial Microbiology and Biotechnology 24, 421-430.

Cottrell, T. R., Doering, T. L. (2003) Silence of the strands: RNA interference in eukaryotic pathogens. Trends in Microbiology 11, 37-43.

Curless, C., Fu, K., Swank, R., Menjares, A., Fieschko, J., Tsai, L. (1991) Design and evaluation of a two-stage, cyclic, recombinant fermentation process. Biotechnology and Bioengineering 38, 1082-1090.

Datsenko, K. A., Wanner, B. L. (2000) One-step inactivation of chromosomal genes in *E. coli* K-12 using PCR products. Proceedings of the National Academy of Science 97, 6640-6645.

De Backer, M. D., Nelissen, B., Logghe, M., Viaene, J., Loonen, I., Vandoninck, S., De Hoogt, R., Dewaele, S., Simons, F. A., Verhasselt, P., Vanhoof, G., Contreras, R., Luyten, W. H. M. L. (2001) An antisense-based functional genomics approach for identification of genes critical for growth of *Candida albicans*. Nature Biotechnology 19, 235-241.

de Boer H.A., Comstock L.J., Vasser M. (1983) The tac promoter: a functional hybrid derived from the trp and lac promoters. Proceedings of the National Academy of Science 80, 21-25.

Delihas, N., Forst, S. (2001) *MicF*: An antisense RNA gene involved in response of *E. coli* to global stress factors. Journal of Molecular Biology 313, 1-12.

Demain, A. L. (2000) Small bugs, big business: The economic power of the microbe. Biotechnology Advances 18, 499-514.

Desai, R. P., Harris, L. M., Welker, N. E., Papoutsakis, E. T. (1999) Metabolic flux analysis elucidates the importance of the acid-formation pathways in regulating solvent production by *Clostridium acetobutylicum*. Metabolic Engineering 1, 206-213.

Desai, R. P., Papoutsakis, E. T. (1999) Antisense RNA strategies for metabolic engineering of *Clostridium acetobutylicum*. Applied and Environmental Microbiology 65, 936-945.

Diaz-Ricci, J. C., Regan, L., Bailey, J. E. (1991) Effect of alteration of the acetic acid synthesis pathway on the fermentation pattern of *E. coli*. Biotechnology and Bioengineering 38, 1318-1324.

Dubois, M., Gilles, K. A., Hamilton, J. K., Rebers, P. A., Smith, F. (1956) Colorimetric method for determination of sugars and related substances. Analytical Chemistry 28, 350-356.

Edwards, J. S., Covert, M. W., Palsson, B. O. (2002) Metabolic modelling of microbes: the flux balance approach. Environmental Microbiology 4, 133-140.

Edwards, J. S., Ibarra, R. U., Palsson, B. O. (2001) *In silico* predictions of *E. coli* metabolic capabilities are consistent with experimental data. Nature Biotechnology 19, 125-130.

Edwards, J. S., Palsson, B. O. (2000) The *E. coli* MG1655 *in silico* metabolic genotype: Its definition, characteristics, and capabilities. Proceedings of the National Academy of Science 97, 5528-5533.

Edwards, J. S., Ramakrishna, R., Schilling, C. H. , Palsson, B. O. (1999). Metabolic Flux Balance Analysis, In: Metabolic Engineering. Ed. Lee, S. Y. and Papoutsakis, E. T. Marcel Dekker, New York. Chapter 2, 13-57.

El-Mansi, E. M. T., Holms, W. H. (1989) Control of carbon flux to acetate excretion during growth of *E. coli* in batch and continuous cultures. Journal of General Microbiology 135, 2875-2883.

El-Mansi, M. (2004) Flux to acetate and lactate excretions in industrial fermentations: physiological and biochemical implications. Journal of Industrial Microbiology and Biotechnology 31, 295-300.

Engdahl, H. M., Lindell, M., Wagner, E. G. H. (2001) Introduction of an mRNA stability element at the 5'-end of an antisense RNA cassette increases the inhibition of target RNA translation. Antisense & Nucleic Acid Drug Development 11, 29-40.

Esterling, L., Delihas, N. (1994) The regulatory RNA gene micF is present in several species bacteria and its phylogenetically conserved. Molecular Microbiology 12, 639-646.

Famulok, M., Verma, S. (2002) In vivo-applied functional RNAs as tools in proteomics and genomics research. Trends in Biotechnology 20, 462-466.

Farmer, W. R., Liao, J. C. (1997) Reduction of aerobic acetate production by E. coli. Applied and Environmental Microbiology 63, 3205-3210.

Fell, D. A. (1998) Increasing the flux in metabolic pathways: A metabolic control analysis perspective. Biotechnology and Bioengineering 58, 121-124.

Feng, J., Atkinson, M. R., McCleary, W. R., Stock, J. B., Wanner, B. L., Ninfa, A. J. (1992) Role of phosphorylated metabolic intermediates in the regulation of glutamine synthesis in E. coli. Journal of Bacteriology 174, 6061-6070.

Fox, D. K., Meadow, N. D., Roseman, S. (1986b) Phosphate transfer between acetate kinase and enzyme I of the bacterial phosphotransferase system. Journal of Biological Chemistry 261, 13489-13503.

Fox, D. K., Roseman, S. (1986a) Isolation and characterisation of homogenous acetate kinase from Salmonella typhimurium and E. coli. Journal of Biological Chemistry 261, 13487-13497.

Furste, J. P., Pansegrau, W., Frank, R., Blocker, H., Scholz, P., Bagdasarian, M., Lanka, E. (1986) Molecular cloning of the plasmid RP4 primase region in a multi-host range tacP expression vector. Gene 48, 119-131.

Galperin, M. Y., Grishin, N. V. (2000) The synthetase domains of cobalamin biosynthesis amidotransferases CobB and CobQ belong to a new family of ATP-dependent amidoligases related to dethiobiotin synthetase. Proteins:Structure, Function and Genetics 41, 238-247.

Gerdes, K., Bech, F. W., Jorgensen, S. T., Lobner-Olesen, A., Rasmussen, P. B., Atlung, T., Boe, L., Karlstrom, O., Molin, S., von Meyenberg, K. (1986b) Mechanism of postsegregational

killing by the *hok* gene product of the *parB* system of plasmid R1 and its homology with the *relF* gene product of the *E. coli relB* operon. EMBO Journal 5, 2023-2029.

Gerdes, K., Rasmussen, P. B., Molin, S. (1986a) Unique type of plasmid maintenance function: postsegregational killing of plasmid-free cells. Proceedings of the National Academy of Science USA 83, 3116-3120.

Gimenez, R., Nunez, M. F., Badia, J., Aguilar, J., Baldoma, L. (2003) The gene *yjcG*, cotranscribed with the gene *acs*, encodes an acetate permease in *E. coli*. Journal of Bacteriology 185, 6448-6455.

Granstrom, T., Aristidou, A. A., Leisola, M. (2002) Metabolic flux analysis of *Candida tropicalis* growing on xylose in an oxygen-limited chemostat. Metabolic Engineering 4, 248-256.

Hahm, D. H., Pan, J., Rhee, J. S. (1994) Characterisation and evaluation of a *pta* (phosphotransacetylase) negative mutant of *E. coli* HB101 as production host of foreign lipase. Applied Microbiology and Biotechnology 42, 100-107.

Han, K., Hong, J., Lim, H. C. (1993) Relieving effects of glycine and methionine from acetic acid inhibition in *E. coli* fermentation. Biotechnology and Bioengineering 41, 316-324.

Han, K., Lim, H. C., Hong, J. (1992) Acetic acid formation in *E. coli* fermentation. Biotechnology and Bioengineering 39, 663-671.

Heinrich, R., Rapoport, T. A. (1974) A linear steady state treatment of enzymatic chains. General properties, control and effector strength. European Journal of Biochemistry 42, 89-95.

Hershberg, R., Altuvia, S., Margalit, H. (2003) A survey of small RNA-encoding genes in *E. coli*. Nucleic Acids Research 31, 1813-1820.

Heyde, M., Laloi, P., Portalier, R. (2000) Involvement of carbon source and acetyl phosphate in the external-pH-dependent expression of porin genes in *E. coli*. Journal of Bacteriology 182, 198-202.

Higgins, J. (1963) Analysis of sequential reactions. Annals of the New York Academy of Science 108, 305-321.

Holms, W. H. (1986) The central metabolic pathways of *E. coli*: Relationship between flux and control at a branch point, efficiency of conversion to biomass and excretion of acetate. Current Topics in Cellular Regulation 28, 69-105.

Holms, W. H. (1999). Metabolic Flux Analysis, In: Applied Microbial Physiology: A Practical Approach. Ed. Rhodes, P. M. and Stanbury, P. F. Oxford University Press, Chapter 9, 213-248.

Jensen, E. B., Carlsen, S. (1990) Production of recombinant human growth hormone in *E. coli*: Expression of different precursors and physiological effects of glucose, acetate and salts. Biotechnology and Bioengineering 36, 1-11.

Jensen, K. F. (1993) The *E. coli* K-12 "Wild Types" W3110 and MG1655 have a *rph* frameshift mutation that leads to pyrimidine starvation due to low *pyrE* expression levels. Journal of Bacteriology 175, 3401-3407.

Jones, K. L., Keasling, J. D. (1998) Construction and characterization of F plasmid-based expression vectors. Biotechnology and Bioengineering 59, 659-665.

Kacser, H., Burns, J. A. (1973) The control of flux. Symposia of the Society for Experimental Biology 27, 65-104.

Kakuda, H., Kosono, K., Shiroishi, K., Ichihara, S. (1994) Identification and characterisation of the *ackA* (acetate kinase A) - *pta* (phosphotransacetylase) operon and complementation analysis of acetate utilization by an *ackA* - *pta* deletion mutant of *E. coli*. Journal of Biochemistry 116, 916-922.

Kakuda, H., Shiroishi, K., Hosono, K., Ichihara, S. (1994) Construction of Pta-Ack pathway deletion mutants of *E. coli* and characteristic growth profiles of the mutants in rich media. Bioscience, Biotechnology and Biochemistry 58, 2232-2235.

Kasemets, K., Drews, M., Nisamedtinov, I., Adamberg, K., Paalme, T. (2003) Modification of A-stat for the characterisation of microorganisms. Journal of Microbiological Methods 55, 187-200.

Kelleher, J. K. (2001) Flux estimation using isotopic tracers: common ground for metabolic physiology and metabolic engineering. Metabolic Engineering 3, 100-110.

Kim, J. Y. H., Cha, H. J. (2003) Down-regulation of acetate pathway through antisense strategy in E. coli: improved foreign protein production. Biotechnology and Bioengineering 83, 841-853.

Kirkpatrick, C., Maurer, L. M., Oyelakin, N. E., Yoncheva, Y. N., Maurer, R., Slonczewski, J. L. (2001) Acetate and formate stress: Opposite responses in the proteome of E. coli. Journal of Bacteriology 183, 6466-6477.

Klamt, S., Stelling, J. (2003) Two approaches for metabolic pathway analysis. Trends in Biotechnology 21, 64-69.

Kleman, G. L., Strohl, W. R. (1994) Acetate metabolism by E. coli in high-cell-density fermentation. Applied and Environmental Microbiology 60, 3952-3958.

Knappe, J., Sawers, G. (1990) A radical chemical route to acetyl-CoA: the anaerobically induced pyruvate formate-lyase of E. coli. FEMS Microbiology Reviews 75, 383-398.

Koffas, M., Roberge, C., Lee, K., Stephanopoulos, G. N. (1999) Metabolic engineering. Annual Review of Biomedical Engineering 1, 535-557.

Konstantinov, K., Kishimoto, M., Seke, T., Yoshida, T. (1990) A balanced DO-stat and its application to the control of acetic acid excretion by recombinant E. coli. Biotechnology and Bioengineering 36, 750-758.

Kumari, S., Beatty, C., Browning, D. F., Busby, S. J. W., Simel, E. J., Hovel-Miner, G., Wolfe, A. (2000) Regulation of acetyl coenzyme A synthetase in E. coli. Journal of Bacteriology 182, 4173-4179.

Kumari, S., Tishel, R., Eisenbach, M., Wolfe, A. (1995) Cloning, characterisation, and functional expression of acs the gene which encodes acetyl coenzyme A synthetase in E. coli. Journal of Bacteriology 177, 2878-2886.

Lease, R. A., Cusick, M. E., Belfort, M. (1998) Riboregulation in E. coli: DrsA RNA acts by RNA:RNA interactions at multiple loci. Proceedings of the National Academy of Science 95, 12456-12461.

Lee, I.-D., Palsson, B. O. (1991) A comprehensive model of human erythrocyte metabolism: Extensions to include pH effects. Biomedica et Biochimica acta 49, 771-789.

Lee, P. S., Lee, K. H. (2003) *E. coli* - A model system that benefits from and contributes to the evolution of proteomics. Biotechnology and Bioengineering 84, 801-814.

Lee, P. S., Shaw, L. B., Choe, L. H., Mehra, A., Hatzimanikatis, V., Lee, K. H. (2003) Insights into the relation between mRNA and protein expression patterns: II. Experimental observations in *E. coli*. Biotechnology and Bioengineering 84, 834-841.

Lee, S. Y. (1996) High cell density culture of *E. coli*. Trends in Biotechnology 14, 98-105.

Lin-Chao, S., Bremer, H. (1986) Effect of the bacterial growth rate on replication control of plasmid pBR322 in *E. coli*. Molecular Genes and Genetics 203, 143-149.

Luli, G. W., Strohl, W. R. (1990) Comparison of growth, acetate production, and acetate inhibition of *E. coli* strains in batch and fed-batch fermentations. Applied and Environmental Microbiology 56, 1004-1011.

Majdalani, N., Cunning, C., Sledjeski, D. D., Elliott, T., Gottesman, S. (1998) DsrA RNA regulates translation of RpoS message by an anti-antisense mechanism, independent of its action as an antisilencer of transcription. Proceedings of the National Academy of Science USA 95, 12456-12461.

Majewski, R. A., Domach, M. M. (1989) Simple constrained optimization view of acetate overflow in *E. coli*. Biotechnology and Bioengineering 35, 732-738.

Masse, E., Escorcia, F. E., Gottesman, S. (2003) Coupled degradation of a small regulatory RNA and its mRNA targets in *E. coli*. Genes & Development 17, 2374-2383.

Masse, E., Gottesman, S. (2002) A small RNA regulates the expression of genes involved in iron metabolism in *E. coli*. Proceedings of the National Academy of Science USA 99, 4620-4625.

Matsuyama, A., Yamamoto, H., Nakano, E. (1989) Cloning, expression and nucleotide sequence of the *E. coli* K-12 *ackA* gene. Journal of Bacteriology 171, 577-580.

McCleary, W. R., Stock, J. B. (1994) Acetyl phosphate and the activation of two-component response regulators. The Journal of Biological Chemistry 269, 31567-31572.

Mehra, A., Lee, K. H., Hatzimanikatis, V. (2003) Insights into the relation between mRNA and

protein expression patterns: I. Theoretical considerations. Biotechnology and Bioengineering 84, 822-833.

Miller, J. H. (1972) Experiments in molecular genetics. Cold Spring Harbour Laboratory, New York, USA.

Mirochnitchenko, O., Inouye, M. (2000) Antisense RNA and DNA in E. coli. Methods in Enzymology 313, 467-484.

Mizuno, T., Chou, M., Inouye, M. (1983) Regulation of gene expression by a small RNA transcript (micRNA) in E. coli K-12. Proceedings of the Japanese Academy 59, 335-338.

Mizuno, T., Chou, M., Inouye, M. (1984) A unique mechanism regulating gene expression: Translational inhibition by a complementary RNA transcript (micRNA). Proceedings of the National Academy of Science 81, 1966-1970.

Molina, F., Jimenez-Sanchez, A., Guzman, E. C. (1998) Determining the optimal thymidine concentration for growing Thy- E. coli strains. Journal of Bacteriology 180, 2992-2994.

Moller, T., Franch, T., Hojrup, P., Keene, D. R., Bachinger, H. P., Brennan, R. G., Valentin-Hansen, P. (2002a) Hfq: a bacterial Sm-like protein that mediates RNA-RNA interaction. Molecular Cell 9, 23-30.

Moller, T., Franch, T., Udesen, C., Gerdes, K., Valentin-Hansen, P. (2002b) Spot 42 RNA mediates discoordinate expression of the E. coli galactose operon. Genes & Development 16, 1696-1706.

Morales, V. M., Backman, A. , Bagdasarian, M. (1990). Promiscuous plasmids of the IncQ group. Mode of replication and use for gene cloning in Gram-negative bacteria, In: Pseudomonas, Biotransformations, Pathogenesis and Evolving Biotechnology. Ed. Silver, S., Chakrabarty, A. M., Gunsalus, B., and Iglewski, B. Academic Press, New York. Chapter 23,

Neidhardt, F. C., Ingraham, J. L., Brooks Low, K., Magasanik, B., Schaechter, M., Umbarger, H. E. (1987) E. coli and Salmonella typhimurium. American society for microbiology, Washington D.C., USA.

Nellen, W., Sczakiel, G. (1996) In vitro and in vivo action of antisense RNA. Molecular Biotechnology 6, 7-15.

Nielsen, J. (2001) Metabolic engineering. Applied Microbial Biotechnology 55, 263-283.

Nystrom, T. (1994) The glucose-starvation stimulon of *E. coli*: induced and repressed synthesis of enzymes of central metabolic pathways and role of acetyl phosphate in gene expression and starvation survival. Molecular Microbiology 12, 833-843.

Paalme, T., Kahru, A., Elken, R., Vanatalu, K., Tiisma, K., Vilu, R. (1995) The computer-controlled continuous culture of *Escherichia coli* with smooth change of dilution rate (A-stat). Journal of Microbiological Methods 24, 145-153.

Phue, J.-N., Shiloach, J. (2004) Transcriptional levels of key metabolites are the cause for different glucose utilization pathways in *E. coli* B (BL21) and *E. coli* K (JM109). Journal of Biotechnology 109, 21-30.

PruB, B. M. (1998) Acetyl phosphate and the phosphorylation of OmpR are involved in the regulation of the cell division rate in *E. coli*. Archives of Microbiology 170, 141-146.

PruB, B. M., Wolfe, A. J. (1994) Regulation of acetyl phosphate synthesis and degradation, and the control of flagellar expression in *E. coli*. Molecular Microbiology 12, 973-984.

Puerta-Fernandez, E., Romero-Lopez, C., Barroso-delJesus, A., Berzal-Herranz, A. (2003) Ribozymes: recent advances in the development of RNA tools. FEMS Microbiology Reviews 27, 75-97.

Riise, E., Stougaard, P., Bindslev, B., Nordstrom, K., Molin, S. (1982) Molecular cloning and characterisation of a copy number control gene *copB* of plasmid R1. Journal of Bacteriology 151, 1136-1145.

Roe, A. J., O'Byrne, C., McLaggan, D., Booth, I. R. (2002) Inhibition of *E. coli* growth by acetic acid: a problem with methionine biosynthesis and homocysteine toxicity. Microbiology 148, 2215-2222.

Ruijun, G., Nikolova, S., Clark, D. P. (2001) Regulation of the *ldhA* gene, encoding the fermentative lactate dehydrogenase of *E. coli*. Microbiology 147, 2437-2446.

San, K. Y., Bennett, G. N., Berrios-Rivera, S. J., Vadali, R. V., Yang, Y. T., Horton, E., Rudolph, F. B., Sariyar, B., Blackwood, K. (2002) Metabolic engineering through cofactor manipulation and its effects on metabolic flux redistribution in *E. coli*. Metabolic Engineering 4,

182-192.

Savageau, M. A. (1970) Biochemical systems analysis: III Dynamic solution using power-law approximation. Journal of Theoretical Biology 26, 215-226.

Schmidt, M., Delihas, N. (1995) micF RNA is a substrate for RNase E. FEMS Microbiology Letters 133, 209-213.

Shimizu, M., Suzuki, T., Kameda, K.-Y., Abiko, Y. (1969) Phosphotransacetylase of *E. coli* B, purification and properties. Biochimica et Biophysica Acta 191, 550-558.

Shin, S., Park, C. (1995) Modulation of flagellar expression in *E. coli* by acetyl phosphate and the osmoregulator OmpR. Journal of Bacteriology 177, 4696-4702.

Shuey, D. J., McCallus, D. E., Giordano, T. (2002) RNAi: gene-silencing in therapeutic intervention. Drug Discovery Today 7, 1040-1046.

Sledjeski, D. D., Whitman, C., Zhang, A. (2001) Hfq is necessary for regulation by the untranslated RNA DsrA. Journal of Bacteriology 183, 1997-2005.

Srivastava, R., Cha, H. J., Peterson, M. S., Bentley, W. E. (2000) Antisense downregulation of sigma 32 as a transient metabolic controller in *E. coli*: Effects on yield of active organophosphorus hydrolase. Applied and Environmental Microbiology 66, 4366-4371.

Stefan, A., Reggiani, L., Cianchetta, S., Radeghieri, A., Gonzalez, A., Rodriguez, V., Hochkoeppler, A. (2003) Silencing of the gene coding for the ε subunit of DNA polymerase III slows down the growth rate of *E. coli* populations. FEBS Letters 546, 295-299.

Stephanopoulos, G. N. (1999) Metabolic fluxes and Metabolic Engineering. Metabolic Engineering 1, 1-11.

Stephanopoulos, G. N., Aristidou, A. A., Nielsen, J. (1998) Metabolic Engineering: Principles and Methodologies. Academic Press, San Diego, USA.

Stephanopoulos, G. N., Vallino, J. J. (1991) Network rigidity and metabolic engineering in metabolite overproduction. Science 252, 1675-1681.

Stolt, P., Zillig, W. (1993) Structure specific ds/ss-RNase activity in the extreme halophile

Halobacterium salinarium. Nucleic Acids Research 21, 5595-5599.

Storz, G., Opdyke, J. A., Zhang, A. (2004) Controlling mRNA stability and translation with small, noncoding RNAs. Current Opinion in Microbiology 7, 140-144.

Stougaard, P., Molin, S., Nordstrom, K. (1981) RNAs involved in copy number control and incompatibility of plasmid R1. Proceedings of the National Academy of Science 78, 6008-6012.

Summers, D. K. (1996) The Biology of Plasmids. Blackwell Science Ltd., London.

Suzuki, T. (1969) Phosphotransacetylase of *E. coli* B, activation by pyruvate and inhibition by NADH and certain nucleotides. Biochimica et Biophysica Acta 191, 559-569.

Taylor, L. A., Rose, R. E. (1988) A correction in the nucleotide sequence of the Tn903 kanamycin resistance determinant in pUC4K. Nucleic Acids Research 16, 358

Thompson, J. D. (2002) Applications of antisense and siRNAs during preclinical drug development. Drug Discovery Today 7, 912-917.

Tomizawa, J. (1984) Control of ColE1 plasmid replication: the process of binding RNA I to the primer transcript. Cell 38, 861-870.

Tomizawa, J. (1986) Control of plasmid ColE1 replication: binding of RNA I to RNA II and inhibition of primer formation. Cell 47, 97

Tomizawa, J., Itoh, T. (1981) Plasmid ColE1 incompatibility determined by interaction of RNA I with primer transcript. Proceedings of the National Academy of Science 78, 6096-6100.

Tomizawa, J., Itoh, T., Selzer, G., Som, T. (1981) Inhibition of ColE1 RNA primer formation by a plasmid-specified small RNA. Proceedings of the National Academy of Science 78, 1421-1425.

Tummala, S. B., Welker, N. E., Papoutsakis, E. T. (2003) Design of antisense RNA constructs for downregulation of the acetone formation pathway of *Clostridium acetobutylicum.* Journal of Bacteriology 185, 1923-1934.

van de Walle, M., Shiloach, J. (1998) Proposed mechanism of acetate accumulation in two

recombinant *E. coli* strains during high density fermentation. Biotechnology and Bioengineering 57, 71-78.

van den Berg, W. A. M., van Dongen, W. M. A. M., Veeger, C. (1991) Reduction of the amount of periplasmic hydrogenase in *Desulfovibrio vulgaris* (Hildenborough) with anti-sense RNA: Direct evidence for an important role of this hydrogenase in lactate metabolism. Journal of Bacteriology 173, 3688-3694.

Varma, A., Palsson, B. O. (1994) Metabolic flux balancing: Basic concepts, scientific and practical use. Bio/Technology 12, 994-998.

Varma, A., Palsson, B. O. (1994) Stoichiometric flux balance models quantitatively predict growth and metabolic by-product secretion in wild-type *E. coli* W3110. Applied and Environmental Microbiology 60, 3724-3731.

Voet, D., Voet, J. G. (1995) Biochemistry. John Wiley & Sons, Inc., New Jersey, USA.

Wagner, E. G. H., Simons, R. W. (1994) Antisense RNA control in bacteria, phages, and plasmids. Annual Review of Microbiology 48, 713-742.

Wanner, B. L., Wilmes-Riesenberg, M. R. (1992) Involvement of phosphotransacetylase, acetate kinase, and acetyl phosphate synthesis in control of the phosphate regulon in *E. coli*. Journal of Bacteriology 174, 2124-2130.

Warren, J. W., Walker, J. R., Roth, J. R., Altman, E. (2000) Construction and characterisation of a highly regulable expression vector, pLAC11, and its multipurpose derivatives, pLAC22 and pLAC33. Plasmid 44, 138-151.

Woodcock, D. M., Crowther, P. J., Doherty, J., Jefferson, S., Decruz, E., Noyerweidner, M., Smith, S. S., Michael, M. Z., Graham, M. W. (1989) Quantitative evaluation of *E. coli* host strains for tolerance to cytosine methylation in plasmid and phage recombinants. Nucleic Acids Research 17, 3469-3478.

Yamamoto-Otake, H., Matsuyama, A., Nakano, E. (1990) Cloning of a gene coding for phosphotransacetylase from *E. coli*. Applied Microbial Biotechnology 33, 680-682.

Yang, Y. T., Aristidou, A. A., San, K. Y., Bennett, G. N. (1999a) Metabolic flux analysis of *E. coli* deficient in the acetate production pathway and expressing the *Bacillus subtilis*

acetolactate synthase. Metabolic Engineering 1, 26-34.

Yang, Y. T., Bennett, G. N., San, K. Y. (1998) Genetic and Metabolic Engineering. Electronic Journal of Biotechnology 3, 1-8.

Yang, Y. T., San, K. Y., Bennett, G. N. (1999b) Redistribution of metabolic fluxes in *E. coli* with fermentative lactate dehydrogenase overexpression and deletion. Metabolic Engineering 1, 141-152.

Yanisch-Perron, C., Vieira, J., Messing, J. (1983) Construction of improved M13 vectors using oligodeoxynucleotide-directed mutagenesis. Gene 26, 101-106.

Zhang, A., Altuvia, S., Tiwari, A., Argaman, L., Hengge-Aronis, R., Storz, G. (1998) The OxyS regulatory RNA represses *rpoS* translation and binds the Hfq (HF-1) protein. EMBO Journal 17, 6061-6068.

Zhang, A., Wassarman, K. M., Ortega, J., Steven, A. C., Storz, G. (2002) The Sm-like Hfq protein increases OxyS RNA interaction with target mRNAs. Molecular Cell 9, 11-22.

Zhang, A., Wassarman, K. M., Rosenow, C., Tiaden, B. C., Storz, G., Gottesman, S. (2003) Global analysis of small RNA and mRNA targets of Hfq. Molecular Microbiology 50, 1111-1124.

Zhao, J., Shimizu, K. (2003) Metabolic flux analysis of *E. coli* K 12 grown on ^{13}C-labeled acetate and glucose using GC-MS and powerful flux calculation method. Journal of Biotechnology 101, 101-117.

CHAPTER 9

APPENDICES

9.1   CATABOLIC REACTIONS AND SYNTHESIS OF MONOMERS IN STOICHIOMETRIC MODEL OF *E. COLI* METABOLISM

Reaction 1: mue :   0.14176 Glyc3P + 26.2949 ATP + 0.60097 Ala + 0.10124 Cys + 0.26647 Asp + 0.30747 Glu + 0.2048 Phe + 0.67725 Gly + 0.10473 His + 0.32116 Ile + 0.37935 Lys + 0.49804 Leu + 0.16989 Met + 0.26647 Asn + 0.24436 Pro + 0.29091 Gln + 0.32698 Arg + 0.38031 Ser + 0.28044 Thr + 0.46778 Val + 0.062835 Trp + 0.15244 Tyr + 0.1489 rATP + 0.18319 rGTP + 0.11366 rCTP + 0.12273 rUTP + 0.023904 dATP + 0.024582 dGTP + 0.024582 dCTP + 0.023904 dTTP + 0.28352 avg_FS + 0.0069264 UDPGlc + 0.010368 CDPEth + 0.010368 OH_myr_ac + 0.010368 C14_0_FS + 0.010368 CMP_KDO + 0.010368 NDPHep + 0.0069264 TDPGlcs + 0.01656 UDP_NAG + 0.01656 UDP_NAM + 0.01656 di_am_pim + 0.0924 ADPGlc =

Reaction 2: O2_up :		= 1 O2
Reaction 3: N_up :		= 1 N
Reaction 4: CO2_ex :		1 CO2 =
Reaction 5: S_up :		4 ATP + 4 NADPH = 1 S
Reaction 6: Glc_PTS_up :		1 PEP = 1 G6P + 1 Pyr
Reaction 7: Glc_ATP_up :		1 ATP = 1 G6P
Reaction 8: Succ_ex :		1 Succ =
Reaction 9: Glyc_up :		= 1 Glyc
Reaction 10: Glyc::Glyc3P :		1 ATP + 1 Glyc = 1 Glyc3P
Reaction 11: DHAP::Glyc3P :		1 DHAP + 1 NADH = 1 Glyc3P
Reaction 12: Lac_ex :		1 Lac =
Reaction 13: Eth_ex :		1 Eth =
Reaction 14: Ac_ex :		1 Ac =
Reaction 15: Glucn_up :		= 1 Glucn
Reaction 16: Form_ex :		1 Form =
Reaction 17: G6P::F6P :		1 G6P = 1 F6P
Reaction 18: F16P::F6P :		1 F16P = 1 F6P
Reaction 19: F6P::F16P :		1 F6P + 1 ATP = 1 F16P
Reaction 20: F16P::T3P :		1 F16P = 1 DHAP + 1 G3P
Reaction 21: DHAP::G3P :		1 DHAP = 1 G3P
Reaction 22: G3P::DPG :		1 G3P = 1 DPG + 1 NADH
Reaction 23: DPG::3PG :		1 DPG = 1 3PG + 1 ATP
Reaction 24: 3PG::2PG :		1 3PG = 1 2PG
Reaction 25: 2PG::PEP :		1 2PG = 1 PEP
Reaction 26: PEP::PYR :		1 PEP = 1 Pyr + 1 ATP
Reaction 27: Pyr::PEP :		1 Pyr + 2 ATP = 1 PEP
Reaction 28: PYR::AcCoA :		1 Pyr = 1 AcCoA + 1 NADH + 1 CO2
Reaction 29: AcCoA::Cit :		1 AcCoA + 1 OxA = 1 Cit
Reaction 30: Cit::ICit :		1 Cit = 1 ICit
Reaction 31: ICit::alKG :		1 ICit = 1 alKG + 1 NADPH + 1 CO2
Reaction 32: alKG::SuccCoA :		1 alKG = 1 SuccCoA + 1 NADH + 1 CO2

Reaction 33: SuccCoA::Succ :   1 SuccCoA = 1 Succ + 1 ATP

Reaction 34: Succ::Fum :   1 Succ = 1 Fum + 1 QuiH2

Reaction 35: Fum::Succ :   1 Fum + 1 QuiH2 = 1 Succ

Reaction 36: Fum::Mal :   1 Fum = 1 Mal

Reaction 37: Mal::OxA :   1 Mal = 1 OxA + 1 NADH

Reaction 38: ICit::Glyox :   1 ICit = 1 Succ + 1 Glyox

Reaction 39: Glyox::Mal :   1 AcCoA + 1 Glyox = 1 Mal

Reaction 40: G6P::PGlac :   1 G6P = 1 PGlac + 1 NADPH

Reaction 41: AcCoA::Adh :   1 AcCoA + 1 NADH = 1 Adh

Reaction 42: Adh::Eth :   1 NADH + 1 Adh = 1 Eth

Reaction 43: PGlac::PGluc :   1 PGlac = 1 PGluc

Reaction 44: Glucn::PGluc :   1 Glucn + 1 ATP = 1 PGluc

Reaction 45: PGluc::RI5P :   1 PGluc = 1 RI5P + 1 NADPH + 1 CO2

Reaction 46: RI5P::X5P :   1 RI5P = 1 X5P

Reaction 47: RI5P::R5P :   1 RI5P = 1 R5P

Reaction 48: Transket1 :   1 R5P + 1 X5P = 1 G3P + 1 S7P

Reaction 49: Transaldo :   1 G3P + 1 S7P = 1 F6P + 1 E4P

Reaction 50: Transket2 :   1 E4P + 1 X5P = 1 F6P + 1 G3P

Reaction 51: PGluc::KetoPGluc :   1 PGluc = 1 KetoPGluc

Reaction 52: KetoPGluc::G3P_Pyr : 1 KetoPGluc = 1 G3P + 1 Pyr

Reaction 53: OxA::PEP :   1 OxA + 1 ATP = 1 PEP + 1 CO2

Reaction 54: PEP::OxA :   1 PEP + 1 CO2 = 1 OxA

Reaction 55: AcCoA::AcP :   1 AcCoA = 1 AcP

Reaction 56: AcP::Ac :   1 AcP = 1 ATP + 1 Ac

Reaction 57: Pyr::Form :   1 Pyr = 1 AcCoA + 1 Form

Reaction 58: Pyr::Lac :   1 Pyr + 1 NADH = 1 Lac

Reaction 59: NADHDehydro :   1 NADH = 1 QuiH2 + 2 H_ex

Reaction 60: Oxidase :   1 QuiH2 + 0.5 O2 = 2 H_ex

Reaction 61: TransHydro :   1 NADH + 1 H_ex = 1 NADPH

Reaction 62: ATPSynth :   3 H_ex = 1 ATP

Reaction 63: ATPdrain :   1 ATP =

Reaction 64: Chor_Synth :   2 PEP + 1 E4P + 1 ATP + 1 NADPH = 1 Chor

Reaction 65: PRPP_Synth :   1 R5P + 2 ATP = 1 PRPP

Reaction 66: MTHF_Synth :   1 ATP + 1 NADPH = 1 MTHF

Reaction 67: Ala_Synth :   1 Pyr + 1 Glu = 1 alKG + 1 Ala

Reaction 68: Val_Synth :   2 Pyr + 1 NADPH + 1 Glu = 1 alKG + 1 CO2 + 1 Val

Reaction 69: Leu_Synth :   2 Pyr + 1 AcCoA + 1 NADPH + 1 Glu = 1 alKG + 1 NADH + 2 CO2 + 1 Leu

Reaction 70: Asn_Synth :   2 ATP + 1 N + 1 Asp = 1 Asn

Reaction 71: Asp_synth :   1 OxA + 1 Glu = 1 alKG + 1 Asp

Reaction 72: Lys_Synth :   1 di_am_pim = 1 CO2 + 1 Lys

Reaction 73: Met_Synth :   1 SuccCoA + 1 ATP + 2 NADPH + 1 MTHF + 1 Cys + 1 Asp = 1 Pyr + 1 Succ + 1 N + 1 Met

Reaction 74: Thr_Synth :   2 ATP + 2 NADPH + 1 Asp = 1 Thr

Reaction 75: Ile_Synth :   1 Pyr + 1 NADPH + 1 Glu + 1 Thr = 1 alKG + 1 CO2 + 1 N +

1 Ile

Reaction 76: His_Synth :	1 ATP + 1 PRPP + 1 Gln = 1 alKG + 2 NADH + 1 His
Reaction 77: Glu_synth :	1 alKG + 1 NADPH + 1 N = 1 Glu
Reaction 78: Gln_Synth :	1 ATP + 1 N + 1 Glu = 1 Gln
Reaction 79: Pro_Synth :	1 ATP + 2 NADPH + 1 Glu = 1 Pro
Reaction 80: Arg_Synth :	1 AcCoA + 4 ATP + 1 NADPH + 1 CO2 + 1 N + 1 Asp + 2 Glu = 1 alKG + 1 Fum + 1 Ac + 1 Arg
Reaction 81: Trp_Synth :	1 Chor + 1 PRPP + 1 Gln + 1 Ser = 1 G3P + 1 Pyr + 1 CO2 + 1 Glu + 1 Trp
Reaction 82: Tyr_Synth :	1 Chor + 1 Glu = 1 alKG + 1 NADH + 1 CO2 + 1 Tyr
Reaction 83: Phe_Synth :	1 Chor + 1 Glu = 1 alKG + 1 CO2 + 1 Phe
Reaction 84: Ser_Synth :	1 3PG + 1 Glu = 1 alKG + 1 NADH + 1 Ser
Reaction 85: Gly_Synth :	1 Ser = 1 MTHF + 1 Gly
Reaction 86: Cys_Synth :	1 AcCoA + 1 S + 1 Ser = 1 Ac + 1 Cys
Reaction 87: rATP_Synth :	5 ATP + 1 CO2 + 1 PRPP + 2 MTHF + 2 Asp + 1 Gly + 2 Gln = 2 Fum + 1 NADPH + 2 Glu + 1 rATP
Reaction 88: rGTP_Synth :	6 ATP + 1 CO2 + 1 PRPP + 2 MTHF + 1 Asp + 1 Gly + 3 Gln = 2 Fum + 1 NADH + 1 NADPH + 3 Glu + 1 rGTP
Reaction 89: rCTP_Synth :	1 ATP + 1 Gln + 1 rUTP = 1 Glu + 1 rCTP
Reaction 90: rUTP_Synth :	4 ATP + 1 N + 1 PRPP + 1 Asp = 1 NADH + 1 rUTP
Reaction 91: dATP_Synth :	1 NADPH + 1 rATP = 1 dATP
Reaction 92: dGTP_Synth :	1 NADPH + 1 rGTP = 1 dGTP
Reaction 93: dCTP_Synth :	1 NADPH + 1 rCTP = 1 dCTP
Reaction 94: dTTP_Synth :	2 NADPH + 1 MTHF + 1 rUTP = 1 dTTP
Reaction 95: avg_FS_Synth :	8.24 AcCoA + 7.24 ATP + 13.91 NADPH = 1 avg_FS
Reaction 96: UDPGlc_Synth :	1 G6P + 1 ATP = 1 UDPGlc
Reaction 97: CDPEth_Synth :	1 3PG + 3 ATP + 1 NADPH + 1 N = 1 NADH + 1 CDPEth
Reaction 98: OH_myr_ac_Synth :	7 AcCoA + 6 ATP + 11 NADPH = 1 OH_myr_ac
Reaction 99: C14_0_FS_Synth :	7 AcCoA + 6 ATP + 12 NADPH = 1 C14_0_FS
Reaction 100: CMP_KDO_Synth :	1 PEP + 1 R5P + 2 ATP = 1 CMP_KDO
Reaction 101: NDPHep_Synth :	1.5 G6P + 1 ATP = 4 NADPH + 1 NDPHep
Reaction 102: TDPGlcs_Synth :	1 F6P + 2 ATP + 1 N = 1 TDPGlcs
Reaction 103: UDP_NAG_Synth :	1 F6P + 1 AcCoA + 1 ATP + 1 Gln = 1 Glu + 1 UDP_NAG
Reaction 104: UDP_NAM_Synth :	1 PEP + 1 NADPH + 1 UDP_NAG = 1 UDP_NAM
Reaction 105: di_am_pim_Synth :	1 Pyr + 1 SuccCoA + 1 ATP + 2 NADPH + 1 Asp + 1 Glu = 1 alKG + 1 Succ + 1 di_am_pim
Reaction 106: ADPGlc_Synth :	1 G6P + 1 ATP = 1 ADPGlc

Synthesis of Macromolecules:

Prot = 39.9455 ATP + 0.88727 Ala + 0.15818 Cys + 0.41636 Asp + 0.45455 Glu + 0.32 Phe + 1.0582 Gly + 0.16364 His + 0.50182 Ile + 0.59273 Lys + 0.77818 Leu + 0.26546 Met + 0.41636 Asn + 0.38182 Pro + 0.45455 Gln + 0.51091 Arg + 0.37273 Ser + 0.43818 Thr + 0.73091 Val + 0.09818 Trp + 0.23818 Tyr

RNA = 1.2488 ATP + 0.80488 rATP + 0.99024 rGTP + 0.61436 rCTP + 0.66341 rUTP

DNA = 4.4129 ATP + 0.7968 dATP + 0.8194 dGTP + 0.8194 dCTP + 0.7968 dTTP

Lip = 1.4176 Glyc3P + 2.8352 ATP + 1.4176 Ser + 2.8352 avg_FS

LPS = 0.46176 UDPGlc + 0.69118 CDPEth + 0.69118 OH_myr_ac + 0.69118 C14_0_FS + 0.69118 CMP_KDO + 0.69118 NDPHep + 0.46176 TDPGlcs

PepGly = 5.52 ATP + 2.208 Ala + 1.104 Glu + 1.104 UDP_NAG + 1.104 UDP_NAM + 1.104 di_am_pim

Glyc = 6.16 ADPGlc

PolyPhos = 12.66 ATP

9.2   LIST OF METABOLITE ABBREVIATIONS

Abbreviation	Metabolite Name
AcCoA	Acetyl-coenzyme A
ADP	Adenosine diphosphate
alKG	α-Ketoglutarate
Ala	Alanine
AMP	Adenosine monophosphate
Arg	Arginine
Asn	Asparagine
Asp	Aspartate
ATP	Adenosine triphosphate
Chor	Chorismate
Cit	Citrate
CMP	Cytosine monophosphate
CO2	Carbon dioxide
CoA	Coenzyme A
Cys	Cysteine
DHAP	Dehydroxyacetone phosphate
E4P	Erythrose-4-phosphate
F6P	Fructrose-6-phosphate
FAD	Flavin adenine dinucleotide-O
FADH	Flavin adenine dinucleotide-R
FTHF	N5-Formyl-tetrahydrofolate
Fum	Fumarate
G1P	Glucose-1-phosphate
G3P	Glyceraldehyde-3-phosphate
G6P	Glucose-6-phosphate
Glc	Glucose
Gln	Glutamine
Glu	Glutamate
Gly	Glycine
Glyc	Glycerol
Glyc3P	Glycerol-3-phosphate
Glyox	Glyoxylate
GMP	Guanosine monophosphate
H20	Water
His	Histidine

ICit	Isocitrate
Ile	Isoleucine
IMP	Inosine monophosphate
Leu	Leucine
Lip	Lipid
LPS	Lipopolysaccharide
Lys	Lysine
Mal	Malate
MDAP	meso-diaminopimelate
Met	Methionine
MTHF	N5-Methyl-tetrahydrofolate
MUR	Murine
MYC	Mycarose
N	Nitrogen
NAD	Nicotinamide adenine dinucleotide-O
NADH	Nicotinamide adenine dinucleotide-R
NADP	Nicotinamide adenine dinucleotide phosphate-O
NADPH	Nicotinamide adenine dinucleotide phosphate-R
NH4	Ammonia
NO2	Nitrite
NO3	Nitrate
O2	Oxygen
OxA	Oxaloacetate
PCOA	Propionyl-Coenzyme A
PEP	Phosphoenolpyruvate
2PG	2-Phosphoglycerate
3PG	3-Phosphoglycerate
PHE	Phenylalanine
Pro	Proline
Prot	Protein
PRPP	5-Phosphoribosyl-1-pyrophosphate
Pyr	Pyruvate
R5P	Ribose-5-phosphate
RI5P	Ribulose-5-phosphate
RMMCoA	R-Methylmalonyl Coenzyme A
RNA	Ribonucleic acid
S7P	Sedoheptulose-7-phosphate
Ser	Serine

225

SMMCoA	S-Methylmalonyl Coenzyme A
Succ	Succinate
SuccCoA	Succinyl Coenzyme A
THF	Tetrahydrofolate
THR	Threonine
TMP	Thymidine monophosphate
Trp	Tryptophan
Tyr	Tyrosine
UDPNAG	Uridine diphosphate-N-acetyl glucosamine
UDPNAM	Uridine diphosphate-N-acetyl muramic acid
UMP	Uridine monophosphate
Val	Valine
X5P	Xylulose-5-phosphate